Functional analysis of the T-box transcription factor Tbx18 in murine urogenital system development

Von der Naturwissenschaftlichen Fakultät

der Gottfried Wilhelm Leibniz Universität Hannover

zur Erlangung des Grades

Doktorin der Naturwissenschaften

(Doktor rer. nat.)

genehmigte Dissertation

von

Eva Bettenhausen, M.Sc.

2017

Referent:	Prof. Dr. rer. nat. Andreas Kispert
Korreferent:	PD Dr. med. Roland Schmitt
Vorsitzender der Prüfungskommission:	Prof. Dr. rer. nat. Hansjörg Küster
Tag der Promotion:	13.12.2016

Meinem Vater

„Leben ist Brückenschlagen über Ströme, die vergehen“

-Konstantin Wecker-

1. Summary

The organs of the excretory system of mouse and men, the kidney, ureter, bladder and urethra are needed for blood filtration, urine production, storage and release. Defects in the development of the ureter, which transports the urine from the kidney to the bladder by peristaltic contractions, can lead to impaired urine transport due to physical or functional obstruction. The consequences are urine accumulation and increasing hydrostatic pressure, which cause damage to the ureter (hydroureter) and kidney (hydronephrosis). These kinds of malformations belong to a spectrum of congenital anomalies of the kidney and urinary tract (CAKUT), which are the most common cause of chronic kidney disease in children.

Loss of the T-box transcription factor Tbx18 results in a hydroureter and hydronephrosis phenotype in mice. The defects are caused by failing ureteric smooth muscle development. At E11.5, *Tbx18* is expressed in a mesenchymal precursor population of the metanephrogenic field, where ureter and kidney development is initiated. This mesenchymal precursor population is associated with the newly formed ureteric epithelium and borders on the mesenchymal precursors of the newly formed kidney primordium. During further ureter development *Tbx18* expression is maintained in the undifferentiated coat of mesenchyme along the ureter. After the examination of the *Tbx18*-loss of function phenotype, it remained unclear, if *Tbx18* is involved in the early specification of ureteric smooth muscle precursors or in the later regulation of smooth muscle development and differentiation.

In this thesis the functional analysis of *Tbx18* in ureter development has been followed-up in three different *in vivo* approaches. The first approach addressed the early establishment of the *Tbx18*$^{+}$ precursor lineage and its later fate. The expression of *Tbx18* and other known markers of mesenchymal compartments of the urogenital precursor ridge was analyzed. This analysis revealed that *Tbx18* expression is initiated as early as day 9.5 of embryonic development (E9.5) in the cranial part of the urogenital ridge (UGR), the gonadal ridge mesenchyme and its coelomic surface epithelium. Further caudally, in the metanephrogenic field, *Tbx18* became detectable between E10.0 and E10.5, with the outgrowth of the ureter from the nephric duct. At no time point, there was an overlap between the strand of nephrogenic mesenchyme,

which gives rise to the nephric structures of the urogenital ridge, and the *Tbx18*$^{+}$ population. The *Foxd1*$^{+}$ renal stroma precursor population, and the mesenchyme along the ureter, which maintained *Tbx18* expression were established as two separate lineages at E11.5.

Fate mapping of the *Tbx18*$^{+}$ lineage in the organs of the urogenital system proved that the smooth muscle layer and all connective tissue layers of the ureter wall are derived from the *Tbx18*$^{+}$ precursor population. *Tbx18*-derived cells were also found to invade the kidney and contribute to the renal stroma and to most other organs of the developing urogenital system. In the Tbx18-loss-of-function mutant the distribution of *Tbx18*-derived cells shifted from the ureteric smooth muscle coat to the stroma surrounding the renal pelvis. No *Tbx18*-derived smooth muscle layer was detectable. Hence *Tbx18* is needed in the cells derived from the common stroma and ureteric mesenchyme precursor population to impose a ureteric instead of the default stromal fate.

In a second approach we analyzed the consequences of temporal and spatial misexpression of *Tbx18* or a transcription activating *Tbx18VP16*-allele in different mesenchymal domains of the urogenital ridge. Misexpression of *Tbx18* throughout the lower trunk mesenchyme, including the complete metanephrogenic field, revealed that *Tbx18* is sufficient to repress the development of nephrogenic mesenchyme, resulting in kidney and ureter agenesis. The examination of the *Tbx18*-loss-of-function mutant at early stages showed, that it is also needed to repress the early metanephric mesenchyme in the ureteric mesenchyme precursor population. *Eya1* was identified as a possible direct target gene of Tbx18 in this process. *In vivo* analysis of two conditional *Eya1*-misexpression mutants revealed, that deregulation of *Eya1*, after the loss of *Tbx18,* might contribute to the *Tbx18*-loss of function phenotype.

Maintained expression of *Tbx18* throughout the ureteric mesenchyme and in *Tbx18*-derived renal stroma cells resulted in an expansion of the ureteric smooth muscle layer towards the epithelium at the expense of the *lamina propria* connective tissue layer of the ureter wall. The fact that the expansion of smooth muscle differentiation occurred only in the direction towards the epithelium indicates that another signal is needed for this ectopic smooth muscle differentiation. In the renal stroma we

detected a less even distribution of the *Tbx18* misexpressing cells and an accumulation of affected cells in the cortex, close to the ureter entry site. These results indicate that Tbx18 can activate ectopic smooth muscle differentiation in a subset of ureteric mesenchyme cells and that it might regulate cell adhesion or motility. Expression of the *Tbx18VP16*-allele in the ureteric mesenchyme and *Tbx18*-derived stroma prevented smooth muscle development cell autonomously. From this finding, it can be concluded, that *Tbx18* is needed as a repressing transcription factor to allow ureteric development.

In a third approach, canonical Wnt-signaling between the ureteric epithelium and the *Tbx18*-derived ureteric mesenchyme and its significance for ureteric smooth muscle development were analyzed. This analysis revealed that canonical Wnt-signals are needed in the mesenchyme to suppress adventitial fibroblast differentiation and allow smooth muscle development in the inner layer of mesenchymal cells. This analysis also revealed new findings about the connection between the regulation and function of Tbx18 and canonical Wnt-signaling in the ureteric mesenchyme. Mouse mutants showing misexpression of *Tbx18* throughout the ureteric mesenchyme in a canonical Wnt-signaling-loss-of-function background were analyzed. The results of this analysis, taken together with the results from the Tbx18-gain and loss-of-function mutant analysis, indicate that *Tbx18* expression and the perception of canonical Wnt-signals by the ureteric mesenchyme depend on each other. Furthermore, Tbx18 and Wnt-signaling are needed in combination for ureteric smooth muscle development.

Key words: Tbx18; ureter; smooth muscle

2. Zusammenfassung

Das Ausscheidungssystem von Maus und Mensch besteht aus Nieren, Harnleitern, der Blase und der Harnröhre. Diese Organe sind für die Filtration des Blutes, die Produktion und Sammlung von Urin und seinen Transport aus dem Körper verantwortlich. Der Harnleiter übernimmt hierbei den aktiven Transport des Urins, indem er ihn durch peristaltische Bewegungen von der Niere zur Blase befördert. Defekte in der Harnleiterentwicklung können den Harnabfluss stören, wenn sie zu physikalischen Blockaden im Transportweg führen oder die peristaltischen Bewegungen der Harnleiterwand beeinträchtigen. Hierdurch kann es zur Aufstauung des Urins und somit zu einem steigenden hydrostatischen Druck in Harnleiter und Niere kommen, der beide Organe schädigt. Die Folgen sind die Bildung von sog. Hydroureteren (stark dilatierter Harnleiter), häufig gefolgt von Hydronephrose (Erweiterung des Nierenbeckens und des Nierenholsystems, oft mit Schädigung des Nierengewebes). Dieses Krankheitsbild gehört zu einem Spektrum von angeborenen Fehlbildungen der Niere und ableitenden Harnwege (CAKUT), die die häufigste Ursache für chronisches Nierenversagen bei Kindern darstellen.

Der Verlust des T-box Transkriptionsfaktors Tbx18 führt in der Maus, in Folge einer fehlenden Entwicklung der glatten Muskulatur des Harnleiters, zur Ausbildung eines Hydroureter- und Hydronephrosephänotyps. Die Organanlagen von Niere und Harnleiter entwickeln sich im sog. metanephrogenen Feld. *Tbx18* wird in einer streifenförmigen, mesenchymalen Zellpopulation des metanephrogenen Feldes, exprimiert, die das Harnleiterepithel umhüllt. Die *Tbx18*$^{+}$ Population grenzt zu diesem frühen Zeitpunkt an die mesenchymale Voräuferpopulation der sich entwickelnden Niere. *Tbx18*-Expression wird von nun an im undifferenzierten Mesenchym des Harnleiters aufrechterhalten und mit einsetzender Differenzierung der glatten Muskulatur runterreguliert. Nach der Untersuchung des *Tbx18*-Verlust-Phänotyps war es unklar, ob die Funktion von Tbx18 in der frühen Spezifizierung der Harnleitermuskulatur-Vorläuferzellen oder in der späteren Regulation ihrer Entwicklung und Differenzierung liegt.

Im Zuge meiner Doktorarbeit wurde die Funktion von *Tbx18* während der Harnleiterentwicklung weiter untersucht. Die Arbeiten hierzu können drei

verschiedenen Ansätzen zugeordnet werden. Im erste Ansatz wurde die frühe *Tbx18*$^{+}$-Vorläuferpopulation in der Urogenitalleiste und das Schicksal der von ihr abgeleiteten Zellen genauer charakterisiert. Zu diesem Zweck wurde die frühe Expression von *Tbx18* und anderer Markergene beschriebener Zellpopulationen der Urogenitalleiste untersucht. Es zeigte sich, dass *Tbx18* am Tag 9.5 der Embryonalentwicklung (E9.5) im cranialen Bereich der Urogenitalleiste, im Oberflächenepithel der Genitalleiste und dem darunterliegenden Mesenchym exprimiert ist. Im weiter caudal gelegenen metanephrogenen Feld ist *Tbx18* bereits zwischen E10.0 und E10.5 mit dem Auswachsen des Harnleiters exprimiert. Von Anfang an waren die *Tbx18*$^{+}$ Population und das nephrogene Mesenchym, das alle nephrischen Strukturen der Urogenitalleiste bildet, klar voneinander abgegrenzt. Die *Foxd1*$^{+}$ Vorläuferpopulation des renalen Stromas und das *Tbx18* exprimierende Uretermesenchym unterschieden sich molekular ab E11.5 voneinander. Eine Schicksalskartierung in den Organen des Urogenitalsystems bewies, dass die glatte Muskulatur und alle Bindegewebeschichten der Harnleiterwand aus *Tbx18*-abgeleiteten Zellen entstehen. Auch im Stroma der Niere und in anderen Organen des Urogenitalsystems wurden *Tbx18*-abgeleitete Zellen gefunden. In der *Tbx18*-Verlustmutante stellten wir eine Umverteilung der Harnleitermesenchymzellen ins Stroma, das das Nierenbecken umgibt, fest. Eine *Tbx18*-abgeleitete glatte Muskelschicht des Harnleiters war nicht nachweisbar. Daraus lässt sich schließen, dass *Tbx18* benötigt wird, um in einem Teil der Uretermesenchym- und Stroma-Vorläuferpopulation das Uretermesenchym-Schicksal zu vermitteln im Gegensatz zum Stroma-Schicksal der Zellen, die die *Tbx18*-Expression verlieren.

In einem zweiten Ansatz untersuchten wir die Auswirkungen von zeitlicher und räumlicher Misexpression von *Tbx18* oder einer Transkription-aktivierenden *Tbx18VP16*-Variante in verschiedenen mesenchymalen Populationen der Urogenitalleiste. Misexpression von *Tbx18* im Mesenchym des gesamten caudalen Rumpfbereichs, inklusive des gesamten metanephrogenen Feldes, zeigte, dass *Tbx18* die Entwicklung von nephrogenem Mesenchym verhindert, wodurch die Entwicklung von Niere und Harnleiter ausbleibt. Die Untersuchung der *Tbx18*-Verlustmutante zeigte, dass *Tbx18* nicht nur dieses Potenzial hat, sondern auch benötigt wird um das frühe Expressionsprogramm des Nierenmesenchyms in der benachbarten Harnleitermesenchym-Population zu unterdrücken. *Eya1* wurde als ein mögliches direktes Zielgen von Tbx18 in diesem Prozess identifiziert. Die *in vivo*-

Analyse zweier konditioneller *Eya1*-Missexpressionsmutanten wies darauf hin, dass die Fehlregulation von *Eya1* in der *Tbx18*-Verlustmutante zur Entstehung des Phänotyps beiträgt.

Misexpression im gesamten Harnleitermesenchym und in den *Tbx18*-abgeleiteten Zellen des Nierenstromas führte zu einem Verlust der *Lamina propria*, der inneren Bindegewebsschicht der Harnleiterwand. Das an das Ureterepithel angrenzende Gewebe zeigte nun ektopische Entwicklung von glatter Muskulatur. Diese Ergebnisse weisen darauf hin, dass *Tbx18* eine Funktion in die Spezifizierung oder Differenzierung der Harnleitermuskulatur hat, vermutlich gemeinsam mit anderen vom Harnleiterepithel ausgehenden Signalen. Im Nierenstroma führte die Missexpression zu einer veränderten Verteilung der betroffenen Zellen, die eine Regulation von Zelladhäsion durch Tbx18 hinweisen könnten. Expression eines *Tbx18-VP16*-Allels im Harnleitermesenchym und in den *Tbx18*-abgeleiteten Zellen im Nierenstroma verhinderte die Differenzierung von glatter Muskulatur zellautonom, was darauf hinweist, dass *Tbx18* in der Entwicklung der Harnleitermuskulatur als reprimierender Transkriptionsfaktor gebraucht wird.

In einem dritten Ansatz wurde der Austausch von kanonischen Wnt-Signalen zwischen Harnleiterepithel und –mesenchym und die Bedeutung dieses Signalweges für die Entwicklung der glatten Muskulatur des Harnleiters untersucht. Diese Analyse zeigte, dass kanonische Wnt-Signale im Mesenchym gebraucht werden, um die Entwicklung von *Lamina propria*-Fibroblasten im inneren Harnleitermesenchym zu verhindern und stattdessen die Entwicklung der glatten Muskulatur zu ermöglichen. Diese Untersuchung brachte auch neue Erkenntnisse über den Zusammenhang zwischen Tbx18-Expression und –Funktion und dem kanonischen Wnt-Signalweg im Harnleitermesenchym. Mausmutanten, die Misexpression von *Tbx18* im gesamten Harnleitermesenchym bei einem gleichzeitigen genetischen Verlust des kanonischen Wnt-Signalweges zeigten, wurden analysiert. Die Ergebnisse wiesen, zusammen mit den Ergebnissen der *Tbx18*-Verlustmutantenanalyse und der Analyse der *Tbx18*-Misexpressionsmutanten darauf hin, dass *Tbx18*-Expression und das Empfangen von kanonischen Wnt-Signalen im Harnleitermesenchym voneinander abhängen. Tbx18 und kanonische Wnt-Signale werden gemeinsam für die Entwicklung der glatten Muskulatur am Harnleiter benötigt.

Schlagwörter: Tbx18; Ureterentwicklung; Glatte Muskulatur

3. Table of content

4. Index of Abbreviations

ACTA	α-smooth muscle actin
BOR	branchio-oto-renal-syndrome
BrdU	Bromodeoxyuridine
CAKUT	Congenital Anomalies of the Kidney and the Urinary Tract
CDS	Collecting duct system
CM	Cap mesenchyme
Cre	Cre recombinase
Ctnnb1	β-Catenin
DAB	3, 3 –diaminobenzidine
DAPI	4',6-diamidino-2-phenylindole
DMSO	Dimethylsulfoxid
DNA	Deoxyribonucleic acid
E	Day of embryonic development
EGFP	Enhanced GFP
Fig	Figure
FITC	Fluorescein
GFP	Green fluorescent protein
H&E	Hematoxylin & Eosin labeling
Hprt	Hypoxanthine phosphoribosyltransferase
IgG	Immunoglobulin G
IM	Intermediate mesoderm
IRES	Internal ribosome entry site
KO	Knock out
LacZ	β-Galactosidase
Mes	Mesonephric tubules
MET	Mesenchymal to epithelial transition
MM	Metanephric mesenchyme
ND	Nephric duct / Wolffian duct
NM	Nephrogenic mesenchyme
ORF	Open reading frame

PBS	Phosphate-buffered saline
PBST	0,05% Tween 20 in PBS
PCR	Polymerase chain reaction
PFA	Paraformaldehyde
PGC	Primordial germ cell
RNA	Ribonucleic acid
SM	smooth muscle
SMCs	Smooth muscle cells
TSA	Tetramethylrhodamine amplification
TUNEL	TdT-mediated dUTP-biotin nicked end
UB	Ureteric bud
UE	Ureteric epithelium
UGR	Urogenital ridge
UGS	Urogenital organ system
UM	Ureteric mesenchyme
UT	Ureteric tip
γm	Micrometer

5. Erklärung zur kumulativen Dissertation

von Eva Christina Bettenhausen (geboren am 14.10.1984 in Kassel)

Diese kumulative Dissertation basiert auf folgenden Artikeln und zwei bisher unveröffentlichten Manuskripten:

Artikel 1:

Bohnenpoll T (1) and Bettenhausen E (2), Weiss AC, Foik AB, Trowe MO, Blank P, Airik R and Kispert A.

„*Tbx18* expression demarcates multipotent precursor populations in the developing urogenital system but is exclusively required within the ureteric mesenchymal lineage to suppress a renal stroma fate“

Developmental Biology 2013, August 380(1), 25-36

Autor (1) und (2) teilen sich die Erstautorenschaft für diese Publikation

Ich habe für Artikel 1 die Abbildungen **Abb. 2B, Abb. 3** (außer **B** und **C**)**, Abb. 4 A, B, C+E, Abb. S2, S3 A-I, S4,** und **S5** erstellt und die zu Grunde liegenden Daten generiert. Diese Abbildungen enthalten die Ergebnisse der Zellschicksalsanalyse der *Tbx18*-abgeleiteten Zellen in den Organen des Urogenitalsystems, die Quantifizierung der *Tbx18*-abgeleiteten Zellen, die zum renalen Stroma beitragen, die Dokumentation der Einwanderung dieser Zellen *in vivo*, sowie die vergleichende Schicksalskartierung und Quantifizierung der *Tbx18*-abgeleiteten Zellen in der *Tbx18*-Verlust-Mutante und der heterozygoten Kontrolle. Des Weiteren habe ich zum inhaltlichen Konzept des Manuskripts beigetragen. Tobias Bohnenpoll hat zu diesem Manuskript die frühe vergleichende Expressionsanalyse in **Abb. 1**, die *Ex vivo*-Zellschicksalsanalyse von *Tbx18*-abgeleiteten Zellen in explantierten Nieren-Organanlagen in **Abb. 4 F**, die Abstammungs- und Apoptose-Analyse in explantierten Nieren-Organanlagen in **Abb. 5 A-C**, die Analyse der *Tbx18*-Regulation im Uretermesenchym in **Abb. 6 A+C** sowie die frühe Zellschicksalsanalyse in **Abb. S1** und die *ex vivo* Zellschicksalsanalyse des $Tbx18^{+}$ Uretermesenchyms in **Abb. S6** beigetragen. Anna-Carina Weiss hat die Vergleichende Expressionsanalyse in **Abb. 2A**, die Apoptose-Analyse mittels Terminal deoxynucleotidyl transferase dUTP nick and labeling (TUNEL) -Untersuchung in **Abb. 5D**, die Expressionsanalyse im

Uretermesenchym in **Abb. 6B** und die Expressionsanalyse in der Nebenniere in **Abb. S3 J-P** durchgeführt. Mark-Oliver Trowe hat die adulten Urogenitalsysteme in **Abb. 3 B** und **C** präpariert und dokumentiert. Rannar Airik hat Vorarbeiten für die Erstellung von **Abb. 1** geleistet. Mark-Oliver Trowe, Patrick Blank und Anna-Barbara Foik haben technische Hilfestellungen geleistet. Andreas Kispert hat das Manuskript geplant und verfasst, war an der Züchtung der verwendeten Mausstämme beteiligt, leistete technische Hilfestellungen und hat das Projekt finanziert.

Artikel 2:

Trowe MO and Airik R, Weiss AC, Farin HF, Foik AB, Bettenhausen E, Schuster-Gossler K, Taketo MM and Kispert A.

„Canonical Wnt signaling regulates smooth muscle precursor development in the mouse ureter“

Development 2012, September 139(17), 3099-108.

Zu Artikel 2 habe ich die experimentelle Arbeit zur Generierung der **Abb. S1 B-E** beigetragen. Mark-Oliver Trowe und Rannar Airik haben den Großteil der Arbeiten an diesem Artikel durchgeführt. Anna-Barbara Foik hat technische Hilfestellung geleistet. Henner Farin und Karin Schuster-Gossler sowie Makoto Mark Taketo haben Mauslinien generiert oder zur Verfügung gestellt. Mark-Oliver Trowe und Andreas Kispert haben das Manuskript geschrieben und Andreas Kispert hat das Projekt finanziert.

Manuskript 1:

Bettenhausen E, Trowe MO, Foik AB, Rudat C, Farin HF and Kispert A.

“Tbx18 suppresses metanephric development”

Manuskript in Vorbereitung

Alle experimentellen Arbeiten und Abbildungen für Manuskript 1 mit Ausnahme eines Teils von **Abb. S5** wurden von mir erstellt. Das Manuskript wurde von mir skizziert und überarbeitet. Die Expressionsanalyse im Uretermesenchym bei E12.5 in **Abb. S5** wurde von Anna-Carina Weiss durchgeführt. Henner Farin hat den *Hprt*^{Tbx18}-Mausstamm generiert. Mark-Oliver Trowe, Anna-Barbara Foik und Carsten Rudat

haben technische Hilfestellungen geleistet. Die Daten auf denen **Abb. 1** basiert, und Vorarbeiten zur **Abb. 2** wurden im Zuge meiner Masterarbeit generiert, die ich ebenfalls im Institut für Molekularbiologie, in der Arbeitsgruppe von Andreas Kispert angefertigt habe („Missexpressionsexperimente *in vivo* zur Analyse der Funktion des T-box-Transkriptionsfaktors *Tbx18* in der Entwicklung des Uretermesenchyms“, Eva Bettenhausen, 2010). Die $Hprt^{Eya1}$-Mauslinie wurde, im Zuge dieser Arbeit, von mir nach einem etablierten Verfahren generiert. Die anderen verwendeten Mausstämme waren im Labor vorhanden. Andreas Kispert verfasste das Manuskript, war beteiligt an der Zucht der verwendeten Mausstämme, leistete technische Hilfestellung und finanzierte das Projekt.

Manuskript 2:

Bettenhausen E, Weiss AC, Trowe MO, Farin HF and Kispert A.

“Misexpression of *Tbx18* in the ureter wall and renal stroma prevents *lamina propria* development and alters distribution of stromal cells”

Manuskript in Vorbereitung

Für Manuskript 2 wurden alle experimentellen Arbeiten und Abbildungen, außer **Abb. 3 G-H`**, die von Anna-Carina Weiss erstellt wurden, von mir erstellt. Die Daten auf denen **Abb. 1**, **Abb. 2**, **Abb. 3 A-L`** (außer **G-H`**), **Abb. 4 E-V** und **Abb. S1** beruhen, wurden im Zuge meiner Masterarbeit generiert, die ich ebenfalls im Institut für Molekularbiologie, in der Arbeitsgruppe von Andreas Kispert angefertigt habe. Henner Farin hat den $Hprt^{Tbx18}$- und den $Hprt^{Tbx18VP16}$-Mausstamm generiert. Mark-Oliver Trowe und Tobias Bohnenpoll haben technische Hilfestellung geleistet. Das Manuskript wurde von Andreas Kispert und mir geplant und von mir geschrieben. Andreas Kispert editierte Teile des Manuskripts und finanzierte das Projekt.

6. Introduction

6.1. Anatomy and function of the murine urogenital organ system

The urogenital system (UGS) of the mouse and of all other amniotes (mammals, birds and reptiles) can be divided into two units, which are functionally and anatomically tightly connected (**Fig.1**). One of these units is the reproductive system, which consists of the gonads and the sex ducts. The second unit is composed of the excretory organs. In the mouse these are the paired kidneys, the ureters, the bladder and the urethra. Urine produced by the kidneys is drained to the bladder by the ureters, two tube shaped organs consisting of a multilayered epithelium, clad in layers of connective tissue and smooth muscle tissue [1]. The bladder stores the urine until micturition, when it is released from the body by the urethra. The three main functions of the excretory organ system are the removal of waste products of protein and nucleotide metabolism and other potentially harmful substances from the blood, the resorption of beneficial substances like glucose from the primary urine, and the regulation of the blood pressure by balancing the amount of water and salt retained in the body [2]. The site of blood filtration and urine production in the kidney is the nephron (**Fig.1**). The adult mouse kidney harbors about 11.000 nephrons [3]. Blood filtration takes place inside the renal corpuscle. A renal corpuscle consists of a tuft of capillaries, the glomerulus, enclosed by Bowman`s capsule, a cup-like epithelial structure. Bowman`s capsule is the first epithelial segment of the nephron. It is followed by a long, segmented epithelial tube. While the primary filtrate, generated in the glomerulus, passes through this tube, specific molecules are resorbed from it into the tightly associated blood vessels. All nephrons finally drain the urine they produce into the collecting duct system (CDS), which can resorb more water if necessary. The CDS opens into the pelvis at the tip of the renal papilla. Unlike the human kidney, the murine kidney possesses only a single, central papilla. In the pelvis urine accumulates until a peristaltic contraction, which is propagated along the ureteric smooth muscle layer, actively pumps the fluid down to the bladder. To fulfil this function the mature ureteric wall is equipped with a coat of smooth muscle tissue and its inner surface is lined by a specialized urothelium, which can withstand the high osmolarity of the urine [1]. The distal end of the ureter opens into the urinary bladder via the valve-like ureteral orifice, which prevents reflux of the urine up to the kidney.

The mature bladder wall consists of a thick layer of randomly oriented smooth muscle fibers and its inner lumen is also lined by a multilayered urothelium [4,5]. This tissue architecture allows the collection and storage of urine until it is released from the body through the urethra. During embryonic development the organs of the excretory system are established in a stepwise process. This process involves the early specification of precursor tissues and later signal exchange between them to allow the development of organ primordia, growth and differentiation.

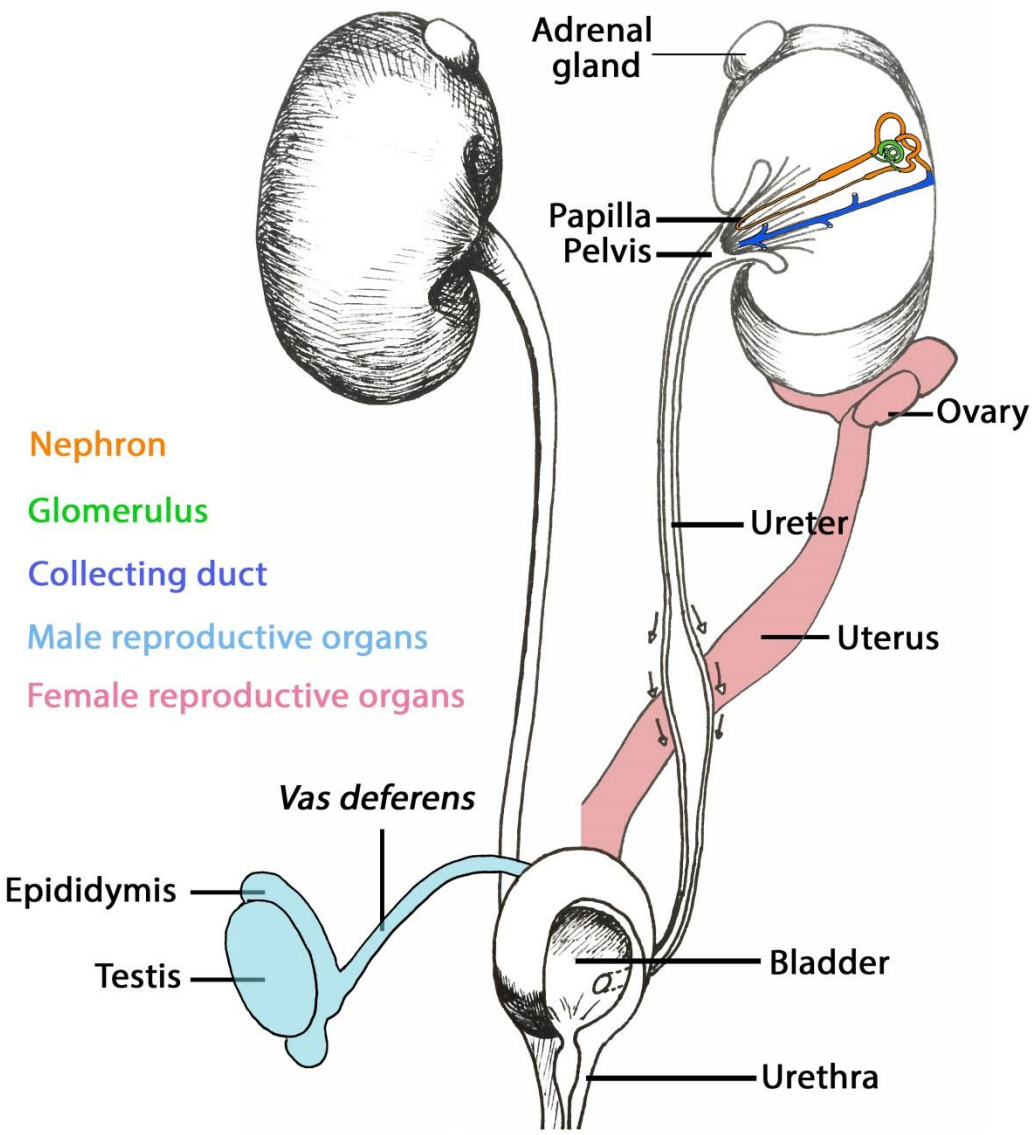

Fig.1: Anatomy of the adult murine urogenital organ system

6.2. Development of the mouse UGS and its molecular regulation

Two progenitor tissues contribute to the developing organs of the UGS, these are the intermediate mesoderm (IM) and the endoderm. An endodermal infolding, the cloaca, gives rise to the bladder, and urethra as well as to parts of the female vagina [6]. The intermediate mesoderm (IM) is the main progenitor tissue of the kidneys and ureters. The IM also gives rise to the gonads of both sexes, testes and ovaries and to the *vas deferens,* the male sex ducts [7–9].

The IM becomes first detectable after gastrulation between the paraxial mesoderm and the lateral plate mesoderm (**Fig. 2**). It gives rise to the urogenital ridge (UGR), paired strands of mesenchymal tissue, which stretch along the dorsal body wall from the heart region to the tailbud region of the embryo on either side of the gut mesentery [3]. Their ventral side is covered by the coelomic epithelium. In amniotes three generations of nephric organs, the pronephros, the mesonephros and the metanephros, are established within the UGR consecutively and in a cranial to caudal progression [3]. While the first two generations degenerate nearly completely before birth and are never functional as excretory organs, the metanephros, as the last and most caudally established kidney generation persists in the mouse to become the mature kidney.

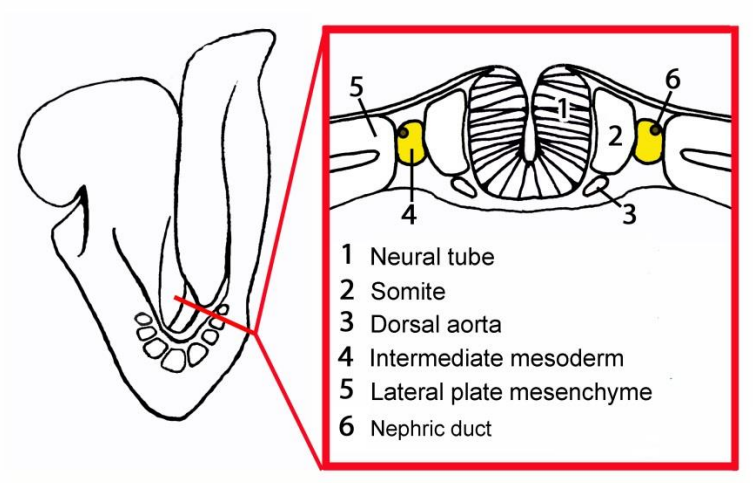

Fig. 2: The intermediate mesoderm (IM) at E8.5 The figure is based on information from EMAP eMouse Atlas Project (http://www.emouseatlas.org)[10].

In the further course of development progenitor populations or lineages are established within the UGR by the expression of specific sets of transcription factors

(**Fig. 3**). These precursor populations will then establish the organ primordia. Initially, at E7.5, the complete UGR is marked by expression of the zinc finger transcription factor *Osr1* [7,11]. The paired-box transcription factors *Pax2* and *Pax8* are the first two markers, which are restricted to the nephrogenic lineage, a mesenchymal population within the UGR, which is capable to give rise to epithelial nephric structures by mesenchymal to epithelial transition (MET) when induced by external signals [12]. MET leads to the formation of the pronephric tubules at about E8.0. These tubules fuse to initiate the formation of the Wolffian or nephric duct (ND) at the level of the forelimb buds [3,13]. While the pronephros exists only transiently in the mouse, the ND, which is marked by expression of *Lhx1*, *Ret, Pax2, Pax8* and *Wnt9b* [14–17] grows out in the caudal direction until it reaches the cloaca and connects with it between E9.5 and E10.0 [18]. With the formation of the ND the epithelial precursor structure, which induces the formation of the two following generations of nephric structures in the surrounding nephrogenic mesenchyme (NM) is established [15,19].

The strand of NM runs along the UGR on the dorsal side of the ND. It is capable to respond to the inductive Wnt9b signals coming from the ND epithelium by MET. The NM lineage is also marked by expression of a specific combination of transcriptional regulators. *Osr1* and *Wt1,* which earlier showed a broader expression domain within the IM, are later restricted to the NM, whereas *Sall1 Six1, Six2* and *Eya1* are specific markers of the NM lineage [20–22]. Expression of *Pax2* and *Pax8* is maintained in the epithelium of the ND as well as in the NM. The mesonephros, the second transitory generation of kidneys in the embryo, becomes detectable at about E9.0 at a level between the fore- and the hindlimb bud [15,19]. It consists of several NM-derived epithelial tubules. In female mammals the mesonephric second kidney generation degenerates completely, while some of the cranial mesonephric tubules persist in the male to establish the connection between the *vas deferens* and the testis. The gonads themselves are derived from the gonadal ridge, a precursor field within the UGR next to the mesonephros, which becomes detectable shortly before E10.5 by a thickening of the coelomic epithelium [23]. The early, bi-potential gonad contains primordial germ cells as well as somatic cells, which provide a kind of matrix to support the germ cells [24]. In the testis of male embryos the somatic portion of the gonad primordium gives rise to the following cell types of the testis: Sertoli cells of the epithelial testis cords, in which the germ cells are embedded, peritubular myoid cells,

which surround the testis cords, fetal Leydig cells, which fill the interstitium between the chords, and endothelial cells. The germ cells migrate into the organ primordium between E10.5 and E11.5, coming from the base of the allantois [23–25].

Finally, the development of the third, persistent kidney generation, the metanephros, is initiated. At E10.0 the metanephric blastema or metanephric mesenchyme (MM) becomes morphologically and molecularly distinguishable. It is located at the level of the hindlimb bud in the so-called metanephrogenic field at the caudal end of the strand of NM. The MM expresses a unique combination of transcription factors specifying it as the main mesenchymal precursor population of the developing kidney. *Osr1, Wt1, Sall1, Six1, Eya1* and *Pax2* were earlier expressed throughout the strand of NM and become restricted to the MM with the onset of metanephric kidney development. The three functionally redundant paralogous *Homeobox* (*Hox*)-genes *Hoxa11*, *Hoxc11* and *Hoxd11* are expressed only in the most caudal part of the strand of NM and thereby determine the position of the MM along the cranio-caudal body axis [26]. All of these factors are required for normal metanephric development and the loss of either of them results in renal agenesis in mouse mutants. But only the knock out mutants of *Osr1* and *Eya1,* which is thought to act downstream of *Osr1*, show a failing initial establishment of the MM [11,20]. This indicates their function in the early specification of the MM or the NM in general. In contrast, knock-out mutants of *Six1, Wt1, Pax2, Sall1* or the three *Hox11* paralogs initially establish the MM but lose it subsequently [22,27–30]. In the MM *Eya1* interacts with *Pax2, Six1* and the *Hox11* paralogous factors in a transcriptional complex to activate the expression of the MM specific genes *Six2* and *Gdnf* [30,31]. Spatio-temporal restriction of *Gdnf* expression is a prerequisite for metanephric kidney development, as GDNF, secreted by MM cells, induces the outgrowth of the epithelial ureteric bud (UB) from the ND. Ureteric budding is induced by GDNF signaling via the receptor tyrosine kinase RET and the GPI-linked cell surface co-receptor Gfrα1, expressed in the ND epithelium [32]. At E10.5 the UB enters the MM. This invasion is needed for further metanephric development, as the UB induces the mesenchyme to survive and proliferate. Without *Gdnf* expression ureteric outgrowth and invasion of the MM does not occur, which explains the subsequent loss of the MM in *Pax2*, *Hox11* and *Six1*-mutants.

Between E10.5 and E11.5 the mesenchymal precursor population, which will give rise to all nephrons of the developing kidney, the so called cap mesenchyme (CM),

becomes distinguished as a sub-population of the MM. The CM cells condense around the ureteric tip to form cap-like clusters [3]. Nephron formation will later be induced in a subset of the CM cells by Wnt9b emanating from the epithelium of the ureteric tips [33]. In response to this signal the induced CM cells give rise to a renal vesicle, the epithelial precursor structure of the nephron via MET. To maintain the CM as a nephron precursor pool until the termination of nephron induction, it establishes a balance between proliferation and differentiation [33].

At E11.5, MM markers, like *Eya1*, *Six1*, *Six2*, *Pax2* and *Gdnf* are still expressed throughout the metanephric blastema. After this stage expression of most of these factors will be maintained only in the CM clusters [32,34–36]. Only *Six1* is downregulated after E11.5 [37]. Two other mesenchymal precursor populations become detectable in the metanephrogenic field at E11.5. One of them is the renal stroma lineage, which is marked by expression of *Foxd1*. Spindle-shaped, *Foxd1*$^+$ stroma precursors cover the surface of the first CM clusters at E11.5 [38,39]. The origin of the stroma population is still under investigation. Traditionally these cells are described as the outer part of the MM, which is not reached by inductive signals from the UB epithelium and therefore does not condense around it [40]. Also the tailbud mesenchyme [41] and the neural crest [42] are discussed as possible sources for renal stroma cells. During embryonic development the fetal stroma cells will establish a kind of fibrocyte framework, embedding all epithelial structures of the kidney. Their developmental function in the kidney is still under investigation. The third mesenchymal population of the metanephrogenic field at E11.5 expresses neither MM nor stroma markers. It is a stripe-shaped population of cells, which stretches along the UGR, between the MM and the mesenchymal coat of the ND. The population is marked by expression of the T-box transcription factor *Tbx18*, as Airik and colleagues found out in a previous expression analysis [43]. At E11.5 the epithelium of the distal ureteric bud is embedded in this *Tbx18*$^+$ mesenchyme.

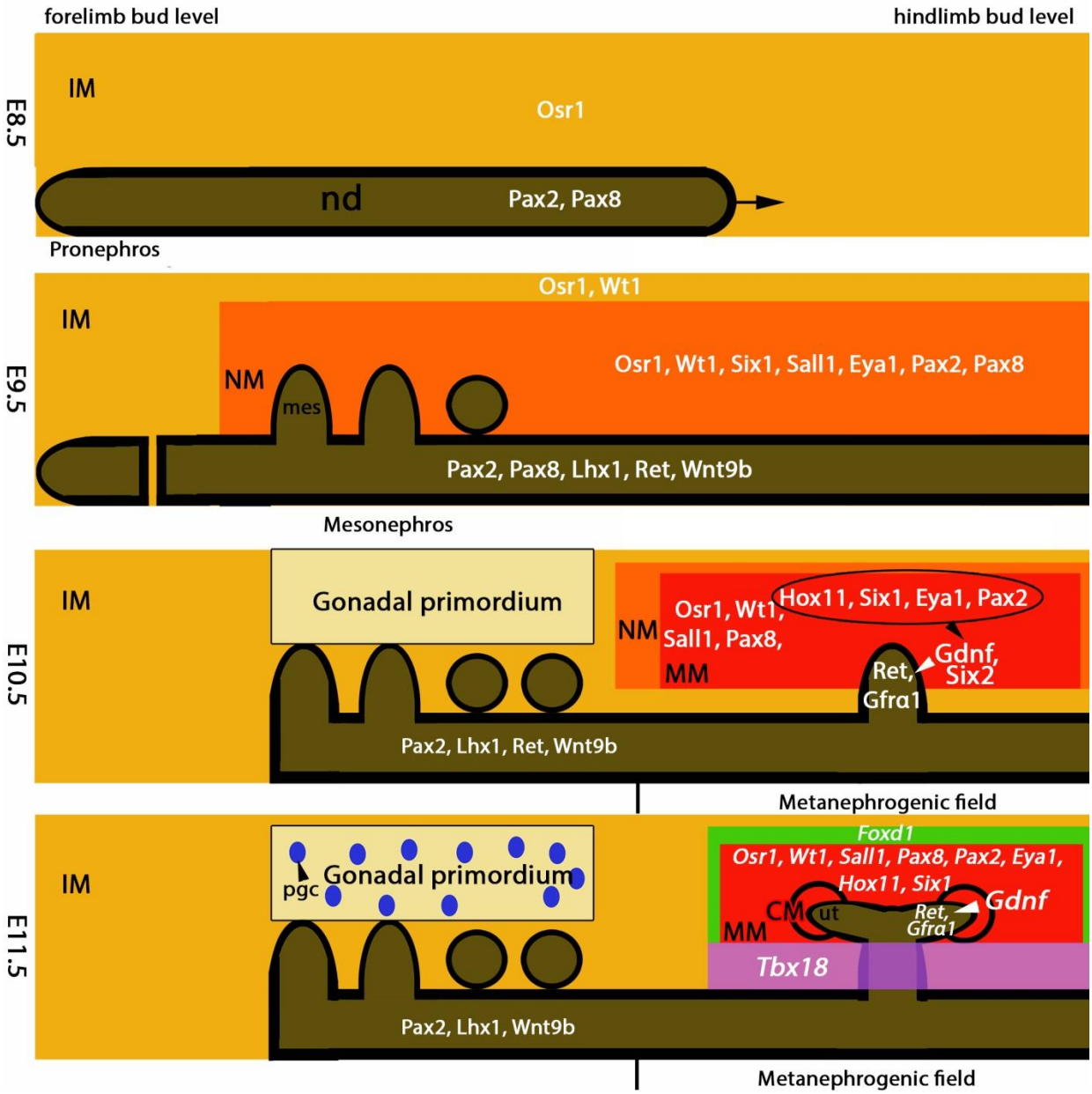

Fig. 3: Early kidney and ureter development within the UGR

CM, cap mesenchyme; IM, intermediate mesoderm; NM, nephrogenic mesenchyme; MM, metanephric mesenchyme; mes, mesonephric tubules; nd, nephric duct; ut, ureteric tip; pgc, progenitor germ cells. (The figure is based on informations from publications cited in the text)

After the main mesenchymal and epithelial precursor tissues have been established and the ureteric bud has invaded the MM, further development of the kidney and ureter is regulated by signal exchange between these tissues. Patterning of the ureteric bud epithelium into a proximal segment, which establishes the renal collecting duct system and a distal segment, which gives rise to the ureter stalk, is regulated by the surrounding mesenchyme [44–46]. The part of the UB which has invaded the MM undergoes several rounds of dichotomous branching in response to

GDNF-RET signaling, which is maintained between the CM-clusters and the UB-tip epithelium. This repetitive branching generates the collecting duct system of the kidney. The ureter stalk, the part of the ureteric bud which remains outside the kidney, shows mainly longitudinal growth. It will give rise to the ureter, which finally establishes the direct connection between kidney and bladder. During further development the ureter establishes a more elaborate tissue architecture. While the cells of the mesenchyme, which surrounds the newly formed ureter, are homogenously distributed at E11.5, the density of the mesenchyme increases close to the ureteric epithelium at E12.5 and the cells aquire a more cuboidal morphology [1]. Expression of *Tbx18* is maintained after E11.5 specifically in the undifferentiated ureteric mesenchyme (**Fig. 4A**). At E12.5, *Tbx18* is expressed throughout the mesenchymal coat of the ureteric epithelium. Between E13.5 and E14.5 the ureteric epithelium starts to differentiate to establish the multilayered urothelium, consisting of an apical layer of so called superficial facet cells, followed by a layer of intermediate cells and by the basal cell layer [47]. This architecture is established until E16.5, when the kidney begins to produce urine. Simultaneously, at E14.5, the subdivision of the surrounding mesenchyme into an inner condensed and an outer more loosely organized layer becomes even more obvious. At this stage expression of *Tbx18* is restricted to the tightly packed mesenchyme close to the ureteric epithelium. Between E14.5 and E15.5 smooth muscle differentiation is initiated in the inner layers of the ureteric mesenchyme along the ureter in a proximal to distal direction. After E16.5, when the basic architecture of the ureter has been established, the four-layered organization of the ureter wall is recognizable. The urothelium is surrounded by a layer of fibrous connective tissue, the so-called *lamina propria*. This layer is followed by a thick coat of smooth muscle cells. The outermost layer of the wall consists of the loosely organized fibrocytes of the *lamina adventitia,* which attaches the ureter to the dorsal body wall [1].The structure of the mature ureter wall at E18.5 is shown in (**Fig. 4B**). With the onset of smooth muscle differentiation *Tbx18* is downregulated in the ureteric mesenchyme. At E16.5, its expression is restricted to the layer of smooth muscle cells. At E18.5, it is undetectable in the ureter wall. The development of the different specialized tissue layers of the ureter wall depends on signals from the ureteric epithelium [9,43], but little is known about the molecular regulation of this process. Shh, a member of the Hedgehog family of signaling molecules, is expressed in the UE throughout ureter development, while its receptor *patched homolog 1*

(*Ptch1*) is expressed in the adjacent UM [48]. *Shh* loss-of-function mutants develop a hydroureter and hydronephrosis phenotype, characterized by a strongly dilated ureter. The ureter wall of these mutants lacks a functional smooth muscle layer and the kidney shows a destruction of the renal parenchyme due to increased hydrostatic pressure. It has been shown that Shh-signaling, which is partly mediated by mesenchymal *bone morphogenetic protein 4* (*Bmp4*), is required for normal proliferation and regulation of smooth muscle differentiation in the ureter. Depending on the activated downstream pathways Shh seems to be involved in promotion as well as inhibition of smooth muscle differentiation. In the future it will be a challenge to analyze the mediators of Shh-signaling and to identify more pathways involved in ureter development. Canonical Wnt signaling, which is indispensable for normal kidney development [33], might also be of importance as a signal between the epithelium of the ureter stalk and the UM.

6.3. Tbx18 and its function in ureter development

Tbx18 is a vertebrate-specific member of the family of T-box transcription factors [49,50]. Its expression pattern during ureter development suggested that Tbx18 is involved in the regulation of ureteric smooth muscle development. As the work of Airik and colleagues revealed, it is in fact indispensable for the development of the ureteric smooth muscle coat [43]. The characteristic feature of all T-box factors, the T-box, is a DNA-binding domain, recognizing conserved DNA-motifs, the T-half sites, in the regulatory sequence of target genes [51]. Subsequently, T-box factors influence the transcription of these genes, in a repressing or activating way. Their mode of regulation depends on the kind of co-factors recruited by them [52]. The specificity of target gene regulation is generated by the distribution of T- half sites in the genome, as different T-box factors prefer a different number, spacing and orientation of these binding sites. Competition between activating and repressing T-box factors for the same DNA binding sites [49] and binding of T-box factors as hetero- or homodimers [49,53–55] further increases the specificity of target gene regulation.

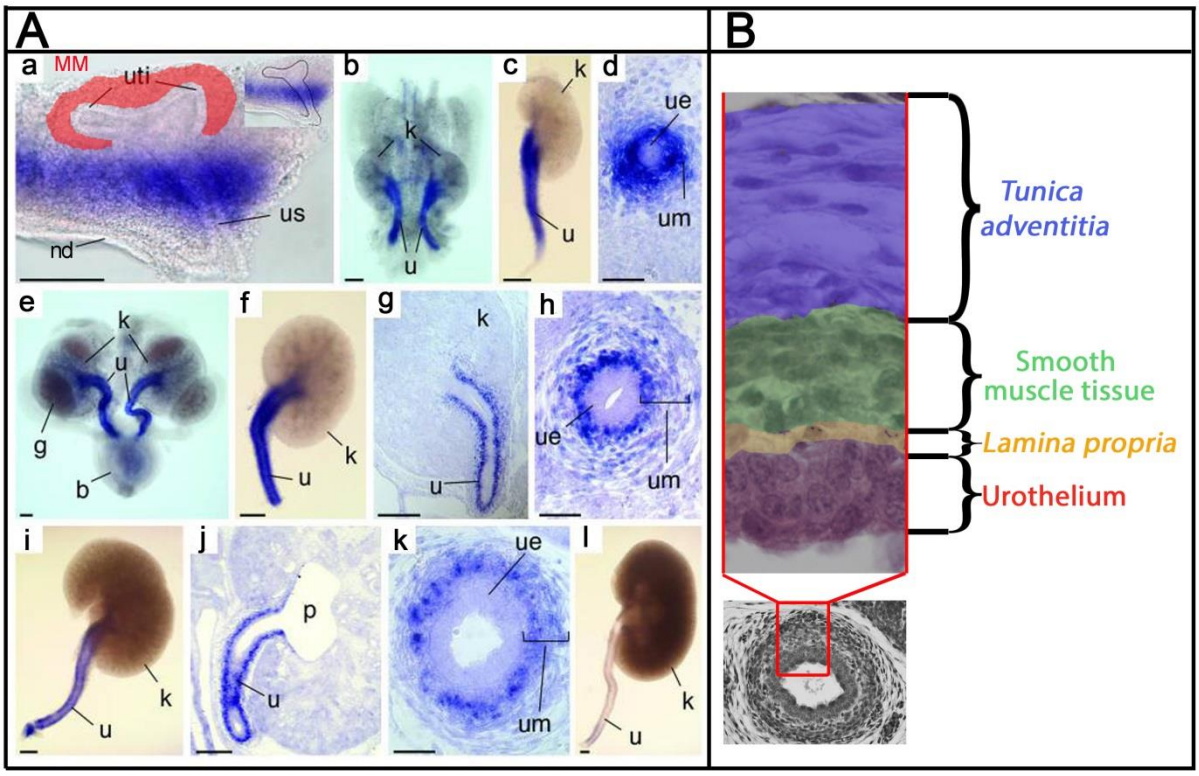

Fig. 4: Expression of Tbx18 during ureter development and structure of the mature ureter wall at E18.5 A: *Tbx18 in situ* hybridization expression analysis in the developing kidney and ureter at E11.5 (**a**), E12.5 (**c**), E14.5 (**f**), E16.5 (**i**), and E18.5 (**l**), in whole urogenital systems at E12.5 (**b**) and E14.5 (**e**), on transverse sections of ureters at E12.5 (**d**), E14.5 (**h**), and E16.5 (**k**), and on longitudinal sections of kidneys with attached ureters of wild-type embryos at E14.5 (**g**) and E16.5 (**j**). b, bladder; g, gonad; k, kidney; MM, metanephric mesenchyme; nd, nephric duct; p, pelvis; u, ureter; ue, ureteric epithelium; um, ureteric mesenchyme; uti, ureter tip; us, ureter stalk. Scale bars: 200 µm (**a**–**c**, **e**–**g**, **i**, **j**, and **l**), 100 µm (**d**, **h**, and **k**). Figure and figure legend adopted with minor modifications from: "*Tbx18* Regulates the Development of the Ureteral Mesenchyme." Airik, Rannar et al. 2006. Permission given by *Journal of Clinical Investigation* **B:** Four-layered structure of the ureter wall at E18.5.

For the Tbx18 protein, interaction with T-box factors and with other transcription factors has been shown *in vitro*. The significance of the interaction with Six1 during smooth muscle development was also shown *in vivo* with the analysis of double heterozygous and homozygous mutants. [56, 57]. Interaction of Tbx18 with Groucho co-repressors was shown to contribute significantly to the transcription repressing function of Tbx18, which has also been identified in *in vitro* experiments [49]. To understand the function of a transcription factor it is necessary to identify direct target genes. In the case of *Tbx18,* a loss-of-function as well as conditional misexpression mouse mutants were generated and analyzed for this purpose. Newborn *Tbx18* loss-of-function pups die shortly after birth, showing malformations of the rib cage and

severe difficulties in taking breath [58]. During embryonic development other defects were found in the development of the inner ear [59], the heart [60] and the UGS [43] of the mutant. In most cases the analysis of the *Tbx18* loss-of-function and gain-of-function phenotype, which was studied during somite development, did not lead to the identification of the molecular mechanisms regulated by Tbx18. The maintenance of the boundary between precursor populations was identified as a common potential function of Tbx18 in different embryonic organ primordia. Also a function in the specification or differentiation of mesenchymal precursors, in the *de novo* establishment of precursor populations or in the regulation of basic processes like adhesion, migration, proliferation or survival were considered [43,50,58,59,61]. Results of *in vitro* analyses and *in vivo* experiments in guinea pigs indicated that Tbx18 was sufficient to convert working myocardium into pacemaker-like cells [62,63]. These findings could be confirmed only partly in the analysis of mice which showed misexpression of *Tbx18* throughout the myocardium. This misexpression resulted in deregulation of a number of genes but in most cases the deregulation was identified as secondary to functional defects of the hearts. Only Gja5, a gap junction protein seemed to be directly regulated under these conditions. Activation of the pacemaker expression program was not observed [64]. Up to now, direct target genes of Tbx18 could not be identified under physiological conditions due to the lack of a specific Tbx18 antibody, which might be used for Chromatin-immunoprecipitation experiments followed by sequencing of the precipitated DNA bound by Tbx18.

The analysis of the *Tbx18*-loss-of-function phenotype in the urogenital system revealed severe defects in ureter and kidney development. Until E18.5 *Tbx18*-loss of function mutants developed hydroureters and severe hydronephrosis, a strong dilatation of the ureter and renal pelvis accompanied by the destruction of the renal parenchyme. This phenotype is commonly caused by strongly increased hydrostatic pressure after the accumulation of urine, which cannot be transported to the bladder or released into the bladder lumen due to physical or functional obstruction of the ureter [65]. In the case of the *Tbx18*-mutant, urine transport was apparently impaired due to a complete loss of the ureteric smooth muscle layer, resulting in a functional obstruction. The kidneys of the mutant showed a ventral rotation of about 90°, which positioned the opening of the pelvis on the ventral side. The ureter was severely shortened and the gonads were attached to the caudal apex of the kidney by ectopic

ligamentous tissue. First changes in the histology of the ureter wall were found at E12.5, when the mutant UM failed to establish an inner ring of tightly packed mesenchymal cells around the ureteric epithelium. The normal three layered organization of the UM around the UE was never established in the mutant. With the onset of urine production at E16.5, the mutant ureter started to dilate and the thin layer of mesenchyme lacked expression of smooth muscle differentiation markers. Most likely secondary to the mesenchymal defects also the urothelium did not show expression of differentiation markers. In a short term lineage tracing using a *Tbx18*^{LacZ}-allele, to mark *Tbx18*-derived cells temporarily, *Tbx18*-derived cells were found only along the developing ureter. In *Tbx18*-mutant embryos, in contrast, *Tbx18*-derived cells spread over the kidney surface, contributing to ligaments which tethered the gonads to the kidney. Proliferation was significantly reduced in both the UM and UE at late developmental stages. Expression of *Uncx4.1*, *Wt1*, *Raldh2* and *Foxd1,* markers for the CM and renal stroma respectively, was unchanged at E12.5 whereas *Ptch1* and *Bmp4* were downregulated and *Secreted frizzled related protein 2* (*Sfrp2*) was undetectable in the mutant UM. The molecular process regulated by Tbx18 during ureteric smooth muscle development remained unclear. A role in the aggregation of the UM along the UE or in the perception of epithelium derived signals by the mesenchyme was suggested. The very early expression of *Tbx18* and early onset of developmental defects pointed towards a function in the specification of the UM. Due to the downregulation of *Tbx18* with the onset of smooth muscle differentiation also a function in maintaining the UM in an undifferentiated state was considered. To identify the biological process regulated by Tbx18 during ureter development and to find target genes mediating the function of Tbx18 in this process, further analysis was necessary. A first analysis of the effect of temporal and spatial misexpression of *Tbx18* was done during my master thesis. This analysis revealed the necessity of a tight regulation of *Tbx18*-expression in the UGS progenitor tissues, to allow normal kidney and ureter development.

6.4. The aim of this thesis

The aim of this thesis is to further analyze the function of *Tbx18* in ureter development and to investigate pathways regulating *Tbx18* expression or mediating its function. This shall be done in three different projects:

The first project aims at a more detailed characterization of the *Tbx18* expressing precursor population in the UGR and its contribution to the developing organs of the UGS. In a short term lineage tracing of the *Tbx18*-derived cells published previously by Airik and colleagues, labeling could be achieved only for a limited period of time by *LacZ* expression [43]. To overcome this problem, a *Tbx18^{cre}*-line in combination with a *Rosa26^{mTmG}*-reporter will be used to permanently label all *Tbx18*-derived cells by GFP expression for a fate mapping in wildtype and *Tbx18*-loss-of-function UGS.

In the second project the effects of conditional misexpression of *Tbx18* will be analyzed *in vivo* in three different mouse models. A phenotypic analysis of these mice will be performed with the aim to identify biological processes, expression programs and finally single genes, which can be regulated by Tbx18. These candidate genes shall than be evaluated for their physiological relevance in the Tbx18-loss of function mutant.

Misexpression experiment 1: During ureter development *Tbx18* expression is progressively restricted to the inner ring of the UM. In the first mouse mutant, the expression of *Tbx18* is maintained in all cells derived from the early stripe-like expression domain in the metanephrogenic field. The analysis of this mutant shall answer the question, if restriction of *Tbx18* is essential for UM patterning and differentiation or for renal stroma development.

Misexpression experiment 2: In the second misexpression mutant, *Tbx18* expression is expanded from the UM-precursor domain to the complete metanephrogenic field and all its derivatives. This experiment is supposed to answer the question, if *Tbx18* has the potential to change the specification of the early mesenchymal compartments in this precursor field.

Misexpression experiment 3: A Tbx18VP16 fusion protein that activates transcription shall be expressed in all *Tbx18*-derived cells. The analysis of this mutant is supposed to provide first evidence for a transcription activating or repressing function of Tbx18 *in vivo*.

In the third project of this thesis the significance of canonical Wnt-signaling for the development of the ureteric smooth muscle layer and its connection to Tbx18 shall be analyzed *in vivo*. For this purpose the phenotype of two conditional mutants, which

show over-activation or a loss of canonical Wnt-signaling in the *Tbx18*-derived ureteric mesenchyme respectively, will be examined.

7. Paper I

Tbx18 expression demarcates multipotent precursor populations in the developing urogenital system but is exclusively required within the ureteric mesenchymal lineage to suppress a renal stromal fate

Tobias Bohnenpoll [1], Eva Bettenhausen[1], Anna-Carina Weiss, Anna B. Foik, Mark-Oliver Trowe, Patrick Blank, Rannar Airik and Andreas Kispert *

Institut für Molekularbiologie, Medizinische Hochschule Hannover, Hannover, Germany

[1] Shared first authorship

* Corresponding author address:
Institut für Molekularbiologie, OE5250, Medizinische Hochschule Hannover, Carl-Neuberg-Str. 1, D-30625 Hannover, Germany. TEL.: +49 (0)511 5324017; fax: +49 (0)511 5324283.
e-mail address: kispert.andreas@mh-hannover.de

Reprinted from: Developmental Biology 380 (2013) 25-36

http://dx.doi.org/10.1016/j.ydbio.2013.04.036

Developmental Biology 380 (2013) 25–36

Contents lists available at SciVerse ScienceDirect

Developmental Biology

journal homepage: www.elsevier.com/locate/developmentalbiology

Tbx18 expression demarcates multipotent precursor populations in the developing urogenital system but is exclusively required within the ureteric mesenchymal lineage to suppress a renal stromal fate

Tobias Bohnenpoll [1], Eva Bettenhausen [1], Anna-Carina Weiss, Anna B. Foik, Mark-Oliver Trowe, Patrick Blank, Rannar Airik, Andreas Kispert *

Institut für Molekularbiologie, OE5250, Medizinische Hochschule Hannover, Carl-Neuberg-Str. 1, D-30625 Hannover, Germany

ARTICLE INFO

Article history:
Received 11 October 2012
Received in revised form
30 April 2013
Accepted 30 April 2013
Available online 15 May 2013

Keywords:
Tbx18
Cre
Lineage tracing
Ureter
Urogenital system

ABSTRACT

The mammalian urogenital system derives from multipotent progenitor cells of different germinal tissues. The contribution of individual sub-populations to specific components of the mature system, and the spatiotemporal restriction of the respective lineages have remained poorly characterized. Here, we use comparative expression analysis to delineate sub-regions within the developing urogenital system that express the T-box transcription factor gene *Tbx18*. We show that *Tbx18* is transiently expressed in the epithelial lining and the subjacent mesenchyme of the urogenital ridge. At the onset of metanephric development *Tbx18* expression occurs in a band of mesenchyme in between the metanephros and the Wolffian duct but is subsequently restricted to the mesenchyme surrounding the distal ureter stalk. Genetic lineage tracing reveals that former *Tbx18*$^+$ cells of the urogenital ridge and the metanephric field contribute substantially to the adrenal glands and gonads, to the kidney stroma, the ureteric and the bladder mesenchyme. Loss of *Tbx18* does not affect differentiation of the adrenal gland, the gonad, the bladder and the kidney. However, ureter differentiation is severely disturbed as the mesenchymal lineage adopts a stromal rather than a ureteric smooth muscle fate. Dil labeling and tissue recombination experiments show that the restriction of *Tbx18* expression to the prospective ureteric mesenchyme does not reflect an active condensation process but is due to a specific loss of *Tbx18* expression in the mesenchyme out of range of signals from the ureteric epithelium. These cells either contribute to the renal stroma or undergo apoptosis aiding in severing the ureter from its surrounding tissues. We show that *Tbx18*-deficient cells do not respond to epithelial signals suggesting that *Tbx18* is required to prepattern the ureteric mesenchyme. Our study provides new insights into the molecular diversity of urogenital progenitor cells and helps to understand the specification of the ureteric mesenchymal sub-lineage.

Introduction

The urinary system is a multi-component entity consisting of the kidneys, the ureters, the bladder and the urethra that together control the water and ionic balance of the blood by excretion of excess water, solutes and waste products. The urinary system is structurally and functionally tightly associated with the adrenal glands, as well as with the genital system that consists of sexually dimorphic gonads, sex ducts and external genitalia.

A number of studies have begun to identify the progenitor populations, their interaction and the temporal specification of sublineages for the different components of the urogenital system in the mouse. While the lower parts of the urogenital system including the bladder epithelium, the urethra, and the lower aspect of the vagina derive from an infolding of the endoderm, the cloaca, and its surrounding mesenchyme, most other components are thought to be derivatives of the intermediate mesoderm (Mugford et al., 2008; Wang et al., 2011). Expression of the transcriptional regulator gene *Osr1* is activated broadly within the intermediate mesoderm starting from embryonic day (E) 7.5, and is required for the development of adrenals, gonads, kidneys and sex ducts suggesting that *Osr1* marks the progenitors for all of these components at this stage (James et al., 2006; Wang et al., 2005). Within the urogenital ridge of E9.5-E10.5 embryos, the first sublineages emerge. *Osr1* expression becomes gradually excluded from the (coelomic) epithelium that lines the urogenital ridge and from the epithelial Wolffian duct to be restricted to the

* Corresponding author. Fax: +49 511 5324283.
E-mail address: kispert.andreas@mh-hannover.de (A. Kispert).
[1] Equal contribution.

0012-1606/$ - see front matter © 2013 Elsevier Inc. All rights reserved.
http://dx.doi.org/10.1016/j.ydbio.2013.04.036

mesenchymal compartment of the intermediate mesoderm, and later at around E10.5, to the most posterior aspect from which all cell types of the metanephros will arise (Mugford et al., 2008). The Wolffian duct epithelium that expresses the transcription factor genes *Lhx1*, *Pax2* and *Gata3* (Grote et al., 2006; Pedersen et al., 2005) contributes exclusively to the vas deferens in the male, the epithelium of the ureter and the collecting duct system of the kidney (Saxen, 1987), whereas the epithelial lining of the ridge harbors a common pool of precursor cells for the gonads and the adrenal glands (Hatano et al., 1996). This adrenogonadal primordium that is marked by expression of the orphan nuclear receptor gene *Sf1* divides between E10-E11 into distinct progenitor populations for the adrenals and gonads (Ikeda et al., 1994; Keegan and Hammer, 2002; Luo et al., 1994). The $Sf1^{+}$ cells eventually differentiate into the cortical cells of the adrenal gland, Sertoli and Leydig cells of the testis, and granulosa and theca cells of the ovary (Bingham et al., 2006). At E10.5, signals from the mesenchymal condensation at the posterior end of the intermediate mesoderm, the metanephric blastema, induce the formation of an epithelial diverticulum from the Wolffian duct, the ureteric bud. During further development the ureteric bud invades the metanephric blastema and initiates a program of branching morphogenesis to generate the collecting duct system of the mature kidney. The distal part merely elongates and differentiates into a highly specialized type of epithelium, the urothelium. With each branching event a portion of the metanephric mesenchyme adjacent to the branch tip, is induced by tip signals to condense and undergo a mesenchymal–epithelial transition and form a renal vesicle from which the nephron will mature (for a recent review see (Little and McMahon, 2012). This cap or metanephrogenic mesenchyme is a self-renewing population of nephron progenitors that expresses the transcription factor genes *Six2* and *Uncx* (Boyle et al., 2008; Karner et al., 2011; Kobayashi et al., 2008; Neidhardt et al., 1997; Self et al., 2006). Nephron progenitors are surrounded by $Foxd1^{+}$ mesenchymal cells that will give rise to the stromal cells of the renal capsule, cortex and medulla as well as to mesangial and vascular smooth muscle cells (Hatini et al., 1996; Humphreys et al., 2010; Levinson et al., 2005). Separation of the $Six2^{+}$ nephron lineage from the $Foxd1^{+}$ stromal lineage within the $Osr1^{+}$ precursor pool is thought to occur between E10.5 and E11.5 (Mugford et al., 2008). Finally, $Flk1^{+}$ cells within the metanephric mesenchyme may contribute to the renal vasculature system (Gao et al., 2005). While the developmental origin of most of the cell types of the mature kidney has been characterized to an appreciable level, much less is known about the specification of the mesenchymal progenitor pool of the smooth muscle and fibroblast coatings of the ureter and the bladder, and the temporal separation of this lineage from the $Six2^{+}$ and $Foxd1^{+}$ progenitors of the metanephros. Notably, it has been suggested that stromal cells of the kidney and the ureteric mesenchyme do not actually arise from the intermediate mesoderm but originate in the paraxial and/or tail-bud mesoderm (Brenner-Anantharam et al., 2007; Guillaume et al., 2009).

We have previously shown that the T-box transcription factor gene *Tbx18* marks the undifferentiated ureteric mesenchyme from E12.5 to E14.5. At E11.5, *Tbx18* is expressed in a narrow band of cells between the mesenchyme surrounding the Wolffian duct and the metanephros (Airik et al., 2006). Prior to metanephric development expression of *Tbx18* was also noted in the mesonephros (Kraus et al., 2001). In $Tbx18^{-/-}$ mice, descendants of former *Tbx18*-positive cells (short: $Tbx18^{+}$ descendants) do not differentiate into smooth muscle cells of the ureter but dislocalize to the kidney and differentiate into fibroblast-like cells. As a consequence, the renal pelvis becomes dramatically enlarged at the expense of the ureter, and hydronephrosis develops at birth (Airik et al., 2006). This suggested that the ureteric mesenchymal lineage is separated early from other mesenchymal lineages of the renal system, and that separation is disturbed in *Tbx18*-deficient mice. Fate mapping efforts based on a cre knock-in in the *Tbx18* locus harbored on a BAC identified smooth muscle cells of the ureter and the bladder as derivatives of former $Tbx18^{+}$ progenitor cells (Wang et al., 2009). However, it remained unclear whether the genomic region covered by the BAC contained all *Tbx18* control elements for specific urogenital expression. Further, we neither know when the ureteric lineage is specified nor do we know the mechanisms by which the ureteric mesenchyme becomes localized around the ureteric epithelium.

Here, we characterize the expression of *Tbx18* in the developing urogenital system. We describe the cell lineages to which $Tbx18^{+}$ descendants contribute in the mature urogenital system, and analyze their *Tbx18*-dependancy. We investigate the mechanisms that restrict *Tbx18* expression to the ureteric mesenchyme, and provide evidence for the role that *Tbx18* plays within this tissue.

Materials and methods

Mice

$R26^{mTmG}$ ($Gt(ROSA)26Sor^{tm4(ACTB-tdTomato-EGFP)Luo}$) reporter mice (Muzumdar et al., 2007), $Tbx18^{lacZ}$ ($Tbx18^{tm3Akis}$), $Tbx18^{GFP}$ ($Tbx18^{tm2Akis}$) and $Tbx18^{cre}$ ($Tbx18^{tm4(cre)Akis}$) knock-in alleles (Bussen et al., 2004; Christoffels et al., 2006; Trowe et al., 2010) were all maintained on an NMRI outbred background. Embryos for gene expression analysis were derived from matings of NMRI wildtype mice. $Tbx18^{cre/+};R26^{mTmG/+}$ mice were obtained from matings of $Tbx18^{cre/+}$ males and $R26^{mTmG/mTmG}$ females. $Tbx18^{cre/lacZ};R26^{mTmG/+}$ mice were obtained from matings of $Tbx18^{cre/+};R26^{mTmG/mTmG}$ males and $Tbx18^{lacZ/+}$ females. $Tbx18^{GFP/+}$ embryos were obtained from matings of $Tbx18^{GFP/+}$ males with NMRI females. For timed pregnancies, vaginal plugs were checked in the morning after mating, noon was taken as embryonic day (E) 0.5. Embryos, whole urogenital systems and kidneys were dissected in PBS. For *in situ* hybridization and immunofluorescence analyses specimens were fixed in 4% paraformaldehyde (PFA) in PBS and stored in methanol at −20 °C. Genomic DNA prepared from yolk sacs or tail biopsies was used for genotyping by PCR.

Organ cultures

Explant cultures of embryonic kidneys or urogenital systems were performed as previously described (Airik et al., 2010). The culture medium was replaced every 24 h.

For labeling experiments with the fluorescent carbocyanine dye DiI, a tungsten wire was dipped into the DiI tissue labeling paste (Invitrogen) and excessive material was removed with a tissue towel. The tungsten wire was then clamped into a micromanipulator. Labeling of mesenchymal subpopulations within the metanephric field of E11.5 $Tbx18^{GFP/+}$ kidney rudiments was performed under visual control. Kidney explants were documented before and after treatment and the perpendicular distance of labeled cells from the ureteric epithelium was measured using ImageJ software (Schneider et al., 2012). After two days of culture the distribution of DiI labeled cells was assessed and plotted against the distance.

For the detection of apoptotic tissue in the metanephric field E11.5 kidney rudiments ($Tbx18^{GFP/+}$) were explanted and cultured for 24 h. The medium was subsequently replaced with 1 ml of 2.5 μM LysoTracker red DND-99 (L-7528, Invitrogen) in PBS and the explant cultures were incubated for 30 min at 37 °C. Cultures were then rinsed in PBS and documented.

For tissue recombination experiments, E11.5 acceptor kidney rudiments ($Tbx18^{GFP/+}$) were explanted. E12.5 ureters ($Tbx18^{cre/+}$;

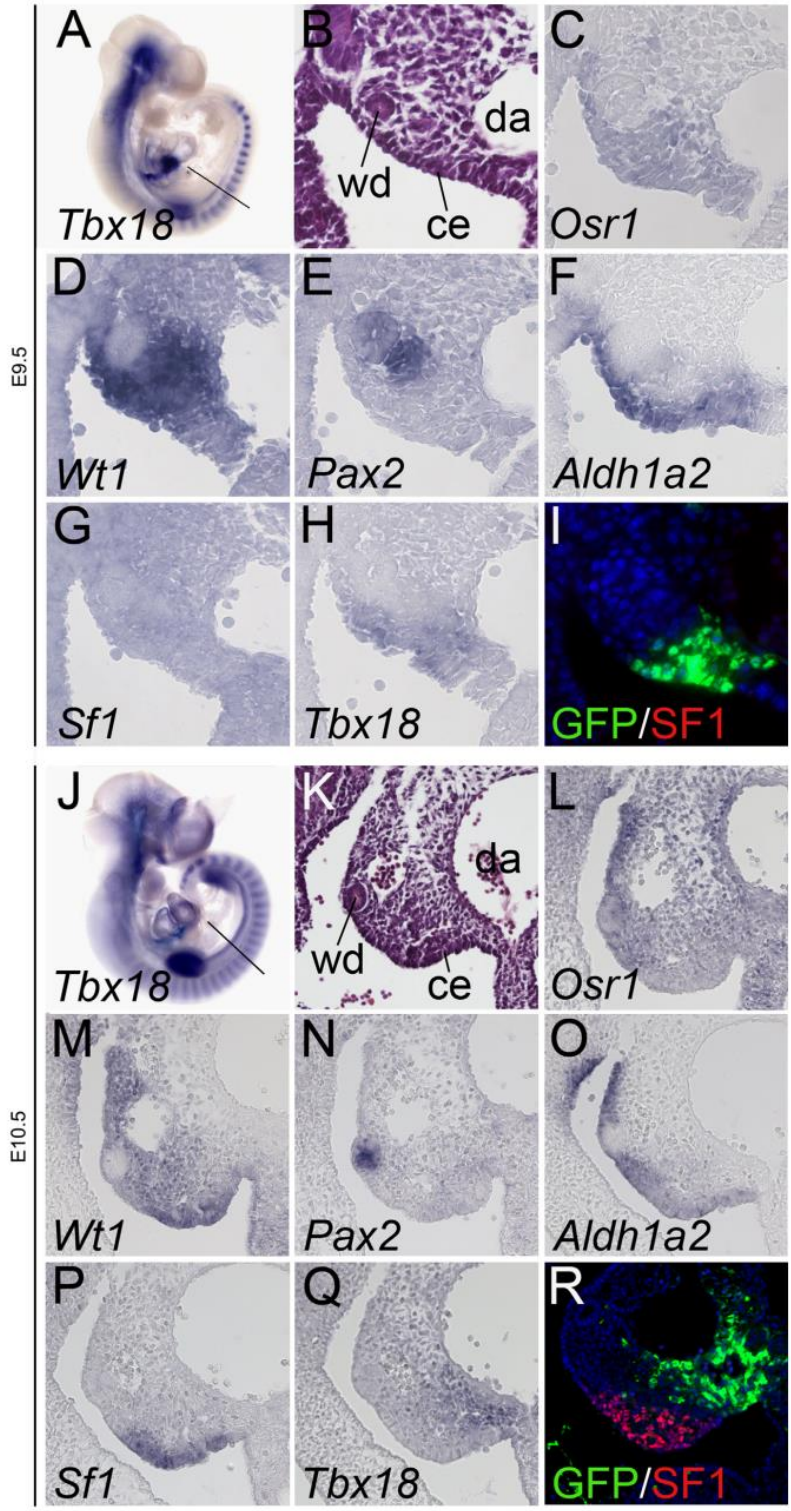

Fig. 1. *Tbx18* expression during early urogenital development: (A,J) *In situ* hybridization analysis of whole wildtype embryos for *Tbx18*: (B,D). Histological staining (HE) of transverse sections through the posterior trunk region on the planes indicated in (A,J) to describe anatomical landmarks. (C–H,L–Q) *In situ* hybridization analysis on adjacent sections to compare expression of *Tbx18* and markers of the intermediate mesoderm. (I,R) Co-immunofluorescence analysis for SF1 and GFP on adjacent sections of *Tbx18*$^{GFP/+}$ embryos. Probes and stages are as indicated. ce: coelomic epithelium; da: dorsal aorta; wd: Wolffian duct.

R26$^{mTmG/+}$) were subsequently prepared and the ureteric epithelium was mechanically separated from the mesenchyme using forceps. The uncoated ureteric epithelium was transplanted into the *Tbx18*$^{+}$ domain of the acceptor tissue distant to the endogenous ureteric epithelium. The recombined tissues were cultured for 3 days with daily documentation.

For bead implantation experiments, E11.5 acceptor kidney rudiments (*Tbx18*$^{GFP/+}$) were explanted. AffiGel Blue beads (153-7302, Bio-Rad) were rinsed in PBS and incubated with 50 μg/ml rmWNT9B (3669-WN, R&D Systems), 1.6 μg/ml rmSHH (PMC8034, Invitrogen), both or 1 mg/ml BSA for 4 hours at 4 °C. Beads were implanted into the GFP^{+} domain of the acceptor kidneys. Cultures were maintained for 2 days and GFP expression was documented daily.

Histological and histochemical analyses

Fixed embryos were dehydrated, paraffin embedded, and sectioned to 5 μm. For histological analyses sections were stained with haematoxylin and eosin. For the detection of antigens on these sections, the following primary antibodies and dilutions were used: mouse anti-UPK1B (WH0007348M2-100UG, Sigma, 1:200), mouse anti-ACTA2 (F3777 and C6198, Sigma, 1:200), rabbit anti-CDH1 (kindly provided by R. Kemler, MPI for Immunobiology and Epigenetics, Freiburg, Germany, 1:200), rabbit anti-SF1 (Trans-Genic Inc., preparation of antibodies by Dr. Ken-Ichirou Morohashi, 1:200), rabbit anti-DDX4 (ab13840, Abcam, 1:50), rabbit anti-FOXD1 (kindly provided by A.P. McMahon, Harvard University, MA, USA, 1:2000), rabbit anti-SIX2 (kindly provided by A.P. McMahon, Harvard University, MA, USA, 1:1000), anti-SOX9 (AB5535, Millipore Chemicon, 1:200), rat anti-EMCN (kindly provided by D. Vestweber, MPI for Molecular Medicine, Münster, Germany, 1:10), mouse anti-GFP (11 814 460 001, Roche, 1:200), rabbit anti-GFP (sc-8334, Santa Cruz, 1:200). Fluorescent staining was performed using Alexa 488/555-conjugated secondary antibodies (A11034; A11008; 711-487-003; A21202; A21422; A21428, Invitrogen/Dianova; 1:500) or biotin-conjugated secondary antibodies (Dianova; 1:500) and the TSA Tetramethylrhodamine Amplification Kit (Perkin-Elmer).

Labeling with primary antibodies was performed at 4 °C overnight after antigen retrieval (Antigen Unmasking Solution, Vector Laboratories; 15 min, 100 °C), blocking of endogenous peroxidases with 3% H_2O_2/PBS for 10 min (required for TSA) and incubation in

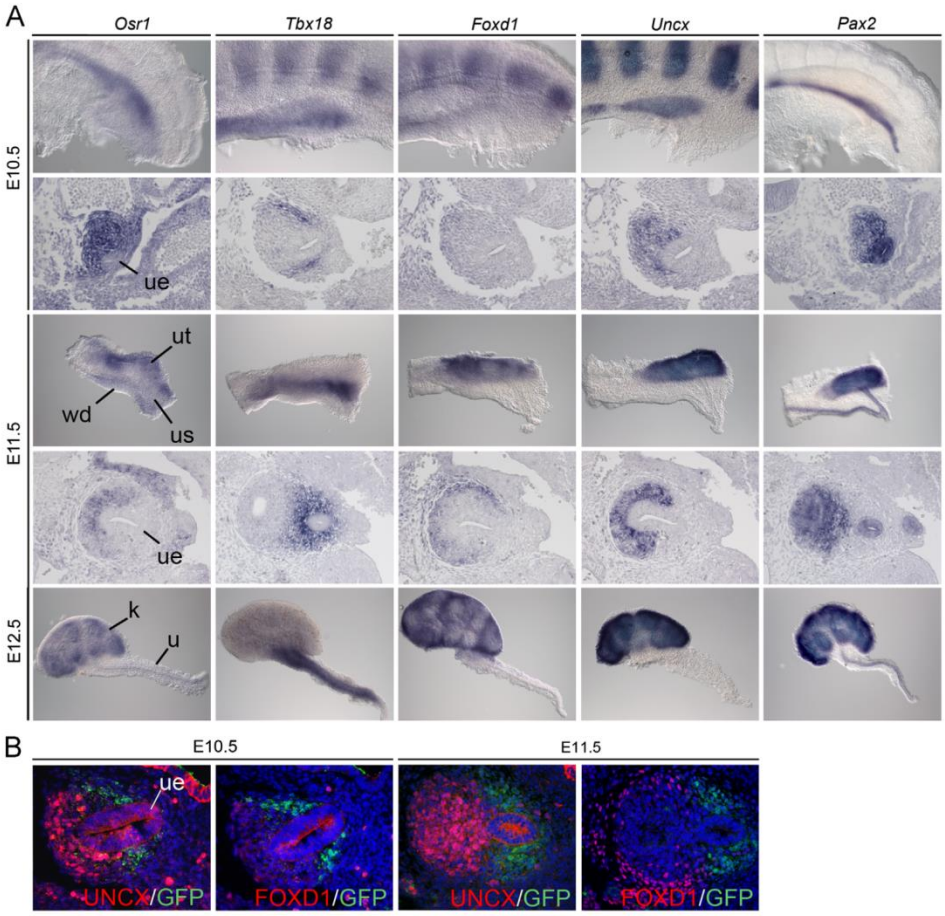

Fig. 2. *Tbx18* expression during early metanephric and ureter development. (A) *In situ* hybridization analysis of whole posterior trunk halves at E10.5 (first row), of transverse sections through the metanephric anlagen of the posterior trunk region at E10.5 (posterior is to the right, ventral to the bottom, second row), of whole E11.5 kidneys (third row), of transverse sections through the E11.5 metanephric kidney (fourth row) and of E12.5 kidneys with ureters (fifth row) to compare expression of *Tbx18* with an early pan-metanephric marker (*Osr1*), and with markers of the nephron lineage (*Uncx*, *Pax2*), of the collecting duct and ureter epithelium (*Pax2*) and of the stromal lineage (*Foxd1*) in wildtype embryos. and (B) Co-immunofluorescence analysis on sections through the metanephros at E10.5 and E11.5 with antibodies against GFP (visualizing TBX18 expression), FOXD1 and UNCX in *Tbx18*$^{GFP/+}$ embryos. k: kidney; u: ureter; ue: ureteric epithelium; us: ureter stalk; wd: Wolffian duct.

blocking solutions provided with the kits. For monoclonal mouse antibodies an additional IgG blocking step was performed using the Mouse-on-Mouse Kit (Vector Laboratories). Sections were mounted with Mowiol (Roth) or IS mounting medium (Dianova).

Paraffin sections used for TUNEL assay were deparaffinized, rehydrated and than treated according to the protocol provided with the Apop Tag Fluorescence Apoptosis detection kit (S7111, Millipore).

In situ hybridization analysis

Whole-mount *in situ* hybridization was performed following a standard procedure with digoxigenin-labeled antisense riboprobes (Wilkinson and Nieto, 1993). Stained specimens were transferred in 80% glycerol prior to documentation. *In situ* hybridization on 10 μm paraffin sections was done essentially as described (Moorman et al., 2001). For each marker at least three independent specimens were analyzed.

Image analysis

Whole-mount specimens were photographed on Leica M420 with Fujix digital camera HC-300Z, sections on Leica DM5000 B with Leica digital camera DFC300 FX. All images were processed in Adobe Photoshop CS4.

Results

Tbx18 is expressed in a subregion of the urogenital ridge

Earlier work showed expression of *Tbx18* in the urogenital ridge but failed to delineate the precise subdomain (Kraus et al., 2001). We therefore performed comparative *in situ* hybridization analysis of expression of *Tbx18* and of markers of (subregions of) the urogenital ridge on transverse sections of E9.5 and E10.5 wildtype embryos (Fig. 1). At E9.5, the entire urogenital ridge was marked by expression of *Osr1* and *Wt1*; the Wolffian duct by expression of *Pax2*, the adjacent tubule-forming mesonephric mesenchyme by *Pax2*, and the epithelial (coelomic) lining of the ridge by *Aldh1a2*. *Sf1* was not expressed at this stage. *Tbx18* expression was never detected in the epithelial Wolffian duct and the *Pax2*$^{+}$ mesonephric mesenchyme but was present in the more medially located mesenchyme close to the dorsal aorta, and overlapping with *Aldh1a2* expression in the coelomic epithelium (Fig. 1C H). At E10.5, the coelomic epithelium of the urogenital ridge was positive for *Sf1* and *Aldh1a2*, and the Wolffian duct for *Pax2* expression. *Osr1* was confined to the mesenchymal compartment of the intermediate mesoderm. *Tbx18* was found in a subregion of the *Osr1*$^{+}$ mesenchyme in the medial aspect close to the hinge between the urogenital ridge and the dorsal mesenterium, complementary to *Wt1* that was expressed in the epithelium and the lateral mesenchyme. Expression of *Tbx18* was no longer detected in the epithelial lining of the ridge that was positive for *Sf1* at this stage (Fig. 1K Q). Co-immunofluorescence analysis for GFP and SF1 (in *Tbx18*$^{GFP/+}$ embryos) confirmed the expression domain of *Tbx18*

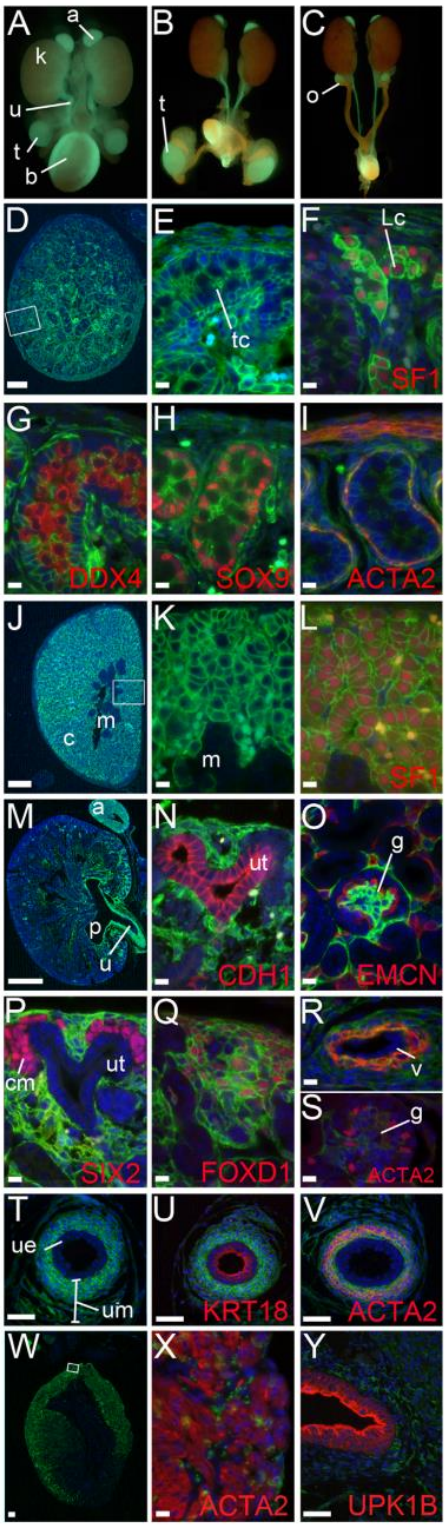

Fig. 3. Lineage analysis of *Tbx18*$^{+}$ descendants in the urogenital system. (A–C) GFP/RFP epifluorescence analysis of urogenital systems from *Tbx18*$^{cre/+}$;*R26*$^{mTmG/+}$ embryos at E18.5 (A) and at 3-weeks of age (B,C) of both male (A,B) and female sex (C). GFP (green) marks *Tbx18*$^{+}$ cells and their descendants, RFP (red) marks all other cells in the urogenital system. (D–Y) Immunofluorescence analysis of expression of the lineage marker GFP on sections of E18.5 testis (D–I), adrenal gland (J–L), kidney (M–S), ureter (T–V) and bladder (W–Y). Boxed areas are magnified for co-expression analysis of GFP and cell type markers as indicated. Scale bars represent 100 μm (D,J), 500 μm (M,W), 50 μm (T–V,Y), 10 μm (E–I,K,L,N–S, X). a: adrenal gland; b: bladder; c: cortex; cm: cap mesenchyme; g: glomerulus; k: kidney; Lc: Leydig cell; m: medulla; p: pelvis; t: testis; tc: testis cord; u: ureter; ue: ureteric epithelium; um: ureteric mesenchyme; ut: ureter tip; v- vessel. (For interpretation of the references to color in this figure legend, the reader is referred to the web version of this article.)

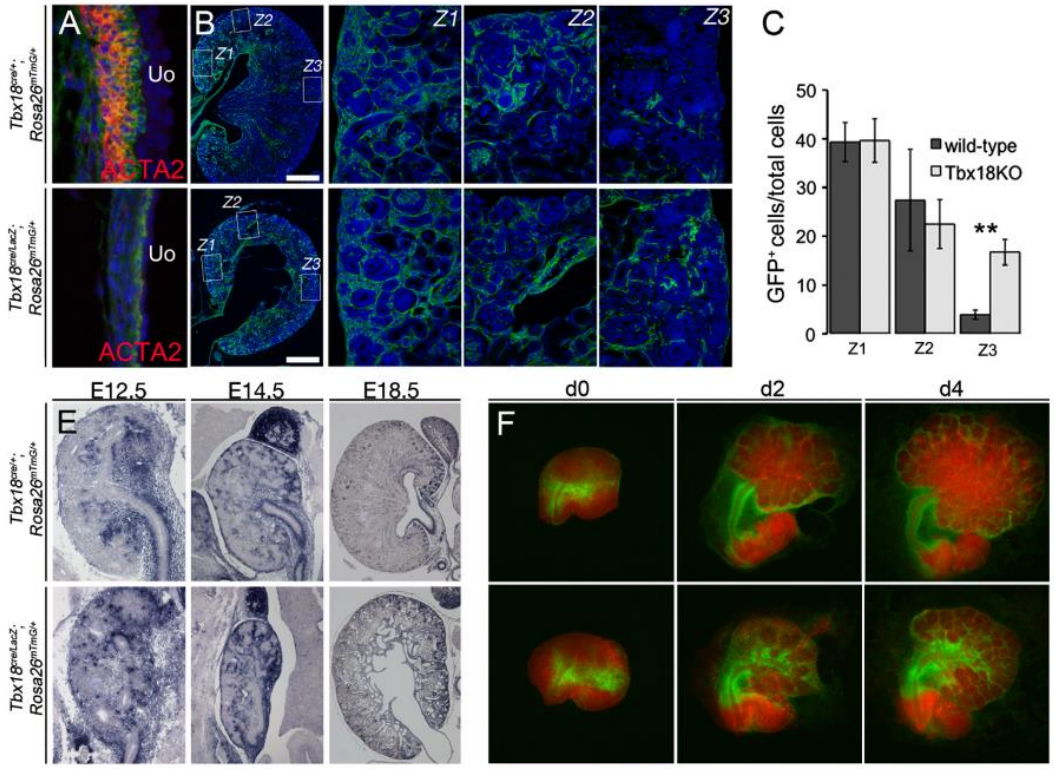

Fig. 4. Lineage analysis of *Tbx18*$^{+}$ descendants in the metanephric/ureteric development. (A) Co-immunofluorescence analysis of expression of the lineage marker GFP and the marker of smooth muscle cells, ACTA2 on sagittal sections of the ureter at E18.5. (B) Co-immunofluorescence analysis of expression of the lineage marker GFP on sagittal sections of the kidney at E18.5. Z1-3 relate to three regions used to determine the contribution of GFP^{+} cells. (C) Quantification of the contribution of GFP^{+} cells to stromal cells in the three regions of the kidney. *Z1*: control: 39+/−4, mutant: 40+/−4, $p=0.935$; *Z2*: control: 27+/−10, mutant: 23+/−5, $p=0.504$; *Z3*: control: 4+/−1, mutant: 17+/−3, $p= 0.001$. (D) *in situ* hybridization analysis of *GFP* expression in *Tbx18*$^{cre/+}$;*R26*$^{mTmG/+}$ kidneys at different developmental stages as indicated. (E) GFP/RFP epifluorescence analysis of metanephric explants from E11.5 *Tbx18*$^{cre/+}$;*R26*$^{mTmG/+}$ embryos at 0, 2 and 4 days of culture. GFP (green) marks *Tbx18*$^{+}$ cells and their descendants, RFP (red) marks all other cells in the explants. a: adrenal; k: kidney; u: ureter; ut: ureter tip. (For interpretation of the references to color in this figure legend, the reader is referred to the web version of this article.)

at both stages and the exclusion from SF1^{+} cells (Fig. 1I,R). Hence, *Tbx18* is expressed transiently in the coelomic epithelium and in a mesenchymal subdomain of the urogenital ridge.

Tbx18 is expressed in a mesenchymal subregion of the metanephric field before it is restricted to the ureteric mesenchyme

Our previous work showed that during metanephric development *Tbx18* is expressed in a narrow band of mesenchymal cells abutting the mesenchyme of the Wolffian duct and the metanephric kidney at E11.5 before expression becomes confined to the mesenchyme surrounding the ureter from E12.5 onwards (Airik et al., 2006). To determine the onset of *Tbx18* expression in the mesenchymal cells of the metanephric anlage (the metanephric field) and define the relationship to the precursor populations of known metanephric cell lineages, we performed *in situ* hybridization analysis of whole kidney rudiments as well as of adjacent sections through the posterior trunk at E10.5 and E11.5. At each stage, we compared expression of *Tbx18* to that of *Foxd1*, a marker for the stromal lineage of the metanephros (Hatini et al., 1996), to that of *Uncx*, a marker for the cap mesenchyme (Karner et al., 2011), to *Pax2* which marks the cap mesenchyme as well as the Wolffian duct and its epithelial outgrowths (Dressler et al., 1990), and to *Osr1* (Mugford et al., 2008; So and Danielian, 1999).

At E10.5, *Osr1* expression encompassed the mutually exclusive domains of *Tbx18* and *Uncx*/*Pax2*. Expression of *Foxd1* was scarcely detectable at this stage. At E11.5, *Foxd1* expression surrounded in a circle-like fashion the cap mesenchyme that was positive for *Osr1*, *Uncx* and *Pax2*. *Tbx18* expression surrounded the ureter stalk in an exclusive fashion. At E12.5, *Tbx18* was restricted to the mesenchyme surrounding the distal ureter whereas expression of *Foxd1* and *Uncx*/*Pax2*/*Osr1* was restricted to the stromal and the cap mesenchyme of the kidney, respectively (Fig. 2A). Immunofluorescence analysis of GFP (visualizing TBX18) and FOXD1/UNCX expression on transverse sections of E10.5 and E11.5 *Tbx18*$^{GFP/+}$ embryos confirmed that TBX18 protein was not co-expressed with either of these markers (Fig. 2B). These data show that *Tbx18* expression defines a molecularly distinct sub-population of mesenchymal cells in the early metanephric field.

Tbx18^{+} *cells of the urogenital ridge and the early metanephric field contribute to multiple components of the mature urogenital system*

To determine the contribution of *Tbx18*$^{+}$ cells in the urogenital ridge and the early metanephric field to the components of the mature urogenital system, we irreversibly labeled the descendants of these populations using a *cre*/*loxP*-based genetic approach with a *Tbx18*^{cre}-line generated in our laboratory and the sensitive *Rosa26*^{mTmG} reporter (Muzumdar et al., 2007; Trowe et al., 2010). In the *Rosa26*^{mTmG} reporter line cells that have undergone recombination express membrane-bound GFP while non-recombined cells express membrane-bound RFP.

In E18.5 and 3-week old whole urogenital systems, GFP epifluorescence was found in the gonads, the kidneys, the ureters,

the bladder and additionally in the adrenals that are associated with the urogenital system (Fig. 3A–C). To characterize the contribution of *Tbx18*$^{+}$ descendants to the differentiated cell types in these organs, we performed co-immunofluorescence analysis with antibodies directed against GFP and cell-type specific markers on sections of E18.5 *Tbx18*$^{cre/+}$;*Rosa26*$^{mTmG/+}$ embryos. In the testis, GFP expression was found in the tunica albuginea, interstitium and testis cords in a dorsal to ventral gradient (Fig. 3D). Coexpression analysis with cell-type specific markers showed that *Tbx18*$^{+}$ descendants contributed to Leydig cells in the interstitium (SF1) (Luo et al., 1994), to most but not all Sertoli cells (SOX9) (Morais da Silva et al., 1996), to smooth muscle cells of the tunica albuginea (ACTA2) but not to germ cells (DDX4) (Fujiwara et al., 1994) (Fig. 3E–I). In adrenals, GFP^{+} cells were restricted to the SF1^{+} steroidogenic cells of the cortex (Luo et al., 1994) (Fig. 3J–L). Compatible with the notion that *Tbx18*$^{+}$ descendants contribute to steroidogenic cells of the gonad and the adrenal gland, we observed coexpression of the lineage marker GFP with SF1, a marker for the adrenogonadal precursor pool (Bingham et al., 2006), in the coelomic lining of E10.5 *Tbx18*$^{cre/+}$;*Rosa26*$^{mTmG/+}$ embryos (Supplementary Fig. S1).

In E18.5 kidneys, the distribution of GFP expression appeared graded being more prominent at the medial (where *Tbx18*$^{+}$ cells originally resided) than at the lateral side of the organ (Fig. 3M). In the medial region of the kidney, GFP expression was excluded from cells expressing the epithelial marker CDH1 (Vestweber et al., 1985), the endothelial marker EMCN (Morgan et al., 1999), and the cap mesenchyme marker SIX2 (Karner et al., 2011; Self et al., 2006) indicating that *Tbx18*$^{+}$ descendants do not contribute to the collecting duct system, the endothelial network of the kidney, or the nephron lineage, respectively (Fig. 3N–P). Coexpression in the cortical stroma with FOXD1 and with the smooth muscle marker ACTA2 in arteries and in glomeruli argue that a substantial fraction of interstitial cells, vascular smooth muscle and mesangial cells in the medial kidney region derive from *Tbx18*$^{+}$ progenitors (Fig. 3Q–S). In the ureter, all cells of the mesenchymal coating (fibroblasts of the lamina propria, smooth muscle cells and adventitial fibroblasts) expressed GFP confirming earlier results

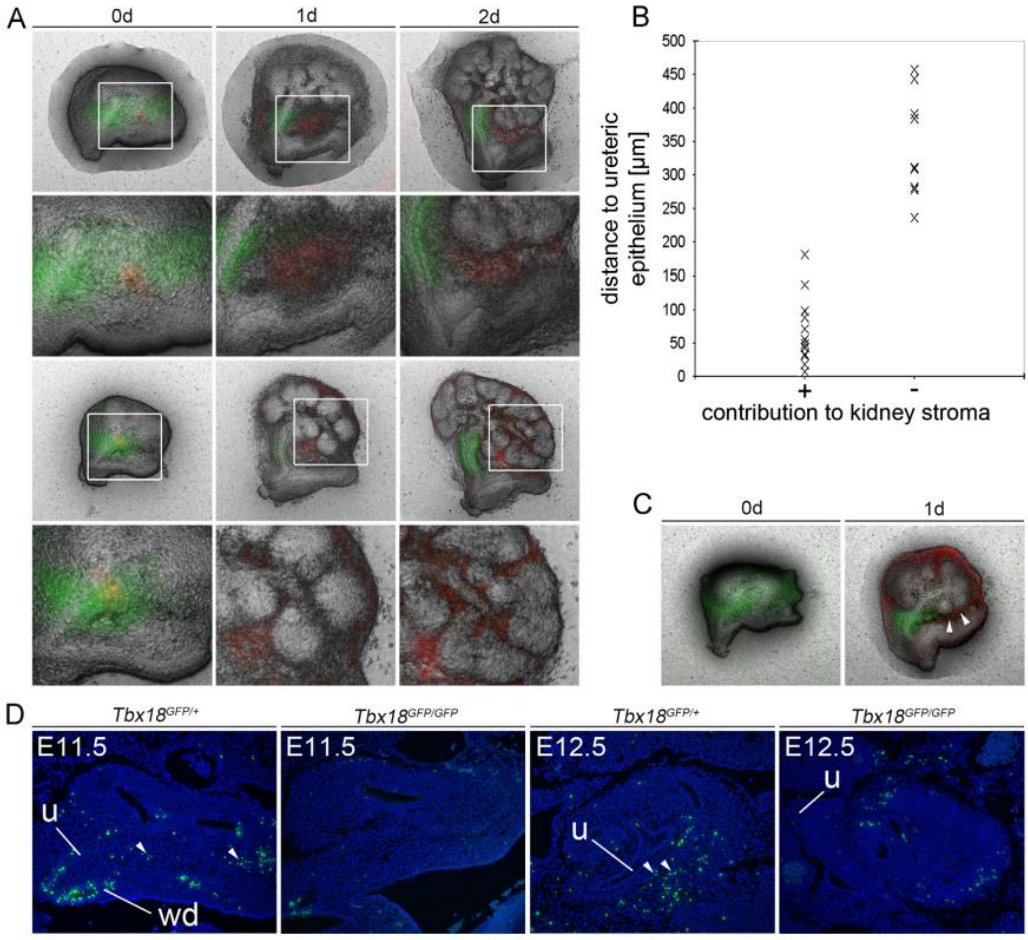

Fig. 5. Lineage analysis and apoptosis of *Tbx18*$^{+}$ mesenchymal cells in early kidney rudiments. (A) Combined brightfield and epifluorescence analysis of metanephric explants from E11.5 *Tbx18*$^{GFP/+}$ embryos at 0, 1 and 2 days of culture. GFP (green) marks the *Tbx18* expression domain, the red fluorescence indicates DiI-injected cell clusters. Shown are two representative examples of DiI-injected cells ending up in the renal stroma (upper row), and of cells localizing to the space between kidneys and the Wolffian duct (lower row). Boxed regions are shown in higher magnifications below. (B) Quantitative evaluation of localization of DiI-injected cells in dependence from the distance from the ureteric epithelium at E11.5. (C) Analysis of cell death by lysotracker staining in explants of E11.5 kidney rudiments from *Tbx18*$^{GFP/+}$ embryos cultured for 0 and 1 day. Arrows point to cell death in the lateral ureteric mesenchyme. (D) Analysis of cell death by the TUNEL assay in E11.5 and E12.5 kidneys rudiments from *Tbx18*$^{GFP/+}$ and *Tbx18*$^{GFP/GFP}$ embryos. Arrows point to cell death in the lateral ureteric mesenchyme. u, ureter; Wd, Wolffian duct. (For interpretation of the references to color in this figure legend, the reader is referred to the web version of this article.)

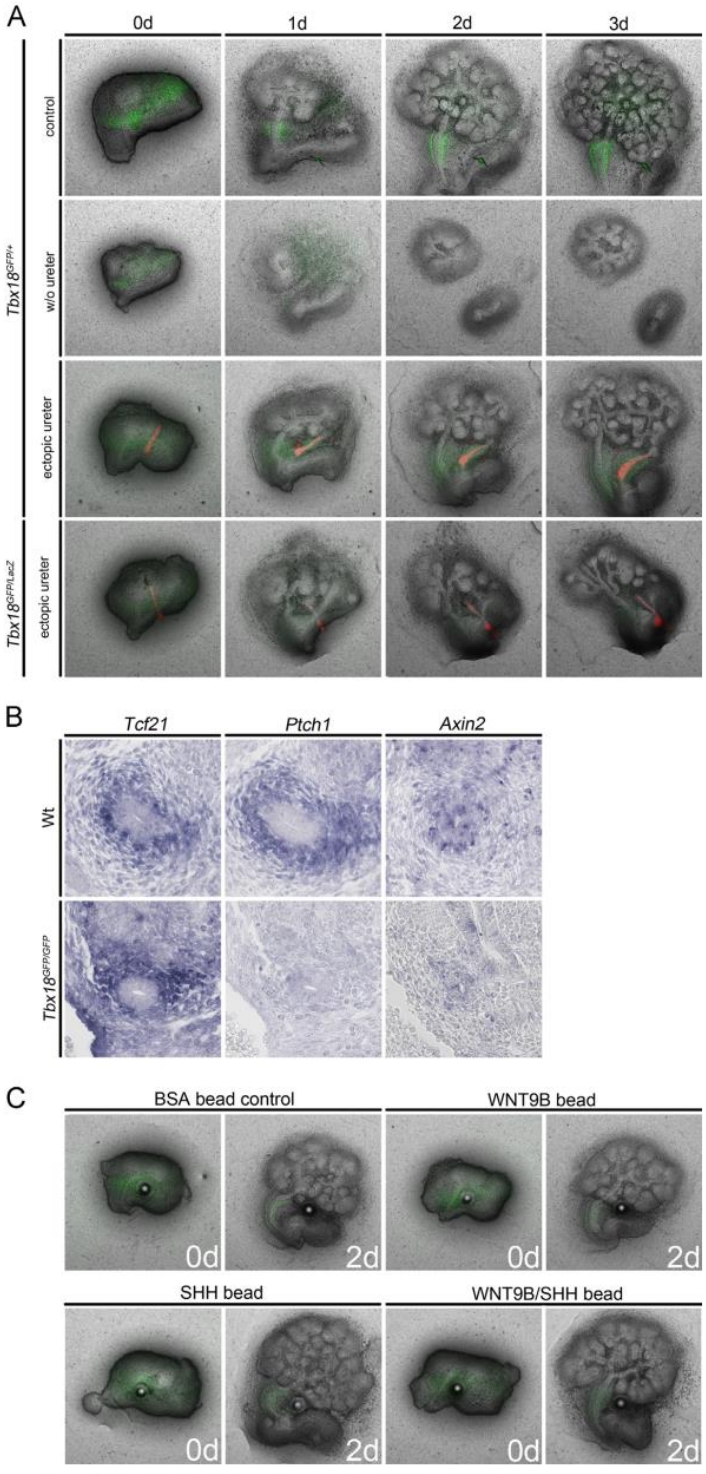

Fig. 6. Regulation of *Tbx18* expression and ureteric fates by signals from the ureteric epithelium. (A) Combined brightfield and GFP/RFP epifluorescence analysis of E11.5 metanephric explants from E11.5 $Tbx18^{GFP/+}$ embryos at 0, 1, 2 and 3 days of culture; GFP (green) marks $Tbx18^{+}$ cells in unmanipulated cultures (control), in cultures from which the ureter was removed (w/o ureter); after transplantation of an RFP^{+} (red) $R26^{mTmG/+}$ ureter stripped of mesenchymal cells into the distal domain of $Tbx18^{+}$ cells (ectopic ureter) in $Tbx18^{GFP/+}$ and $Tbx18^{GFP/GFP}$ rudiments. (B) *In situ* hybridization analysis of transverse ureter sections of E12.5 control (wt) and $Tbx18^{GFP/GFP}$ embryos of expression of *Tcf21*, of the target of SHH-signaling, *Ptch1*, and of the target of canonical WNT-signaling, *Axin2*. (C) GFP epifluorescence analysis of explants from E11.5 $Tbx18^{GFP/+}$ embryos cultured for 0 and 2 days in the presence of BSA-, WNT9B-, SHH- or WNT9B/SHH-soaked beads. (For interpretation of the references to color in this figure legend, the reader is referred to the web version of this article.)

of our group that the ureteric mesenchyme completely derives from *Tbx18*$^{+}$ mesenchymal cells (Fig. 3T–V) (Trowe et al., 2012). In the bladder, GFP expression was graded from dorsal to ventral within the smooth muscle cell layer but was absent from the urothelium (Fig. 3W–Y).

We conclude, that *Tbx18*$^{+}$ cells in the developing urogenital system are multipotent and contribute to all mesenchymal cell types in the ureter but also to a large degree to the stromal, mesangial and smooth muscle cells of the medial region of the kidney, to the bladder mesenchyme, to the cortical steroidogenic cells of the adrenal gland and to somatic cells of the gonads.

Tbx18 is required for ureteric differentiation of mesenchymal cells

Our previous analysis has shown that *Tbx18* is required for differentiation of the ureteric mesenchyme into smooth muscle cells but has not addressed a critical involvement of the gene in the development of the other organs of the urogenital system, to which *Tbx18*$^{+}$ descendants largely contribute. We, therefore, analyzed *Tbx18*-deficient embryos (*Tbx18*$^{cre/lacZ}$;*R26*$^{mTmG/+}$) at E18.5, *i.e.* shortly before these mice die due to skeletal defects, for histological and molecular changes in the development of these organs. Analysis of the adrenal gland by histological staining, co-immunofluorescence of the lineage marker GFP and the marker of steroidogenic cells SF1, and quantification of GFP^{+} cells in the cortex did not detect any difference in the distribution and differentiation of *Tbx18*$^{+}$ descendants in wildtype and *Tbx18*-deficient adrenals at this stage. Expression of *Akr1c18* and *Cyp11b1*, markers of the inner cortical layer (Lalli, 2010), and of *Wnt-4*, a marker of the outer cortical layer (Heikkila et al., 2002), was unaffected in the mutant showing that zonation into medulla and inner and outer cortex occurred normally (Supplementary Fig. S2). Histological staining and co-expression analysis with subsequent quantification of the previously used differentiation markers SOX9 (Sertoli cells), DDX4 (germ cells), and SF1 (Leydig cells) did not detect any difference between wildtype and *Tbx18*-deficient testes at this stage either (Supplementary Fig. S3). Differentiation of mesenchymal and epithelial lineages was also unaffected in the bladder and the kidney in the absence of *Tbx18* (Supplementary Figs. S4,S5).

However, in the kidney, the contribution of GFP^{+} cells to both the medullary and cortical stroma on the lateral side was enhanced, whereas the few GFP^{+} cells of the ureter failed to differentiate into smooth muscle cells (Fig. 4A–C). *In situ* hybridization of the lineage marker *Gfp* on sections of kidneys of earlier stages revealed that *Tbx18*$^{+}$ descendants dislocalized laterally onto the kidney as early as E12.5 (Fig. 4D). To further visualize the altered contribution to stromal cells in *Tbx18*-deficient kidneys, we explanted E11.5 metanephric rudiments and followed the GFP epifluorescence in culture (Fig. 4E). In the control (*Tbx18*$^{cre/+}$;*R26*$^{mTmG/+}$) GFP^{+} cells localized to the ureteric mesenchyme and the stromal cells of the kidney particularly those of the medial cortex. In *Tbx18*-deficient embryos (*Tbx18*$^{cre/lacZ}$;*R26*$^{mTmG/+}$), GFP expression was reduced around the short ureter but strongly enhanced in the medullary stroma around the distorted pelvic region. Of note, GFP^{+} cells now surrounded branching ureteric epithelium unlike in the control (Fig. 4E). We conclude from this analysis that *Tbx18* is required in uncommitted precursor cells to adopt the ureteric fate. In absence of *Tbx18* these cells contribute to the renal stroma.

A spatially restricted subset of Tbx18^{+} *mesenchymal cells contributes to the definite ureteric mesenchyme after E11.5*

As *Tbx18* is exclusively required within the ureteric mesenchymal lineage, we wished to learn about the mechanisms that confine *Tbx18* expression in the early metanephric field, and suppress the stromal in favor of the ureteric mesenchymal fate. To determine whether *Tbx18*$^{+}$ cells of the early metanephric field contribute randomly or in a spatially defined manner to the ureteric mesenchyme, we isolated kidney rudiments of E11.5 *Tbx18*$^{GFP/+}$ embryos and explanted them onto filter membranes. The red fluorescent dye DiI was injected at defined distances from the ureteric epithelium onto small cell clusters within the *Tbx18*$^{+}$ domain (as visualized by GFP fluorescence from the *Tbx18*^{GFP} allele) and the distribution of the red fluorescence was determined after 2 days (Fig. 5A, Supplementary Fig. S6). Two outcomes were observed: DiI injected into mesenchymal cells in a distance of up to 200 μm from the ureteric epithelium contributed to the kidney stroma whereas DiI injected more distally ended up as an amorphous mass in between the Wolffian duct and the kidney. Localization of DiI^{+} cells to the GFP^{+} ureteric mesenchyme was never observed (Fig. 5B). Lysotracker staining of E11.5 metanephric rudiments explanted for 1 day detected apoptotic cells in the lateral domain of the ureteric mesenchyme that had lost *Tbx18* expression at this time but not in those adjacent to the ureteric epithelium (Fig. 5C). To exclude a culture artefact, we also analyzed apoptosis by TUNEL staining in sections of E11.5 and E12.5 embryos. At both stages we detected apoptosis in mesenchymal cells lateral to but not adjacent to the short ureter stalk. Intriguingly, apoptosis in this domain was completely lost in *Tbx18*-deficient embryos (Fig. 5D).

We conclude that only a minor fraction of the mesenchymal cells initially positive for *Tbx18* contribute to the definite ureteric mesenchyme, most likely those in direct proximity to the epithelium (that we were unable to label by this technique). Cells within a 200-μm range of the ureteric epithelium contribute to the kidney stroma whereas cells further away undergo apoptosis. In *Tbx18*-deficient embryos, lateral *Tbx18*$^{+}$ descendants fail to undergo apoptosis but may additionally contribute to the renal stroma.

Epithelial signals impose a ureteric fate onto Tbx18^{+} *cells*

Given the finding that only cells in direct vicinity of the ureteric epithelium are likely to contribute to the definitive ureteric mesenchyme, we wished to test the role of epithelial signals in maintaining *Tbx18* expression and directing a ureteric fate to cells in the early metanephric field, and performed tissue recombination experiments in cultured explants of metanephric rudiments of E11.5 *Tbx18*$^{GFP/+}$ embryos (Fig. 6A). In a control experiment, GFP expression was confined to the mesenchymal tissue layer covering the ureteric epithelium after 3 days of culture. Removal of the ureter from E11.5 kidney explants resulted in a dispersal of GFP^{+} cells and their complete loss after 3 days. We then transplanted an RFP-labeled ureteric epithelium (obtained from E12.5 *R26*$^{mTmG/+}$ embryos) into the *Tbx18*$^{+}$ domain in a position distant from the ureteric epithelium of the host tissue. Interestingly, GFP expression was maintained in the lateral mesenchyme and GFP^{+} cells accumulated around the ectopic RFP^{+} ureteric epithelium. In contrast, when a RFP-labeled ureteric epithelium was transplanted into the lateral GFP^{+} domain of kidney explants of E11.5 *Tbx18*$^{GFP/lacZ}$ embryos, GFP^{+} cells did not accumulate around the ectopic ureter (Fig. 6A). Together, these results strongly suggest that epithelial signals are required and sufficient to maintain *Tbx18* expression and to impose a ureteric fate onto *Tbx18*$^{+}$ cells. Epithelial signals do not act in a distance to induce a condensation process but merely seem to impinge onto the adjacent layer of mesenchymal cells. In absence of *Tbx18*, mesenchymal cells can no longer respond to signals from the ureteric epithelium.

We have recently shown that canonical (*Ctnnb1*-dependent) WNT signaling is required to maintain *Tbx18* expression and induce smooth muscle differentiation in the ureteric mesenchyme

(Trowe et al., 2012). The latter process also requires SHH signals from the epithelial compartment (Yu et al., 2002). In *Tbx18*-deficient ureters, *Tcf21*$^{+}$-mesenchymal cells surrounding the ureter did not express *Axin2* and *Ptch1*, targets of the canonical WNT- and SHH-signals that are secreted from the epithelial compartment in the mutant (Fig. 6B). We conclude that *Tbx18* is required in uncommitted precursor cells to respond to epithelial signals and to adopt the ureteric fate.

To address the question whether WNT and/or SHH signals are sufficient to maintain *Tbx18* expression in the lateral domain in which it is lost after E11.5, we explanted E11.5 kidney rudiments and implanted beads soaked with SHH and/or WNT9B protein (*Wnt9b* is co-expressed with *Wnt7b* in the ureteric epithelium) into this domain (Trowe et al., 2012). Neither BSA control nor WNT9B-, SHH- or WNT9B/SHH-beads maintained GFP, *i.e. Tbx18* expression, in the lateral domain (Fig. 6C), arguing that WNTs cooperate with other as yet unknown epithelial signals to maintain *Tbx18* expression and possibly determine the ureteric fate.

Discussion

Tbx18^{+} *progenitors contribute to multiple cell types in the urogenital system*

We have demonstrated that descendants of *Tbx18*$^{+}$ cells contribute to a variety of cell types within the urogenital system including cells within the gonads, the kidney, ureter, bladder and adrenal gland. Our expression analysis together with the genetic lineage tracing of *Tbx18*$^{+}$ cells argue that cellular contribution to the adrenal gland and gonads on one hand and to the kidney, ureter and bladder on the other hand reflect two independent expression domains of *Tbx18*; one in the urogenital ridge and the other one in the metanephric field, and that the latter represents a novel subpool of progenitors from which the ureteric mesenchyme will eventually arise.

Transient expression in the epithelial lining of the urogenital ridge around E9.5 is likely to present a common precursor pool for the gonads and the adrenals. In fact, the contribution to interstitial, Sertoli and tunica albuginea cells in the gonad and steroidogenic cells of the adrenal cortex is virtually identical to that identified by a genetic approach based on expression of *Sf1*, a marker for this primordium (Bingham et al., 2006). *Tbx18* expression in the epithelial lining of the ridge is transient and seems to slightly precede that of *Sf1* in this domain. Compatible with expression in the unseparated progenitor pool for both tissues, we recently noted sex reversal and loss of adrenals in mice with conditional *Tbx18*^{cre}-mediated deletion of *Ctnnb1* (Trowe et al., 2012). In fact, identical phenotypes were observed upon an *Sf1*^{cre}-mediated deletion of this mediator of the canonical branch of WNT signaling in mice (Kim et al., 2008; Liu et al., 2009). At this point, we do not have the technical means to independently evaluate the contribution of the mesenchymal expression domain of *Tbx18* in the early urogenital ridge. However, since this domain does not overlap with *Pax2* in the mesonephros, we suggest that it does not mark progenitors for mesonephric tubules but for stromal cells that are associated with these structures.

In contrast to our initial expectations, we found that the *Tbx18*$^{+}$ cells that are located in the metanephric field between the mesenchymal populations of the metanephros and the Wolffian duct, are not yet specified to a ureteric mesenchymal fate but are a multipotent population that contributes to interstitial cells of the kidney (cortical and medullary stromal cells, mesangial cells and vascular smooth muscle cells), to all mesenchymal cells of the ureter and to a subset of smooth muscle cells of the bladder. Most notably, our expression analysis as well as the fate mapping clearly shows that the *Tbx18*$^{+}$ lineage is at all time points separated from the *Six2*$^{+}$*Uncx*$^{+}$ progenitors from which nephrons will develop. *Tbx18* expression does not overlap with the stromal marker *Foxd1* at E11.5. However, *Foxd1* is not expressed at E10.5 in the metanephric field strongly suggesting that *Tbx18* expression at this stage encompasses progenitors of renal stromal cells as well as of the ureteric mesenchyme. Hence, within the *Osr1*$^{+}$ metanephric field two lineages are established at E10.5: the *Six2*$^{+}$*Uncx*$^{+}$ nephron lineage and the *Tbx18*$^{+}$ lineage of kidney stromal cells/ureter and bladder mesenchyme. Between E10.5 and E11.5 the *Tbx18*$^{+}$ and *Foxd1*$^{+}$ lineages are completely separated. *Tbx18*$^{+}$ cells lying in direct proximity to the ureteric epithelium will maintain *Tbx18* and differentiate into all mesenchymal cell types of the ureter. Cells which loose *Tbx18* expression will either die or contribute to the renal stroma and the bladder mesenchyme. Due to lack of appropriate markers and adequate culture settings we cannot firmly state when the mesenchymal lineages of the ureter and bladder separate but assume that it occurs around the same time.

Tbx18-Cre cell lineage tracing with a BAC-based approach recently reported contribution of *Tbx18*$^{+}$ descendants to smooth muscle cells of the bladder and the ureter in the mature urogenital system. The more restricted contribution in this genetic setting may relate to a less sensitive detection system used but more likely reflects the lack of regulatory elements in the BAC used for construction of a *Tbx18–Cre* transgene (Wang et al., 2009). Our *Tbx18*^{cre} allele was constructed by inserting a *cre* orf into the start codon of the *Tbx18* locus (Trowe et al., 2010). Analysis of *cre* expression in the urogenital system as well as at extrarenal sites showed that expression of *cre* faithfully mimics endogenous expression of *Tbx18* strongly arguing that all control elements of *Tbx18* are preserved and direct appropriate expression of *cre* from this allele (Christoffels et al., 2009; Trowe et al., 2012). Furthermore, the sensitive *Rosa26*^{mTmG} reporter line allows a cellular resolution of all recombination events. Hence, we are convinced that our genetic lineage tracing system is technically sound and provides a true image of the widespread distribution of *Tbx18*$^{+}$ descendants in the urogenital system.

Tbx18^{+} *cells do not condense to form the definitive ureteric mesenchyme*

We previously suggested that the band of *Tbx18*$^{+}$ mesenchymal cells in the E11.5 metanephric field condenses around the ureteric epithelium to form the definite ureteric mesenchyme until E12.5. Our genetic lineage tracings as well as our DiI injection in the *Tbx18*$^{+}$ domain at E11.5 contradict this "condensation" model but suggest that only a minor fraction of the cells initially positive for *Tbx18* become the precursors for smooth muscle cells and fibroblasts of the ureter. In fact, the majority of cells in this domain switch off *Tbx18* expression, and depending on the distance from the ureter contribute to the kidney stroma (the more proximal ones) or localize to the tissue in between the kidney and the Wolffian duct (the more distal ones). The latter population undergoes apoptosis, a process that may aid in severing the connections between the two organs. Only the few cells in proximity to the ureteric epithelium maintain *Tbx18* expression. Our further experiments suggest that the ureteric mesenchyme is specified between E11.5 and E12.5 by signals from the ureteric epithelium. Data from canonical WNT pathway manipulation presented in this study as well in a recent report from our lab strongly suggest that WNT signals are required to maintain but are not sufficient to induce *Tbx18* expression (Trowe et al., 2012). We suggest that other signals from the epithelium, but not SHH, cooperate with WNT signals to maintain *Tbx18* expression and specify a ureteric fate to allow further differentiation of ureteric fibroblasts and smooth muscle cells.

Our analysis of *Tbx18*-deficient embryos has shown that *Tbx18* is not required for development of any of the components of the urogenital system except the ureter. *Tbx18* seems to act in a sub-pool of mesenchymal precursors of the metanephric field to favor a ureteric at the expense of a renal stromal fate. Since target genes for signals from the ureteric epithelium (*i.e.* SHH and WNTs) are not activated in *Tbx18*-deficient cells, we suggest that *Tbx18* acts as a prepatterning gene to make the cells competent to receive signals emanating from the epithelial compartment. However, our analysis has also shown that transient *Tbx18* expression in mesenchymal cells of the early metanephric field is required to induce apoptosis in the lateral domain to avoid the formation of ectopic ligaments between the gonads, the kidney and the ureter as observed in *Tbx18*-deficient urogenital systems.

Acknowledgments

This work was supported by a grant from the Deutsche Forschungsgemeinschaft (German Research Foundation) to A.K. (DFG Ki728/7-1). We would like to thank Rolf Kemler, Andrew P. McMahon, Dietmar Vestweber, Tamara Rabe and Ahmed Mansouri for antibodies.

Appendix A. Supporting information

Supplementary data associated with this article can be found in the online version at http://dx.doi.org/10.1016/j.ydbio.2013.04.036.

References

Airik, R., Bussen, M., Singh, M.K., Petry, M., Kispert, A., 2006. Tbx18 regulates the development of the ureteral mesenchyme. J. Clin Invest. 116, 663–674.
Airik, R., Trowe, M.O., Foik, A., Farin, H.F., Petry, M., Schuster-Gossler, K., Schweizer, M., Scherer, G., Kist, R., Kispert, A., 2010. Hydroureternephrosis due to loss of Sox9-regulated smooth muscle cell differentiation of the ureteric mesenchyme. Hum. Mol. Genet. 19, 4918–4929.
Bingham, N.C., Verma-Kurvari, S., Parada, L.F., Parker, K.L., 2006. Development of a steroidogenic factor 1/Cre transgenic mouse line. Genesis 44, 419–424.
Boyle, S., Misfeldt, A., Chandler, K.J., Deal, K.K., Southard-Smith, E.M., Mortlock, D.P., Baldwin, H.S., de Caestecker, M., 2008. Fate mapping using Cited1-CreERT2 mice demonstrates that the cap mesenchyme contains self-renewing progenitor cells and gives rise exclusively to nephronic epithelia. Dev. Biol. 313, 234–245.
Brenner-Anantharam, A., Cebrian, C., Guillaume, R., Hurtado, R., Sun, T.T., Herzlinger, D., 2007. Tailbud-derived mesenchyme promotes urinary tract segmentation via BMP4 signaling. Development 134, 1967–1975.
Bussen, M., Petry, M., Schuster-Gossler, K., Leitges, M., Gossler, A., Kispert, A., 2004. The T-box transcription factor Tbx18 maintains the separation of anterior and posterior somite compartments. Genes Dev. 18, 1209–1221.
Christoffels, V.M., Grieskamp, T., Norden, J., Mommersteeg, M.T., Rudat, C., Kispert, A., 2009. Tbx18 and the fate of epicardial progenitors. Nature 458, E8–E9; discussion E9-10.
Christoffels, V.M., Mommersteeg, M.T., Trowe, M.O., Prall, O.W., de Gier-de Vries, C., Soufan, A.T., Bussen, M., Schuster-Gossler, K., Harvey, R.P., Moorman, A.F., Kispert, A., 2006. Formation of the venous pole of the heart from an Nkx2-5-negative precursor population requires Tbx18. Circ. Res. 98, 1555–1563.
Dressler, G.R., Deutsch, U., Chowdhury, K., Nornes, H.O., Gruss, P., 1990. Pax2, a new murine paired-box-containing gene and its expression in the developing excretory system. Development 109, 787–795.
Fujiwara, Y., Komiya, T., Kawabata, H., Sato, M., Fujimoto, H., Furusawa, M., Noce, T., 1994. Isolation of a DEAD-family protein gene that encodes a murine homolog of Drosophila vasa and its specific expression in germ cell lineage. Proc. Natl. Acad. Sci. USA 91, 12258–12262.
Gao, X., Chen, X., Taglienti, M., Rumballe, B., Little, M.H., Kreidberg, J.A., 2005. Angioblast-mesenchyme induction of early kidney development is mediated by Wt1 and Vegfa. Development 132, 5437–5449.
Grote, D., Souabni, A., Busslinger, M., Bouchard, M., 2006. Pax 2/8-regulated Gata 3 expression is necessary for morphogenesis and guidance of the nephric duct in the developing kidney. Development 133, 53–61.
Guillaume, R., Bressan, M., Herzlinger, D., 2009. Paraxial mesoderm contributes stromal cells to the developing kidney. Dev. Biol. 329, 169–175.
Hatano, O., Takakusu, A., Nomura, M., Morohashi, K., 1996. Identical origin of adrenal cortex and gonad revealed by expression profiles of Ad4BP/SF-1. Genes Cells 1, 663–671.
Hatini, V., Huh, S.O., Herzlinger, D., Soares, V.C., Lai, E., 1996. Essential role of stromal mesenchyme in kidney morphogenesis revealed by targeted disruption of Winged Helix transcription factor BF-2. Genes Dev. 10, 1467–1478.
Heikkila, M., Peltoketo, H., Leppaluoto, J., Ilves, M., Vuolteenaho, O., Vainio, S., 2002. Wnt-4 deficiency alters mouse adrenal cortex function, reducing aldosterone production. Endocrinology 143, 4358–4365.
Humphreys, B.D., Lin, S.L., Kobayashi, A., Hudson, T.E., Nowlin, B.T., Bonventre, J.V., Valerius, M.T., McMahon, A.P., Duffield, J.S., 2010. Fate tracing reveals the pericyte and not epithelial origin of myofibroblasts in kidney fibrosis. Am. J. Pathol. 176, 85–97.
Ikeda, Y., Shen, W.H., Ingraham, H.A., Parker, K.L., 1994. Developmental expression of mouse steroidogenic factor-1, an essential regulator of the steroid hydroxylases. Mol. Endocrinol. 8, 654–662.
James, R.G., Kamei, C.N., Wang, Q., Jiang, R., Schultheiss, T.M., 2006. Odd-skipped related 1 is required for development of the metanephric kidney and regulates formation and differentiation of kidney precursor cells. Development 133, 2995–3004.
Karner, C.M., Das, A., Ma, Z., Self, M., Chen, C., Lum, L., Oliver, G., Carroll, T.J., 2011. Canonical Wnt9b signaling balances progenitor cell expansion and differentiation during kidney development. Development 138, 1247–1257.
Keegan, C.E., Hammer, G.D., 2002. Recent insights into organogenesis of the adrenal cortex. Trends Endocrinol. Metab. 13, 200–208.
Kim, A.C., Reuter, A.L., Zubair, M., Else, T., Serecky, K., Bingham, N.C., Lavery, G.G., Parker, K.L., Hammer, G.D., 2008. Targeted disruption of beta-catenin in Sf1-expressing cells impairs development and maintenance of the adrenal cortex. Development 135, 2593–2602.
Kobayashi, A., Valerius, M.T., Mugford, J.W., Carroll, T.J., Self, M., Oliver, G., McMahon, A.P., 2008. Six2 defines and regulates a multipotent self-renewing nephron progenitor population throughout mammalian kidney development. Cell Stem Cell 3, 169–181.
Kraus, F., Haenig, B., Kispert, A., 2001. Cloning and expression analysis of the mouse T-box gene Tbx18. Mech. Dev. 100, 83–86.
Lalli, E., 2010. Adrenal cortex ontogenesis. Best Pract. Res. Clin. Endocrinol. Metab. 24, 853–864.
Levinson, R.S., Batourina, E., Choi, C., Vorontchikhina, M., Kitajewski, J., Mendelsohn, C.L., 2005. Foxd1-dependent signals control cellularity in the renal capsule, a structure required for normal renal development. Development 132, 529–539.
Little, M.H., McMahon, A.P., 2012. Mammalian kidney development: principles, progress, and projections. Cold Spring Harbor Perspect. Biol. 4.
Liu, C.F., Bingham, N., Parker, K., Yao, H.H., 2009. Sex-specific roles of beta-catenin in mouse gonadal development. Hum. Mol. Genet. 18, 405–417.
Luo, X., Ikeda, Y., Parker, K.L., 1994. A cell-specific nuclear receptor is essential for adrenal and gonadal development and sexual differentiation. Cell 77, 481–490.
Moorman, A.F., Houweling, A.C., de Boer, P.A., Christoffels, V.M., 2001. Sensitive nonradioactive detection of mRNA in tissue sections: novel application of the whole-mount *in situ* hybridization protocol. J. Histochem. Cytochem. 49, 1–8.
Morais da Silva, S., Hacker, A., Harley, V., Goodfellow, P., Swain, A., Lovell-Badge, R., 1996. Sox9 expression during gonadal development implies a conserved role for the gene in testis differentiation in mammals and birds. Nat. Genet. 14, 62–68.
Morgan, S.M., Samulowitz, U., Darley, L., Simmons, D.L., Vestweber, D., 1999. Biochemical characterization and molecular cloning of a novel endothelial-specific sialomucin. Blood 93, 165–175.
Mugford, J.W., Sipila, P., McMahon, J.A., McMahon, A.P., 2008. Osr1 expression demarcates a multi-potent population of intermediate mesoderm that undergoes progressive restriction to an Osr1-dependent nephron progenitor compartment within the mammalian kidney. Dev. Biol. 324, 88–98.
Muzumdar, M.D., Tasic, B., Miyamichi, K., Li, L., Luo, L., 2007. A global double-fluorescent Cre reporter mouse. Genesis 45, 593–605.
Neidhardt, L.M., Kispert, A., Herrmann, B.G., 1997. A mouse gene of the paired-related homeobox class expressed in the caudal somite compartment, and in the developing vertebral column, kidney and nervous system. Dev. Genes Evol. 207, 330–339.
Pedersen, A., Skjong, C., Shawlot, W., 2005. Lim 1 is required for nephric duct extension and ureteric bud morphogenesis. Dev. Biol. 288, 571–581.
Saxen, L., 1987. Organogenesis of the Kidney. Camridge University Press, Cambridge, UK.
Schneider, C.A., Rasband, W.S., Eliceiri, K.W., 2012. NIH image to image J: 25 years of image analysis. Nat. Methods 9, 671–675.
Self, M., Lagutin, O.V., Bowling, B., Hendrix, J., Cai, Y., Dressler, G.R., Oliver, G., 2006. Six2 is required for suppression of nephrogenesis and progenitor renewal in the developing kidney. EMBO J. 25, 5214–5228.
So, P.L., Danielian, P.S., 1999. Cloning and expression analysis of a mouse gene related to Drosophila odd-skipped. Mech. Dev. 84, 157–160.
Trowe, M.O., Airik, R., Weiss, A.C., Farin, H.F., Foik, A.B., Bettenhausen, E., Schuster-Gossler, K., Taketo, M.M., Kispert, A., 2012. Canonical Wnt signaling regulates smooth muscle precursor development in the mouse ureter. Development 139, 3099–3108.
Trowe, M.O., Shah, S., Petry, M., Airik, R., Schuster-Gossler, K., Kist, R., Kispert, A., 2010. Loss of Sox9 in the periotic mesenchyme affects mesenchymal expansion and differentiation, and epithelial morphogenesis during cochlea development in the mouse. Dev. Biol. 342, 51–62.

Vestweber, D., Kemler, R., Ekblom, P., 1985. Cell-adhesion molecule uvomorulin during kidney development. Dev. Biol. 112, 213–221.
Wang, C., Gargollo, P., Guo, C., Tang, T., Mingin, G., Sun, Y., Li, X., 2011. Six1 and Eya1 are critical regulators of peri-cloacal mesenchymal progenitors during genitourinary tract development. Dev. Biol. 360, 186–194.
Wang, Q., Lan, Y., Cho, E.S., Maltby, K.M., Jiang, R., 2005. Odd-skipped related 1 (Odd 1) is an essential regulator of heart and urogenital development. Dev. Biol. 288, 582–594.
Wang, Y., Tripathi, P., Guo, Q., Coussens, M., Ma, L., Chen, F., 2009. Cre/lox recombination in the lower urinary tract. Genesis 47, 409–413.
Wilkinson, D.G., Nieto, M.A., 1993. Detection of messenger RNA by *in situ* hybridization to tissue sections and whole mounts. Methods Enzymol. 225, 361–373.
Yu, J., Carroll, T.J., McMahon, A.P., 2002. Sonic hedgehog regulates proliferation and differentiation of mesenchymal cells in the mouse metanephric kidney. Development 129, 5301–5312.

Supplementary Figures

for

Tbx18 expression demarcates multipotent precursor populations in the developing urogenital system but is exclusively required within the ureteric mesenchymal lineage to suppress a renal stromal fate

Tobias Bohnenpoll[1], Eva Bettenhausen[1], Anna-Carina Weiss, Anna B. Foik, Mark-Oliver Trowe, Patrick Blank, Rannar Airik, and Andreas Kispert[*]

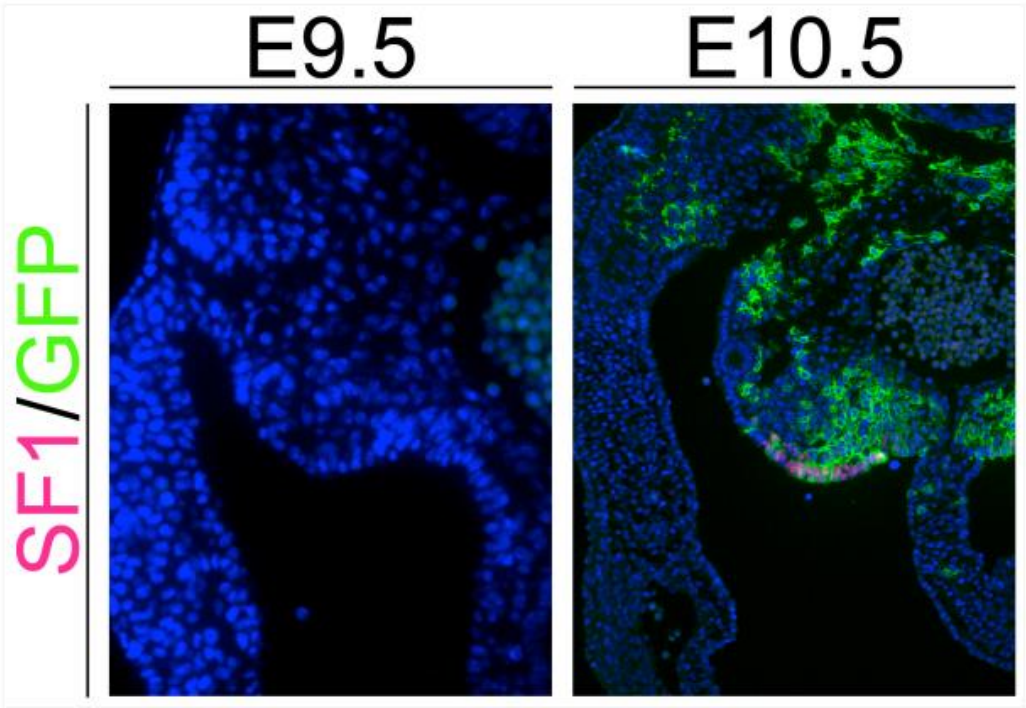

Supplementary Fig. S1. *Tbx18*$^{+}$-descendants are positive for SF1 in the coelomic lining at E10.5. (Co-)immunofluorescence analysis of expression of the lineage marker GFP (green) and the marker for the adrenogonadal primordium, SF1 (red), on transverse sections through the posterior trunk of E9.5 and E10.5 *Tbx18*$^{cre/+}$;*R26*$^{mTmG/+}$ embryos. At E9.5, SF1 protein is not yet expressed in the coelomic lining and recombination of the lineage reporter has not yet occurred. At E10.5, cells formerly positive for *Tbx18* in the coelomic lining express SF1.

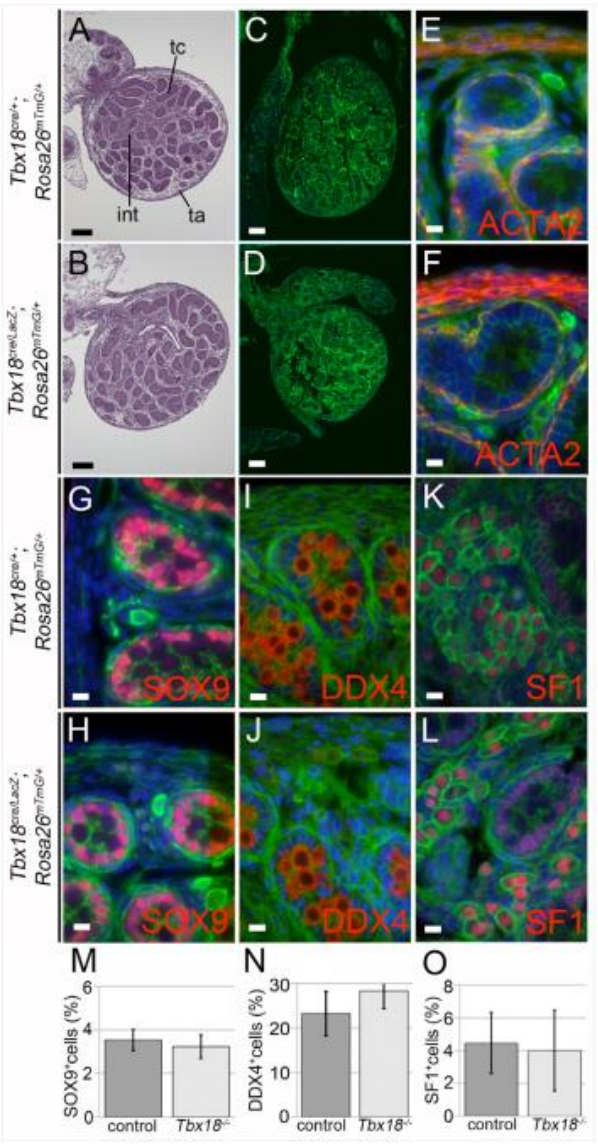

Supplementary Fig. S2. Loss of *Tbx18* does not affect testis development. (A,B) Histological analysis by haematoxylin and eosin staining of sagittal testis sections in E18.5 control (*Tbx18*$^{cre/+}$;*R26*$^{mTmG/+}$) and *Tbx18*-deficient embryos (*Tbx18*$^{cre/lacZ}$;*R26*$^{mTmG/+}$) does not detect changes of the testicular tissue organization. (C-L) (Co-)immunofluorescence analysis of expression of the lineage marker GFP and markers of differentiated cell types on sections of E18.5 testis does not detect changes in the number and distribution of smooth muscle cells of the capsule (ACTA2), of Sertoli cells (SOX9), of germ cells (DDX4) and of Leydig cells (SF1) between control and *Tbx18*-deficient embryos. Scale bars represent 100 µ m (A,B,C,D) and 10 µm (E-L). (M-O) Quantification of SOX9^{+} Sertoli cells, DDX4 germ cells and SF1^{+} Leydig cells in the testis. (M) SOX9^{+} cells/all cells in the counted area (in%), control: 3.5+/-0.5, mutant: 3.2+/-0.5 p=0.515. (N) DDX4^{+} cells/testis cord cells (somatic and germ cells) (in %). control: 23.3+/-5.0, mutant: 28.3+/-4.0 p=0.093. (O) SF1^{+} Leydig cells/all interstitial cells (in %), control: 4.5+/-1.9, mutant: 4.0+/-2.5 p=0.801.

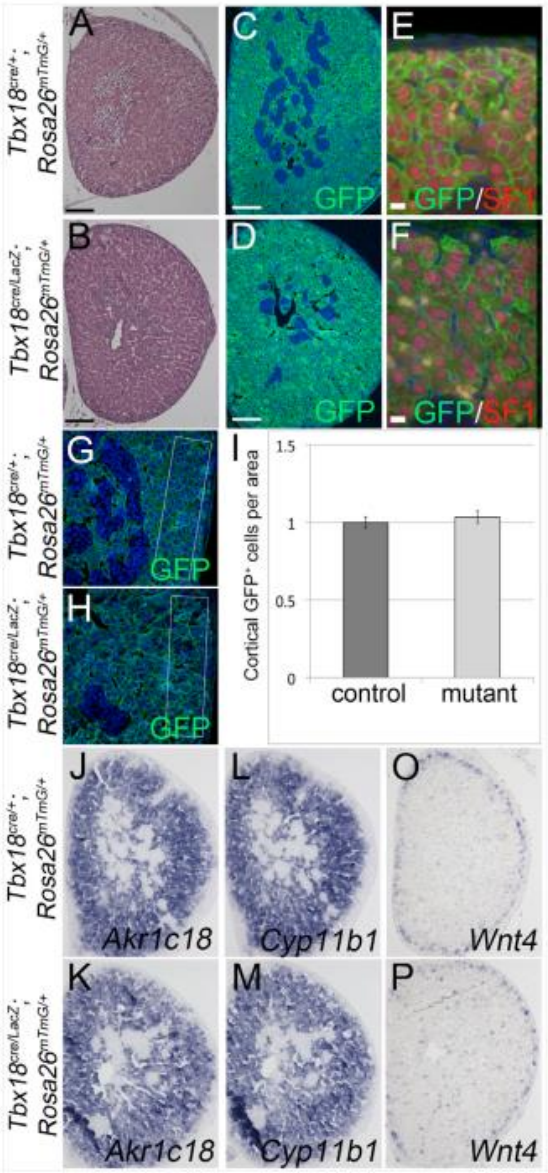

Supplementary Fig. S3. Loss of *Tbx18* does not affect adrenal development at E18.5. (A,D) Histological analysis by haematoxylin and eosin staining, (B,E) immunofluorescence analysis of expression of the lineage marker GFP, (C,F) co-immunofluorescence analysis of expression of the lineage marker GFP and of the steroidogenic marker SF1, on sections of control ($Tbx18^{cre/+};R26^{mTmG/+}$) and *Tbx18*-deficient embryos ($Tbx18^{cre/lacZ};R26^{mTmG/+}$) does not detect changes in adrenal development. Size bars represent 0.1 mm (A-D) and 10 µm (C,F). (G-I) Immunofluorescence analysis of cells expressing the lineage marker GFP in a defined cortical area and subsequent quantification of GFP^+ cells (control is set to 1) reveals unchanged contribution of $Tbx18^+$ descendants to the cortical area of the *Tbx18*-deficient adrenal gland. Control: 1+/-0.037, mutant: 1.034+/-0.04, p=0.26 (J-M) *In situ* hybridization analysis of markers of the inner cortical region shows normal zonation in the mutant adrenal gland. Genotypes, probes and antigens are as shown.

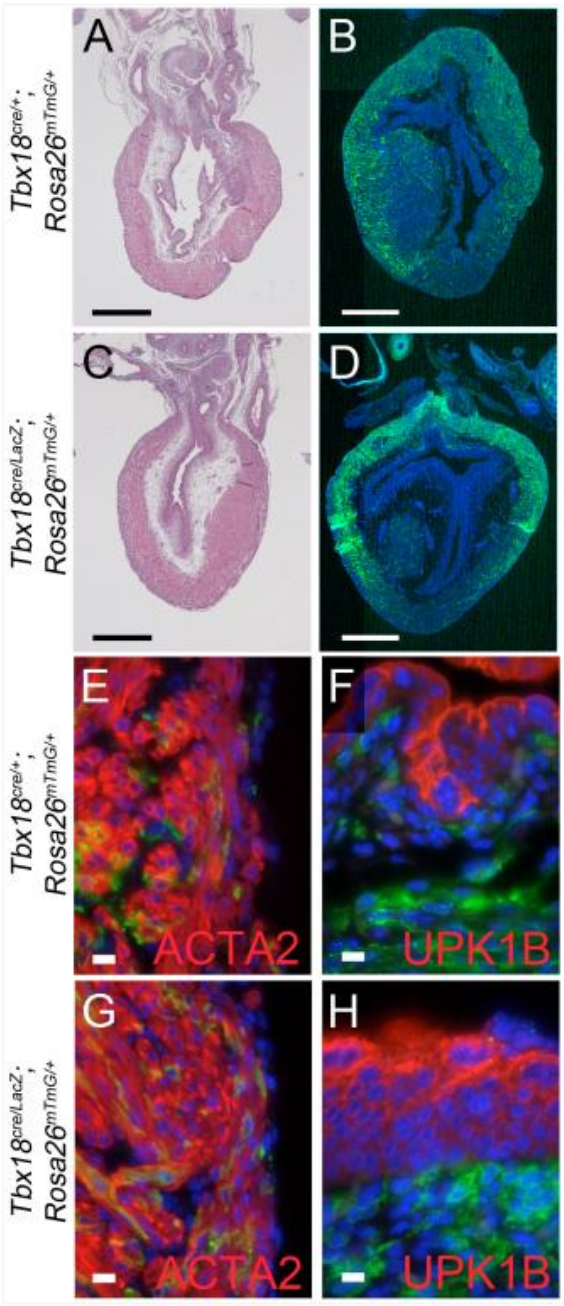

Supplementary Fig. S4. Loss of *Tbx18* does not affect bladder development. (A,C) Histological analysis by haematoxylin and eosin staining, (B,D) immunofluorescence analysis of expression of the lineage marker GFP, (E,G) co-immunofluorescence analysis of expression of the lineage marker GFP and the smooth muscle marker ACTA2, (F,H) co-immunofluorescence analysis of expression of the lineage marker GFP and of the urothelial marker UPK1B on sections of control (*Tbx18*$^{cre/+}$;*R26*$^{mTmG/+}$) and *Tbx18*-deficient embryos (*Tbx18*$^{cre/lacZ}$;*R26*$^{mTmG/+}$) does not detect changes in contribution of *Tbx18*$^{+}$ descendants and cellular differentiation in the bladder. Size bars represent 0.5 mm (A-D) and 10 µm (E-H).

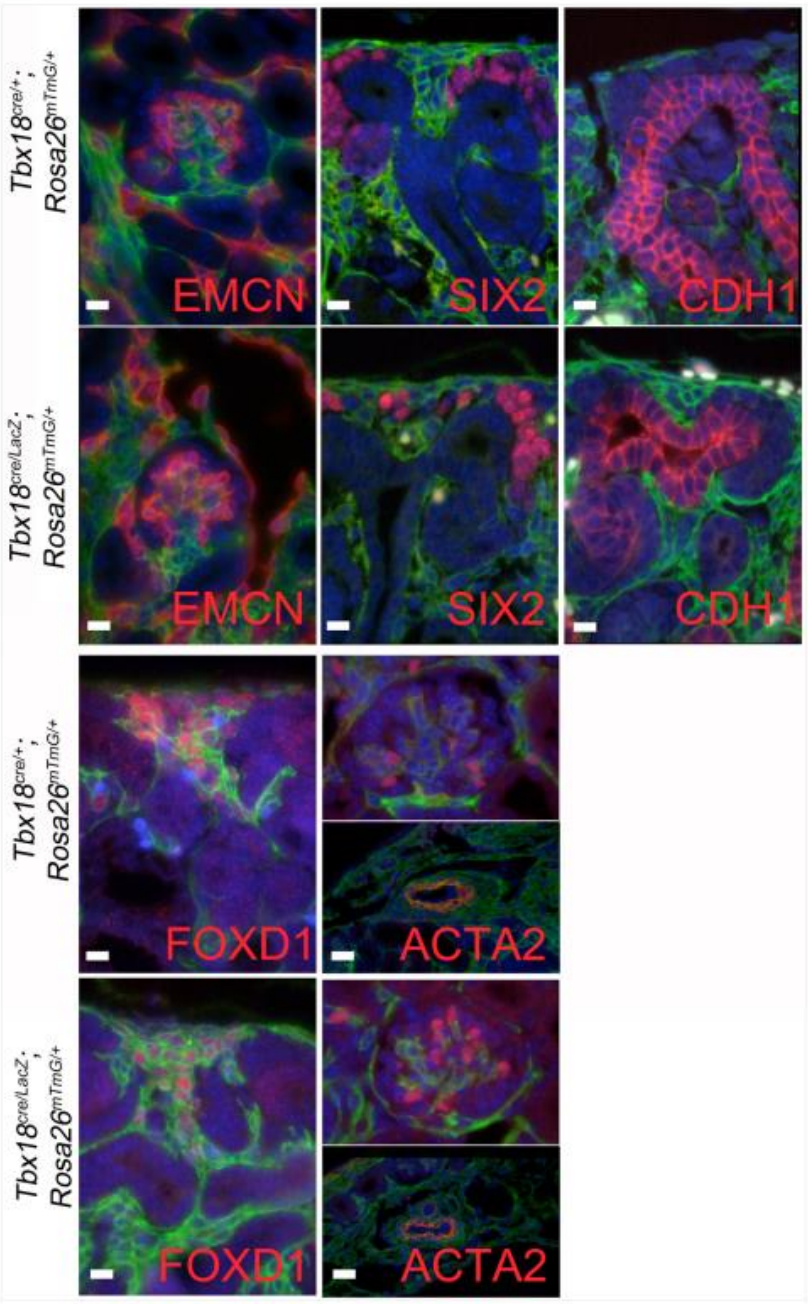

Supplementary Fig. S5. Loss of *Tbx18* does not affect differentiation of renal cell lineages. Co-immunofluorescence analysis of expression of the lineage marker GFP, with the endothelial marker EMCN, the cap mesenchyme marker SIX2, the epithelial marker CDH1, the cortical stroma marker FOXD1 and the smooth muscle marker ACTA2 on sections of control (*Tbx18*$^{cre/+}$;*R26*$^{mTmG/+}$) and *Tbx18*-deficient embryos (*Tbx18*$^{cre/lacZ}$;*R26*$^{mTmG/+}$) does not detect changes in contribution of *Tbx18*$^{+}$ descendants and cellular differentiation in the kidney. Size bars represent 10 µm.

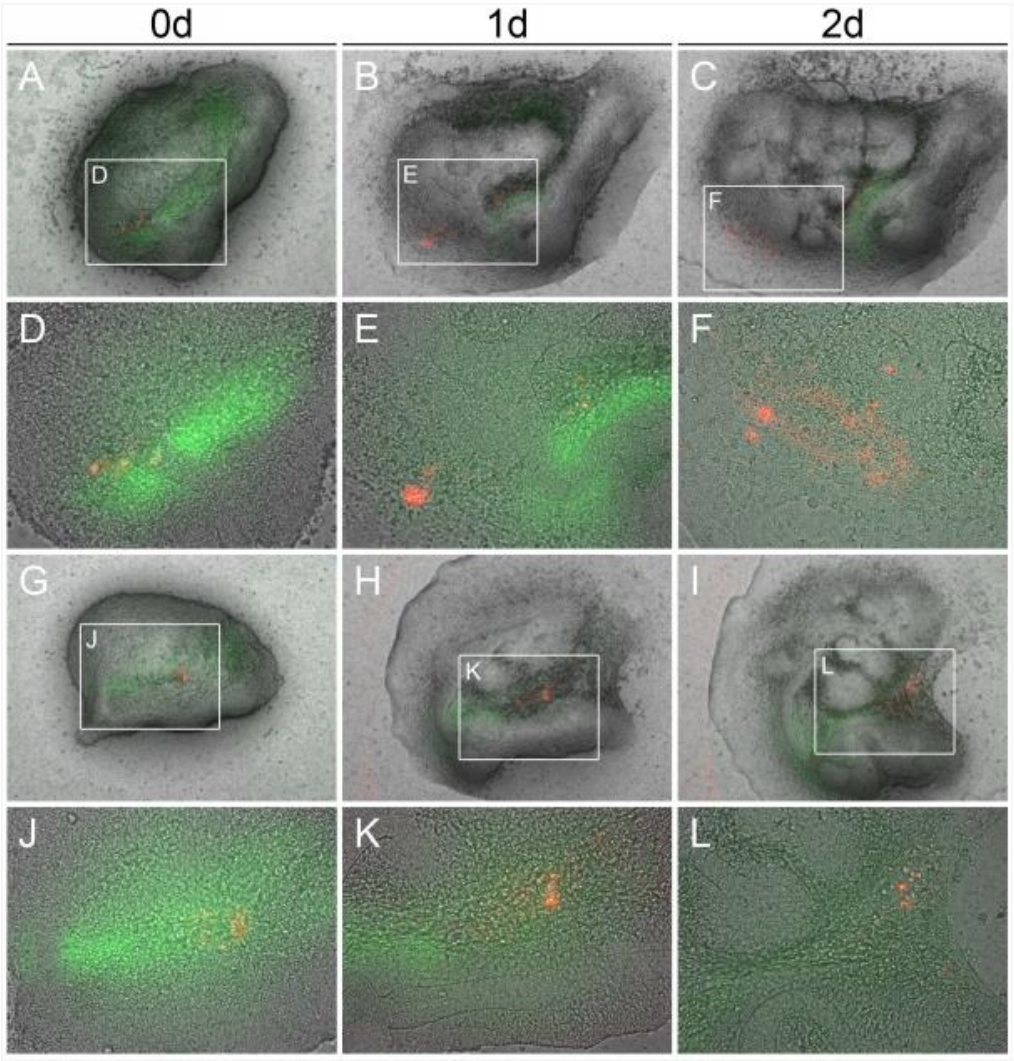

Supplementary Figure S6. Lineage analysis of *Tbx18*$^{+}$ mesenchymal cells in early kidney rudiments. (A) Combined brightfield and epifluorescence analysis of metanephric explants from E11.5 *Tbx18*$^{GFP/+}$ embryos at 0, 1 and 2 days of culture. GFP (green) marks the *Tbx18* expression domain, the red fluorescence indicates DiI-injected cell clusters. Shown are two representative examples of DiI-injected cells localizing to the space between kidneys and the Wolffian duct (lower row). Boxed regions are shown in higher magnifications below.

8. Paper II

Canonical Wnt signaling regulates smooth muscle precursor development in the mouse ureter

Mark-Oliver Trowe[1],*, Rannar Airik[1],*, Anna-Carina Weiss[1], Henner F. Farin[1], Anna B. Foik[1], Eva Bettenhausen[1], Karin Schuster-Gossler[1], Makoto Mark Taketo[2] and Andreas Kispert[1],‡

[1]Institut für Molekularbiologie, Medizinische Hochschule Hannover, Hannover, Germany
[2]Department of Pharmacology, Kyoto University, Kyoto 606- 8501, Japan.

*Equal contribution

‡Corresponding author Address:
Institut für Molekularbiologie, OE5250, Medizinische Hochschule Hannover, Carl-Neuberg-Str. 1, D-30625 Hannover, Germany. TEL.: +49 (0)511 5324017; fax: +49 (0)511 5324283.
e-mail address: kispert.andreas@mh-hannover.de (A. Kispert)

Reprinted from: Development 139, (2012) 3099-3108

http://dx.doi.org/10.1242/dev.077388

Development 139, 3099-3108 (2012) doi:10.1242/dev.077388

Canonical Wnt signaling regulates smooth muscle precursor development in the mouse ureter

Mark-Oliver Trowe[1,*], Rannar Airik[1,*], Anna-Carina Weiss[1], Henner F. Farin[1], Anna B. Foik[1], Eva Bettenhausen[1], Karin Schuster-Gossler[1], Makoto Mark Taketo[2] and Andreas Kispert[1,‡]

SUMMARY

Smooth muscle cells (SMCs) are a key component of many visceral organs, including the ureter, yet the molecular pathways that regulate their development from mesenchymal precursors are insufficiently understood. Here, we identified epithelial Wnt7b and Wnt9b as possible ligands of Fzd1-mediated β-catenin (Ctnnb1)-dependent (canonical) Wnt signaling in the adjacent undifferentiated ureteric mesenchyme. Mice with a conditional deletion of *Ctnnb1* in the ureteric mesenchyme exhibited hydroureter and hydronephrosis at newborn stages due to functional obstruction of the ureter. Histological analysis revealed that the layer of undifferentiated mesenchymal cells directly adjacent to the ureteric epithelium did not undergo characteristic cell shape changes, exhibited reduced proliferation and failed to differentiate into SMCs. Molecular markers for prospective SMCs were lost, whereas markers of the outer layer of the ureteric mesenchyme fated to become adventitial fibroblasts were expanded to the inner layer. Conditional misexpression of a stabilized form of Ctnnb1 in the prospective ureteric mesenchyme resulted in the formation of a large domain of cells that exhibited histological and molecular features of prospective SMCs and differentiated along this lineage. Our analysis suggests that Wnt signals from the ureteric epithelium pattern the ureteric mesenchyme in a radial fashion by suppressing adventitial fibroblast differentiation and initiating smooth muscle precursor development in the innermost layer of mesenchymal cells.

KEY WORDS: Wnt, Ctnnb1, Ureter, Tbx18, Smooth muscle cell

INTRODUCTION

The mammalian ureter is a simple tube that mediates by unidirectional peristaltic contractions the efficient removal of urine from the renal pelvis to the bladder. The structural basis of the flexibility and contractile activity of this tubular organ is a two-layered tissue architecture of an outer mesenchymal wall composed of radially organized layers of fibroelastic material, contractile smooth muscle cells (SMCs) and adventitial fibroblasts, and an inner specialized highly expandable impermeable epithelial lining. Whether acquired or inherited, compromised drainage of the urine to the bladder by physical barriers or by functional impairment of the SMC layer results in fluid pressure-mediated dilation of the ureter (hydroureter) and the pelvis and collecting duct system of the kidney (hydronephrosis), a disease entity that may progress to pressure-mediated destruction of the renal parenchyme (Chevalier et al., 2010; Rosen et al., 2008; Song and Yosypiv, 2011).

The three-layered mesenchymal coating of the mature ureter arises from a homogenous precursor tissue that is established in the metanephric field after formation of the ureter as an epithelial outgrowth of the Wolffian duct. In the mouse, this mesenchymal precursor pool remains undifferentiated from embryonic day (E) 11.5 to E15.5 and supports the elongation of the distal ureter stalk. From E15.5, i.e. shortly before onset of urine production in the developing kidney at E16.5, the mesenchyme in direct proximity to the ureteric epithelium differentiates in a proximal-to-distal wave into SMCs that will form layers with longitudinal and transverse orientations. Between the SMCs and the urothelium, a thin layer of stromal cells develops that contributes to elasticity of the ureteric tube. The outer mesenchymal cells remain more loosely organized and differentiate into adventitial fibroblasts (Airik and Kispert, 2007).

Despite its simple design and the relevance of congenital defects of the ureteric wall, only a small number of genes crucial for development of the ureteric mesenchyme have been characterized in recent years (Airik and Kispert, 2007; Uetani and Bouchard, 2009). Phenotypic analyses of mutant mice suggested that the T-box transcription factor gene 18 (*Tbx18*) specifies the ureteric mesenchyme (Airik et al., 2006); that Bmp4, a member of the family of secreted bone morphogenetic proteins, inhibits budding and branching morphogenesis of the distal ureteric epithelium, directs a ureteric fate and/or promotes SMC differentiation (Brenner-Anantharam et al., 2007; Dunn et al., 1997; Miyazaki et al., 2003); that the transcriptional regulators GATA binding protein 2 (Gata2), teashirt zinc finger family member 3 (Tshz3) and SRY-box containing gene 9 (Sox9) act as downstream mediators of Bmp4 function in the mesenchyme to activate expression of myocardin (*Myocd*), the key regulator of SMC differentiation (Airik et al., 2010; Caubit et al., 2008; Wang and Olson, 2004; Zhou et al., 1998); and that sonic hedgehog (Shh) signaling from the ureteric epithelium maintains *Bmp4* in the mesenchyme and dose-dependently inhibits SMC fates (Yu et al., 2002).

The Wnt gene family encodes secreted growth and differentiation factors that have been implicated in numerous processes of vertebrate development and disease. Wnt proteins signal via at least three distinct pathways, of which only the canonical pathway has been implicated in transcriptional control of cell proliferation and differentiation. This pathway uniquely and critically involves the cytoplasmic protein β-catenin (Ctnnb1),

[1]Institut für Molekularbiologie, Medizinische Hochschule Hannover, 30625 Hannover, Germany. [2]Department of Pharmacology, Kyoto University, Kyoto 606-8501, Japan.

*These authors contributed equally to this work
‡Author for correspondence (kispert.andreas@mh-hannover.de)

Accepted 8 June 2012

which is stabilized upon binding of a Wnt ligand to a Frizzled (Fzd) receptor complex on the cell surface, and translocates to the nucleus to activate target gene transcription (Barker, 2008; MacDonald et al., 2009; Miller and McCrea, 2010).

Here, we study the functional involvement of Wnt signaling in the development of the (distal) ureter, particularly its mesenchymal component, in the mouse. We provide evidence for a crucial function of the Ctnnb1-dependent sub-branch of this pathway in the specification of the SMC lineage and radial patterning of the ureteric mesenchyme.

MATERIALS AND METHODS

Mouse strains and husbandry

For the production of a conditional misexpression allele of *Tbx18*, a knock-in strategy into the X-chromosomal hypoxanthine guanine phosphoribosyl transferase (*Hprt*) gene locus was employed (Luche et al., 2007). Construction of the targeting vector, ES cell work and generation of chimeras followed exactly the procedure established for the generation of an $Hprt^{Sox9}$ allele (Airik et al., 2010). *Beta-catenin*^{flox} ($Ctnnb1^{fx}$, $Ctnnb1^{tm2Kem}$) (Brault et al., 2001), *beta-catenin*$^{lox(ex3)}$ [$Ctnnb1^{(ex3)fx}$, $Ctnnb1^{tm1Mmt}$] (Harada et al., 1999), $Hprt^{Tbx18}$, $R26^{mTmG}$ [$Gt(ROSA)26Sor^{tm4(ACTB-tdTomato-EGFP)Luo}$] (Muzumdar et al., 2007) and $Tbx18^{cre}$ [$Tbx18^{tm4(cre)Akis}$] mice (Trowe et al., 2010) were maintained on an NMRI outbred background. Embryos for Wnt (pathway) gene expression analysis were derived from matings of NMRI wild-type mice. $Tbx18^{cre/+}$;$Ctnnb1^{fx/fx}$ mice were obtained from matings of $Tbx18^{cre/+}$;$Ctnnb1^{fx/+}$ males and $Ctnnb1^{fx/fx}$ females. $Tbx18^{cre/+}$;$Ctnnb1^{fx/+}$ and $Tbx18^{+/+}$;$Ctnnb1^{fx/+}$ littermates were interchangeably used as controls. $Tbx18^{cre/+}$;$Ctnnb1^{(ex3)fx/+}$;$R26^{mTmG/+}$ and $Tbx18^{cre/+}$;$R26^{mTmG/mTmG}$ mice were obtained from matings of $Tbx18^{cre/+}$;$R26^{mTmG/mTmG}$ males and $Ctnnb1^{(ex3)fx/(ex3)fx}$ and NMRI females, respectively. For timed pregnancies, vaginal plugs were checked on the morning after mating and noon was taken as E0.5. Embryos and urogenital systems were dissected in PBS and fixed in 4% paraformaldehyde (PFA) in PBS and stored in methanol at –20°C. Genomic DNA prepared from yolk sacs or tail biopsies was used for genotyping by PCR.

Organ cultures

Explant cultures of embryonic kidneys or urogenital systems were performed as previously described (Airik et al., 2010). The pharmacological Wnt pathway inhibitor IWR1 (Sigma, dissolved in DMSO) was used at final concentrations of 50 μM and 10 μM. Culture medium was replaced every 24 hours.

Morphological, histological and histochemical analyses

Ink injection experiments to visualize the ureteropelvic lumen were performed as previously described (Airik et al., 2010). Kidneys for histological stainings were fixed in 4% PFA, paraffin embedded, and sectioned to 5 μm. Sections were stained with Hematoxylin and Eosin. For the detection of antigens on 5-μm paraffin sections, the following primary antibodies and dilutions were used: polyclonal rabbit antisera against Cdh1 (E-cadherin; a kind gift from Rolf Kemler, Max-Planck-Institute for Immunobiology and Epigenetics, Freiburg, Germany; 1:200), Myh11 (SMMHC, smooth muscle myosin heavy chain; a kind gift from R. Adelstein, NIH, Bethesda, MD, USA; 1:200), transgelin (Tagln, SM22a; Abcam, ab14106-100; 1:200), GFP (Santa Cruz; 1:100) and mouse monoclonal antibodies against Acta2 (alpha smooth muscle actin, aSMA; clone 1A4, NatuTec; 1:200), cytokeratin 18 (Ck18, Krt18; Acris; 1:200) and GFP (Roche; 1:200).

Fluorescent staining was performed using Alexa 488/555-conjugated secondary antibodies (Invitrogen; 1:200) or Biotin-conjugated secondary antibodies (Dianova; 1:200) and the TSA Tetramethylrhodamine Amplification Kit (PerkinElmer). Non-fluorescent staining was performed using kits from Vector Laboratories [Vectastain ABC Peroxidase Kit (rabbit IgG), Mouse-on-Mouse Kit, DAB Substrate Kit]. Labeling with primary antibodies was performed at 4°C overnight after antigen retrieval (Antigen Unmasking Solution, Vector Laboratories; 15 minutes, 100°C), blocking of endogenous peroxidases with 3% H_2O_2/PBS for 10 minutes (required for DAB and TSA) and incubation in 2.5% normal goat serum in PBST (0.05% Tween 20 in PBS) or blocking solutions provided with the kits. For monoclonal mouse antibodies an additional IgG blocking step was performed using the Mouse-on-Mouse Kit (Vector Laboratories).

Cellular assays

Cell proliferation rates in tissues of E12.5 and E14.5 wild-type and *Ctnnb1* mutant embryos were investigated by the detection of incorporated BrdU on 5-μm paraffin sections according to published protocols (Bussen et al., 2004). For each specimen (three embryos per genotype for E12.5, five embryos per genotype for E14.5), ten sections of the proximal ureter were assessed. The BrdU labeling index was defined as the number of BrdU-positive nuclei relative to the total number of nuclei as detected by DAPI counterstaining in histologically defined regions. Statistical analysis was performed using the two-tailed Student's *t*-test. Data are expressed as mean ± s.d. Differences were considered significant when $P<0.05$. Apoptosis in tissues was assessed by TUNEL assay using the ApopTag Plus Fluorescein In Situ Apoptosis Detection Kit (Chemicon) on 5-μm paraffin sections. All sections were counterstained with DAPI.

In situ hybridization analysis

Whole-mount in situ hybridization was performed following a standard procedure with digoxigenin-labeled antisense riboprobes (Wilkinson and Nieto, 1993). Stained specimens were transferred in 80% glycerol prior to documentation. In situ hybridization on 10-μm paraffin sections was essentially as described (Moorman et al., 2001). For each marker, at least three independent specimens were analyzed.

Image documentation

Whole-mount specimens were photographed on a Leica M420 Macroscope with a Fujix HC-300Z digital camera, and sections on a Leica DM5000 B microscope with a Leica DFC300 FX digital camera. All images were processed in Adobe Photoshop CS.

RESULTS

(Canonical) Wnt signaling in ureter development

To determine the involvement of Wnt signaling in ureter development, the expression of genes encoding Wnt ligands (*Wnt1* to *Wnt16*) and Frizzled receptors (*Fzd1* to *Fzd10*) was analyzed by in situ hybridization of whole ureters at E12.5 and E16.5, i.e. before and after cell differentiation has occurred in this tissue. This screen identified *Wnt7b*, *Wnt9b* and *Fzd1* as Wnt components with specific expression in the ureter at these stages (Fig. 1). To better resolve the spatiotemporal expression profile of these genes, we performed an in situ hybridization analysis both in whole ureters and on transverse ureter sections from E11.5 to E18.5. *Wnt7b* and *Wnt9b* were co-expressed in the ureteric epithelium from E11.5 to E14.5. Expression of *Wnt9b* was downregulated after that stage, whereas *Wnt7b* was maintained at least until E18.5 (Fig. 1A-D). Expression of *Fzd1* was detected in the ureteric mesenchyme from E11.5 to E18.5, with lower levels being confined to the innermost ring after E14.5 (Fig. 1E,F).

As Wnt7b and Wnt9b have previously been associated with the canonical branch of Wnt signaling (Karner et al., 2011; Yu et al., 2009), we investigated ureteric expression of *Axin2*, a bona fide target of this pathway (Jho et al., 2002). At E11.5, expression of *Axin2* was found in the ureteric epithelium and weakly in the surrounding mesenchyme. Epithelial expression was no longer detectable at subsequent stages, whereas mesenchymal expression was maintained and confined to the innermost cell layer at E12.5 and E14.5. *Axin2* expression in this domain was markedly downregulated after the onset of SMC differentiation at E15.5 (Fig. 1G,H).

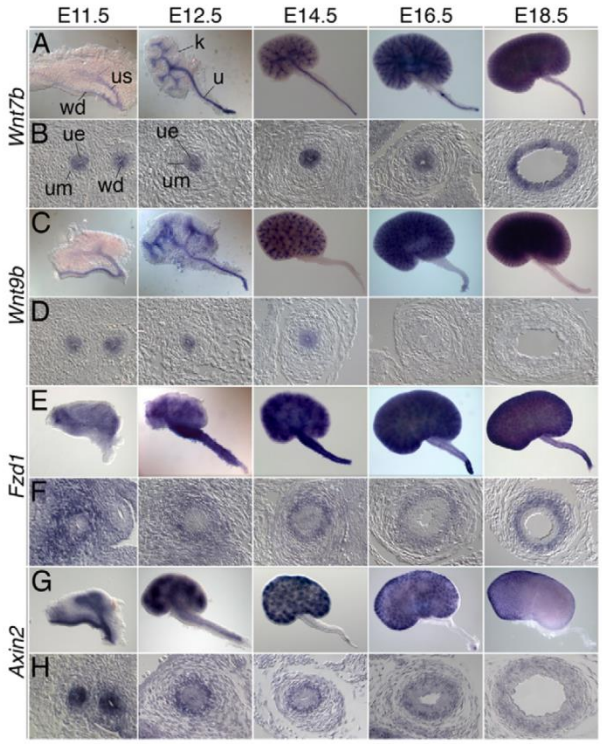

Fig. 1. Wnt expression during mouse ureter development. In situ hybridization analysis (**A**,**C**,**E**,**G**) on whole kidneys with ureters and (**B**,**D**,**F**,**H**) on transverse sections of the proximal ureter for expression of Wnt pathway components and the target of canonical Wnt signaling *Axin2* in wild-type embryos. (F,H) Note that stainings were overdeveloped to better visualize the weak expression domain. k, kidney; u, ureter; ue, ureteric epithelium; um, ureteric mesenchyme; us, ureter stalk; wd, Wolffian duct.

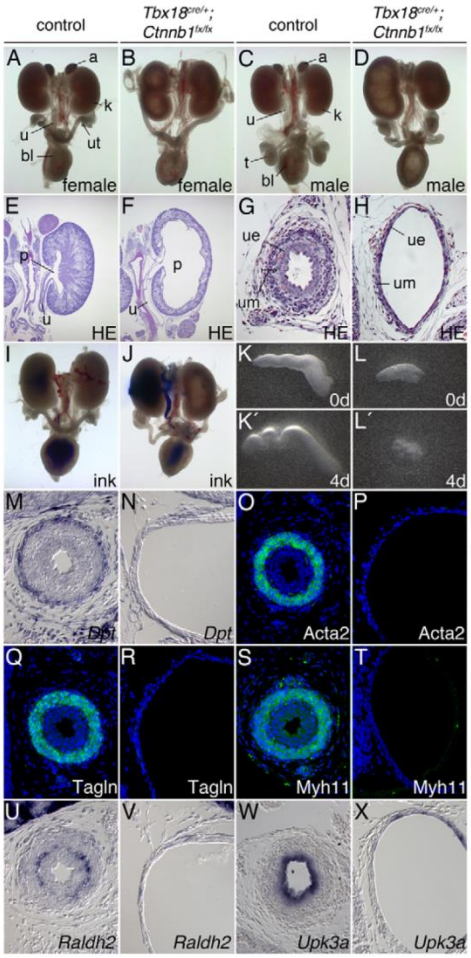

Fig. 2. Kidney and urogenital tract anomalies in *Tbx18*$^{cre/+}$;*Ctnnb1*$^{fx/fx}$ mouse embryos at E18.5. (**A-D**) Morphology of whole urogenital systems of female (A,B) and male (C,D) embryos. (**E-H**) Hematoxylin and Eosin stainings (HE) of sagittal sections of kidneys (E,F) and of transverse sections of the proximal ureter (G,H). (**I**,**J**) Absence of physical obstruction in the *Tbx18*$^{cre/+}$;*Ctnnb1*$^{fx/fx}$ ureter as revealed by ink injection experiments. (**K-L′**) Explants of E15.5 ureters after 0 and 4 days (d) in culture. (**M-X**) Cytodifferentiation of the ureteric mesenchyme (M-V) and epithelium (W,X) as shown by in situ hybridization analysis (M,N,U-X) and immunohistochemistry (O-T) on transverse sections of the proximal ureter at E18.5. a, adrenal gland; bl, bladder; k, kidney; p, pelvis; t, testis; u, ureter; ue, ureteric epithelium; um, ureteric mesenchyme; ut, uterus.

Together, this analysis suggests that Wnt7b and Wnt9b from the ureteric epithelium activate the canonical signal transduction pathway via Fzd1 in the adjacent undifferentiated mesenchyme.

Conditional inactivation of *Ctnnb1* in the ureteric mesenchyme results in hydroureter

To investigate the role of canonical Wnt signaling in the ureteric mesenchyme, we employed a tissue-specific gene inactivation approach using a *Tbx18*^{cre} line generated in our laboratory (Airik et al., 2010) and a floxed allele of *Ctnnb1* (*Ctnnb1*^{fx}), the unique intracellular mediator of this signaling pathway (Brault et al., 2001). We tested the efficiency of *Tbx18*^{cre}-mediated recombination in the ureteric mesenchyme with the sensitive reporter line *R26*^{mTmG}. In this line, recombination is visualized by bright membrane-bound GFP expression in a background of membrane-bound red fluorescence. Anti-GFP immunofluorescence analysis on sections provides additional cellular resolution of Cre-mediated recombination events (Muzumdar et al., 2007). In *Tbx18*$^{cre/+}$;*R26*$^{mTmG/+}$ mice, GFP activity was observed in a domain abutting the mesenchyme of the Wolffian duct and of the metanephric kidney at E11.5, as expected from the *Tbx18* expression pattern (Airik et al., 2006). Analysis of ureter sections at E12.5, E14.5 and E18.5 revealed GFP expression throughout the entire mesenchymal compartment, confirming that *Tbx18*^{cre} mediates recombination in precursors of all differentiated cell types of the ureteric mesenchyme, i.e. fibroblasts of the inner lamina propria and outer adventitia, and SMCs (supplementary material Fig. S1). The tissue-specific inactivation of the canonical Wnt signaling pathway in *Tbx18*$^{cre/+}$;*Ctnnb1*$^{fx/fx}$ ureters was validated by the absence of *Axin2* expression in the mesenchymal but not in the epithelial compartment at E11.5 and E12.5 (supplementary material Fig. S2).

At E18.5, urogenital systems of *Tbx18*$^{cre/+}$;*Ctnnb1*$^{fx/fx}$ embryos displayed a prominent hydroureter and hydronephrosis phenotype. These abnormalities were fully penetrant and occurred bilaterally in both sexes (Fig. 2A-D). In the female mutant, the uterus appeared stretched, the translucent ovaries were attached more anteriorly to the kidneys, and the Wolffian duct had not regressed. In the male mutant, the testes and epididymides were tethered to the posterior pole of the kidneys. Adrenals were absent from the mutant urogenital systems of both sexes (Fig. 2B,D). Adrenogenital defects are compatible with a requirement of *Ctnnb1* in female differentiation and adrenal development (Chassot et al., 2008; Kim et al., 2008). They most likely derive from *Tbx18*^{cre}-mediated recombination in adrenogenital precursors in the mesonephros rather than in the ureteric mesenchyme (Kraus et al., 2001). Heterozygous loss of *Ctnnb1* in *Tbx18*$^{cre/+}$;*Ctnnb1*$^{fx/+}$ embryos was not associated with morphological defects in the urogenital system, arguing against a dose-dependent requirement for *Ctnnb1* and genetic interaction of *Tbx18* and *Ctnnb1* in ureter development (data not shown).

Histological analyses revealed dilation of the entire renal collecting system, including the collecting ducts, calyx and pelvis, and absence of the papilla in mutant kidneys (Fig. 2E,F). The ureter was strongly dilated and featured a flat and single-layered urothelium with a thin layer of surrounding mesenchyme (Fig. 2G,H).

Hydroureternephrosis can result from structural or functional deficits of the peristaltic machinery and from physical obstruction along the ureter and its junctions. To distinguish these possibilities, we analyzed the continuity of the ureteric lumen and the patency of the junctions by injecting ink into the renal pelvis. In all genotypes the ink readily passed into the bladder (Fig. 2I,J), excluding physical barrier formation as a cause of obstruction. To further analyze the nature of functional ureter impairment, we cultured E15.5 ureter explants for 4 days, monitoring daily for peristaltic activity and contraction patterns. Wild-type ureters elongated extensively in culture and initiated unidirectional peristaltic contractions, whereas *Tbx18*$^{cre/+}$;*Ctnnb1*$^{fx/fx}$ ureters never contracted and degenerated over time (Fig. 2K-L′). To characterize the cellular changes that caused this behavior, we analyzed the expression of markers that indicate cell differentiation within the epithelial and mesenchymal tissue compartments of the ureter at E18.5. In the *Ctnnb1*-deficient ureteric mesenchyme, expression of the adventitial fibroblast marker dermatopontin (*Dpt*), the smooth muscle (SM) structural proteins Acta2, Tagln and Myh11, and of aldehyde dehydrogenase family 1, subfamily A2 (*Raldh2*, or *Aldh1a2*), a marker for the lamina propria, was absent (Fig. 2M-V). Urothelial differentiation was also affected in the mutant, as shown by the strong reduction of the urothelial marker *Upk3a* (Fig. 2W,X). Taken together, loss of *Ctnnb1* in the ureteric mesenchyme results in ureter dysfunction, probably caused by a complete loss of the SMC layer.

The requirement of canonical Wnt signaling for differentiation of the ureteric mesenchyme was independently confirmed by a pharmacological inhibition experiment. Exposure of explant cultures of E11.5 wild-type metanephric rudiments to 50 μM IWR1, a Wnt pathway inhibitor that was recently shown to block expression of Wnt9b target genes in the metanephric mesenchyme at 100 μM (Karner et al., 2011), resulted in tissue degeneration similar to that observed in explanted *Tbx18*$^{cre/+}$;*Ctnnb1*$^{fx/fx}$ ureters. Wild-type ureters cultured in 10 μM IWR1 survived for 8 days but showed a dramatic reduction of Acta2-positive SMCs (supplementary material Fig. S3).

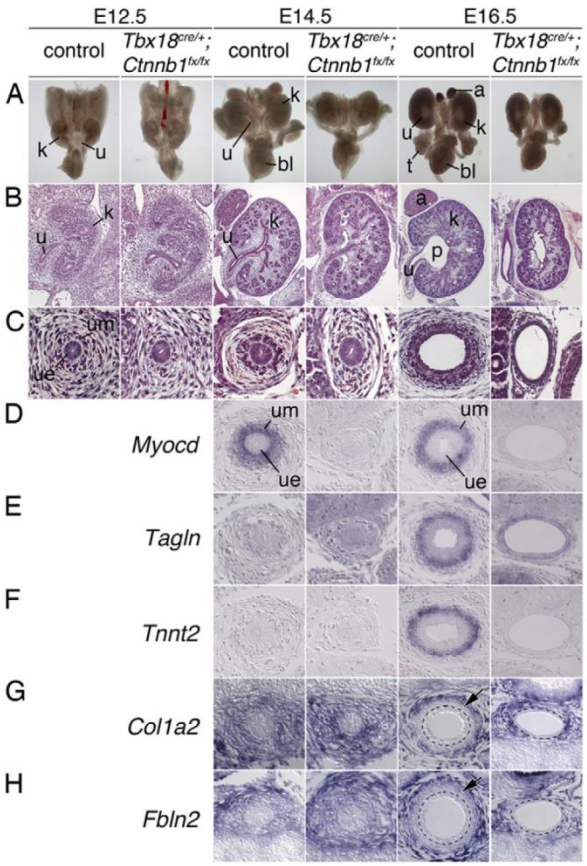

Fig. 3. Early onset of kidney and ureter anomalies in *Tbx18*$^{cre/+}$;*Ctnnb1*$^{fx/fx}$ mouse embryos. (**A**) Morphology of whole urogenital systems. (**B**,**C**) Hematoxylin and Eosin stainings of sagittal sections of kidneys (B) and of transverse sections of proximal ureters (C). (**D-H**) Cytodifferentiation of the ureteric mesenchyme into SMCs and fibroblasts as shown by in situ hybridization analysis on transverse sections of the proximal ureter. (G,H) Arrows indicate the inner ring of mesenchymal cells; the ureteric epithelium is outlined (dashed line). adrenal gland; bl, bladder; k, kidney; p, pelvis; t, testis; u, ureter; ue, ureteric epithelium; um, ureteric mesenchyme.

Early onset of ureter defects in *Tbx18*$^{cre/+}$;*Ctnnb1*$^{fx/fx}$ embryos

To define both the onset and progression of urogenital malformations in *Tbx18*$^{cre/+}$;*Ctnnb1*$^{fx/fx}$ embryos, we analyzed urogenital systems from E12.5 to E16.5. On the morphological level, *Tbx18*$^{cre/+}$;*Ctnnb1*$^{fx/fx}$ embryos were distinguished by the absence of the adrenals at E14.5. At E16.5, the failure of the testes to separate from the kidneys was apparent, and a mild dilation of the proximal ureter was observed in some mutant specimens (Fig. 3A). Histological analysis revealed the first hydronephrotic lesions (dilation of the pelvicalyceal space) in the mutant kidney at this stage, i.e. shortly after onset of urine production (Fig. 3B). In the *Ctnnb1*-deficient ureter, a mesenchymal compartment was established at E12.5 but all cells remained loosely organized with small cell bodies arranged in a tangential fashion at subsequent stages. This contrasted with the

situation in the wild-type ureteric mesenchyme, where loosely organized cells of typical fibroblast appearance with large protrusions were restricted to an outer layer, while cells adjacent to the epithelium were denser in appearance with large cell bodies from E12.5 onwards (Fig. 3C).

To examine whether these histological changes were accompanied or followed by changes in differentiation of the ureteric mesenchyme, we analyzed expression of the SM regulatory gene *Myocd*, the SM structural genes *Tagln* and troponin T2, cardiac (*Tnnt2*), and of markers of the adventitial fate collagen 1a2 (*Col1a2*) and fibulin 2 (*Fbln2*). In the wild type, *Myocd* was activated at E14.5 in the proximal region of the ureter (Fig. 3D), whereas *Tagln* and *Tnnt2* were first expressed at E16.5. *Col1a2* and *Fbln2* expression was homogenous in the ureteric mesenchyme at E14.5, but was excluded from the inner mesenchymal layers comprising lamina propria fibroblasts and SMCs at E16.5. In the mutant ureter, *Myocd* and SM structural genes were never expressed. *Col1a2* and *Fbln2* expression, by contrast, was found throughout the ureteric mesenchyme (Fig. 3D-H).

In summary, morphological and histological analyses revealed the onset of ureter anomalies in *Tbx18*$^{cre/+}$;*Ctnnb1*$^{fx/fx}$ embryos at E12.5, with a progression of phenotypic severity during subsequent embryonic stages and onset of hydroureter at E16.5. This, together with the absence of SMC differentiation and expanded expression of adventitial fibroblast markers argues for a function of canonical Wnt signaling in ureteric mesenchymal patterning and/or in the initiation of the SM developmental program.

Defects in mesenchymal patterning precede SM differentiation defects

In order to analyze the molecular changes that caused the defective SMC differentiation in *Tbx18*$^{cre/+}$;*Ctnnb1*$^{fx/fx}$ ureters, we screened for expression of a panel of genes that have been implicated in the early development of the ureteric mesenchyme and the initiation of the SM program by in situ hybridization analysis on ureter sections. In E12.5 wild-type ureters, *Bmp4*, *Gata2*, the target of Shh signaling patched 1 (*Ptch1*) (Ingham and McMahon, 2001), podocyte-expressed 1 (*Pod1*, also known as *Tcf21*), *Tshz3*, *Tbx18*, *Sox9* and secreted frizzled-related protein 2 (*Sfrp2*) were expressed throughout the mesenchymal compartment with increased levels in cells adjacent to the epithelium. Expression of chemokine (C-X-C motif) ligand 12 (*Cxcl12*) and BMP-binding endothelial regulator (*Bmper*) appeared uniformly high throughout the entire ureteric mesenchyme. In *Tbx18*$^{cre/+}$;*Ctnnb1*$^{fx/fx}$ ureters, only the expression of *Tbx18*, *Sox9* and *Sfrp2* was altered, as these were no longer detected at this stage (Fig. 4A-J). The normal expression of *Tbx18* in *Tbx18*$^{cre/+}$;*Ctnnb1*$^{fx/+}$ embryos excluded a gene-dosage effect as the cause for *Tbx18* downregulation in the *Ctnnb1* mutant ureter (supplementary material Fig. S4).

In E14.5 wild-type ureters, *Bmp4*, *Gata2*, *Ptch1*, *Pod1* and *Tshz3* were expressed in the inner layer of the mesenchymal cells from which SMCs will arise. Expression of *Bmper* and *Cxcl12* was restricted to the outer layer from which adventitial fibroblasts will differentiate. In the *Ctnnb1*-deficient ureter, mesenchymal expression of *Bmp4* and *Pod1* was absent, and *Gata2* and *Tshz3* were strongly reduced. Expression of *Ptch1* was less affected, arguing that Shh signaling was still present to some degree (Fig. 4A-E). Expression of *Bmper* and *Cxcl12* was found throughout the mutant ureteric mesenchyme at this stage (Fig. 4F,G, arrows). To exclude the possibility that the *Ctnnb1*-deficient ureteric mesenchyme acquires the fate of an adjacent tissue, we additionally checked the expression of markers of the somitic mesoderm (*Tcf15*, also known as *paraxis*), the hindlimb mesenchyme (*Tbx4*), adrenogenital tissue (*Nr5a1*, also known as *SF1*), the cap mesenchyme of nephron progenitors (*Osr1*, *Uncx4.1*, *Six2*), and chondrocytes (*Col2a1*). None of these markers was ectopically activated in the ureteric mesenchyme of *Tbx18*$^{cre/+}$;*Ctnnb1*$^{fx/fx}$ embryos (supplementary material Fig. S5). Together, this suggests that the initial specification of the ureteric mesenchyme occurs

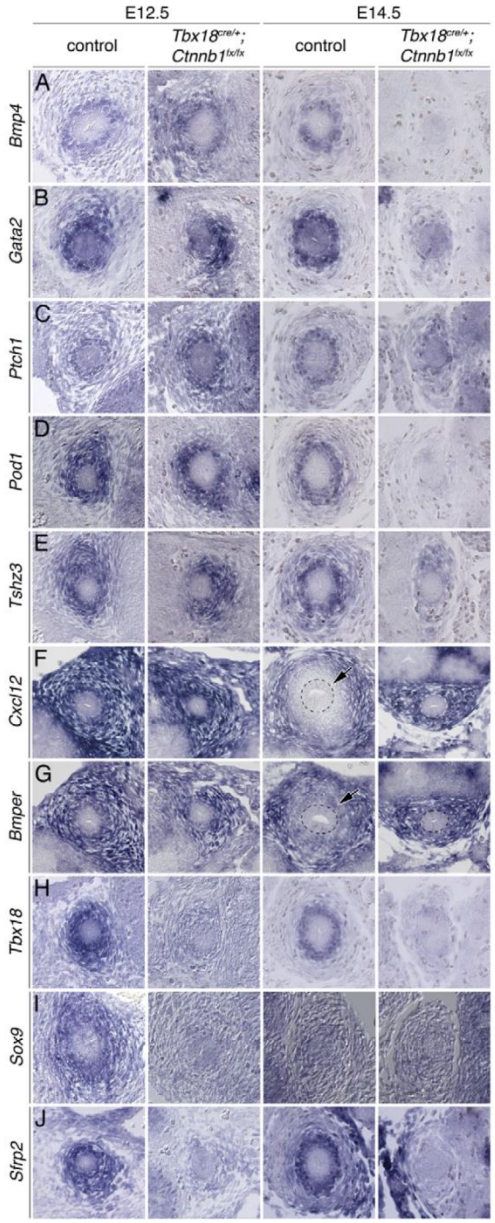

Fig. 4. Molecular characterization of *Ctnnb1*-deficient ureteric mesenchyme. (**A-J**) In situ hybridization analysis on transverse ureter sections at E12.5 and E14.5. (F,G) Arrows indicate the inner ring of mesenchymal cells; the ureteric epithelium is outlined (dashed line).

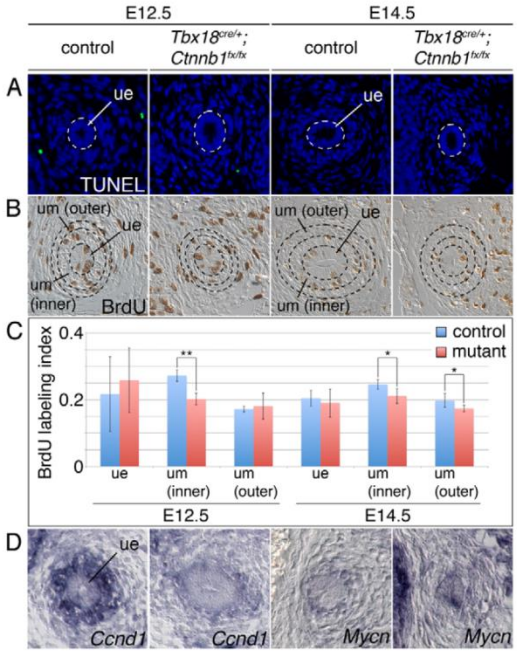

Fig. 5. Cellular defects in *Ctnnb1*-deficient ureteric mesenchyme. (**A-C**) Analysis of cell death by TUNEL assay (A) and of cell proliferation by BrdU incorporation assay (B,C) on transverse sections of mouse proximal ureter at E12.5 and E14.5. White dashed circles in A indicate the ureteric epithelium (ue); black dashed circles in B mark the ureteric epithelium and the inner and outer layers of ureteric mesenchymal cells (um) that were analyzed for proliferation. (C) Quantification of BrdU-positive cells. E12.5 (n=3), wild type versus mutant: ue, 0.217±0.113 versus 0.258±0.097, P=0.653; um (inner layer), 0.272±0.017 versus 0.202±0.017, P=0.008; um (outer layer), 0.172±0.009 versus 0.181±0.039, P=0.727. E14.5 (n=5), wild type versus mutant: ue, 0.204±0.024 versus 0.19±0.042, P=0.527; um (inner layer), 0.246±0.014 versus 0.211±0.022, P=0.034; um (outer layer), 0.198±0.021 versus 0.174±0.01, P=0.047. Error bars indicate s.d. *, P<0.05; **, P<0.01; two-tailed Student's t-test. (**D**) Expression analysis of *Ccnd1* and *Mycn* by in situ hybridization on transverse sections of the proximal ureter at E12.5.

normally in *Tbx18*$^{cre/+}$;*Ctnnb1*$^{fx/fx}$ embryos but that during the subsequent differentiation step fibroblasts expand at the expense of (prospective) SMC fates.

As *Tbx18*-deficient ureters also exhibit a severe reduction of SMCs (Airik et al., 2006), we examined whether the early loss of *Tbx18* expression contributed to the observed defects in *Ctnnb1*-deficient ureters. We tested this hypothesis by re-expressing *Tbx18* in the *Ctnnb1*-deficient ureteric mesenchyme. We generated an *Hprt*^{Tbx18} allele by integrating a bicistronic transgene cassette containing the mouse *Tbx18* ORF followed by IRES-GFP into the ubiquitously expressed X-chromosomal *Hprt* locus, similar to a previously published strategy for *Sox9* (Airik et al., 2010) (supplementary material Fig. S6). To activate transgene expression, we used the *Tbx18*^{cre} mouse line. Re-expression of *Tbx18* in *Tbx18*$^{cre/+}$;*Ctnnb1*$^{fx/fx}$;*Hprt*$^{Tbx18/Y}$ embryos did not rescue hydroureter formation and loss of SMC differentiation at E18.5, nor did it reconstitute the expression of markers that were absent or reduced in *Tbx18*$^{cre/+}$;*Ctnnb1*$^{fx/fx}$ ureters at E14.5 (supplementary material Figs S7, S8). Since we found normal expression of *Tbx18* in the ureteric mesenchyme of *Tbx18*$^{cre/+}$;*Ctnnb1*$^{fx/fx}$ embryos at E11.5 (supplementary material Fig. S9), we conclude that the loss of *Tbx18* at E12.5 or after contributes only to a minor degree, if at all, to the observed molecular and histological changes in the *Ctnnb1*-deficient ureteric mesenchyme.

Cellular changes in the ureteric mesenchyme of *Tbx18*$^{cre/+}$;*Ctnnb1*$^{fx/fx}$ mice

The loss of expression of markers of the inner, and expansion of markers of the outer, mesenchymal cell layer in *Ctnnb1*-deficient ureters might reflect a role of canonical Wnt signaling in maintaining SMC precursors. The TUNEL assay did not detect apoptotic cells at E12.5 or E14.5 in the mutant ureteric mesenchyme (Fig. 5A) making it unlikely that Wnts simply act as survival factors for these cells. However, Wnt signaling contributed to some degree to the proliferation of the inner ring of *Axin2*-positive mesenchymal cells at E12.5 and E14.5, as detected by reduced BrdU incorporation in this domain of the *Ctnnb1*-deficient ureteric mesenchyme (Fig. 5B,C). Strong reduction of the cell-cycle regulator gene cyclin D1 (*Ccnd1*) and slightly reduced expression of the pro-proliferative factor *Mycn* (Fig. 5D), which are regulated by canonical Wnt signaling in other contexts (Shtutman et al., 1999; ten Berge et al., 2008), might contribute to this finding.

Canonical Wnt signaling is sufficient to induce SMC development in the ureteric mesenchyme

Our loss-of-function analysis indicated an essential role of *Ctnnb1*-dependent Wnt signaling for SM development in the ureter, possibly by specifying an SMC precursor. To further test this hypothesis, we performed a complementary gain-of-function study with conditional (*Tbx18*^{cre}-mediated) overexpression of a stabilized form of Ctnnb1 [*Ctnnb1*$^{(ex3)fx}$] in the ureteric mesenchyme in vivo (Fig. 6) (Harada et al., 1999). As shown above, *Tbx18*^{cre}-mediated recombination is not restricted to the SMC lineage but occurs in the precursor pool of all mesenchymal cell types of the ureter (supplementary material Fig. S1), allowing ectopic activation of canonical Wnt signaling in prospective fibroblasts as well.

We validated this experimental strategy by comparative expression analysis of the lineage marker GFP and the target of canonical Wnt signaling *Axin2* on adjacent sections. In control embryos (*Tbx18*$^{cre/+}$;*R26*$^{mTmG/+}$), GFP expression marked a band of mesenchymal cells between the metanephric mesenchyme and the Wolffian duct at E11.5, and labeled all mesenchymal cells surrounding the distal ureter stalk at E12.5. At both stages, *Axin2* expression was barely detectable under the conditions used (we developed the color reaction for a shorter time than shown in Fig. 1) in the innermost layer of mesenchymal cells adjacent to the ureteric epithelium. In *Tbx18*$^{cre/+}$;*R26*$^{mTmG/+}$;*Ctnnb1*$^{(ex3)fx/+}$ embryos, *Axin2* expression was strongly activated in almost all GFP-positive cells in the E11.5 and E12.5 ureter, confirming the premature and ectopic activation of canonical Wnt signaling at high levels in precursor cells for all differentiated cell types of the ureteric mesenchyme (Fig. 6A-H′). Histological analysis revealed that the enlarged GFP$^+$ *Axin2*$^+$ domain in E12.5 *Tbx18*$^{cre/+}$;*R26*$^{mTmG/+}$;*Ctnnb1*$^{(ex3)fx/+}$ ureters almost exclusively harbored densely packed large mesenchymal cells that were rhomboid in shape. In control embryos, this cell morphology was restricted to the innermost ring of the ureteric mesenchyme at E12.5 and E14.5, whereas the rest of the GFP$^+$ ureteric mesenchyme featured cells that were slender and loosely packed,

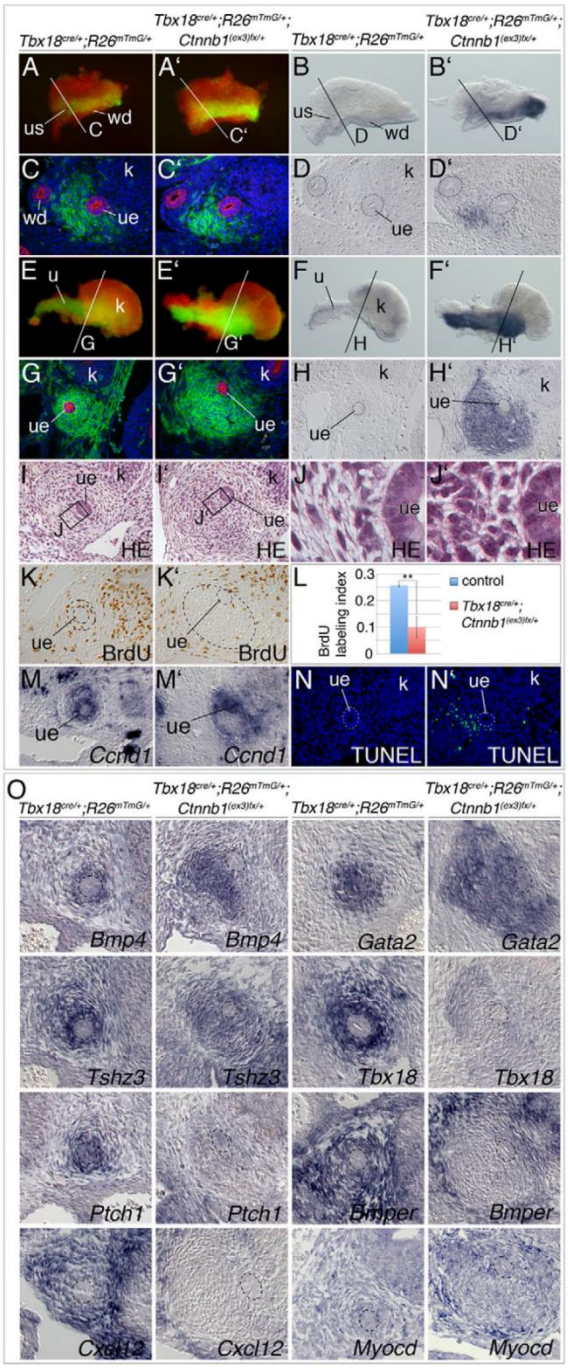

Fig. 6. Stabilization of Ctnnb1 in the ureteric mesenchyme triggers ectopic differentiation of SMC progenitors.
(**A**,**A′**,**E**,**E′**) GFP/RFP epifluorescence in whole mouse kidneys at E11.5 (A,A′) and E12.5 (E,E′). (**B**,**B′**,**D**,**D′**,**F**,**F′**,**H**,**H′**) In situ hybridization analysis of *Axin2* expression in whole kidneys at E11.5 (B,B′) and E12.5 (F,F′) and in sections of these kidneys (planes as indicated) (D,D′,H,H′). (**C**,**C′**,**G**,**G′**) Immunofluorescent staining against GFP of the $R26^{mTmG}$ reporter allele in sections of E11.5 (C,C′) and E12.5 (G,G′) kidneys. (**I-J′**) Hematoxylin and Eosin stainings of transverse sections of the proximal ureter at E12.5. (**K-L**) Analysis of cell proliferation by the BrdU incorporation assay on transverse sections of the proximal ureter at E12.5. The regions counted, as marked by dashed lines in K,K′, are the GFP^+ $Axin2^+$ region of mesenchymal cells of the ureter. (L) Quantification of BrdU-positive cells. Wild type versus mutant: 0.257±0.006 versus 0.1±0.04, P=0.003; n=3. Error bars indicate s.d. **, P<0.01; two-tailed Student's t-test. (**M**,**M′**,**O**) In situ hybridization analysis on transverse ureter sections at E12.5. (**N**,**N′**) Analysis of cell death (green) by the TUNEL assay. Sections were counterstained with DAPI. k, kidney; ue, ureteric epithelium; us, ureter stalk; wd, Wolffian duct.

as is typical for fibroblasts (Fig. 6I-J′). The BrdU incorporation assay demonstrated that cell proliferation was actually decreased, correlating with the absence of *Ccnd1* expression, while TUNEL staining detected increased levels of apoptosis in the GFP^+ $Axin2^+$ domain of the ureteric mesenchyme in $Tbx18^{cre/+};R26^{mTmG/+};Ctnnb1^{(ex3)fx/+}$ embryos at E12.5 (Fig. 6K-N′). Together, these findings argue against a selective proliferative expansion of putative SM progenitors by enhanced Wnt signaling but point to a reprogramming of prospective fibroblasts toward an SMC fate.

We further tested this idea by analyzing the expression of a panel of marker genes associated with differentiation of SMCs and fibroblasts in the ureter. *Bmp4*, *Gata2* and *Tshz3*, which are expressed throughout the entire ureteric mesenchyme of wild-type ureters at E12.5 and mark prospective SMCs of the inner ring in the wild type at E14.5, were expressed throughout the large GFP^+ $Axin2^+$ domain of the ureteric mesenchyme of $Tbx18^{cre/+};R26^{mTmG/+};Ctnnb1^{(ex3)fx/+}$ embryos at E12.5. By contrast, *Tbx18*, *Pod1* and *Ptch1*, which have similar expression patterns in the wild type, were severely downregulated in the mutants. Expression of *Bmper* and *Cxcl12*, which are restricted to the non-myogenic lineage of the ureteric mesenchyme in the wild type starting from E14.5, was clearly excluded from the GFP^+ $Axin2^+$ mesenchymal cells in $Tbx18^{cre/+};Ctnnb1^{(ex3)fx/+}$ ureters. To our surprise, we detected weak expression of *Myocd* in the mutant, whereas no expression was found in the wild-type ureteric mesenchyme at this stage (Fig. 6O). These data indicate that stabilization of Ctnnb1/enhanced Wnt signaling prevents fibroblast differentiation and promotes premature SMC differentiation in the ureteric mesenchyme.

As $Tbx18^{cre/+};Ctnnb1^{(ex3)fx/+}$ mice die at ~E12.5 due to cardiovascular lesions (Norden et al., 2011), we could not observe the long-term effect of our misexpression approach on cell differentiation in vivo. Therefore, we explanted whole urogenital systems at E12.5, cultured them for 4 days and examined the histology and expression of SM structural markers on adjacent transverse sections of the proximal ureter (Fig. 7). Analyses at later time points, which might have been more representative of the full differentiation potential of the ureteric mesenchyme, were not possible owing to subsequent degeneration of the mutant ureter by apoptosis (compare with Fig. 6N′). In control specimens, the E-cadherin (Cdh1)-positive ureteric epithelium was encircled by mesenchymal cells that expressed the lineage marker GFP but were negative (at this level of signal development) for the target of canonical Wnt signaling *Axin2* (Fig. 7A,C). Cells in the outer, less dense region expressed the fibroblast marker *Col1a2*, whereas an

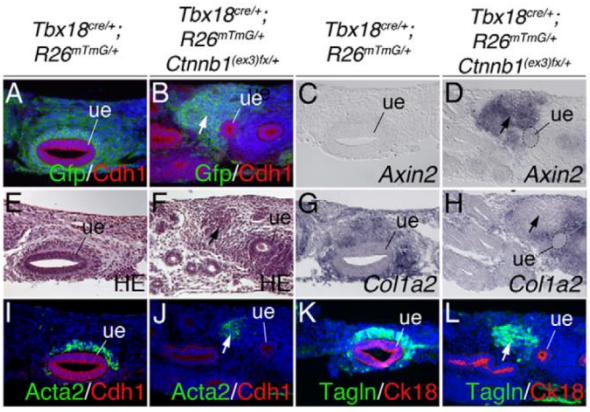

Fig. 7. Stabilization of Ctnnb1 in the ureteric mesenchyme results in ectopic SMC differentiation. Whole urogenital systems of E12.5 *Tbx18*$^{cre/+}$;*R26*$^{mTmG/+}$ (control) and *Tbx18*$^{cre/+}$;*R26*$^{mTmG/+}$;*Ctnnb1*$^{(ex3)fx/+}$ mouse embryos were explanted, cultured for 4 days, sectioned through the proximal ureter region and analyzed by (**A**,**B**,**I-L**) co-immunofluorescence, (**C**,**D**,**G**,**H**) in situ hybridization and (**E**,**F**) Hematoxylin and Eosin staining. Arrows indicate the GFP$^+$ *Axin2*$^+$ domain in the ureteric mesenchyme of *Tbx18*$^{cre/+}$;*R26*$^{mTmG/+}$;*Ctnnb1*$^{(ex3)fx/+}$ embryos. For immunofluorescent stainings, sections were counterstained with DAPI. Cdh1 and Ck18 immunofluorescence visualizes the ureteric epithelium. ue, ureteric epithelium.

inner ring of highly condensed mesenchymal cells was positive for the SMC markers Acta2 and Tagln (Fig. 7C,G,I,K). In *Tbx18*$^{cre/+}$;*R26*$^{mTmG/+}$;*Ctnnb1*$^{(ex3)fx/+}$ explant cultures, the ureteric epithelium appeared mildly hypoplastic, with cells showing enlarged nuclei. An accumulation of GFP-positive mesenchymal cells in proximity to the ureteric epithelium expressed high levels of *Axin2*, demonstrating continuous activity of the canonical Wnt signaling pathway in these cells (Fig. 7B,D). These GFP$^+$ *Axin2*$^+$ cells were not positive for the fibroblast marker *Col1a2* but expressed Acta2 and Tagln, albeit at slightly reduced levels compared with the wild type (Fig. 7H,J,L). These data strongly suggest that forced activation of the Ctnnb1-dependent Wnt signaling pathway is sufficient to induce SMC differentiation in the ureteric mesenchyme.

DISCUSSION

Specification of SMC precursors by epithelial Wnt signals in the ureteric mesenchyme

The development of the distal ureter and its surrounding mesenchymal layer lacks the complex morphogenetic processes of the proximal part. Nonetheless, it is obvious that proliferation rates and differentiation waves require spatial and temporal coordination between the epithelium and the surrounding mesenchyme to achieve continuous elongation and to acquire functional integrity at the onset of urine production in the kidney. In fact, embryological experiments have shown that the urothelium is necessary for the survival of isolated ureteric mesenchyme and induction of SMCs (Cunha, 1976), and that the mesenchymal layer controls urothelial survival, proliferation and differentiation (Airik and Kispert, 2007). However, the molecular nature of the underlying signaling systems has remained largely obscure, with the exception of epithelial Shh signals that are required for patterning and proliferation of the adjacent SMC layer (Yu et al., 2002).

Our data suggest that epithelial signals of the Wnt family play a crucial role in SMC development in the ureteric mesenchyme. Our exhaustive in situ hybridization screen identified expression of *Wnt7b* and *Wnt9b* in the ureteric epithelium but failed to detect expression of Wnt family members in the adjacent mesenchyme. By contrast, we found expression of the Wnt receptor gene *Fzd1* and of the target of canonical Wnt signaling *Axin2* in the mesenchyme but only weakly and transiently (*Axin2* at E11.5) in the epithelium, arguing that Wnt7b and Wnt9b act in a paracrine fashion on the mesenchymal tissue compartment to activate the canonical Wnt signaling pathway. Previous functional analyses of *Wnt7b* and *Wnt9b* have revealed their role as canonical Wnt ligands in the development of the renal medulla and as inducers of nephrogenesis but have not described ureter defects (Carroll et al., 2005; Yu et al., 2009), suggesting that *Wnt7b* and *Wnt9b* act redundantly in the ureteric epithelium. *Axin2* expression was confined to a single layer of mesenchymal cells directly adjacent to the epithelial compartment, indicating that, in this context, epithelial Wnt signals are largely non-diffusible and do not act as morphogens, but act from cell to cell. To our knowledge, *Axin2* is the earliest marker that molecularly distinguishes mesenchymal cells of an inner from that of an outer mesenchymal compartment. Shortly after the onset of *Axin2* expression at E12.5, cells of the inner ring undergo characteristic cell shape changes that clearly distinguish them from outer mesenchymal cells. Although lineage tracing has not yet been performed to confirm this, it is very likely that SMCs arise exclusively from the (*Axin2*$^+$) inner compartment, whereas the outer compartment gives rise to adventitial fibroblasts.

Our genetic experiments and supportive pharmacological inhibition studies showed that loss of *Ctnnb1*-dependent Wnt signaling results in absence of the SMC lineage. This phenotype is compatible with a number of functions for canonical Wnt signaling, including the aggregation, specification or survival of uncommitted precursor cells, proliferation and expansion of specified precursors and/or terminal differentiation of SMCs. Our analysis of *Ctnnb1*-deficient embryos has shown that the ureteric mesenchyme aggregated normally around the distal ureter stalk and exhibited reduced proliferation but survived throughout development. In turn, stabilization of Ctnnb1 did not lead to aggregation of cells but merely to shape changes of resident cells that had reduced proliferation and increased apoptosis, strongly arguing against a primary function of canonical Wnt signaling in the aggregation and survival of the ureteric mesenchyme. We suggest that proliferation of the ureteric mesenchyme, particularly increased proliferation of SMC precursors, is mediated both by Shh (Yu et al., 2002) and by epithelial Wnt signals. We deem it unlikely that canonical Wnts act late on as terminal differentiation signals for SMCs either, as *Axin2* expression was activated early and dropped sharply after the onset of *Myocd* expression. In our opinion, our dataset is most compatible with a role of canonical Wnt signaling in initiating SMC development by specifying SMC precursors at the expense of the alternative fibroblast fate, for the following reasons. First, expression of *Axin2* preceded the characteristic cell shape changes of the inner ureteric mesenchymal cell layer. Second, these cell shape changes were largely prevented when canonical Wnt signaling was absent, whereby SMC differentiation failed completely and the fibroblast layer was expanded instead. Third, expression of all markers of SMC precursors was completely lost by E14.5. Finally, canonical Wnt signaling was sufficient to induce the characteristic cell shape

changes and marker expression in unprogrammed precursor cells, which was followed by SMC development at the expense of fibroblast fates.

Mesenchymal cells expressing stabilized Ctnnb1, i.e. possessing enhanced Wnt signaling, expressed *Myocd* and SM structural genes at much lower levels than in the wild-type ureter. It is conceivable that additional signals emitted from the ureteric epithelium are required for increased proliferation and terminal differentiation of these cells. In fact, cells with ectopic Wnt signaling lacked the Shh signaling that has previously been shown to increase the proliferation of SMCs (Yu et al., 2002). Alternatively, or additionally, prolonged activation of canonical Wnt signaling might actually prevent terminal differentiation.

A requirement for *Ctnnb1*-dependent Wnt signaling in SMC development is not without precedence but the specific function and mode of action seem to vary in different tissues. Loss of *Wnt7b* from the pulmonary epithelium resulted in decreased mesenchymal differentiation and proliferation and, later in development, decreased vascular SMC integrity in the lung (Shu et al., 2002). *Wnt4* was shown to be required in an autocrine fashion for SMC differentiation in the medullary stroma (Itäranta et al., 2006) and for SMC proliferation during intimal thickening in the vascular system (Tsaousi et al., 2011).

Canonical Wnt signaling is independent of Tbx18 but acts upstream of other factors required for SMC differentiation

To date, only a small number of factors have been identified as crucial for ureteric SMC development (Airik and Kispert, 2007): *Tbx18* was implicated in the specification and cohesive aggregation of the ureteric mesenchyme (Airik et al., 2006), *Bmp4* and *Gata2* in control of ureter budding and SMC differentiation (Brenner-Anantharam et al., 2007; Dunn et al., 1997; Miyazaki et al., 2003; Zhou et al., 1998), Shh signaling in the proliferation and patterning of the ureteric mesenchyme (Yu et al., 2002) and *Tshz3* and *Sox9* in SMC differentiation (Airik et al., 2010; Caubit et al., 2008). *Gata2* and Shh signaling are thought to regulate *Bmp4*, which in turn regulates *Tshz3*. Although only specifically shown for *Sox9* and *Tshz3*, all of these genes are likely to act upstream of *Myocd*, the key regulator of SMC differentiation (Wang and Olson, 2004). Therefore, the loss of expression of all of these factors might collectively contribute to the loss of SMCs in the *Ctnnb1*-deficient mesenchyme. Downregulation of *Tbx18* preceded that of the other genes relevant to SMC formation, suggesting a primary requirement of this transcription factor upstream of other molecular circuits. However, re-expression of *Tbx18* in the *Ctnnb1*-deficient ureteric mesenchyme did not induce expression of any of these factors in this tissue, nor did it rescue SMC differentiation and hydroureter formation. Although this finding does not exclude the possibility that *Tbx18* is relevant for SMC differentiation, it shows that Tbx18 is not sufficient to trigger the ureteric SMC differentiation program downstream of canonical Wnt signaling.

Early loss of expression of *Tbx18*, *Sfrp2* and *Sox9* at E12.5 and later loss of *Bmp4*, *Tshz3*, *Gata2* and *Pod1* in the *Ctnnb1*-deficient ureteric mesenchyme argue for differential regulation by Wnt signaling. In the first case, *Ctnnb1*-dependent Wnt signaling might be directly required to maintain the expression of *Tbx18* [*Sfrp2* and *Sox9* depend on *Tbx18* in turn (Airik et al., 2006)], whereas downregulation of the second set of genes might merely reflect a loss of specification of this cell type. The latter contention is

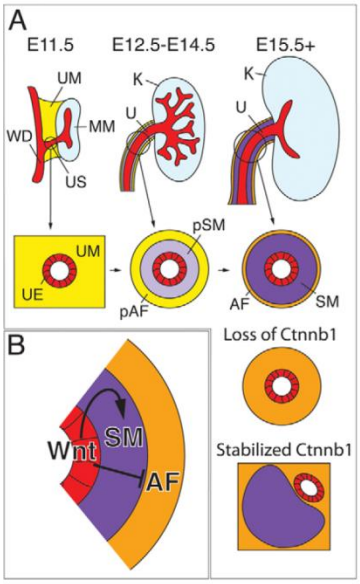

Fig. 8. Model of how canonical Wnt signaling directs the formation of SMCs in the developing mouse ureter. (**A**) Scheme of the developing mouse kidney and ureter. At E11.5, homogenous ureteric mesenchyme surrounds the epithelium in the distal ureter stalk region. Between E12.5 and E14.5, two mesenchymal subdomains become established whose cells differ in shape and gene expression profile. After E15.5, the inner domain differentiates into SMCs, whereas the outer domain differentiates into adventitial fibroblasts. Loss of Wnt signaling by deletion of *Ctnnb1* in the ureteric mesenchyme results in loss of the SMC lineage and expansion of fibroblast fates. Stabilization of Ctnnb1 throughout the entire ureteric mesenchyme induces ectopic SMC differentiation. (**B**) Scheme for radial patterning of the ureteric mesenchyme. Wnt signals from the ureter epithelium may specify SMCs and repress adventitial fibroblast fate. (p)AF, (prospective) adventitial fibroblasts; K, kidney; MM, metanephric mesenchyme; pSM, (prospective) smooth muscle cells; U, ureter; UE, ureteric epithelium; UM, ureteric mesenchyme; US, ureter stalk; WD, Wolffian duct.

supported by the concurrent expansion of markers for prospective fibroblasts. Interestingly, these markers are initially expressed uniformly as well, but become progressively restricted to the outer layer of prospective and definitive fibroblasts after E12.5. Hence, Wnt signaling may pattern the ureteric mesenchyme by inducing SMCs and/or by repressing a fibroblast fate.

Although all of these factors directly or indirectly depend on canonical Wnt signaling, they differentially respond to ectopic activation of this pathway in the prospective ureteric mesenchyme in $Tbx18^{cre/+};Ctnnb1^{(ex3)fx/+}$ embryos: expression of *Tbx18* and *Pod1* is repressed, whereas *Bmp4*, *Gata2* and *Tshz3* are induced. We propose that this regulation reflects a differential cooperation of Wnt signaling with other signaling systems (e.g. Shh) in the ureteric mesenchyme.

It has recently been suggested that in the developing lung epithelial Wnt7b mediates, via the canonical pathway, the direct transcriptional activation of the extracellular matrix protein tenascin C (*Tnc*), which in turn is necessary and sufficient for expression of *Pdgfra/b* in the mesenchymal compartment (Cohen et al., 2009). We did not detect any changes in the expression of

these three genes in the *Ctnnb1*-deficient ureteric mesenchyme, arguing that the molecular pathways downstream of Wnt7b/Ctnnb1 differ in different developmental settings (supplementary material Fig. S10).

In summary, our analysis suggests that Wnt proteins from the ureteric epithelium act as paracrine signals to initiate SM precursor development in adjacent mesenchymal cells, and thus may pattern the mesenchyme in a radial fashion (Fig. 8). Our findings emphasize the importance of epithelial-mesenchymal signaling in ureter development. They will help to further dissect the molecular pathways that are important for SMC differentiation in the excretory system and to develop strategies for the directed formation of this important cell type for therapeutic purposes.

Acknowledgements
We thank Andrew P. McMahon, Brian Parr, Cathy Mendelsohn, Charles J. Sherr, Christer Betsholtz, Gregory Shackleford, Laurent Fasano, Liz Robertson, Luc Leyns, Matthew Scott, Richard Stump, Suzanne Cory and Yingzi Yang for probes; R. Adelstein for the rabbit SMMHC antiserum; Rolf Kemler for the anti-Cdh1 antibody and *Ctnnb1*^{fx} mice; and Achim Gossler and Aravind Shekar for technical help.

Funding
This work was supported by a grant from the Deutsche Forschungsgemeinschaft [DFG KI728/7 to A.K.].

Competing interests statement
The authors declare no competing financial interests.

Supplementary material
Supplementary material available online at
http://dev.biologists.org/lookup/suppl/doi:10.1242/dev.077388/-/DC1

References

Airik, R. and Kispert, A. (2007). Down the tube of obstructive nephropathies: the importance of tissue interactions during ureter development. *Kidney Int.* **72**, 1459-1467.
Airik, R., Bussen, M., Singh, M. K., Petry, M. and Kispert, A. (2006). Tbx18 regulates the development of the ureteral mesenchyme. *J. Clin. Invest.* **116**, 663-674.
Airik, R., Trowe, M. O., Foik, A., Farin, H. F., Petry, M., Schuster-Gossler, K., Schweizer, M., Scherer, G., Kist, R. and Kispert, A. (2010). Hydroureternephrosis due to loss of Sox9-regulated smooth muscle cell differentiation of the ureteric mesenchyme. *Hum. Mol. Genet.* **19**, 4918-4929.
Barker, N. (2008). The canonical Wnt/beta-catenin signalling pathway. *Methods Mol. Biol.* **468**, 5-15.
Brault, V., Moore, R., Kutsch, S., Ishibashi, M., Rowitch, D. H., McMahon, A. P., Sommer, L., Boussadia, O. and Kemler, R. (2001). Inactivation of the beta-catenin gene by Wnt1-Cre-mediated deletion results in dramatic brain malformation and failure of craniofacial development. *Development* **128**, 1253-1264.
Brenner-Anantharam, A., Cebrian, C., Guillaume, R., Hurtado, R., Sun, T. T. and Herzlinger, D. (2007). Tailbud-derived mesenchyme promotes urinary tract segmentation via BMP4 signaling. *Development* **134**, 1967-1975.
Bussen, M., Petry, M., Schuster-Gossler, K., Leitges, M., Gossler, A. and Kispert, A. (2004). The T-box transcription factor Tbx18 maintains the separation of anterior and posterior somite compartments. *Genes Dev.* **18**, 1209-1221.
Carroll, T. J., Park, J. S., Hayashi, S., Majumdar, A. and McMahon, A. P. (2005). Wnt9b plays a central role in the regulation of mesenchymal to epithelial transitions underlying organogenesis of the mammalian urogenital system. *Dev. Cell* **9**, 283-292.
Caubit, X., Lye, C. M., Martin, E., Coré, N., Long, D. A., Vola, C., Jenkins, D., Garratt, A. N., Skaer, H., Woolf, A. S. et al. (2008). Teashirt 3 is necessary for ureteral smooth muscle differentiation downstream of SHH and BMP4. *Development* **135**, 3301-3310.
Chassot, A. A., Ranc, F., Gregoire, E. P., Roepers-Gajadien, H. L., Taketo, M. M., Camerino, G., de Rooij, D. G., Schedl, A. and Chaboissier, M. C. (2008). Activation of beta-catenin signaling by Rspo1 controls differentiation of the mammalian ovary. *Hum. Mol. Genet.* **17**, 1264-1277.
Chevalier, R. L., Thornhill, B. A., Forbes, M. S. and Kiley, S. C. (2010). Mechanisms of renal injury and progression of renal disease in congenital obstructive nephropathy. *Pediatr. Nephrol.* **25**, 687-697.
Cohen, E. D., Ihida-Stansbury, K., Lu, M. M., Panettieri, R. A., Jones, P. L. and Morrisey, E. E. (2009). Wnt signaling regulates smooth muscle precursor development in the mouse lung via a tenascin C/PDGFR pathway. *J. Clin. Invest.* **119**, 2538-2549.
Cunha, G. R. (1976). Epithelial-stromal interactions in development of the urogenital tract. *Int. Rev. Cytol.* **47**, 137-194.
Dunn, N. R., Winnier, G. E., Hargett, L. K., Schrick, J. J., Fogo, A. B. and Hogan, B. L. (1997). Haploinsufficient phenotypes in Bmp4 heterozygous null mice and modification by mutations in Gli3 and Alx4. *Dev. Biol.* **188**, 235-247.
Harada, N., Tamai, Y., Ishikawa, T., Sauer, B., Takaku, K., Oshima, M. and Taketo, M. M. (1999). Intestinal polyposis in mice with a dominant stable mutation of the beta-catenin gene. *EMBO J.* **18**, 5931-5942.
Ingham, P. W. and McMahon, A. P. (2001). Hedgehog signaling in animal development: paradigms and principles. *Genes Dev.* **15**, 3059-3087.
Itäranta, P., Chi, L., Seppänen, T., Niku, M., Tuukkanen, J., Peltoketo, H. and Vainio, S. (2006). Wnt-4 signaling is involved in the control of smooth muscle cell fate via Bmp-4 in the medullary stroma of the developing kidney. *Dev. Biol.* **293**, 473-483.
Jho, E. H., Zhang, T., Domon, C., Joo, C. K., Freund, J. N. and Costantini, F. (2002). Wnt/beta-catenin/Tcf signaling induces the transcription of Axin2, a negative regulator of the signaling pathway. *Mol. Cell. Biol.* **22**, 1172-1183.
Karner, C. M., Das, A., Ma, Z., Self, M., Chen, C., Lum, L., Oliver, G. and Carroll, T. J. (2011). Canonical Wnt9b signaling balances progenitor cell expansion and differentiation during kidney development. *Development* **138**, 1247-1257.
Kim, A. C., Reuter, A. L., Zubair, M., Else, T., Serecky, K., Bingham, N. C., Lavery, G. G., Parker, K. L. and Hammer, G. D. (2008). Targeted disruption of beta-catenin in Sf1-expressing cells impairs development and maintenance of the adrenal cortex. *Development* **135**, 2593-2602.
Kraus, F., Haenig, B. and Kispert, A. (2001). Cloning and expression analysis of the mouse T-box gene Tbx18. *Mech. Dev.* **100**, 83-86.
Luche, H., Weber, O., Nageswara Rao, T., Blum, C. and Fehling, H. J. (2007). Faithful activation of an extra-bright red fluorescent protein in "knock-in" Cre-reporter mice ideally suited for lineage tracing studies. *Eur. J. Immunol.* **37**, 43-53.
MacDonald, B. T., Tamai, K. and He, X. (2009). Wnt/beta-catenin signaling: components, mechanisms, and diseases. *Dev. Cell* **17**, 9-26.
Miller, R. K. and McCrea, P. D. (2010). Wnt to build a tube: contributions of Wnt signaling to epithelial tubulogenesis. *Dev. Dyn.* **239**, 77-93.
Miyazaki, Y., Oshima, K., Fogo, A. and Ichikawa, I. (2003). Evidence that bone morphogenetic protein 4 has multiple biological functions during kidney and urinary tract development. *Kidney Int.* **63**, 835-844.
Moorman, A. F., Houweling, A. C., de Boer, P. A. and Christoffels, V. M. (2001). Sensitive nonradioactive detection of mRNA in tissue sections: novel application of the whole-mount in situ hybridization protocol. *J. Histochem. Cytochem.* **49**, 1-8.
Muzumdar, M. D., Tasic, B., Miyamichi, K., Li, L. and Luo, L. (2007). A global double-fluorescent Cre reporter mouse. *Genesis* **45**, 593-605.
Norden, J., Greulich, F., Rudat, C., Taketo, M. M. and Kispert, A. (2011). Wnt/β-catenin signaling maintains the mesenchymal precursor pool for murine sinus horn formation. *Circ. Res.* **109**, e42-e50.
Rosen, S., Peters, C. A., Chevalier, R. L. and Huang, W. Y. (2008). The kidney in congenital ureteropelvic junction obstruction: a spectrum from normal to nephrectomy. *J. Urol.* **179**, 1257-1263.
Shtutman, M., Zhurinsky, J., Simcha, I., Albanese, C., D'Amico, M., Pestell, R. and Ben-Ze'ev, A. (1999). The cyclin D1 gene is a target of the beta-catenin/LEF-1 pathway. *Proc. Natl. Acad. Sci. USA* **96**, 5522-5527.
Shu, W., Jiang, Y. Q., Lu, M. M. and Morrisey, E. E. (2002). Wnt7b regulates mesenchymal proliferation and vascular development in the lung. *Development* **129**, 4831-4842.
Song, R. and Yosypiv, I. V. (2011). Genetics of congenital anomalies of the kidney and urinary tract. *Pediatr. Nephrol.* **26**, 353-364.
ten Berge, D., Brugmann, S. A., Helms, J. A. and Nusse, R. (2008). Wnt and FGF signals interact to coordinate growth with cell fate specification during limb development. *Development* **135**, 3247-3257.
Trowe, M. O., Shah, S., Petry, M., Airik, R., Schuster-Gossler, K., Kist, R. and Kispert, A. (2010). Loss of Sox9 in the periotic mesenchyme affects mesenchymal expansion and differentiation, and epithelial morphogenesis during cochlea development in the mouse. *Dev. Biol.* **342**, 51-62.
Tsaousi, A., Williams, H., Lyon, C. A., Taylor, V., Swain, A., Johnson, J. L. and George, S. J. (2011). Wnt4/β-catenin signaling induces VSMC proliferation and is associated with intimal thickening. *Circ. Res.* **108**, 427-436.
Uetani, N. and Bouchard, M. (2009). Plumbing in the embryo: developmental defects of the urinary tracts. *Clin. Genet.* **75**, 307-317.
Wang, D. Z. and Olson, E. N. (2004). Control of smooth muscle development by the myocardin family of transcriptional coactivators. *Curr. Opin. Genet. Dev.* **14**, 558-566.
Wilkinson, D. G. and Nieto, M. A. (1993). Detection of messenger RNA by in situ hybridization to tissue sections and whole mounts. *Methods Enzymol.* **225**, 361-373.
Yu, J., Carroll, T. J. and McMahon, A. P. (2002). Sonic hedgehog regulates proliferation and differentiation of mesenchymal cells in the mouse metanephric kidney. *Development* **129**, 5301-5312.
Yu, J., Carroll, T. J., Rajagopal, J., Kobayashi, A., Ren, Q. and McMahon, A. P. (2009). A Wnt7b-dependent pathway regulates the orientation of epithelial cell division and establishes the cortico-medullary axis of the mammalian kidney. *Development* **136**, 161-171.
Zhou, Y., Lim, K. C., Onodera, K., Takahashi, S., Ohta, J., Minegishi, N., Tsai, F. Y., Orkin, S. H., Yamamoto, M. and Engel, J. D. (1998). Rescue of the embryonic lethal hematopoietic defect reveals a critical role for GATA-2 in urogenital development. *EMBO J.* **17**, 6689-6700.

Supplemental Figures

for

Canonical Wnt signaling regulates smooth muscle precursor development in the mouse ureter

Mark-Oliver Trowe[1],*, Rannar Airik[1],*, Anna-Carina Weiss[1], Henner F. Farin[1], Anna B. Foik[1], Eva Bettenhausen[1], Karin Schuster-Gossler[1], Makoto Mark Taketo[2] and Andreas Kispert[1],‡

[1]Institut für Molekularbiologie, Medizinische Hochschule Hannover, Hannover, Germany

[2]Department of Pharmacology, Kyoto University, Kyoto 606- 8501, Japan.

* Equal contribution

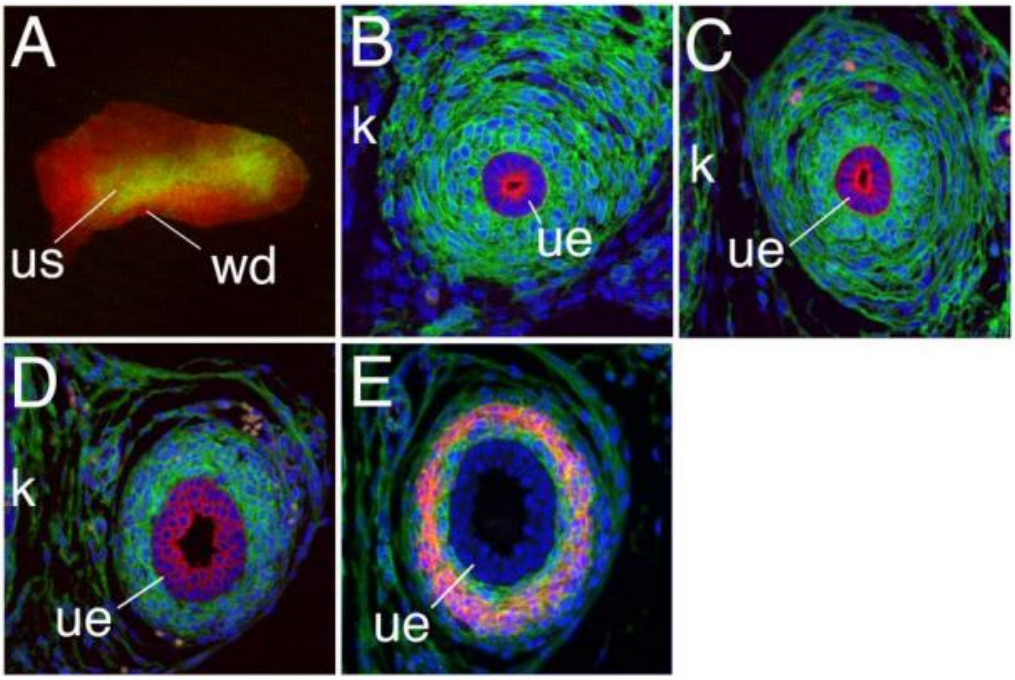

Fig. S1. *Tbx18*^{cre} mediates recombination of a reporter allele in the entire ureteric mesenchyme. (**A-E**) Analysis of GFP expression in whole E11.5 kidneys by epifluorescence (A) and by anti-GFP immunofluorescence on sections through the ureter region at E12.5 (B), E14.5 (C) and E18.5 (D,E) of *Tbx18*$^{cre/+}$;*R26*$^{mTmG/+}$ embryos. GFP-positive cells are in green (A-E), the ureteric epithelium in red by expression of Ck18 (B-D). All mesenchymal cells surrounding the ureteric epithelium are positive for the lineage marker GFP from E12.5 to E18.5. (E) Co-immunofluorescence analysis for expression of the SMC marker Acta2 (red) shows that all differentiated cell types of the ureter mesenchyme at this stage, i.e. SMCs but also fibroblasts of the outer adventitia and the inner lamina propria, derive from Tbx18-positive precursor cells. k, kidney; ue, ureteric epithelium; us, ureter stalk; wd, Wolffian duct.

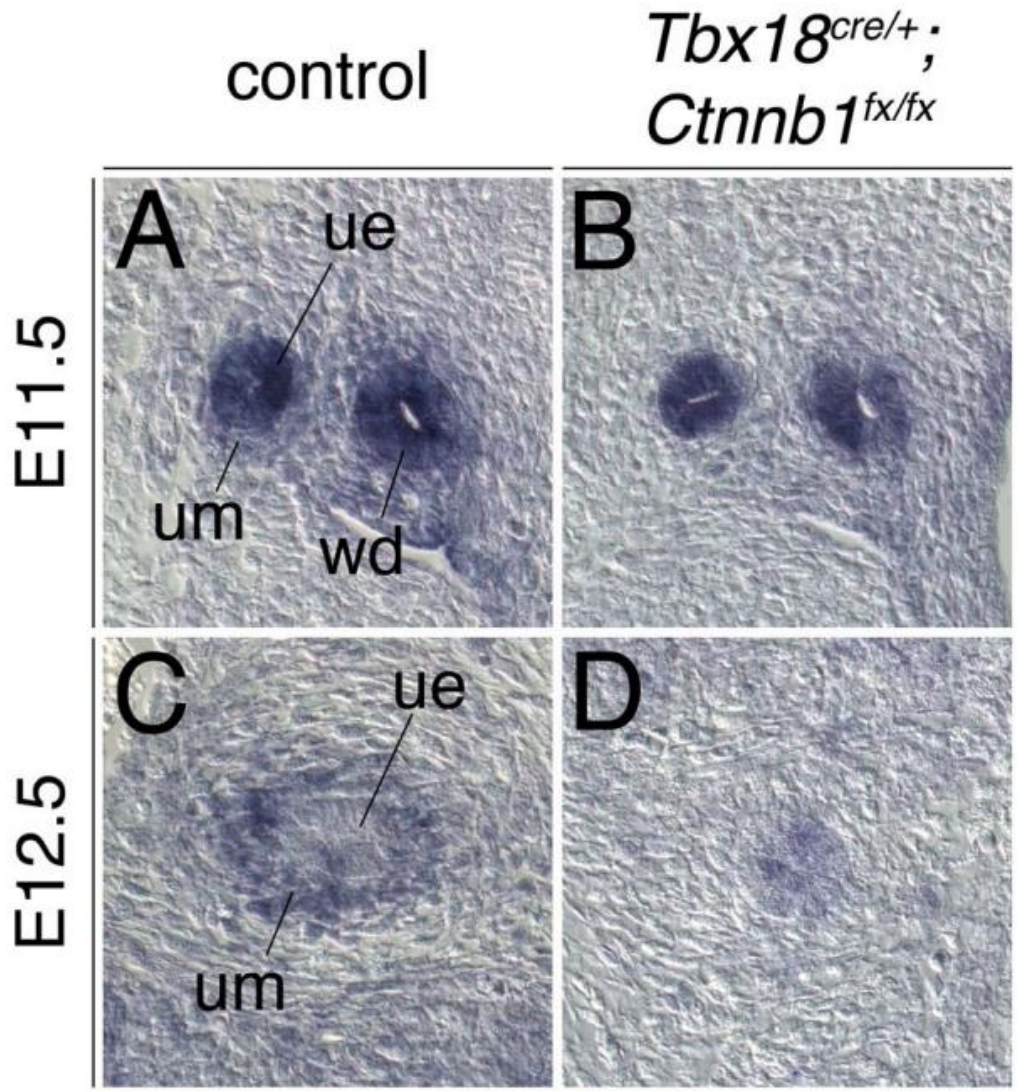

Fig. S2. Conditional inactivation of *Ctnnb1* in the ureteric mesenchyme. (**A-D**) Expression analysis of the *Ctnnb1* downstream target *Axin2* by in situ hybridization on transverse sections of the proximal ureter of *Tbx18*$^{cre/+}$;*Ctnnb1*$^{fx/fx}$ and control embryos at E11.5 and E12.5. Absence of *Axin2* expression indicates that *Tbx18*^{cre}-mediated deletion of *Ctnnb1* completely abrogates canonical Wnt signaling as early as E11.5. ue, ureteric epithelium; um, ureteric mesenchyme; wd, Wolffian duct.

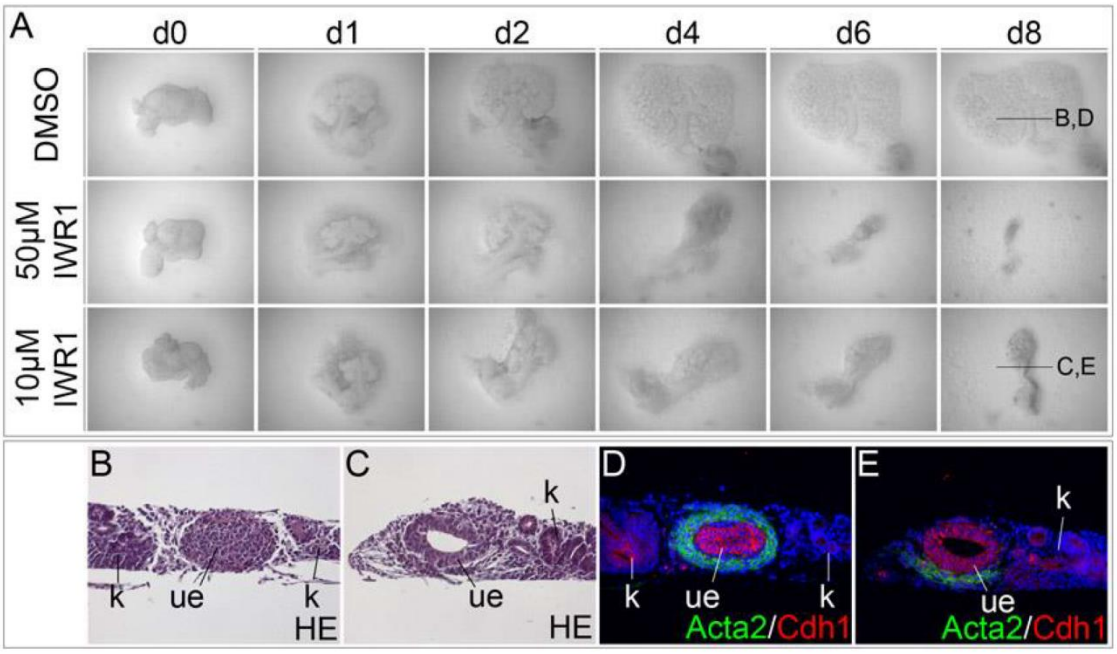

Fig. S3. Pharmacological inhibition of canonical Wnt signaling in kidney explant cultures severely affects differentiation and growth of the ureteric mesenchyme. (**A**) Morphological inspection of explants of E11.5 kidney rudiments at different days (d) of culture. Explants were treated with DMSO (control), 50 µM or 10 µM of the inhibitor of canonical Wnt signaling IWR1. 50 µM IWR1 results in complete degeneration of the ureter, whereas ureters survive in 10 µM IWR1. Note that IWR1 also affects nephron induction in the metanephric mesenchyme leading to reduced branching and nephron formation at both concentrations. (**B**,**C**) Histological analysis by Hematoxylin and Eosin staining of sections through the ureter in 8-day explant cultures treated with DMSO (B) or 10 µM IWR1 (C) (section planes are marked in A). (**D**,**E**) Analysis of SM development by anti-Acta2 immunofluorescence (green) on adjacent sections shows severe reduction of the SMC layer surrounding the ureteric epithelium (visualized by expression of Cdh1, red) in ureters treated with 10 µM IWR1 (E) but not in control explants (D). k, kidney; ue, ureteric epithelium.

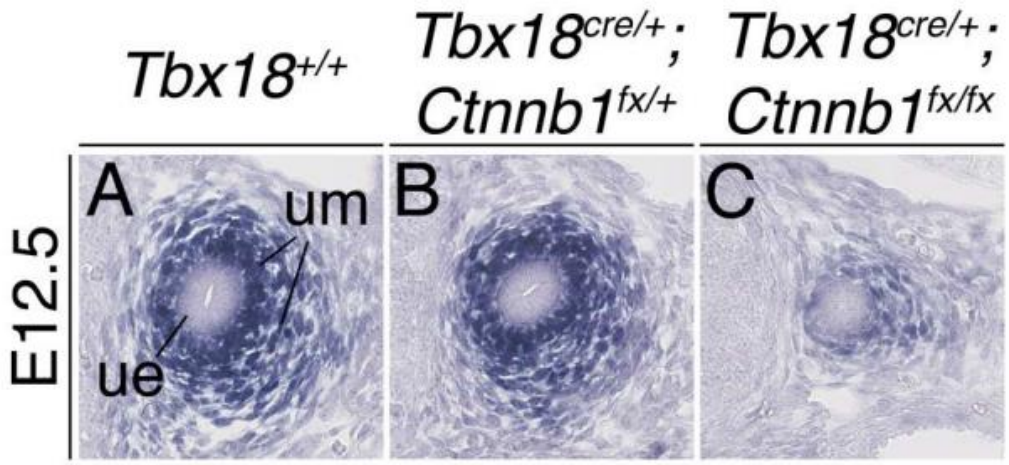

Fig. S4. Downregulation of *Tbx18* expression in the ureteric mesenchyme of *Tbx18*$^{cre/+}$;*Ctnnb1*$^{fx/fx}$ embryos at E12.5. (**A-C**) Expression of *Tbx18* as detected by in situ hybridization analysis on transverse sections of the proximal ureter at E12.5 in different genotypes. Unaltered expression of *Tbx18* in *Tbx18*$^{cre/+}$;*Ctnnb1*$^{fx/+}$ ureteric mesenchyme shows that reduction of *Tbx18* expression in *Tbx18*$^{cre/+}$;*Ctnnb1*$^{fx/fx}$ ureters is due to loss of *Ctnnb1* and not due to the presence of only one functional allele of *Tbx18*. ue, ureteric epithelium; um, ureteric mesenchyme.

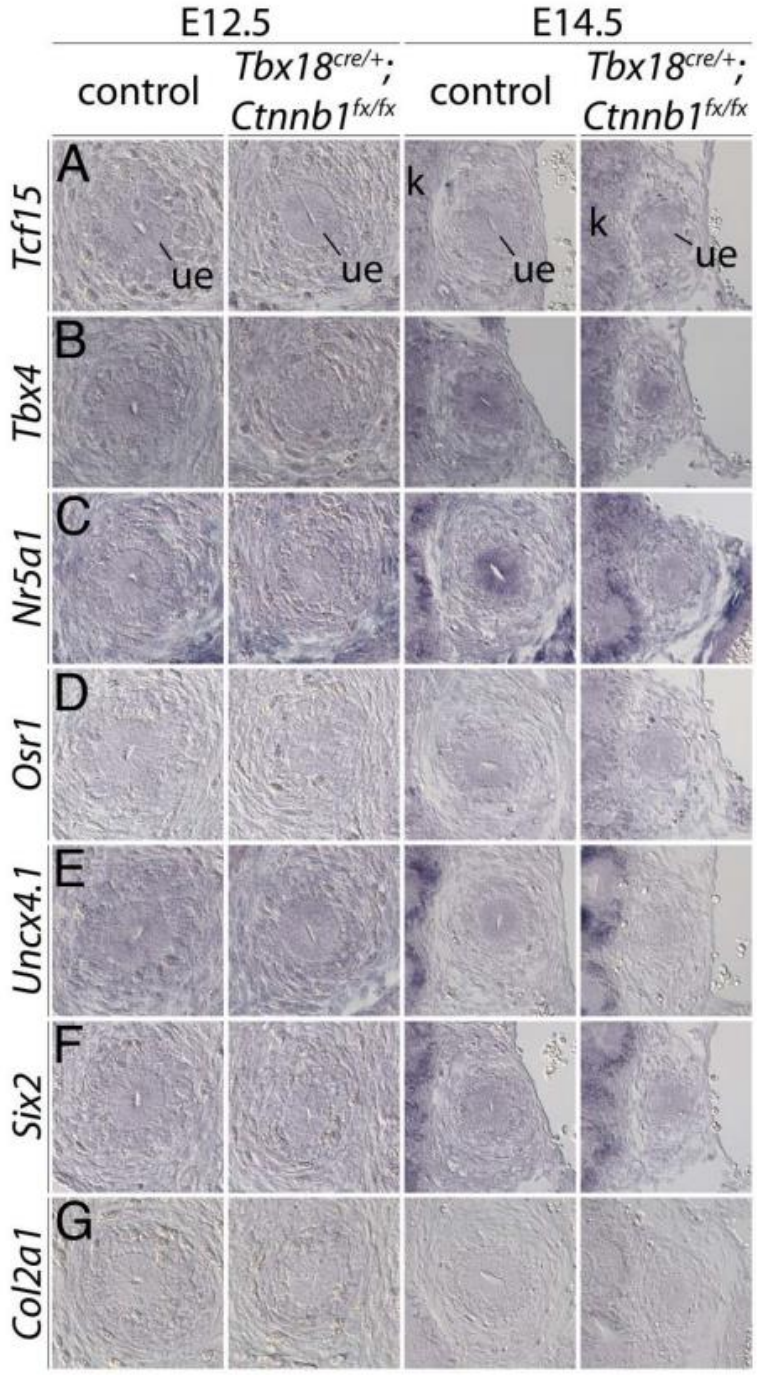

Fig. S5. Molecular characterization of *Ctnnb1*-deficient ureteric mesenchyme. (**A-G**) In situ hybridization analysis on transverse ureter sections at E12.5 and E14.5. Markers for somitic mesoderm (*Tcf15*), the hindlimb mesenchyme (*Tbx4*), adrenogenital tissue (*Nr5a1*), cap mesenchyme of nephron progenitors (*Osr1*, *Uncx4.1*, *Six2*) and chondrocytes (*Col2a1*) are not derepressed in the mesenchyme of *Tbx18*$^{cre/+}$;*Ctnnb1*$^{fx/fx}$ ureters. k, kidney; ue, ureteric epithelium.

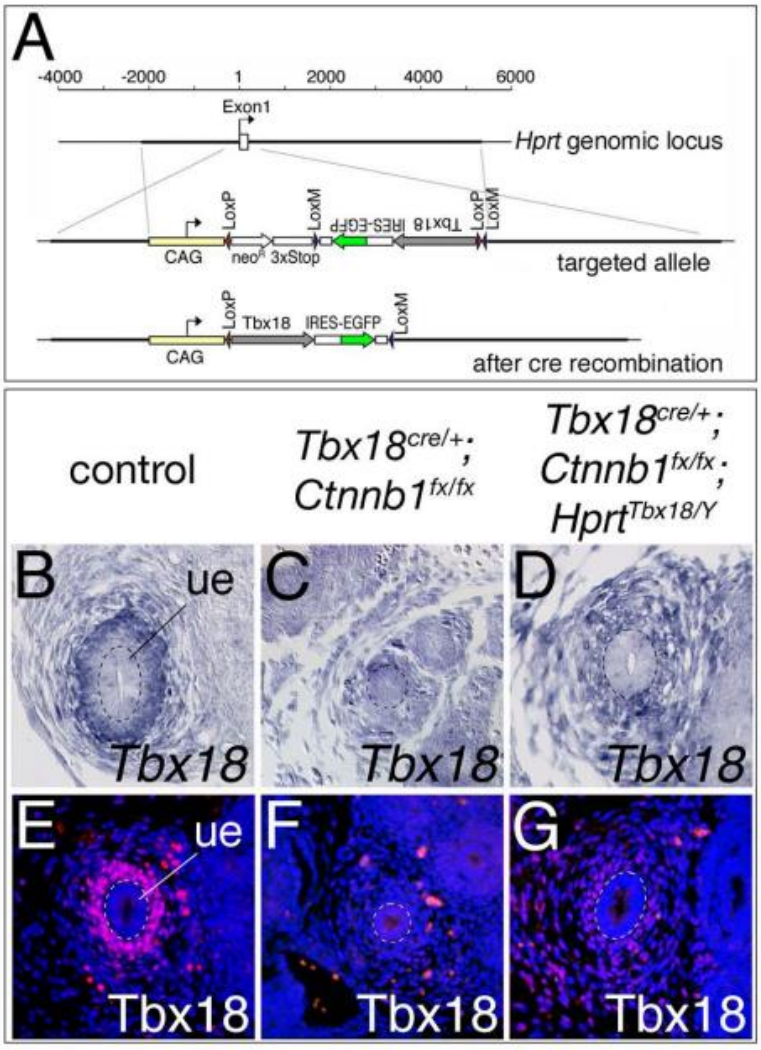

Fig. S6. Generation of an *Hprt*^{Tbx18} knock-in allele. (**A**) Targeting strategy depicting the hypoxanthine guanine phosphoribosyl transferase (*Hprt*) genomic locus in the wild-type (top), after homologous recombination in ES cells (middle) and after Cre-mediated recombination (bottom). The scale bar shows distances (in bp) relative to the *Hprt* transcription start site; homology regions included in the targeting vectors are labeled with thick lines; asterisks mark an SV40 polyadenylation signal. 3xStop, three successive polyadenylation sequences from the bovine growth hormone gene; CAG, CMV early enhancer/chicken beta-actin promoter; IRES, internal ribosomal entry site; neo^{R}, neomycin resistance. (**B-G**) In situ hybridization analysis of *Tbx18* mRNA (B-D) and immunofluorescence analysis of Tbx18 protein expression (E-G) on transverse sections of the proximal ureter at E14.5. Expression of Tbx18 from the *Hprt* allele reconstitutes (low level) expression of *Tbx18* mRNA and Tbx18 protein in the ureteric mesenchyme in the *Ctnnb1*-deficient background. ue, ureteric epithelium.

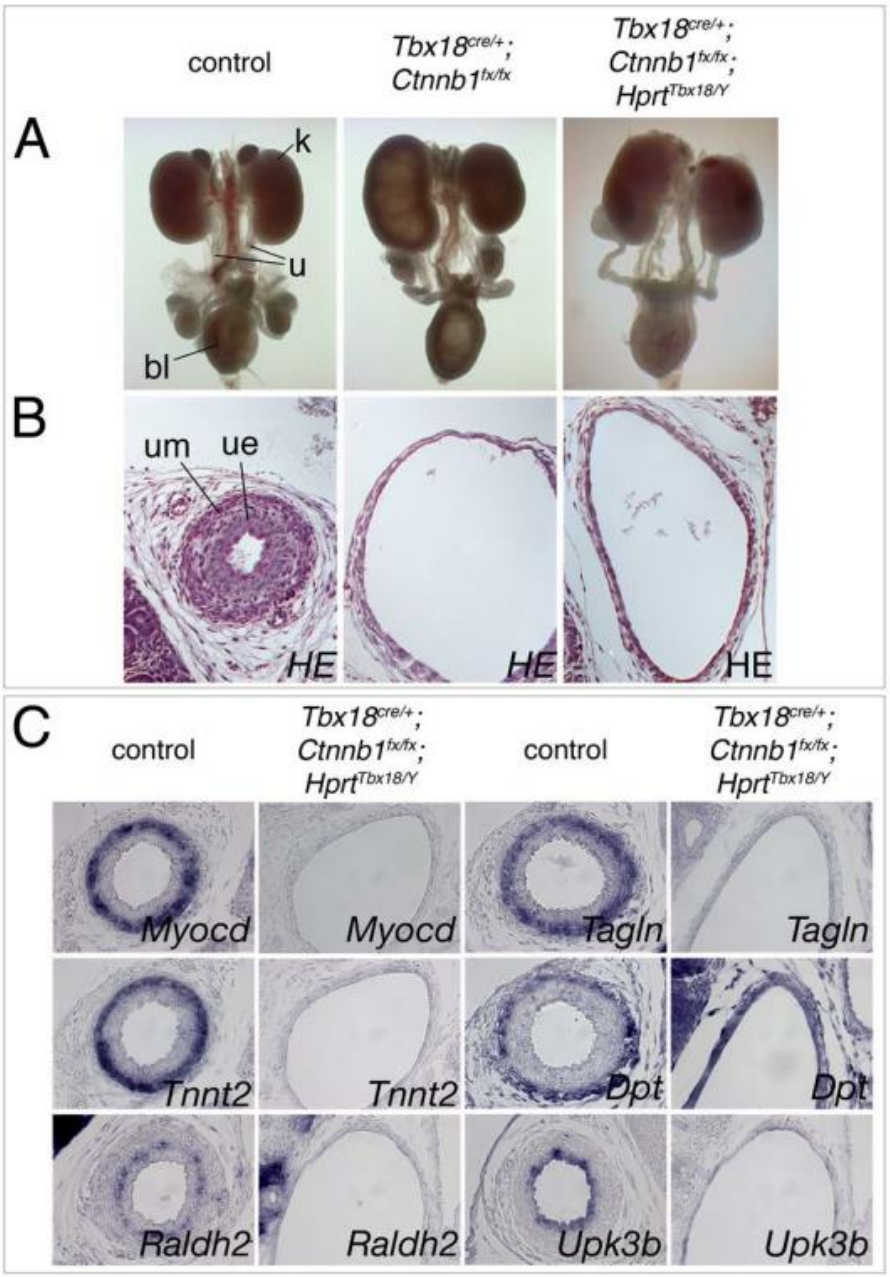

Fig. S7. Re-expression of Tbx18 in *Ctnnb1*-deficient ureteric mesenchyme does not rescue hydroureter formation and the lack of SMC differentiation. (**A**,**B**) Morphology of whole urogenital systems of male embryos (A) and histological stainings (HE) of transverse sections of the proximal ureter (B) at E18.5. (**C**) Cytodifferentiation of the ureter examined by in situ hybridization analysis on transverse sections of the proximal ureter at E18.5 for markers of SMCs (*Myocd*, *Tagln*, *Tnnt2*), adventitial fibroblasts (*Dpt*), lamina propria fibroblasts (*Raldh2*) and urothelium (*Upk3b*). bl, bladder; k, kidney; u, ureter; ue, ureteric epithelium; um, ureteric mesenchyme.

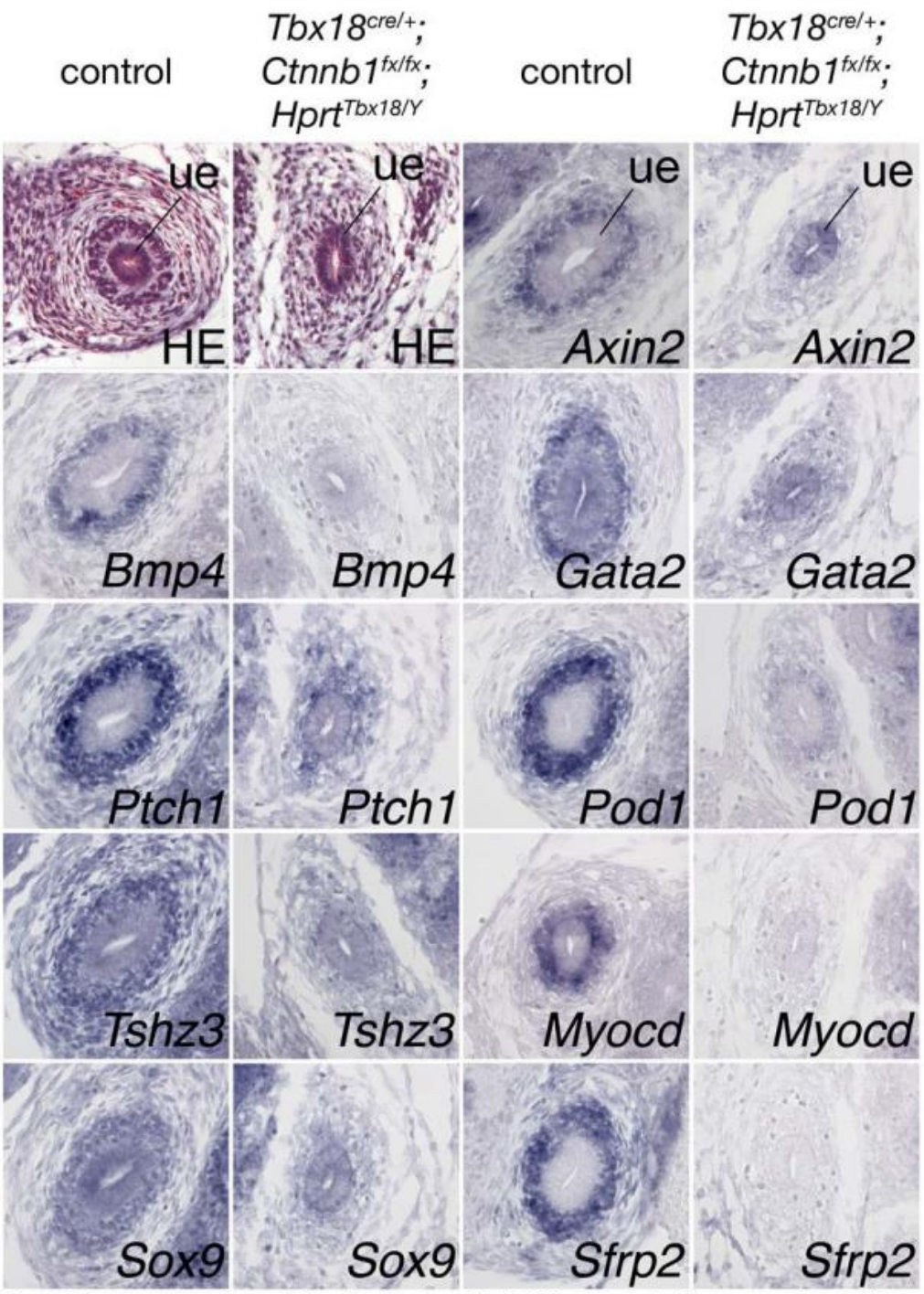

Fig. S8. Re-expression of Tbx18 in *Ctnnb1*-deficient ureteric mesenchyme does not rescue loss of patterning or differentiation of the tissue. Histological stainings (HE) and in situ hybridization analysis on transverse sections of the proximal ureter at E14.5 of markers for patterning and differentiation of the ureteric mesenchyme. ue, ureteric epithelium.

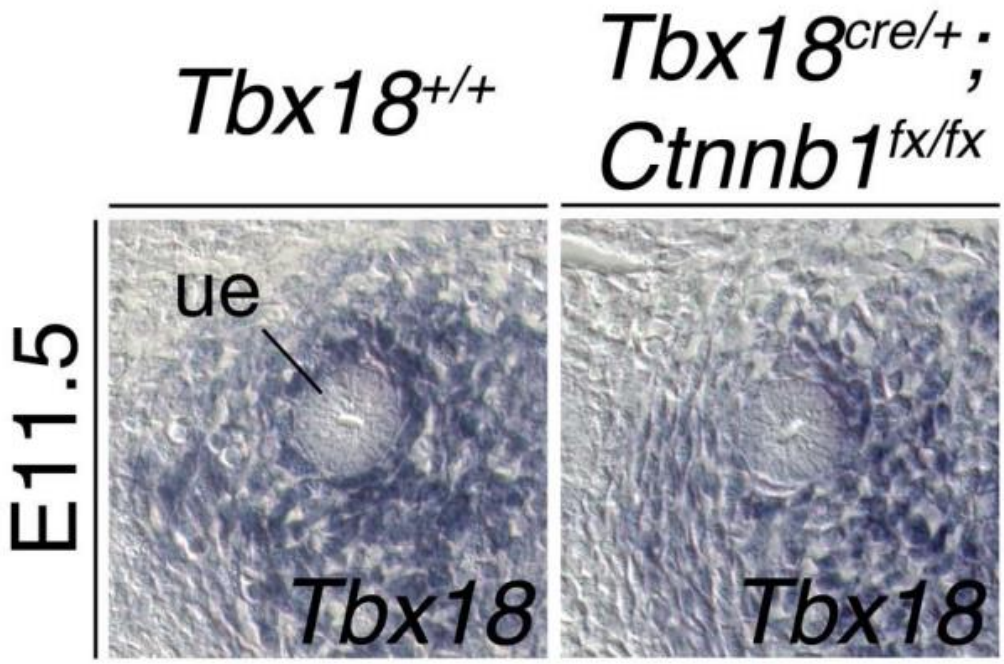

Fig. S9. Expression of *Tbx18* is unchanged in the *Ctnnb1*-deficient prospective ureteric mesenchyme at E11.5. In situ hybridization analysis of *Tbx18* expression in transverse sections of the proximal ureter in wild-type ($Tbx18^{+/+}$) and $Tbx18^{cre/+};Ctnnb1^{fx/fx}$ embryos. ue, ureteric epithelium.

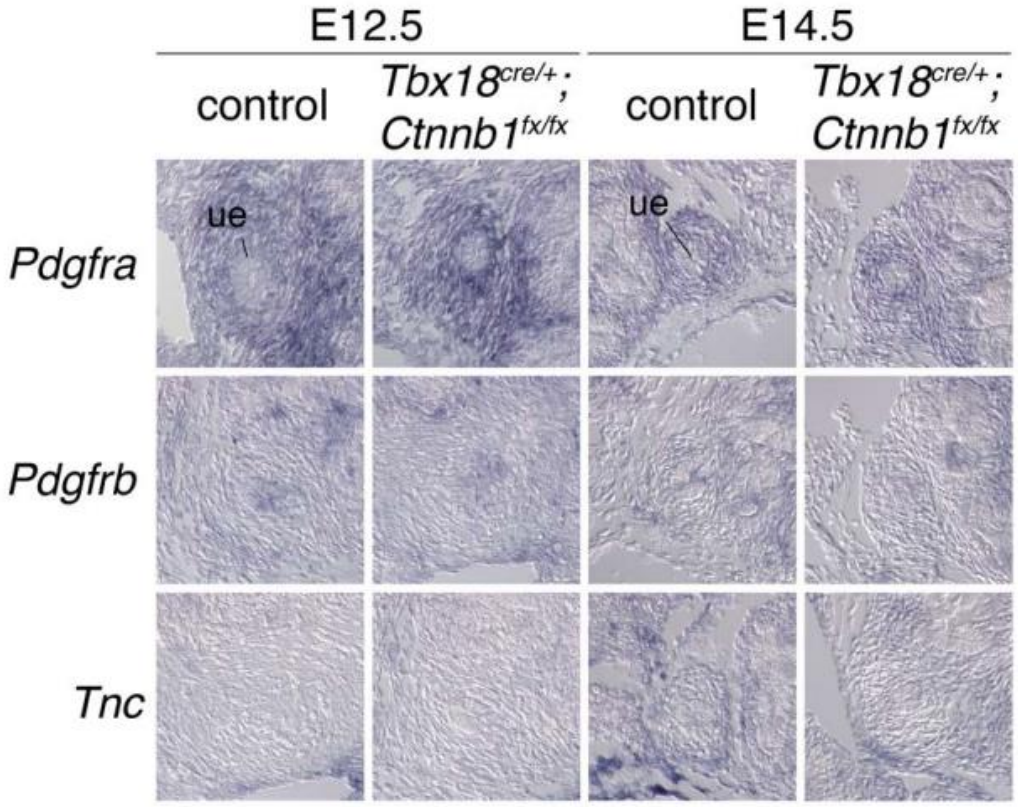

Fig. S10. *Ctnnb1* function in directing SMC development in the ureteric mesenchyme is not mediated by Pdgfr signaling and tenascin C. In situ hybridization analysis of *Pdgfra*, *Pdgfrb* and *Tnc* expression on transverse section of the proximal ureter in wild-type (control) and *Tbx18*$^{cre/+}$;*Ctnnb1*$^{fx/fx}$ embryos at E12.5 and E14.5. ue, ureteric epithelium.

9. Manuscript I

Tbx18 suppresses metanephric development

Eva Bettenhausen[1], Anna-Carina Weiss[1], Mark-Oliver Trowe[1], Anna-Barbara Foik, Carsten Rudat[1], Henner Farin and Andreas Kispert[1,*]

[1]Institut für Molekularbiologie, Medizinische Hochschule Hannover, Hannover, Germany

*Corresponding author
Address:
Institut für Molekularbiologie, OE5250, Medizinische Hochschule Hannover, Carl-Neuberg-Str. 1, D-30625 Hannover, Germany. TEL.: +49 (0)511 5324017; fax: +49 (0)511 5324283.
E-mail address: kispert.andreas@mh-hannover.de (A. Kispert)

Manuscript in preparation

ABSTRACT

The collecting duct system of the kidney, as well as the straight tube of the mature ureter, is derived from a common primordium, the ureteric bud. Differential development is not an autonomous program of this epithelial tissue but is triggered by the surrounding mesenchyme. We have previously shown that the T-box transcription factor Tbx18 is specifically expressed in the undifferentiated ureteric mesenchyme (UM) and marks this lineage in the mouse. Loss of *Tbx18* results in formation of a severely shortened ureter which fails to acquire smooth muscle cells. Here we show that ectopic expression of *Tbx18* in the posterior trunk mesenchyme, including the entire metanephric field of mouse embryos, results in kidney agenesis due to a failure of ureter bud formation after the early loss of the nephrogenic cord by apoptosis. Analysis of *Tbx18*-deficient kidney rudiments revealed ectopic expression of the nephrogenic mesenchyme specific gene *Eya1* and its target gene *Gdnf* in the UM. Ectopic expression of these two markers correlated with formation of an epithelial protrusion from the ureter and altered branching morphogenesis. Misexpression of *Eya1* in the entire mesenchyme of the urogenital ridge (UGR) and the metanephric field led to disturbed ureter budding and branching indicating that de-repression of *Eya1* partly contributes to the phenotypic changes of the *Tbx18*-deficient urogenital systems (UGS). Our study shows that localized expression of *Tbx18* in the metanephrogenic field is required for proper formation of ureter and kidney.

INTRODUCTION

In early embryonic development kidneys and ureters arise from the urogenital ridge (UGR), a precursor field, which is derived from the intermediate mesoderm. Within the mesenchyme of the UGR the nephric duct (ND, also known as Wolffian duct) is established as an epithelial precursor structure of both organs around E8.5 at the level of the forelimb buds. All further development of the organ system depends on signal exchange between the epithelium of the ND and the adjacent strand of nephrogenic mesenchyme. The ND extends in a caudal direction, inducing tubular structures, the mesonephric tubules, in this mesenchyme. At E9.75 it reaches the cloaca, an endodermal infolding at the caudal pole of the UGR. Slightly anterior to the cloaca the ureteric bud (UB), an epithelial diverticulum of the ND, emerges. At E10.5 it invades the metanephric blastema or metanephric mesenchyme (MM), at the caudal end of the strand of nephrogenic mesenchyme. The region, where kidney and ureter development are initiated by this process is also called the metanephrogenic field. From now on the proximal end of the UB which has invaded the MM undergoes repetitive dichotomous branching to generate the highly arborized collecting duct system (CDS) of the kidney. The distal part of the UB merely elongates to give rise to the epithelial component of the mature ureter. Mesenchymal cells surrounding either aspect of the UB take different developmental routes. Those covering the branching tips of the CDS will form nephrons or differentiate into stroma, whereas the mesenchyme along the ureter stalk (and the bladder epithelium) differentiates into SMCs and fibroblasts [1,2].

Tissue separation experiments have revealed that the proximal-distal segmentation of the UB into a kidney and a ureter-forming region does not depend on extrinsic cues but is intrinsic to the ureteric epithelium (UE) and its surrounding mesenchyme. Transplantation experiments of UE into different mesenchymal regions of the early metanephric field have shown that the mesenchyme is specified first and that it dictates the fate of the underlying epithelium [1,3–5]

A large number of studies have characterized a network of transcription factors including *Pax2*, *Wt1*, *Eya1*, *Six1*, *Six2*, *Osr1*, and *Hox11* paralogs, that are coordinately required for formation, proliferation, survival of the nephrogenic mesenchyme and consequently for kidney development [6]. The factor acting most upstream in setting up the nephrogenic precursor tissue is the zinc-finger transcription factor Osr1. Osr1 maintains expression of *Pax2* and *Eya1* which is required for survival of the nephrogenic mesenchyme [7,8]. The transcriptional co-activator Eya1 then teams up with Six (sine oculis) homeobox transcription factors, most likely Six1 and Six4 to regulate survival and proliferation of the nephrogenic mesenchyme and to maintain expression of *Pax2, Pax8* and *Sall1* specifically in the metanephric mesenchyme [9,10]. In the MM Eya1 forms a complex with Hox11 paralogs and Pax2 to induce expression of *Six2* and of glial-derived neurotrophic factor, *Gdnf* [11–13]. Analysis of triple heterozygous *Eya1*$^{+/-}$;*Six1*$^{+/-}$;*Pax2*$^{+/-}$-mutants, which show a strong

reduction of *Gdnf* expression indicates that also Six1 is involved in the regulation of *Gdnf* expression in the (MM). Gdnf binding to the tyrosine-kinase receptor Ret, expressed in the ND epithelium, triggers UB formation and subsequent branching morphogenesis of the collecting duct system [14]. From that stage on expression of MM markers is maintained only in the clusters of nephrogenic mesenchyme which form around the ureteric tips, the so called cap mesenchyme (CM). These nephrogenic precursors will give rise to all nephrons of the developing kidney.

The regulatory network that specifies the ureteric mesenchyme has been less well characterized. Gene expression studies and genetic experiments however have identified a crucial role for the T-box transcription factor Tbx18 [1,15]. Expression of *Tbx18* starts in the UGR around E9.0 in a mesenchymal subdomain distinct from the nephrogenic mesenchyme. Between E10.0 and E10.5, when the UB emerges, *Tbx18* expression becomes detectable in the metanephrogenic field in the mesenchyme between the MM and the ND mesenchyme, indicating a subdivision of the metanephrogenic field into at least three subregions at this stage. Between E11.5 and E12.0, the expression of *Tbx18* becomes restricted to the mesenchyme, which lies inside a certain range of distance from the ureteric epithelium. Expression is downregulated after E14.5 but persists at low levels in the ureteric smooth muscle cells, which start to differentiate at this stage [1,15].

Genetic lineage tracing using a cre knock-in allele of *Tbx18* showed that *Tbx18*-derived cells give rise to all mesenchyme derived cell types of the ureter including the ureteric smooth muscle layer and the inner and outer connective tissue layer, *lamina propria* and *lamina adventitia* [1]. Genetic ablation of *Tbx18* results in severe defects of the urinary tract. The ureter is severely shortened and dilated, appearing more like an expanded pelvis and lacking smooth muscle cells [15]. Further analysis showed that the cells of the UM no longer respond to signals from the ureteric epithelium but adopt a renal stroma fate and disperse from the ureter [1]. Together these results suggest that Tbx18 plays a crucial role in ureter development, possibly by specifying the ureteric mesenchyme (UM).

Here, we investigate the functional consequences of misexpression of *Tbx18* in the early metanephrogenic field in order to identify target genes and the molecular mechanism regulated by Tbx18 in ureter development. We show that *Tbx18* is sufficient to suppress the metanephrogenic fate, and that deregulation of *Eya1/Gdnf* may contribute to the observed changes in *Tbx18* misexpressing and *Tbx18*-deficient mice. These results point towards a function of Tbx18 in specifying the UM-progenitor population by preventing the nephrogenic character in this mesenchymal sub-population of the metanephrogenic field.

MATERIAL AND METHODES

Mice

To generate a conditional misexpression allele of *Eya1* we used a knock-in strategy to integrate a bicistronic transgene-cassette, consisting of the *Eya1* ORF and IRES-GFP into the ubiquitously expressed X-chromosomal hypoxanthine guanine phosphoribosyl transferase (*Hprt*) gene locus [16]. ES cell work and generation of chimeras was done as described for the generation of an $Hprt^{CAG::Sox9}$ allele [17] $Hprt^{CAG::Eya1}$ ($Hprt^{Eya1}$) mice, as well as mice carrying a $Tbx18^{tm2Akis}$ ($Tbx18^{GFP}$) or $Tbx18^{tm4(cre)Akis}$ ($Tbx18^{cre}$) null allele [18,19] or an $Hprt^{Tbx18}$ allele for conditional misexpression of *Tbx18* [20], mice with a $Gt(ROSA)26Sor^{tm4(ACTB-tdTomato-EGFP)Luo}$ ($R26^{mTmG}$) reporter allele [21], and Tg(Pax3-cre)1Joe (*Pax3-cre*) transgenic mice [22] were all maintained on an NMRI outbred background. *Tbx18* misexpressing mice were obtained by mating *Pax3-cre/+* males to $Hprt^{Tbx18/Tbx18}$ females. $Tbx18^{cre/+};R26^{mTmG/+}$ mice were obtained by mating $Tbx18^{cre/+};R26^{mTmG/mTmG}$ males to NMRI wildtype females. $Tbx18^{GFP/GFP}$ mice were generated by mating $Tbx18^{GFP/+}$ males to $Tbx18^{GFP/+}$ females. $Tbx18^{cre/+};Hprt^{Eya1}$ and $Pax3\text{-}cre/+;Hprt^{Eya1}$-misexpression mice were obtained by mating $Tbx18^{cre/+}$ or *Pax3-cre/+* males to $Hprt^{Eya1/Eya1}$ females. As controls we used embryos without a cre-allele.

For timed pregnancy vaginal plugs of mated females were checked in the morning. Noon of the day when a plug was detected was designated E0.5. Embryos were dissected in PBS. After dissection isolated tissues of decapitated embryos were fixed in 4% paraformaldehyde/PBS overnight and washed in PBS and dehydrated in methanol for storage at -20°C on the following day.

In situ hybridization analysis

We performed whole-mount RNA *in situ* hybridizations following a standard procedure with digoxigenin-labeled antisense riboprobes [23]. Stained specimens were transferred in 80% glycerol for documentation. *In situ* hybridization on 10-µm paraffin sections was done essentially as described [24]. For each marker we analyzed at least three independent specimens.

TUNEL assay

To perform the TUNEL (TdT-mediated dUTP-biotin nick end labeling) assay we used the ApopTag kit for in situ apoptosis fluorescein detection (catalog no. NC9815837, Millipore) following the manufacturer's instructions.

Histological and immunohistochemical analyses

Tissues for histological and immuno-histochemical stainings were fixed in 4% PFA and dehydrated stepwise with methanol for storage. After embedding in paraffin, sections of 5 µm thickness were prepared. For histological analysis the tissue sections were stained with hematoxylin and eosin (H&E). For immunohistochemical detection of antigens we used a mouse monoclonal antibody

against ACTA2 (alpha smooth muscle actin; clone 1A4, NatuTec; 1:200), which was labeled with FITC directly and a rabbit polyclonal antibody against GFP (sc-8334, Santa Cruz; 1:100). For fluorescent staining we used Alexa555-conjugated goat-anti-rabbit antibodies (A21428, Invitrogen; 1:500) or biotin-conjugated goat-anti-rabbit antibodies (Dianova; 1:500) for amplified stainings. For amplification we used the TSA Tetramethylrhodamine Amplification Kit (PerkinElmer). After deparaffination of the tissue sections antigen retrieval was done using an acidic Antigen Unmasking Solution (Vector Laboratories) for 10 min in a pressure cooker. Endogenous peroxidases were inactivated by incubation with 3% H_2O_2 for 10 min at room temperature. For blocking prior to incubation with the primary antibodies we used TNB blocking buffer (PerkinElmer) for 30 min and Mouse-on-Mouse Mouse-Ig blocking reagent for 30 min for blocking endogenous mouse immunoglobulins. Incubation with the primary antibodies was done overnight at 4°C.

Organ cultures

Explant cultures of embryonic kidneys were done as previously described {Airik, 2010 #68}. The culture medium was replaced every 24 hours. GFP expression was detected in the cultures via epifluorescence. For tissue recombination experiments we explanted an E11.5 *Pax3-cre/+;Hprt*$^{Tbx18/y}$ acceptor UGS, dissected ureters of *Tbx18*$^{+/+}$*;R26*$^{mTmG/+}$ embryos at E12.5, and separated the ureteric mesenchyme from the ureteric epithelium mechanically using forceps. We then transplanted the ureteric epithelium on the dorsal side of the *Pax3-cre/+;Hprt*$^{Tbx18/y}$ UGS. The recombined tissues were documented every 24 h for 7 days. Videos for documentation of peristaltic movements were recorded on the last day of culture.

Image analysis

Whole-mount specimens were photographed on Leica M420 with Fujix digital camera HC-300Z, sections on Leica DM5000B with Leica digital camera DFC300FX. GFP epifluorescence in living tissues was documented with the Leica DMI 6000 microscope, and the images and movies were processed with Leica Application Suite Advanced Fluorescence Version 2.3.0 software. Confocal images were taken on Leica Inverted-2 with TCS SP2 scan head. Images for figure files were processed in Adobe Photoshop CS4.

RESULTS

Misexpression of *Tbx18* in the posterior trunk mesenchyme suppresses kidney development

In the developing UGS*Tbx18* expression is confined to the prospective and definitive ureteric mesenchyme and is absent from the nephrogenic lineage in the entire UGR [1]. To address the significance of this highly localized expression and to explore the potential of this transcriptional regulator to impose a ureteric fate, we used a conditional Cre/loxP-based transgenic approach to misexpress *Tbx18* in the entire metanephrogenic field. For this purpose, we employed a recently described mouse line harboring a bicistronic transgene-cassette containing the mouse *Tbx18* open reading frame followed by IRES-GFP integrated in the ubiquitously expressed X-chromosomal hypoxanthine guanine phosphoribosyl transferase locus (*Hprt*^{Tbx18}) [20,25], and a *Tg(Pax3-cre)1Joe* (short: *Pax3-cre*) line that mediates recombination in the mesenchyme of the posterior trunk including the entire metanephric field [17,22]. Due to random X-chromosome inactivation, female *Pax3-cre/+;Hprt*$^{Tbx18/+}$ embryos showed a mosaic pattern of misexpression. Male *Pax3-cre/+;Hprt*$^{Tbx18/y}$ embryos expressed the transgene in a uniformly in all recombined cells and were subsequently used for phenotypic analysis. Litter mates without the *Pax3-cre* allele were used as controls (**Fig. 1**).

Morphological analysis of the UGS at E18.5 revealed the absence of kidneys and ureters in male *Pax3-cre/+;Hprt*$^{Tbx18/y}$ mice (N=12). The testis had an elongated, irregular shape and was in direct contact with the adrenal glands rather than being round and descended, like in the wildtype. Female *Pax3-cre/+;Hprt*$^{Tbx18/+}$ mutants exhibited a diverse spectrum of kidney defects including weak and strong hypoplasia and unilateral agenesis (**Fig. S1**, **Table S1**). As in the male all organs of the UGS were embedded in excessive fibrous tissue (**Fig**. **1A**). To visualize the ND and its derivatives, we introduced the *Hoxb7-GFP* transgene into the mutant background. In the male control, GFP epifluorescence was found in the *vas deferens* and the epididymis, the collecting duct system and the ureter. This analysis confirmed the lack of ureter and collecting duct system in the male at E18.5 and revealed the absence of the UB at E11.5 (N=3) in male mutants. In female mutants kidney malformations due to branching defects of the CDS were confirmed, while at E11.5 phenotypic changes were ranging from normal appearance (N=3) to formation of ectopic UBs (N=1) (**Fig. 1B**).

We conclude that ectopic expression of *Tbx18* in the lower trunk mesenchyme, including the whole metanephric field, prevents the formation of the UB and consequently kidney and ureter development.

The metanephric mesenchyme is not detectable in *Pax3-cre/+;Hprt*$^{Tbx18/y}$ embryos at E11.5

The budding of the ureter is triggered by GDNF from the adjacent MM, we wondered whether the observed phenotypic changes in male *Pax3-cre/+;Hprt*$^{Tbx18/y}$ mutants resulted from loss of *Gdnf* expression and/or establishment of the MM. *In situ* hybridization analysis of whole dissected E11.5 UGS revealed absence of *Gdnf* expression in the mesenchyme of the nephrogenic strand region. The same was true for *Uncx*, *Eya1*, *Six2*, *Pax2*, *Sall1*, *Wt1* and *Nr2f2*, which all mark the nephrogenic lineage at this stage. Expression of *Wt1* and *Nr2f2* in the mesenchyme next to the ND and of *Pax2* in the ND epithelium, was, however, maintained in the mutant. In the wildtype *Six1* was detectable in the MM and in the surrounding mesenchyme. In the mutant *Six1* expression was still detectable. We assumed that this *Six1*$^{+}$ mesenchyme is the population which surrounds the MM in the wildtype and not the nephrogenic mesenchyme itself, although we cannot distinguish between these two possibilities explicitly. Expression of markers restricted to the undifferentiated ureteric mesenchyme in the wildtype including *Bmp4*, *Sox9* and *Gata2* was not changed in *Pax3-cre/+;Hprt*$^{Tbx18/y}$ mice (**Fig. 2**). This finding indicates that ectopic expression of *Tbx18* interferes with the establishment or maintenance of the metanephric mesenchyme but does not expand the ureteric mesenchyme.

To address whether the mesenchyme of the metanephrogenic field, including the prospective ureteric lineage, still supports development of the ureteric epithelium, we dissected the UGR from male *Pax3-cre/+;Hprt*$^{Tbx18/y}$ embryos at E11.5 and explanted it onto a membrane. After that the epithelium of an E12.5 wildtype ureter was placed on the explant surface. The epithelium was visualized by expression of the membrane bound red fluorescent Tomato protein, whereas the mesenchyme of the UGR was marked by GFP fluorescence from the *Hprt*^{Tbx18} allele. The ureteric epithelium was quickly surrounded by GFP^{+} (i.e. *Tbx18* expressing) mesenchymal cells. It grew substantially over a 7-day culture period and gained weak peristaltic activity (**Fig. S2**, **Video S1-3**). We conclude that ectopic expression of *Tbx18* is sufficient to prevent the development of the MM in the metanephric field while a ureteric mesenchymal character that supports ureteric epithelial development is maintained.

Nephrogenic cord precursors are lost by apoptosis in the *Pax3-cre/+;Hprt*$^{Tbx18/y}$ mutant

To find out if the loss of the MM in *Pax3-cre;Hprt*$^{Tbx18/y}$ mice derived from failing establishment of the nephrogenic lineage in the UGR or if the nephrogenic precursor tissue is lost at a later stage, we examined the caudal and cranial region of the UGR of E10.5 *Pax3-cre;Hprt*$^{Tbx18/y}$ embryos. In histological stainings of sections at the level of the hindlimb bud, where the MM is established in wildtype embryos, showed tightly packed mesenchymal tissue surrounded the epithelium of the UB. In *Pax3-cre/+;Hprt*$^{Tbx18/y}$ embryos the UB was absent and loose mesenchyme surrounded the ND at this level, indicating that the metanephric blastema and the UB are not established (**Fig. 3A**,

A', **B**, **B'**). More cranially, in the mesonephric region, the UGR was prominently bulged out in wildtype embryos. The mesenchyme beneath the coelomic epithelial lining appeared dense, particularly in the region next to the ND. In contrast, in *Pax3-cre/+;Hprt*$^{Tbx18/y}$ embryos the ridge was little prominent consisted of loose mesenchyme surrounding the ND (**Fig. 3C**, **C'**, **D**, **D'**).

To characterize the mesenchyme of the UGR on the molecular level, we analyzed the expression of a panel of marker genes by *in situ* hybridization (**Fig. 3E-T**). In wildtype embryos *Osr1* and *Wt1* were expressed throughout the mesenchyme and the coelomic epithelium of the ridge, while *Ret* and *Wnt9b* were restricted to the ND epithelium. Expression of all these markers was unchanged in the mutant (**Fig. 3E-L**). *Pax2* expression was detectable in the ND epithelium as well as in the condensed nephrogenic mesenchyme adjacent to the ND in wildtype embryos. While expression in the epithelium was unchanged in *Pax3-cre/+;Hprt*$^{Tbx18/y}$ embryos, it was not detectable in the mesenchymal part of the ridge in the mutant (**Fig. 3 M** and **N**). Whole mount analysis revealed that *Pax2*$^{+}$ anterior mesonephric tubules were present, similar to the wildtype (arrow heads), however, expression in the nephrogenic cord was absent along the complete UGR in the mutant (**Fig. 3O** and **P**). *Six1* and *Eya1* are also expressed in the nephrogenic cord in the wildtype. In the mutant they were not detectable in the UGR mesenchyme (**Fig. 3Q**, **R**, **S**, **and T**). Interestingly, expression of both genes was also reduced in the dermomyotome of the mutant (arrows in **Fig. 3R** and **T**).

Taken together the strand of condensed nephrogenic mesenchyme was neither detectable by molecular expression analysis nor histologically in the *Pax3-cre/+; Hprt*$^{Tbx18/y}$ embryos. We concluded from this that there had to be either a lack of proliferation or increased apoptosis in the mesenchyme of the UGR at an earlier time point, which led to a failing establishment or a loss of the mesenchymal precursors of the nephrogenic lineage. To identify the underlying mechanism we checked for apoptosis in transverse sections of the cranial trunk region by TUNEL assay. Simultaneously we detected GFP by immunohistochemical staining in the same sections to check if apoptosis was specifically increased in *Tbx18* misexpressing tissue (**Fig. 3 U** and **V**). This analysis showed a strongly increased number of apoptotic cells in mesenchyme adjacent to the ND in the cranial trunk region at E10.0 (N=3). We conclude that the nephrogenic precursor tissue is eliminated by apoptosis in *Pax3-cre/+; Hprt*$^{Tbx18/y}$-mutants. This happens before expression of metanephric mesenchyme specific markers or the typical condensed morphology of the nephrogenic mesenchyme is established.

Expression of metanephrogenic markers is expanded into the UM-domain of *Tbx18*-deficient embryos

As our analysis had shown that *Tbx18* is sufficient to repress nephrogenic mesenchyme development within the UGR, we wondered whether *Tbx18* is also required to do so within the ureteric mesenchyme in the wildtype. We therefore analyzed UGS of E11.5 embryos homozygous

for the *Tbx18*^{GFP} null allele (*Tbx18KO)* by *in situ* hybridization for expression of MM specific markers (**Fig. 4A**). *Osr1, Wt1, Nrf2f*, *Hoxd11*, *Sall1, Six2, Uncx* and *Pax2* were confined to the MM, i.e. the cap mesenchyme, in *Tbx18*-deficient embryos as in the wildtype. In contrast, *Eya1* and its target gene *Gdnf* exhibited an expansion of their expression into the mesenchyme along the ureter in *Tbx18KO* kidney rudiments. *Eya1* showed a strong ectopic expression all along the ureter, while ectopic expression of *Gdnf* was restricted to the UM directly adjacent to the cap mesenchyme. *Six1* showed a weak expression in the MM as well as in the UM in both, wildtype and *Tbx18*-KO mutant, though it seems to be slightly increased in its expression in the *Tbx18KO*-mutant.

A thorough analysis of *Eya1* expression in the urogenital system of wildtype and *Tbx18KO*-embryos from E10.0 until E18.5 showed that *Eya1* is expressed in the mesenchyme next to the ND before ureteric budding at about E10.0 in the wildtype as well as in the mutant. Ectopic *Eya1* expression was maintained in the *Tbx18KO* UM until E12.5 and declined thereafter while *Eya1* is never expressed in the UM in the wildtype (**Fig. S3**). After we found, that there are *Eya1*$^{+}$ cells in the UM compartment in the *Tbx18*-loss of function mutant we wanted to know if the *Eya1*$^{+}$ cells were mislocated MM cells or UM cells which had activated *Eya1* expression ectopically. We detected GFP and Eya1 in an immunohistochemical double staining, in sections of E11.5 kidney and ureter primordia of *Tbx18*$^{GFP/GFP}$-mutants and *Tbx18*$^{GFP/+}$ heterozygous controls (**Fig. 4 B**). In the heterozygous control Eya1^{+} cells were found only in the MM. No double staining with GFP was detectable. In the mutant on the other hand, there were several cells detectable along the ureter which were positive for both markers. This result showed, that the ectopic Eya1^{+} cells along the ureter were no mislocated MM cells but belonged to the Tbx18^{+} UM population and had ectopically activated *Eya1* expression after the loss of *Tbx18*.

As GDNF induces UB formation and maintains outgrowth and branching of the collecting duct tree, we wondered if ectopic expression of *Gdnf* affects epithelial gene expression in *Tbx18*-deficient kidneys or ureteric epithelium. We found the receptor tyrosin kinase *Ret* to be expressed weakly in the stem and strongly in the tips of the ureter in the wildtype at E11.5. In the *Tbx18*-mutant we detected up-regulation of *Ret* in an epithelial outgrowth along the ureter stalk, close to the metanephric mesenchyme. However, expression of *Wnt11*, which also marks the ureteric tips of the wildtype, was not detectable in this ectopic epithelial swelling (**Fig. 4C**). To better visualize this epithelial protrusion during early ureter development, we crossed an *Hoxb7-GFP* allele into the *Tbx18*^{GFP} background and explanted E11.5 metanephric rudiments of *Tbx18*$^{GFP/GPF}$*;Hoxb7-GFP* mutant embryos and *Tbx18*$^{GFP/+}$*;Hoxb7-GFP*-controls. We traced GFP epifluorescence from the *Hoxb7-GFP* allele, which marked all ND-derived epithelial structures, including the ureter and collecting duct system, for 3 days (**Fig. 5 A, B, E, F,G, H, I** and **J**).

To correlate the ectopic swelling with the distribution of *Tbx18*-deficient UM cells, we adjusted the detection settings to also detect GFP from the *Tbx18*^{GFP}-allele, marking the complete UM-precursor population at the day of explantation (**Fig. 5 C** and **D**). In the *Hoxb7-GFP*$^{+}$ cultures the epithelial protrusion on the caudal side of the ureter was clearly detectable at E11.5 (d0 of culture) while the control ureter did not show any sign of branching distal from the initial bifurcation surrounded by the MM (**Fig. 5 A** and **B**). The ectopic epithelial bud in the mutant grew out from the ureter stalk surrounded by GFP^{+} UM (**Fig. 5 C** and **D**). 24 hours later the outgrowth of the epithelial protrusion stagnated, the ureter appearing kinked in the affected region (**Fig. 5 E** and **F**). General differences in the branching mode of the collecting duct system were detectable in the *Tbx18* mutant at this stage. In the wildtype both initial branches of the ureteric bud grew out equally strong and the collecting duct tree developed symmetrically. In the *Tbx18KO*-mutant, the outgrowth of the caudal branch was strongly reduced. After the initial bifurcation all further branching took place normally in the *Tbx18KO*-mutant but the initial asymmetry was maintained throughout the documentation of the culture. This analysis shows that *Tbx18* is required to suppress the early metanephric program in the UM. Ectopic expression of *Eya1* together with *Six1* and their target *Gdnf* might cause secondary changes in epithelial marker expression and morphogenesis in the *Tbx18KO*-mutant.

Ectopic expression of *Eya1* in the UM leads to the development of a proximal hydroureter

To find out if the temporary expansion of *Eya1* expression is of any relevance for the phenotype we observed in the *Tbx18*-loss of function mutant, we used a conditional misexpression approach *in vivo* to direct *Eya*1 misexpression to different mesenchymal domains of the early metanephric field. For this purpose we used a knock-in strategy targeting the gene locus of the Hypoxanthine-guanine phosphoribosyltransferase (Hprt) enzyme to introduce the floxed *Eya1* coding sequence followed by a Venus-GFP recapitulating the strategy previously used for the generation of *Hprt* alleles for *Sox9, Tbx18* and *TBX2* misexpression [17,20,26] We first used the *Tbx18*^{cre} line to direct *Eya1* expression into the prospective UM.

Morphological analysis of whole UGS of *Tbx18*$^{cre/+}$;*Hprt*^{Eya1} embryos at E18.5 showed a weak proximal hydroureter in male misexpression mutants (10/14). In two cases we observed a strong proximal hydroureter and in two individuals no morphological changes were detectable (**Fig. 6A** and **B**). In female mutants three out of thirteen individuals showed a weak proximal hydroureter, the rest was phenotypically unaffected (**Fig. S4**). Histological analysis of male mutants which showed a hydroureter phenotype, revealed a slightly dilated pelvis and a more severe ureter dilation (**Fig. 6C**, **D**). The urothelium was stretched to a monolayer and the surrounding fibroblast layer appeared thin (**Fig. 6E**, **F**). Expression of the smooth muscle marker ACTA2 was severely reduced (**Fig. 6G**, **H**).

First phenotypical changes in the *Tbx18KO*-mutant occur between E11.5 and E12.5, when *Eya1* was ectopically detectable in the UM. Thus we were especially interested in the early effects of ectopic *Eya1* expression in the *Tbx18*$^{cre/+}$;*Hprt*$^{Eya1/y}$-mutant. At E11.5 we checked the expression of *Tbx18* by *in situ*-hybridization and found it to be expressed comparably to the wildtype. The same was true for *Six1*, *Gdnf* and *Ret* (**Fig. 6 K-P**). Furthermore, expression of the UM-marker genes *Tshz3, Gata2, Pod1 and Bmp4* was also unchanged at E11.5 and E12.5 (**Fig. S5**). We conclude that ectopic Eya1 is obviously not sufficient to expand *Gdnf* expression into the UM. The partly disturbed development of the ureteric smooth muscle coat most likely occurs due to interference of ectopic Eya1 with later maintenance of the UM or ureteric smooth muscle differentiation.

Ectopic expression of *Eya1* throughout the trunk mesenchyme causes early defects in ureter outgrowth and severe kidney malformations

To test the consequences of a more widespread and earlier misexpression of *Eya1*, we used the *Pax3-cre* line to direct ectopic *Eya1* expression this time into the entire lower trunk mesenchyme from E9.5 on. UGS, dissected from *Pax3-cre/+;Hprt*^{Eya1}-embryos at E18.5, showed severe morphological changes in the kidney and ureter of male mutants (**Fig. 7 B**). In most cases the kidneys showed a ventral rotation so that the opening of the pelvis into the ureter was located on the ventral instead of the medial side (N=11/13). In some individuals the ureter was severely shortened (N=5/13). The testis had not descended, instead it was fixed to the lateral kidney surface by connective tissue (N=12/13). Furthermore, we observed a caudal elongation of the kidney (N=10/13) and the formation of large cysts, which filled up most of the kidney interior. Histological analysis showed a complete loss of the papilla and pelvis structure in the male mutant (**Fig. 7 D**). The pelvic lumen was subdivided in several big cysts and there was a severe dilatation throughout the collecting duct system up to the ureteric tips in the cortex (**Fig. 7E**, **F**). This indicates an increased hydrostatic pressure throughout the upper urinary system. In female *Pax3-cre/+;Hprt*$^{Eya1/+}$ UGS the orientation of the kidney and the general morphology of the ureter, pelvis and papilla were unchanged (N=8) although in fifty percent of the female mutants cysts were detectable in the renal parenchyme (**Fig. S6**). This was confirmed by histological analysis.

To visualize the ND and its derivatives, we again crossed the *Hox7-EGFP*-allele into the mutant background. In total we dissected twenty-six metanephric primordia from male *Pax3-cre/+;Hoxb7-EGFP;Hprt*$^{Eya1/y}$-mutants at E11.5. In general we observed that the epithelium of the outgrowing ureters and their initial branches appeared flattened and its growth appeared unorganized compared to the controls T-shaped first pair of branches. Only in one out of twenty-six specimens the UB reached the normal T-stage. In ten out of twenty-six we did not detect any outgrowth of a ureter. In some of these ten specimens the epithelium of the ND was flattened as if it had grown unorganized in all directions, in others the initial two ureter branches grew out directly from the ND establishing no ureter between the kidney and the ND at all. In thirteen out of twenty-six

specimens the initial outgrowth of the ureter took place but subsequent branching was disturbed. In four out of these thirteen there was a thickening of the UB tip visible but no branches, in others we found an uneven branching pattern. (**Fig. 7 G**, **H**). Taken together, misexpression of *Eya1* in the lower trunk mesenchyme, including the complete metanephric field, leads to early defects in the growth of the ureteric bud epithelium with a penetrance of 38%.

To find out more about the molecular changes which cause the early defects in ureter development in *Pax3-cre;Hprt*$^{Eya1/y}$-mice we performed an expression analysis of transcription factors and signaling molecules which are known to be involved in the early budding and branching of the ureter at E11.5 (**Fig. 7 I-T**).

After we confirmed *Eya1* misexpression in the entire metanephric field by in situ-hybridization, we checked for expression of *Six1*, which is usually confined to the metanephric mesenchyme and the UM. In the *Pax3-cre/+;Hprt*$^{Eya1/y-}$mutant *Six1* was detectable throughout the UGR and appeared strongly increased in its expression intensity. *Gdnf* was ectopically detectable in the UM along the proximal part of the misshaped ureter though not the complete UM-domain was *Gdnf*$^{+}$. We also detected *Gdnf* expression ectopically in the more caudal mesenchyme towards the cloaca. Expression of *Ret* was clearly increased in the ND and UB epithelium of the *Pax3-cre/+;Hprt*$^{Eya1/y-}$ mutant, not showing the typical restriction to the ureteric tips which we observed in the wildtype. Expression of *Tbx18* as a marker for the UM and *Foxd1* which marks the renal interstitial cell progenitors, were unchanged in their expression.

We conclude that the aberrant growth of the ureteric epithelium might occur due to ectopic expression of *Gdnf* and activation of Gdnf-Ret signaling which is not restricted to the tips of the branching ureteric epithelium in the misexpression mutant.

DISCUSSION

We found that misexpression of *Tbx18* in the entire UGR mesenchyme leads to a loss of the mesenchymal kidney precursor tissue, the nephrogenic mesenchyme, by apoptosis resulting in kidney and ureter agenesis. Furthermore early analysis of *Tbx18* loss of function mutants at E11.5 revealed an expanded expression of MM specific markers in the UM domain. From these results we conclude that *Tbx18* is not only sufficient, but also essential to suppress the early metanephric program to allow normal ureter and kidney development. The analysis of two conditional *Eya1* misexpression mutants gave first indications that ectopic Eya1 might contribute to the development of the *Tbx18*-loss of function phenotype in the role of an effector gene of Tbx18 although the mere expansion of *Eya1* expression into the UM does not seem to be sufficient to expand the metanephric program.

Early misexpression of *Tbx18* can repress nephrogenic mesenchyme development

Our analysis showed that ectopic expression of *Tbx18* throughout the lower trunk mesenchyme prevents the development of the nephrogenic cord and, consequently, of ureter and kidney. As molecular expression analysis of the early intermediate mesoderm markers *Osr1* and *Wt-1* revealed, the UGR was established but failed to give rise to the nephrogenic cord, as indicated by the loss of the specific markers *Pax2*, *Six1* and *Eya1*.

It has been shown before that the transcriptional co-activator Eya1 cooperates with different *Six*-family homeobox-transcription factors and members of other transcription factor families, as a key regulator in metanephric kidney development. Besides its function in the transcriptional activation of *Gdnf* in the MM [10,12], Eya1 is also needed for the earlier survival of the nephrogenic cord progenitor population. In *Eya1*-loss of function mutants as well as in *Six1*/*Six4* double mutant embryos this precursor domain is depleted between E9.5 and E10.5 by apoptosis [27]. As a consequence *Eya1*-loss of function embryos show kidney agenesis due to the failing development of the metanephric blastema and a loss of the caudal mesonephric tubules, which are also derived from *Eya1* expressing nephrogenic mesenchyme [27,28]. This phenotype is strikingly similar to the phenotype of the *Pax3-cre;Hprt*$^{Tbx18/y}$-mutant we examined in this analysis. As *in vivo* analyses in the mouse have shown, *Osr1*, *Eya1* and *Nr2f2* (*CoupTFII*), which also acts upstream of *Eya1*, are the only factors of the specification cascade which are required for the initial formation of the metanephric blastema [8,10,29–37]. *Osr1* and *Nr2f2*, were still expressed in the *Pax3-cre;Hprt*$^{Tbx18/y}$-mutant UGR while *Eya1*, the only of these three factors, which specifically marks the nephrogenic cord, was undetectable. Interestingly expression of *Eya1* and *Six1* was also undetectable in the dermomyotom of *Pax3-cre;Hprt*$^{Tbx18/y}$-embryos at E10.5. As this tissue is also affected by *Tbx18* misexpression, the missing expression in the dermomyotom indicates that *Eya1* is regulated directly by Tbx18 and not only missing due to the complete loss of the nephrogenic progenitor cells. Concerning our initial question about the potential role of Tbx18 in specification of

mesenchymal compartments in the metanephrogenic field these results show that ectopic Tbx18 is sufficient to prevent nephrogenic mesenchyme development after the initial establishment of the UGR, at the point of nephrogenic mesenchyme specification. According to our results *Eya1* might be directly repressed by ectopic Tbx18.

Expansion of the early metanephric program in *Tbx18*-loss of function embryos

After the analysis of the *Tbx18* misexpression mutant had shown a loss of nephrogenic mesenchyme markers, we found an expanded expression of the early metanephric markers *Eya1* and *Gdnf* in the UM domain in *Tbx18*-loss of function mutants while *Six1* was increased in its expression intensity in the early UM-domain. Maybe in response to these molecular changes in the mesenchyme the UE gave rise to an ectopic, Ret^{+} epithelial protrusion of the ureter stalk. The question about the epistatic relationship between Eya1, Six1 and Gdnf cannot be answered from the results we obtained in this analysis, although from the analysis of mouse embryos expressing a hypomorphic allele of *Eya1* ($Eya1^{bor/+}$) it is known that *Eya1* regulates the expression of *Six1* and *Gdnf* in the metanephric mesenchyme [10] while *Eya1* itself does not depend on *Gdnf* or *Six1* expression [10,38]. Furthermore *Six1* and *Eya1* were previously found to interact in regulation of *Gdnf* expression [10]. Based on this we hypothesized that expression of *Eya1* might not only be needed for expression of *Gdnf* but also sufficient to expand it temporarily into the UM, maybe in cooperation with Six1. It has been shown before that ectopic GDNF signaling can cause the outgrowth of ectopic epithelial buds from the ND in kidney explant cultures [30,39,40]. Based on this, we presumed that expansion of *Gdnf* expression might also lead to the ectopic development of an epithelial bud on the *Tbx18KO*-mutant ureter. As it is known that expression of *Gdnf*, which provokes further outgrowth and branching of the ureteric epithelium, has to be maintained in the CM by WNT11 signals coming from the ureteric tip epithelium [41], the lack of *Wnt11* in this ectopic bud might explain why its outgrowth did not continue after E11.5. The lack of *Wnt11* in the ureteric tip epithelium, the lack of many MM specific markers and the cessation of the outgrowth of the ectopic bud showed that not the full metanephric program is initiated ectopically in the *Tbx18* misexpression mutant. In accordance with this finding an earlier fate mapping of *Tbx18*-derived UM-cells in the *Tbx18KO*-mutant has shown, that *Tbx18*-derived-cells never contribute to the CM or nephrons [1]. So obviously a loss of *Tbx18* does not lead to a complete respecification of the proximal UM to a CM-like fate. The mesenchyme rather transiently adopts a kind of early metanephric character, which seems to interfere with its later patterning and smooth muscle differentiation. It remains unclear if and in what way the early molecular changes we found in the *Tbx18*-loss of function mutant might influence the first bifurcation of the ureteric epithelium. These alterations in the first branching process seem to lead to the unsymmetrical later development of the Tbx18 loss-of function mutant kidney, which we found in metanephric explant cultures.

Tbx18 might influence activation of *Gdnf* expression by *Eya1* via competitive binding to Six1 in *Eya1*-misexpression mutants

We found that ectopic expression of *Eya1* in the UM domain did not cause any changes in the early expression of *Six1*, *Gdnf*, or *Ret*, the three markers, which were expanded in their expression in *Tbx18-loss of function*-embryos. Also morphologically no early changes were detectable in $Tbx18^{cre/+};Hprt^{Eya1}$-mutants. A possible explanation for this might be that recombination with the $Tbx18^{cre/+}$-allele occurs insufficiently or too late to allow a strong ectopic activation of *Eya1* at the critical time point. The documentation of explanted UGR dissected from $Tbx18^{cre/+};R26^{mTmG/+}$-embryos has shown that first GFP^+, recombined cells are detectable in the metanephrogenic field at E10.0, when ureteric budding is initiated (data not shown). So it appears very unlikely that recombination by the $Tbx18^{cre}$-allele would not be in time to active *Eya1* in the UM domain between E10.0 and E11.5.

It is known that transcriptional regulation of a gene does not only depend on the DNA-binding specificity of the involved transcription factors but also on the interaction between these factors on the protein level. For example whether Six1 acts as a transcriptional activator or repressor depends on the co-factors present in a certain tissue [42]. Considering this, it is possible that Tbx18 prevents the expansion of the metanephric fate into the UM domain in two different ways, by repressing *Eya1* in this domain and also by preventing Six1/Eya1 protein interaction and target gene activation. The second mechanism might not be relevant in the wildtype situation because *Eya1* is not expressed in the UM in the first place, but in the Tbx18-loss of function situation both regulation mechanisms would be lost and ectopic Eya1 might activate target genes in cooperation with Six1, which is co-expressed. When Eya1 is ectopically expressed in the conditional misexpression mutants on the other hand, one functional copy of Tbx18 is still present and it might prevent cooperation between Eya1 and Six1. Also a competition for binding of Eya1 and Tbx18 to Six1 might occur. In the wildtype *Six1* and *Tbx18* are co-expressed between E12.5 and E18.5 in the smooth muscle and connective tissue precursor cells of the UM [43]. They interact physically to regulate smooth muscle development. Compound heterozygous $Tbx18^{+/-};Six1^{+/-}$-mutants show a proximal hydroureter phenotype which is not detectable in the single heterozygous embryos and which is very similar to the $Tbx18^{cre/+};Hprt^{Eya1}$-misexpression -phenotype at E18.5 described in this study [43]. The point mutations, R110W and Y129C, in the Six-domain of Six1 interfere with effective binding of Tbx18 to Six1 [43]. Interestingly these two mutations were initially identified in a study with branchio-oto-renal- (BOR) syndrome patients, where they interfere with binding of Eya1 to Six1 [44]. Obviously the same Six1-binding sites are occupied by Tbx18 and Eya1. Hence a competitive binding is possible and could explain the missing early effect of *Eya1*-misexpression in the $Tbx18^{cre/+};Hprt^{Eya1/y}$-mutant.

Most interestingly, we found that early misexpression of *Eya1* in the complete lower trunk mesenchyme of *Pax3-cre/+;Hprt*^{Eya1}-mutant embryos, does not only lead to an altered expression of *Six1*, *Gdnf* and Ret, but it also severely affects kidney and ureter morphogenesis. At E18.5 we recognized several aspects of the described *Tbx18*-loss of function phenotype in these mutants [15], like the ventral rotation of the kidney and the extremely short, dilated ureter. We were able to trace these changes back to defects in the initial outgrowth of the UB and the establishment of the first bifurcation at E11.5. In 38% of the cases ureteric branching seemed to take place directly from the ND without prior outgrowth of a ureter stalk. These defects in the early epithelial growth occurred most likely due to aberrant expression of *Ret* and *Gdnf*. Ectopic expression of *Six1* in the *Pax3-cre,Hprt*$^{Eya1/y}$-mutant indicates that Eya1 can expand the early metanephric program. Also *Gdnf* is expanded into the UM and towards the cloaca, although there is still a mesenchymal domain along the distal part of the ureter which remains *Gdnf*-negative. The explanation for this might be the same we already suggested for the *Tbx18*$^{cre/+}$*;Hprt*^{Eya1}-mutant: Eya1 competes with *Tbx18* for its binding to Six, which interferes with activation of Gdnf expression. Hence *Gdnf* is not expressed throughout the Eya1^{+}/Six1^{+} domain in *Pax3-cre,Hprt*$^{Eya1/y}$-embryos, which indicates that these two factors, although they can expand *Gdnf* expression to some degree, are still not sufficient to activate ectopic expression of *Gdnf* throughout the UGR. Also, *Gdnf* is not expanded in the cranial direction along the UGR, which implies that the regulation of its expression in this direction by Foxc1 and Robo2-Slit2 signaling [45,46] is still intact in spite of ectopic Eya1 and Six1. Most likely secondary to mesenchymal changes also expression of *Ret* is increased in its intensity in the epithelium of the ureteric bud showing no restriction to the tips of the branching epithelium. This unrestricted expression of *Ret* might well cause the rather unorganized, irregular growth pattern of the ureteric bud in the *Pax3-cre,Hprt*$^{Eya1/y}$-embryos. Taken together these results imply that misexpression of *Eya1* can in fact activate a part of the early metanephric program in the UGR, involving exactly the same factors we found ectopically in the *Tbx18*-mutant, but this ectopic activation does not seem to occur in tissues which still express a functional allele of *Tbx18*.

Taken together the results of the early analysis of the *Tbx18*-loss of function phenotype indicate that Tbx18 is needed during early kidney and ureter development to repress the metanephric program in the UM. This might occur both on the transcriptional and the protein interaction level.

FIGURES AND FIGURE LEGENDS

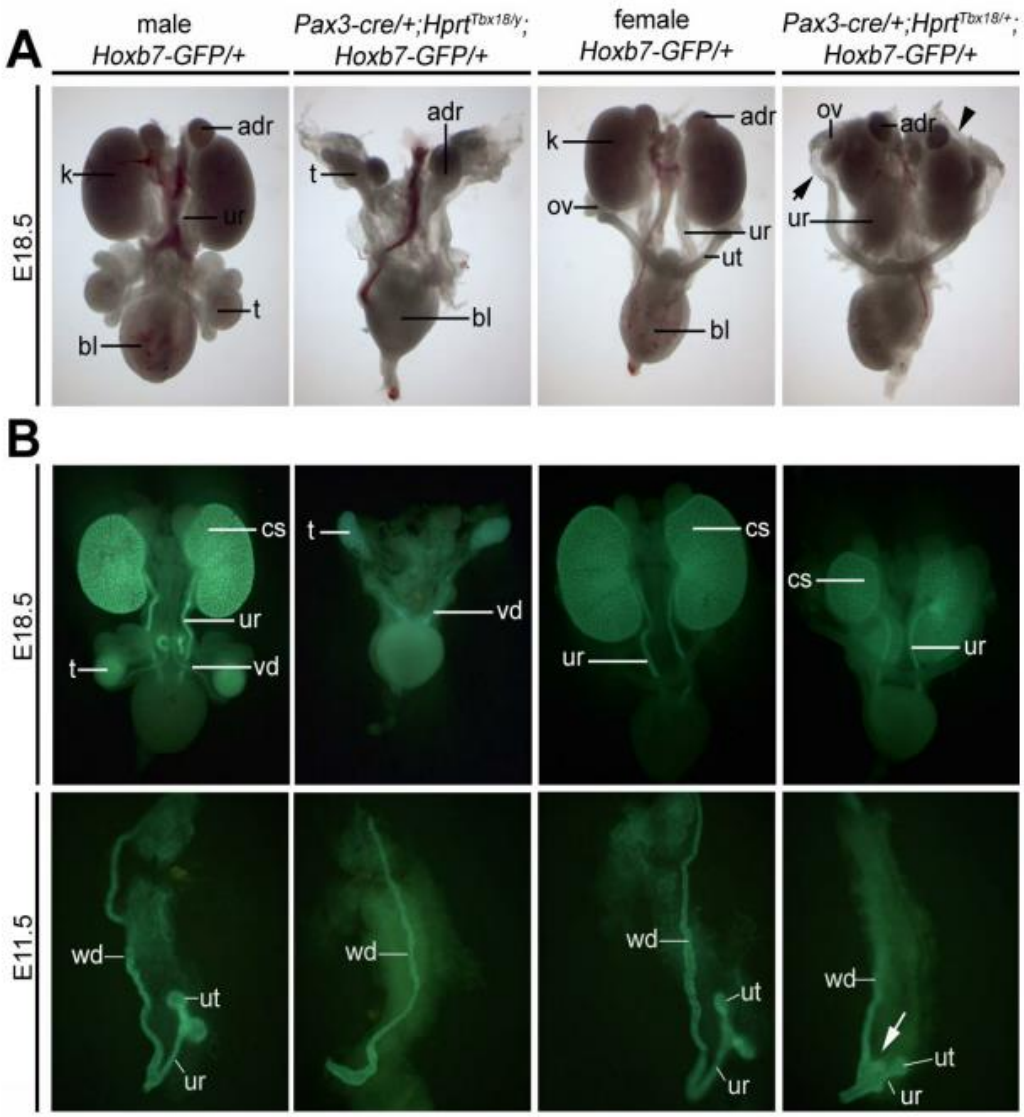

Fig.1: Misexpression of *Tbx18* in the posterior trunk mesenchyme suppresses kidney and ureter development.

Morphological analysis of whole UGS at E18.5 (**A**). Arrowheads point to excessive connective tissue in the mutants. Arrow points to ectopically placed female gonad. Epifluorescent tracing of GFP from the *Hoxb7-GFP* transgene to visualize the ND and its derivatives, the ureteric bud, the renal collecting duct system and the ureters at E18.5 and E11.5 (**B**). Arrow in (**B**) indicates an ectopic ureteric bud. Genotypes and stages are as indicated. adr, adrenal gland; b, bladder; cs, collecting duct system k, kidney; nd, nephric duct; ov, ovary; t, testis; ur, ureter; us, uterus; ut, ureteric tip; vd, *vas deferens*.

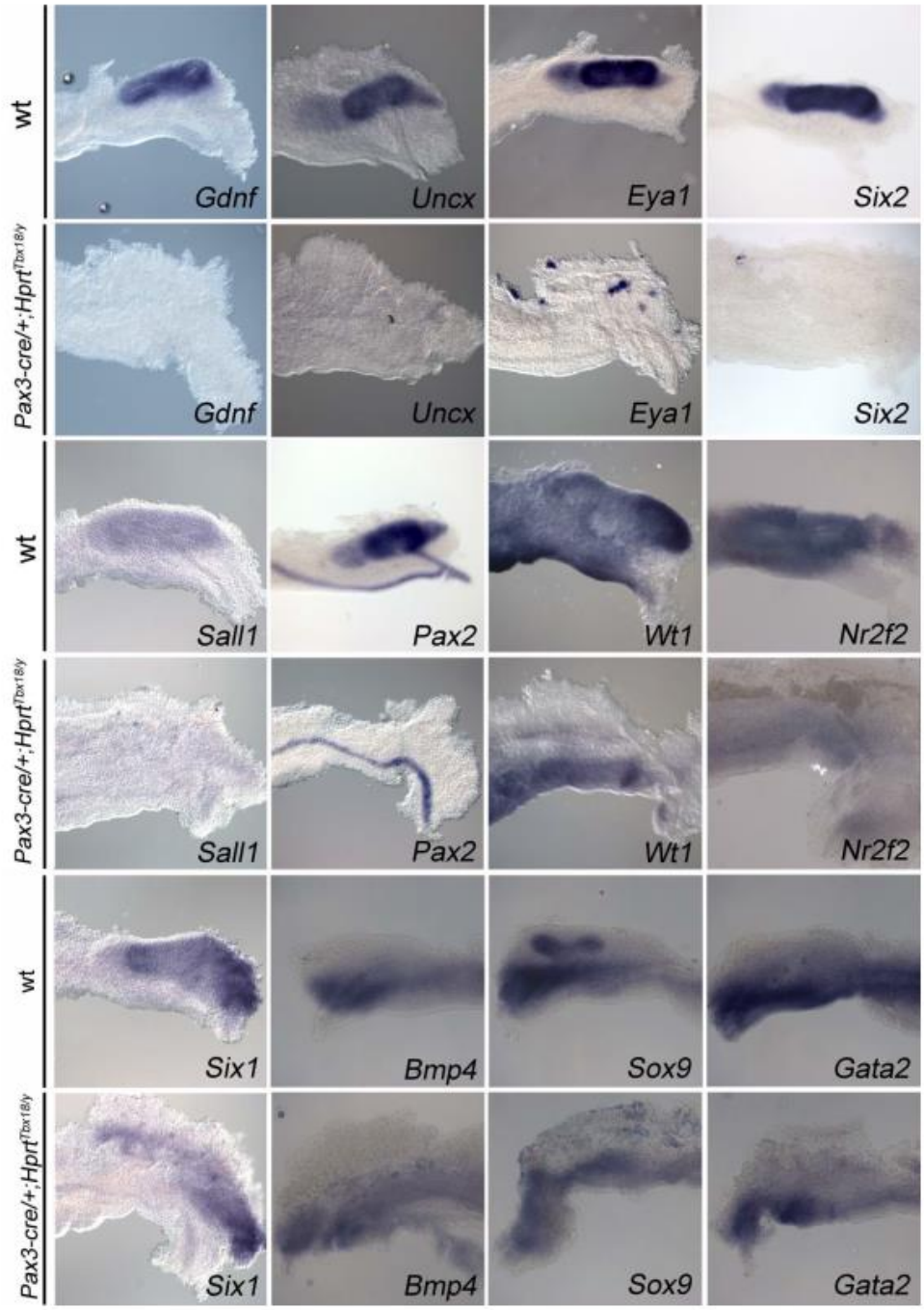

Fig.2: Misexpression of *Tbx18* in the whole metanephric field interferes with expression of markers of the metanephrogenic mesenchyme.

Whole mount *in situ* hybridization expression analysis of markers for different lineages of the early metanephric field in E11.5 UGS. Genotypes and stages are as indicated. nd, nephric duct; ur, ureter; ut, ureteric tip.

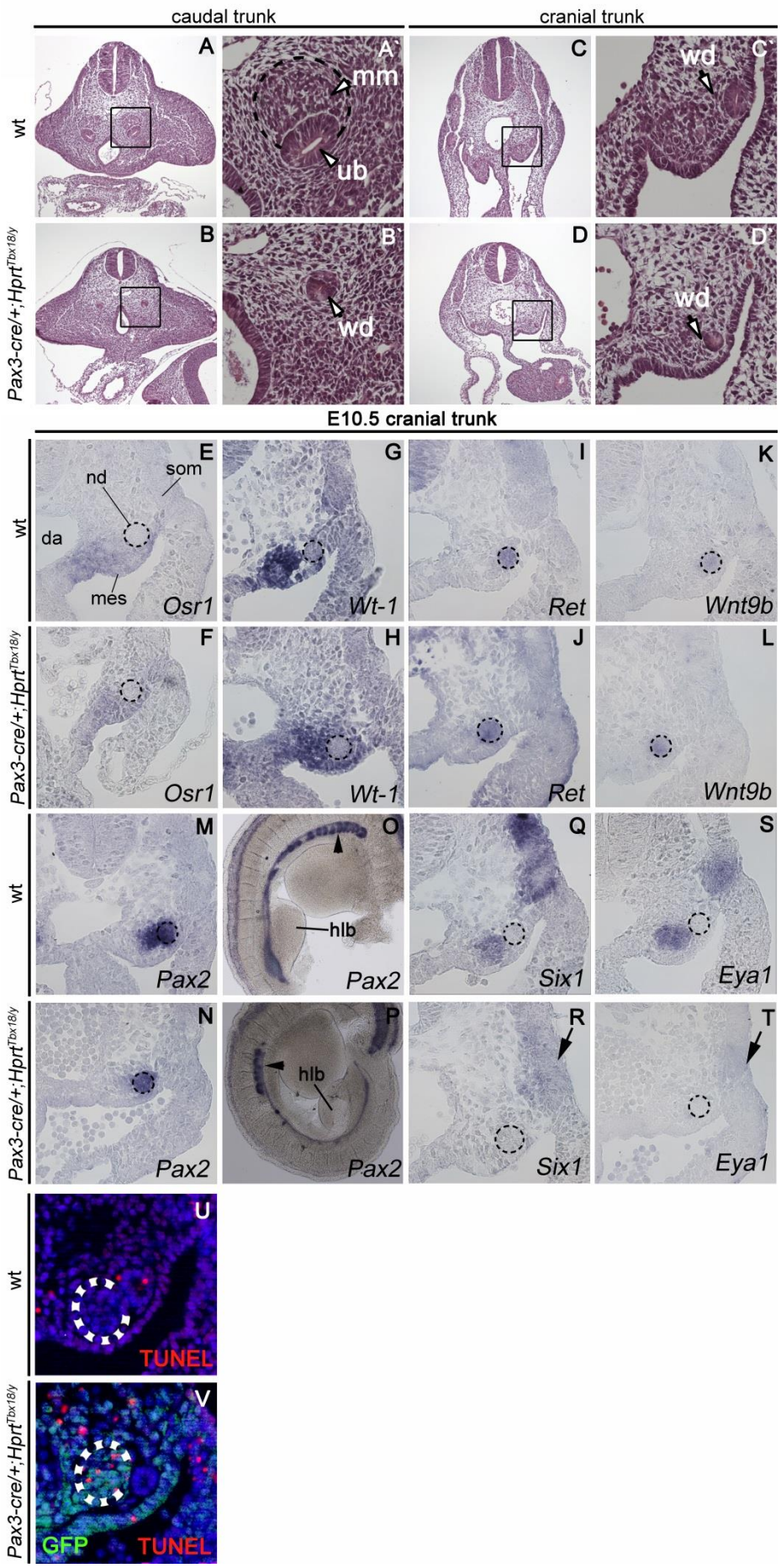
caudal trunk
cranial trunk
wt
Pax3-cre/+;Hprt^Tbx18/y
A
A'
B
B'
C
C'
D
D'
mm
ub
wd
E10.5 cranial trunk
E
F
G
H
I
J
K
L
M
N
O
P
Q
R
S
T
nd
som
da
mes
Osr1
Wt-1
Ret
Wnt9b
Pax2
hlb
Six1
Eya1
U
V
TUNEL
GFP

Fig.3: Ectopic expression of *Tbx18* in the UGR mesenchyme disturbs nephrogenic cord formation.

(**A**- **D'**) Histological analysis by haematoxylin & eosin staining of transverse sections of E10.5 embryos at the level of the hindlimb buds (**A**, **A'**, **B**, **B'**) and the cranial trunk region (**C**, **C'**, **D**, **D'**). Black squares indicate enlarged areas of the MM (**A'**, **B'**) and the mesonephros region (**C'**, **D'**). (**E**) Expression analysis by *In situ* hybridization analysis in transverse sections through the cranial trunk region **(E**-**N** + **Q**-**T**) and in whole posterior trunks (**O**, **P**). Black dashed lines indicate the ND. Arrow heads in **O** and **P** mark mesonephric tubules. Arrows in **R** and **T** indicate the dermomyotome. Detection of apoptosis via TUNEL assay in transverse sections of the cranial trunk area in *Pax3-cre/+;Hprt*$^{Tbx18/y}$ and wt control embryos at E10.0 (**U** and **V**). White dashed line circles indicate the area of the nephrogenic mesenchyme. Genotypes and stages are as indicated. Embryos were stage matched by counting of somites. ce, coelomic epithelium; da, dorsal aorta; dm, ventral region of the dermomyotome; fl, forelimb bud; hl, hindlimb bud; mm, metanephrogenic mesenchyme; mt, mesonephric tubules; nd, nephric duct; ub, ureteric bud; ugr, urogenital ridge.

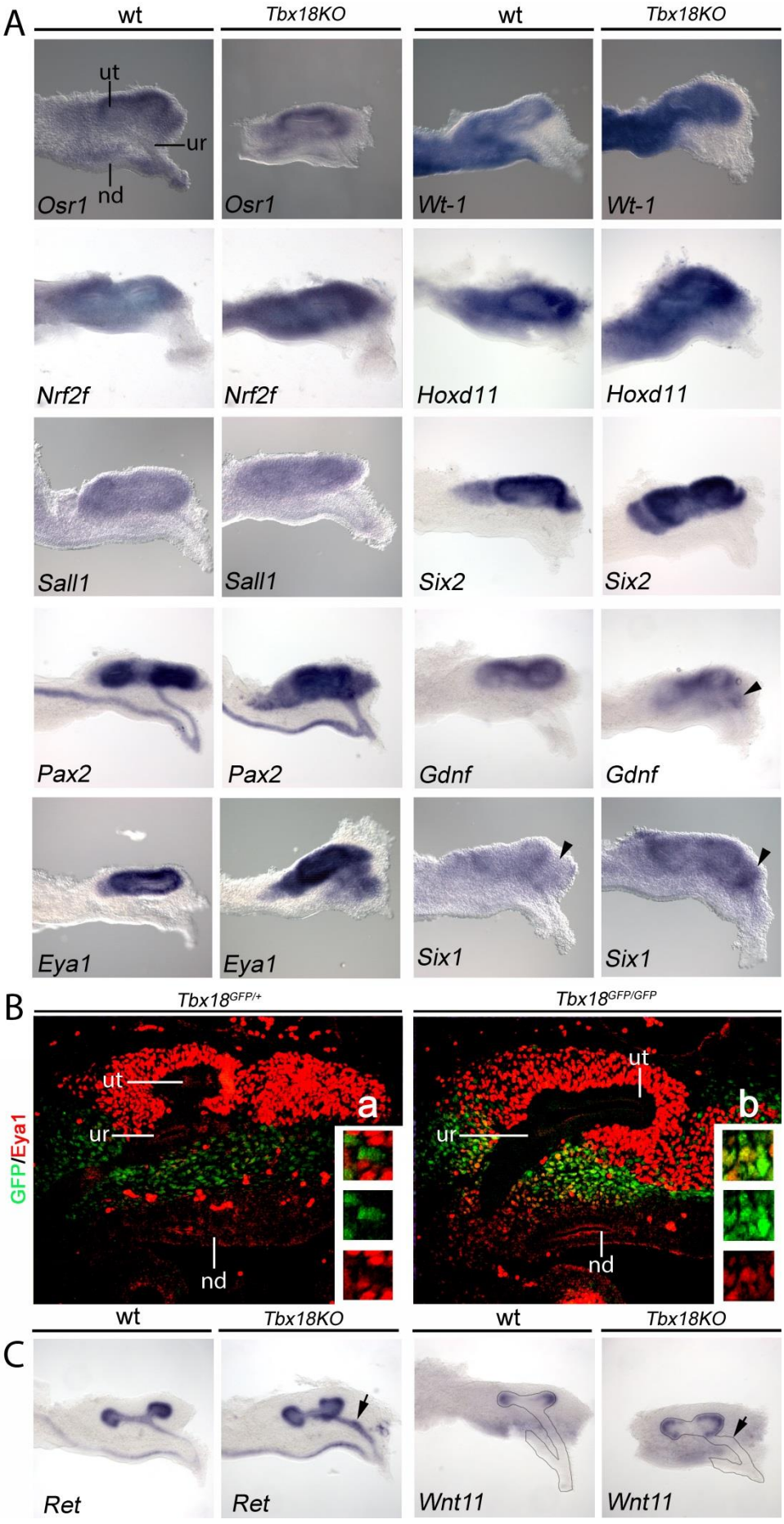
A
wt
Tbx18KO
wt
Tbx18KO
ut
ur
nd
Osr1
Osr1
Wt-1
Wt-1
Nrf2f
Nrf2f
Hoxd11
Hoxd11
Sall1
Sall1
Six2
Six2
Pax2
Pax2
Gdnf
Gdnf
Eya1
Eya1
Six1
Six1
B
Tbx18GFP/+
Tbx18GFP/GFP
GFP/Eya1
ut
ur
nd
a
b
C
wt
Tbx18KO
wt
Tbx18KO
Ret
Ret
Wnt11
Wnt11

Fig.4: Partial expansion of metanephrogenic markers into the UM of *Tbx18*-deficient mice.

Expression analysis of metanephric mesenchyme markers in *Tbx18KO*-mutants at E11.5 via *in situ* hybridization in dissected UGR (**A**). Arrowheads in **A** indicate expanded expression of MM markers in the UM. Detection of Eya1 and GFP in double stainings via immunohistochemistry in sections of $Tbx18^{GFP/+}$ and $Tbx18^{GFP/GFP}$ kidney and ureter primordia at E11.5 (**B**). Detail pictures of nuclei, which show no co-localization of Eya1 and GFP in the *Tbx18*-heterozygous control (**a**) and of nuclei, which show co-localization of both markers in the *Tbx18*-loss of function mutante (**b**). Expression analysis of ureteric epithelium markers in *Tbx18KO*-mutants at E11.5 via *in situ* hybridization in dissected UGR (**C**).Arrows in **C** indicate an ectopic epithelial protrusion of the ureter. cm, cap mesenchyme; nd, nephric duct; ur, (distal) ureter stalk, ut, ureteric tip.

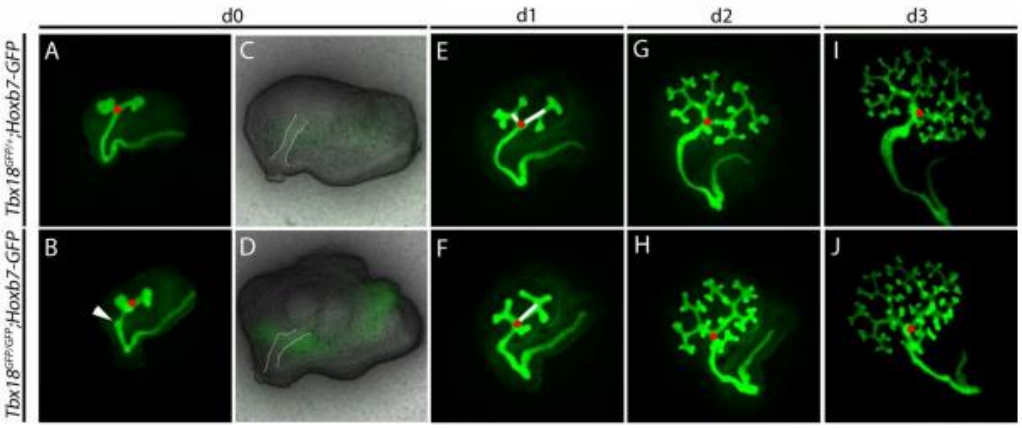

Fig.5: Altered branching morphogenesis in *Tbx18*-deficient ureters and kidneys

Metanephric rudiments of from *Tbx18*$^{GFP/GFP}$-mutant embryos and heterozygous controls were explanted at E11.5 (d0 of culture). To visualize the ureteric epithelium a *Hoxb7-GFP* transgene was used, which marked all ND-derived epithelia by GFP expression. GFP from either the *Hoxb7-GFP* transgene or from the *Tbx18*^{GFP} knock-in allele were detected via epifluorescence. The explants were documented for 3 days after explantation. Red dots mark the point of the first ureter bifurcation, white lines in **E** and **F** mark the first collecting duct system branches. White arrow head in **B** marks ectopic epithelial protrusion on the mutant ureter. *Tbx18*$^{GFP/+}$ heterozygous and *Tbx18*$^{GFP/GFP}$ mutant kidney rudiments (**C**+**D**) White lines outline the ureteric epithelium.

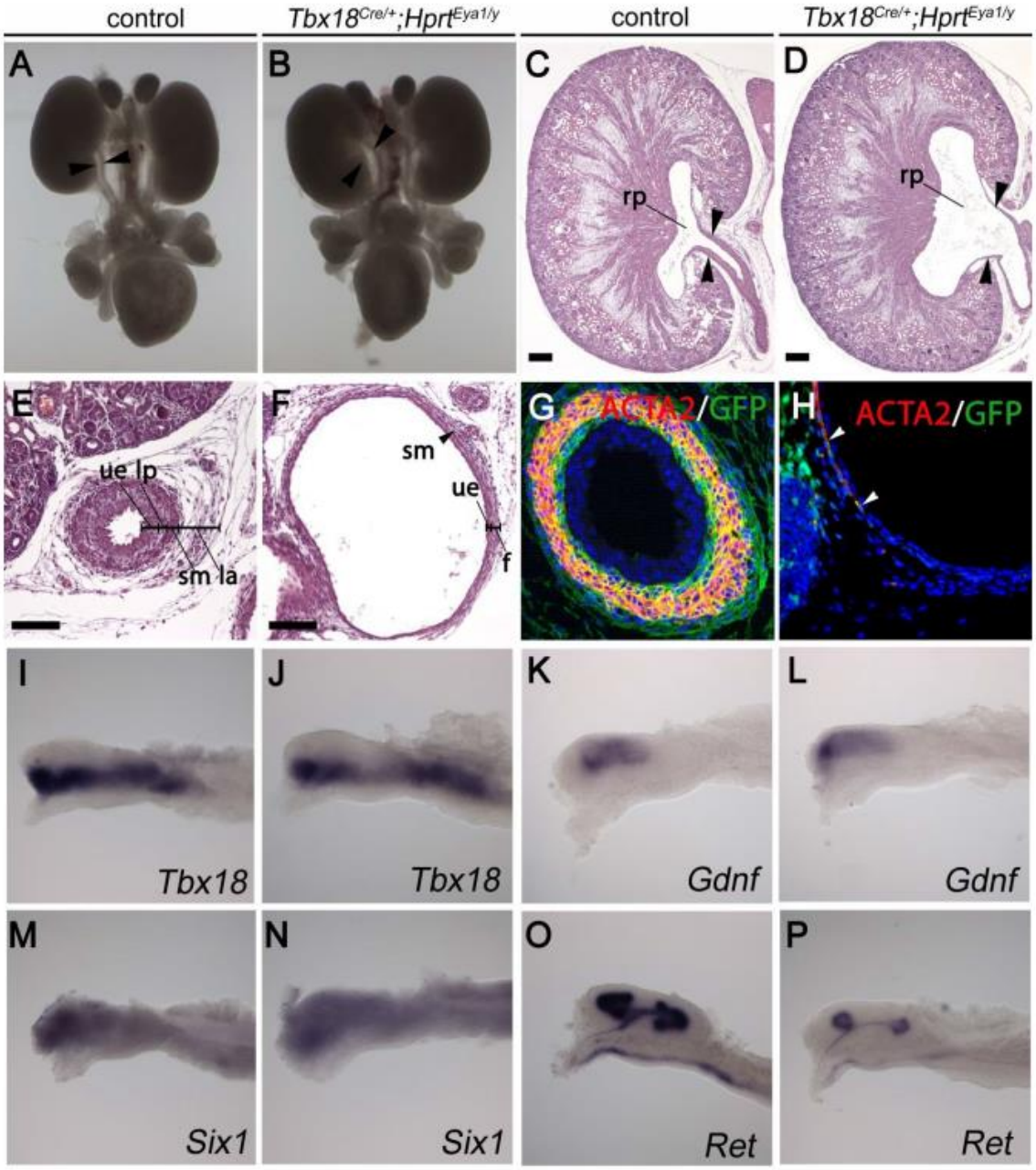

Fig.6: Ectopic expression of *Eya1* in the UM-derived cells causes development of a proximal hydroureter. Morphological analysis of whole UGS at E18.5 (**A** and **B**). Arrow heads frame the proximal ureter. Histological examination by H&E staining of mid-sagittal sections of kidney and proximal ureter (**C** and **D**) and of transverse sections of the proximal ureter of *Tbx18*$^{cre/+}$;*Hprt*$^{Eya1/y}$ embryos at E18.5 (**E** and **F**). Immunohistochemical detection of GFP and ACTA2 in transverse proximal ureter sections of *Tbx18*$^{cre/+}$;*Hprt*$^{Eya1/y}$ embryos at E18.5 (**G** and **H**). White arrow heads in **H** mark remaining scattered ACTA2^{+} cells in the ureter wall of *Tbx18*$^{cre/+}$;*Hprt*$^{Eya1/y}$ embryos. Expression analysis via whole mount *in situ* hybridization on dissected *Tbx18*$^{cre/+}$;*Hprt*$^{Eya1/y}$-UGR at E11.5 (**I**-**P**). f, fibrocytes; la, *lamina adventitia*; lp, *lamina propria;* ue, ureteric epithelium; sm, smooth muscle layer.

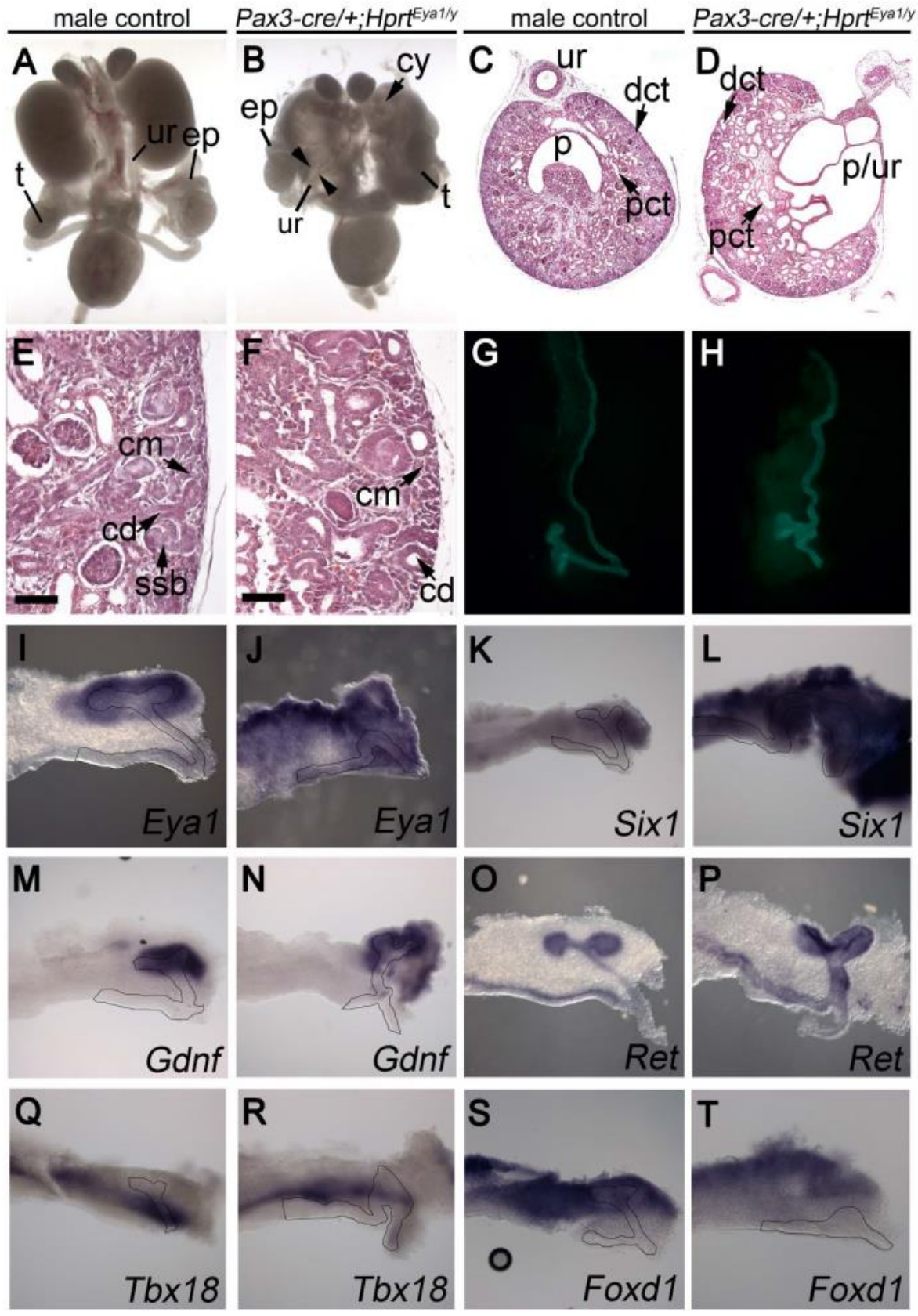
male control
Pax3-cre/+;Hprt^Eya1/y
male control
Pax3-cre/+;Hprt^Eya1/y
A
ur
ep
t
B
cy
ep
ur
t
C
ur
dct
p
pct
D
dct
p/ur
pct
E
cm
cd
ssb
F
cm
cd
G
H
I
Eya1
J
Eya1
K
Six1
L
Six1
M
Gdnf
N
Gdnf
O
Ret
P
Ret
Q
Tbx18
R
Tbx18
S
Foxd1
T
Foxd1

Fig.7: Ectopic expression of Eya1 in the throughout the UGR mesenchyme leads to severe ureter and kidney defects after E11.5.

Morphological analysis of dissected UGS at E18.5 (**A** and **B**). Arrow heads frame the proximal ureter. Histological examination by H&E staining of transverse section of kidney and proximal ureter (**C** and **D**) and detail pictures of the renal cortex histology (**E** and **F**) of *Pax3-cre/+;Hprt*$^{Eya1/y}$ embryos at E18.5. (**G** and **H**) Metanephric rudiments of *Pax3-cre/+;Hoxb7-GFP;Hprt*$^{Eya1/y}$ embryos dissected at E11.5 (**G** and **H**). GFP from the *Hoxb7-GFP* transgene was traced via epifluorescence to visualize the ND and ureteric bud. Expression analysis of molecular markers by *in situ* hybridization on metanephric rudiments, dissected at E11.5 (**I** – **T**). dct, distal convoluted tubule; ep, epididymis; ssb, s-shaped body; cd, collecting duct; cm, cap mesenchyme; ur, ureter; cy, cyst; t, testis; p, pelvis; pct, proximal convoluted tubule.

SUPPLEMENTARY MATERIAL

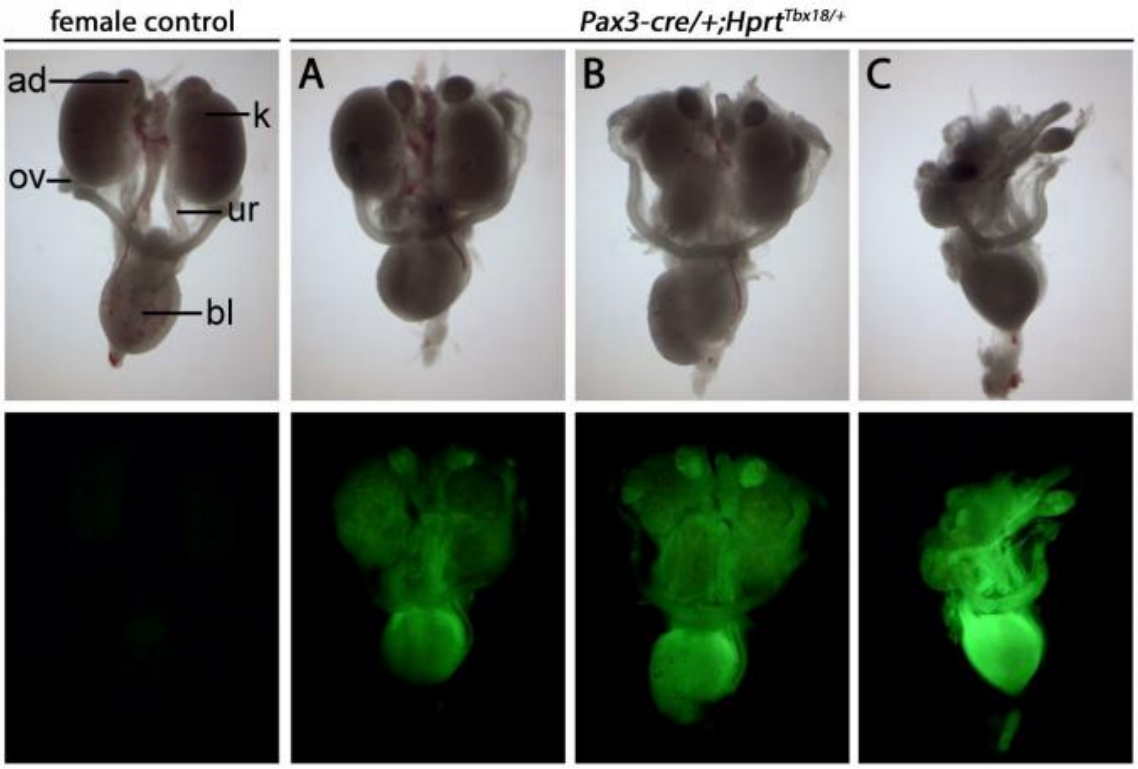

Fig. S1: UGS phenotype of female *Pax3-cre/+;Hprt*$^{Tbx18/+}$ mice.

Morphological analysis of whole UGS of control (A) and *Pax3cre/+;Hprt*$^{Tbx18/+}$ mice (B) at E18.5. A total of 19 mutant UGS were analyzed of which one had a normal appearance (B), 9 had kidneys that were located closer to the midline or caudally extended (C), and 9 had uni- or bilateral kidney hypoplasia or unilateral agenesis (D). adr, adrenal gland; bl, bladder; k, kidney; ur, ureter; us, uterus.

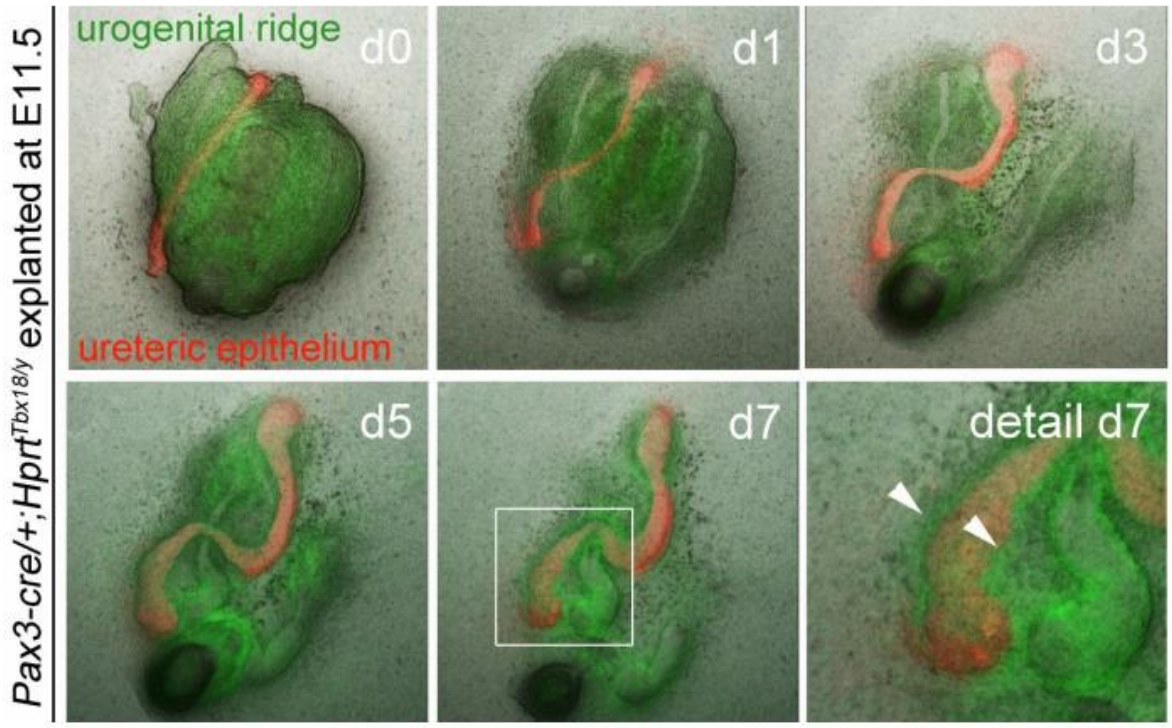

Fig. S2: *Tbx18* expressing mesenchyme supports growth of the ureteric epithelium.

The ureteric epithelium, which is marked by expression of red fluorescent Tomato protein, was dissected from E12.5 *R26,*$^{mTmG/+}$ embryos. The ureteric epithelium was transplanted onto an explanted *Pax3-cre/+;Hprt*$^{Tbx18/y}$ UGR, dissected at E11.5. *Tbx18* misexpressing cells are marked by GFP expression from the *Hprt*^{Tbx18}-misexpression allele. Arrow heads indicate the layer of GFP^{+} cells along the ureteric epithelium in an area, where peristalsis of the ureter was documented in Video S1 nd, nephric duct; ue, ureteric epithelium.

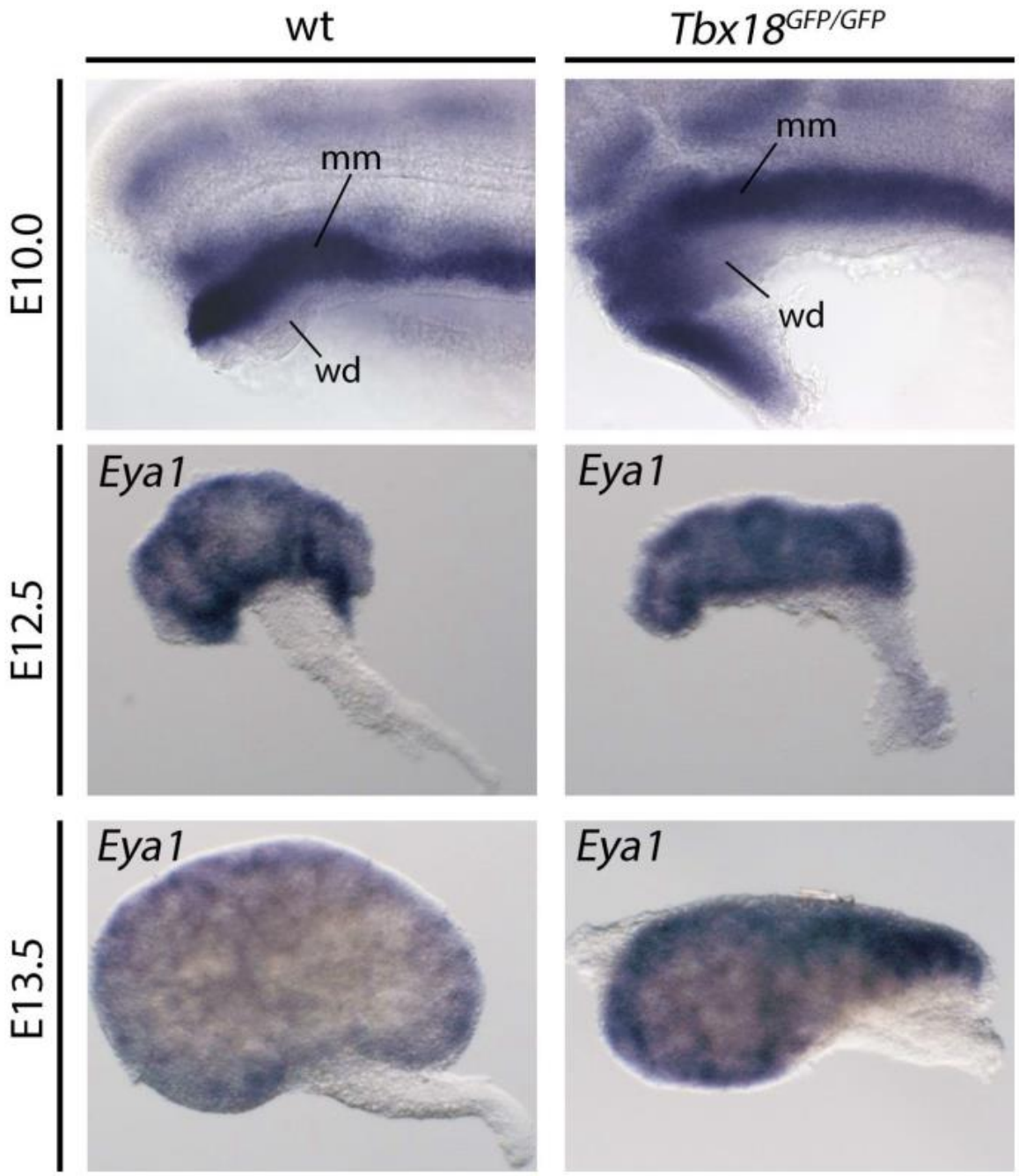

Fig. S3: *Eya1* shows weak ectopic expression in the UM *Tbx18*-deficient embryos until E12.5.
Whole mount *in situ* hybridization expression analysis of *Eya1* in control (*Tbx18*$^{GFP/+}$) and *Tbx18*-deficient kidneys and ureters (*Tbx18*$^{GFP/GFP}$) at E12.5 and E13.5 shows weak ectopic expression of *Eya1* in the ureteric mesenchyme at E12.5 but not at E13.5. ki, kidney; ur, ureter.

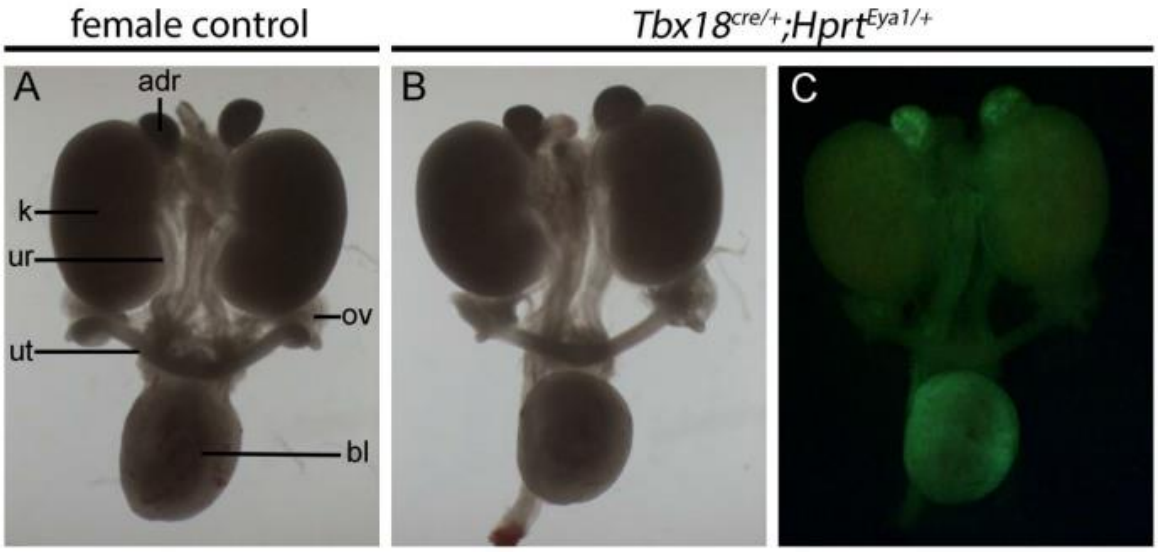

Fig. S4: Phenotypic variability of defects in the UGS of female *Pax3-cre/+;Hprt*$^{Tbx18/+}$ mice.

Morphological analysis of whole UGS of female *Pax3cre/+;Hprt*$^{Tbx18/+}$-mice at E18.5. A total of 13 mutant UGS were analyzed of which ten had no phenotype as shown and three a weak proximal hydroureter. adr, adrenal gland; bl, bladder; k, kidney; ov, ovary; ur, ureter; us, uterus.

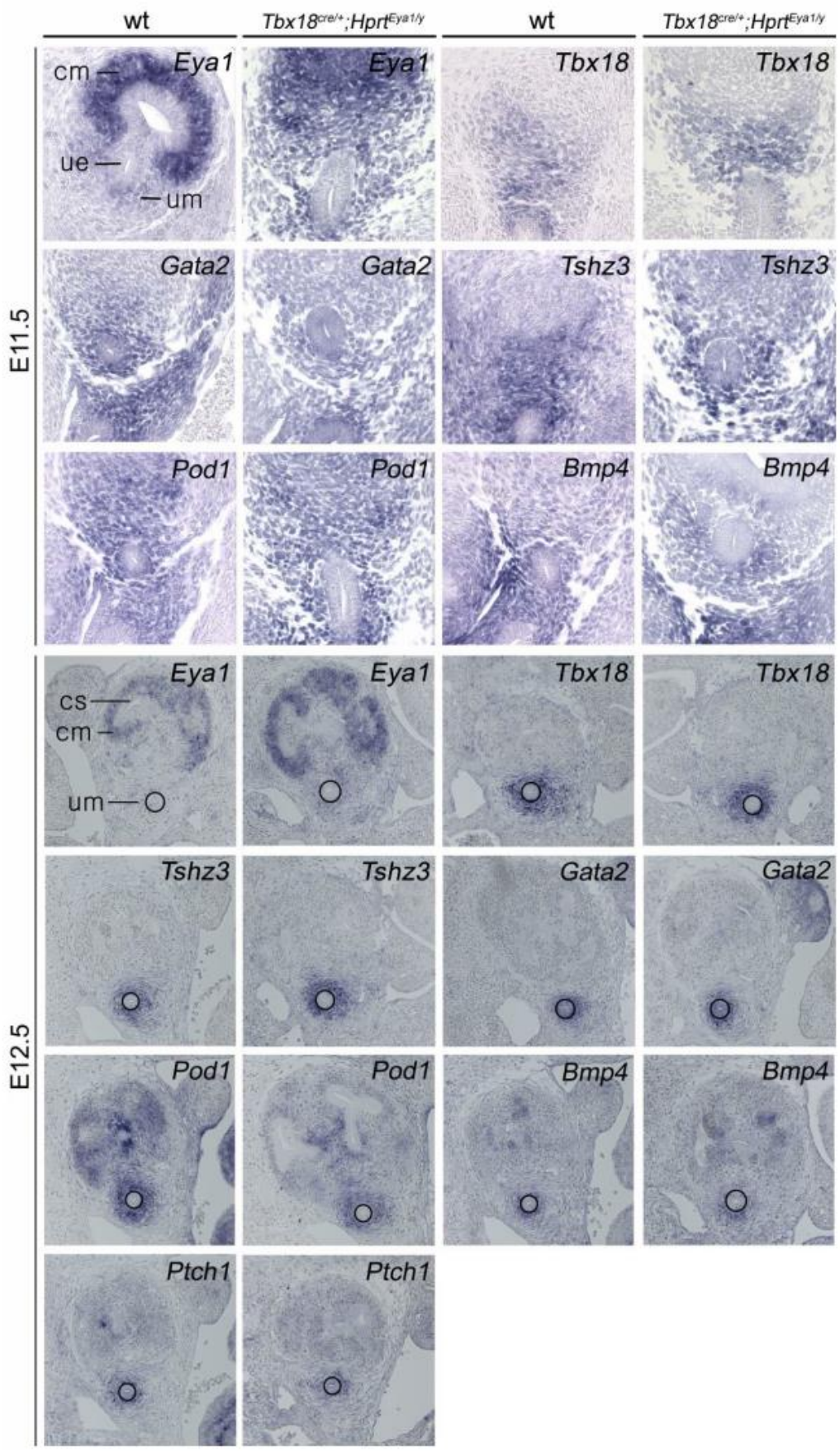
wt
Tbx18cre/+;HprtEya1/y
wt
Tbx18cre/+;HprtEya1/y
E11.5
E12.5
cm
ue
um
cs
Eya1
Tbx18
Gata2
Tshz3
Pod1
Bmp4
Ptch1

Fig. S5: Ureteric mesenchyme markers show an unchanged expression at E11.5 and E12.5 in the *Tbx18$^{cre/+}$;Hprt$^{Eya1/y}$* mutant.

Section *in situ* hybridization analysis of *Eya1* and early ureteric mesenchyme markers at E11.5 and E12.5 showed an unchanged expression of these markers in male *Tbx18$^{cre/+}$;Hprt$^{Eya1/y}$* mutants. cm, cap mesenchyme; cs, collecting duct system; ue, ureteric epithelium, um, ureteric mesenchyme.

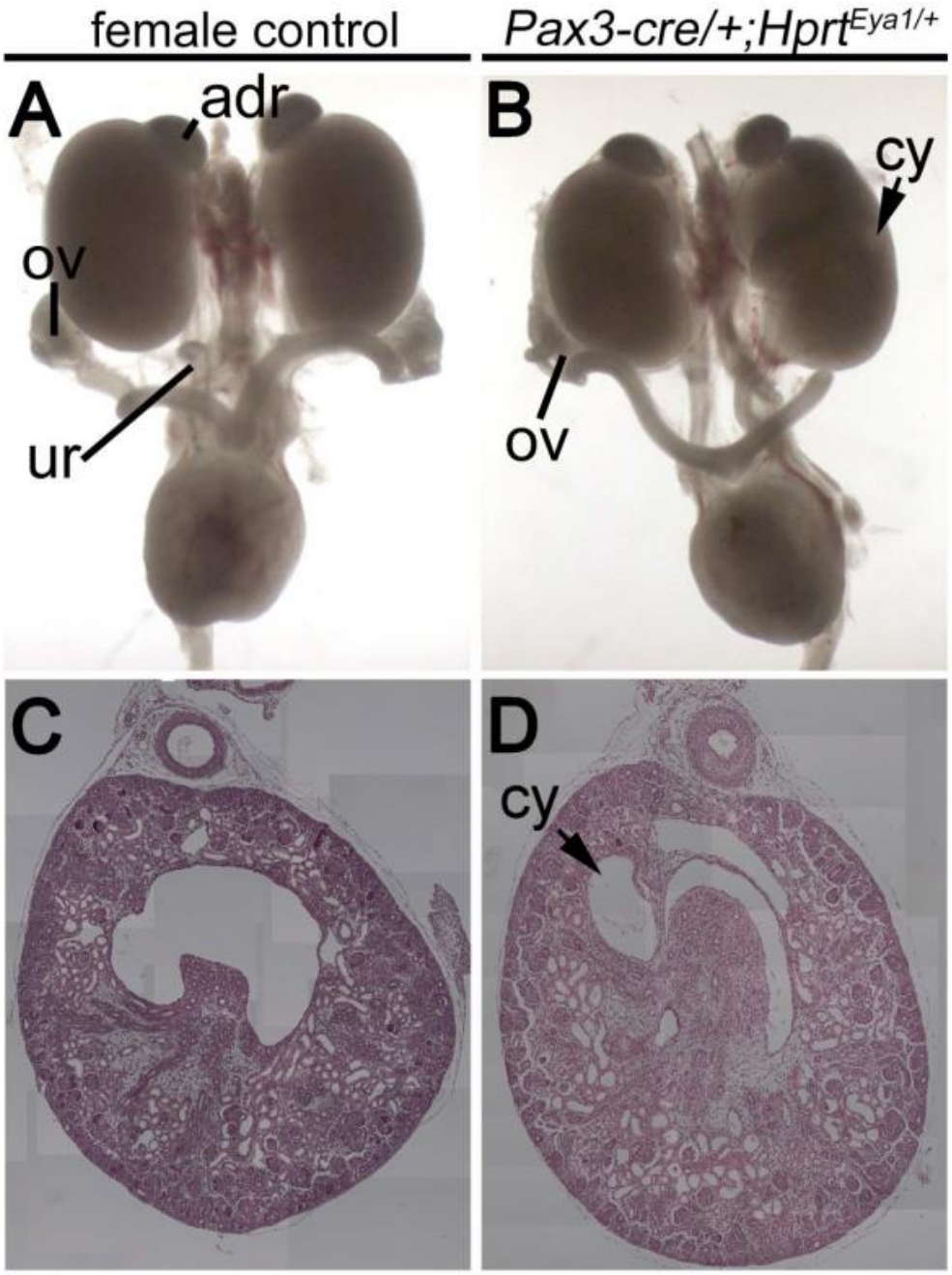

Fig. S6: UGS phenotype of female *Pax3-cre/+;Hprt*$^{Eya1/+}$ mutants at E18.5.

Morphological analysis of dissected UGS at E18.5 (**A** and **B**). Histological examination by H&E staining of transverse section of kidney and proximal ureter (**C** and **D**) at E18.5. adr, adrenal gland; ov, ovary; ur, ureter; cy, cyst.

	N
Total:	19
Uni- or bilateral kidney hypoplasia (Fig.S1C)	7
Unilateral kidney agenesis (Fig.S1C)	2
Kidneys located closer to the body midline (Fig.S1B)	9
Kidney elongated in the caudal direction (Fig.S1B)	10
At least one of the kidneys of irregular shape (Fig.S1B+C)	18
Wildtype phenotype (Fig.S1A)	1

Tab. S1: Features of the UGS phenotype of female *Pax3-cre/+;Hprt*$^{Tbx18/+}$ embryos and their frequence at E18.5.

Video S1. *Tbx18* expressing mesenchyme supports peristaltic activity of the ureter.

Pax3-cre/+;Hprt$^{Tbx18/y}$ explant cultures with transplanted E12.5 R26mTmG/+ ureteric epithelium (see also Fig. S2) Ureteric peristalsis documented at day 8 of culture.

REFERENCES

1. Bohnenpoll, T. *et al.* Tbx18 expression demarcates multipotent precursor populations in the developing urogenital system but is exclusively required within the ureteric mesenchymal lineage to suppress a renal stromal fate. *Dev. Biol.* **380,** 25–36 (2013).

2. Takasato, M. & Little, M. H. The origin of the mammalian kidney: implications for recreating the kidney in vitro. *Development* **142,** 1937–1947 (2015).

3. Cunha, G. R., Young, P., Higgins, S. J. & Cooke, P. S. Neonatal seminal vesicle mesenchyme induces a new morphological and functional phenotype in the epithelia of adult ureter and ductus deferens. *Development* **111,** 145–158 (1991).

4. Baskin, L. S., Hayward, S. W., Young, P. & Cunha, G. R. Role of mesenchymal-epithelial interactions in normal bladder development. *J. Urol.* **156,** 1820–1827 (1996).

5. Lipschutz, J. H., Young, P., Taguchi, O. & Cunha, G. R. Urothelial transformation into functional glandular tissue in situ by instructive mesenchymal induction. *Kidney Int.* **49,** 59–66 (1996).

6. Davidson, A. J. in (2008).

7. Wang, Q., Lan, Y., Cho, E.-S., Maltby, K. M. & Jiang, R. Odd-skipped related 1 (Odd 1) is an essential regulator of heart and urogenital development. *Dev. Biol.* **288,** 582–594 (2005).

8. James, R. G., Kamei, C. N., Wang, Q., Jiang, R. & Schultheiss, T. M. Odd-skipped related 1 is required for development of the metanephric kidney and regulates formation and differentiation of kidney precursor cells. *Development* **133,** 2995–3004 (2006).

9. Xu, P. X. *et al.* Eya1-deficient mice lack ears and kidneys and show abnormal apoptosis of organ primordia. *Nat. Genet.* **23,** 113–117 (1999).

10. Sajithlal, G., Zou, D., Silvius, D. & Xu, P. Eya1 acts as a critical regulator for specifying the metanephric mesenchyme. **284,** 323–336 (2005).

11. Wellik, D. M., Hawkes, P. J. & Capecchi, M. R. Hox11 paralogous genes are essential for metanephric kidney induction. *Genes Dev.* **16,** 1423–1432 (2002).

12. Gong, K. Q., Yallowitz, A. R., Sun, H., Dressler, G. R. & Wellik, D. M. A Hox-Eya-Pax complex regulates early kidney developmental gene expression. *Mol Cell Biol* **27,** 7661–7668 (2007).

13. Kobayashi, A. *et al.* Six2 defines and regulates a multipotent self-renewing nephron progenitor population throughout mammalian kidney development. *Cell Stem Cell* **3,** 169–181 (2008).

14. Costantini, F. & Shakya, R. GDNF/Ret signaling and the development of the kidney. *Bioessays* **28,** 117–127 (2006).

15. Airik, R., Bussen, M., Singh, M. K., Petry, M. & Kispert, A. Tbx18 regulates the development of the ureteral mesenchyme. *J. Clin. Invest.* **116,** 663–674 (2006).

16. Luche, H., Weber, O., Nageswara Rao, T., Blum, C. & Fehling, H. J. Faithful activation of an extra-bright red fluorescent protein in 'knock-in' Cre-reporter mice ideally suited for lineage tracing studies. *Eur. J. Immunol.* **37,** 43–53 (2007).

17. Airik, R. *et al.* Hydroureternephrosis due to loss of Sox9-regulated smooth muscle cell differentiation of the ureteric mesenchyme. *Hum. Mol. Genet.* **19,** 4918–4929 (2010).

18. Trowe, M.-O. *et al.* Loss of Sox9 in the periotic mesenchyme affects mesenchymal expansion and differentiation, and epithelial morphogenesis during cochlea development in the mouse. *Dev. Biol.* **342,** 51–62 (2010).

19. Christoffels, V. M. *et al.* Formation of the venous pole of the heart from an Nkx2-5-negative precursor population requires Tbx18. *Circ. Res.* **98,** 1555–1563 (2006).

20. Greulich, F., Farin, H. F., Schuster-Gossler, K. & Kispert, A. Tbx18 function in epicardial development. *Cardiovasc. Res.* **96,** 476–483 (2012).

21. Muzumdar, M. D., Tasic, B., Miyamichi, K., Li, L. & Luo, L. A global double-fluorescent Cre reporter mouse. *Genesis* **45,** 593–605 (2007).

22. Li, J., Chen, F. & Epstein, J. A. Neural crest expression of Cre recombinase directed by the proximal Pax3 promoter in transgenic mice. *Genesis* **26,** 162–164 (2000).

23. Wilkinson, D. G. & Nieto, M. A. Detection of messenger RNA by in situ hybridization to tissue sections and whole mounts. *Methods Enzymol.* **225,** 361–373 (1993).

24. Moorman, A. F., Houweling, A. C., de Boer, P. A. & Christoffels, V. M. Sensitive nonradioactive detection of mRNA in tissue sections: novel application of the whole-mount in situ hybridization protocol. *J. Histochem. Cytochem.* **49,** 1–8 (2001).

25. Trowe, M.-O. *et al.* Canonical Wnt signaling regulates smooth muscle precursor development in the mouse ureter. *Development* **139,** 3099–3108 (2012).

26. Singh, R. *et al.* Tbx2 and Tbx3 induce atrioventricular myocardial development and endocardial cushion formation. *Cell. Mol. Life Sci.* **69,** 1377–1389 (2012).

27. Xu, J. & Xu, P.-X. Eya-Six are necessary for survival of nephrogenic cord progenitors and inducing nephric duct development prior to ureteric bud formation. *Dev. Dyn.* (2015). doi:10.1002/dvdy.24282

28. Xu, J. *et al.* Eya1 interacts with Six2 and Myc to regulate expansion of the nephron progenitor pool during nephrogenesis. *Dev. Cell* **31,** 434–447 (2014).

29. Esquela, A. F. & Lee, S.-J. Regulation of metanephric kidney development by growth/differentiation factor 11. *Dev. Biol.* **257,** 356–370 (2003).

30. Brophy, P. D., Ostrom, L., Lang, K. M. & Dressler, G. R. Regulation of ureteric bud outgrowth by Pax2-dependent activation of the glial derived neurotrophic factor gene. *Development* **128,** 4747–4756 (2001).

31. Nishinakamura, R. *et al.* Murine homolog of SALL1 is essential for ureteric bud invasion in kidney development. *Development* **128,** 3105–3115 (2001).

32. Dudley, A. T., Godin, R. E. & Robertson, E. J. Interaction between FGF and BMP signaling pathways regulates development of metanephric mesenchyme. *Genes Dev.* **13,** 1601–1613 (1999).

33. Dudley, A. T. & Robertson, E. J. Overlapping expression domains of bone morphogenetic protein family members potentially account for limited tissue defects in BMP7 deficient embryos. *Dev. Dyn.* **208,** 349–362 (1997).

34. Pichel, J. G. *et al.* Defects in enteric innervation and kidney development in mice lacking GDNF. *Nature* **382,** 73–76 (1996).

35. Dudley, A. T., Lyons, K. M. & Robertson, E. J. A requirement for bone morphogenetic protein-7 during development of the mammalian kidney and eye. *Genes Dev.* **9,** 2795–2807 (1995).

36. Kreidberg, J. A. *et al.* WT-1 is required for early kidney development. *Cell* **74,** 679–691 (1993).

37. Yu, C.-T. *et al.* COUP-TFII is essential for metanephric mesenchyme formation and kidney precursor cell survival. *Development* **139,** 2330–2339 (2012).

38. Xu, P.-X. *et al.* Six1 is required for the early organogenesis of mammalian kidney. *Development* **130,** 3085–3094 (2003).

39. Vega, Q. C., Worby, C. A., Lechner, M. S., Dixon, J. E. & Dressler, G. R. Glial cell line-derived neurotrophic factor activates the receptor tyrosine kinase RET and promotes kidney morphogenesis. *Proc. Natl. Acad. Sci. U. S. A.* **93,** 10657–10661 (1996).

40. Sainio, K. *et al.* Glial-cell-line-derived neurotrophic factor is required for bud initiation from ureteric epithelium. *Development* **124,** 4077–4087 (1997).

41. Majumdar, A., Vainio, S., Kispert, A., McMahon, J. & McMahon, A. P. Wnt11 and Ret/Gdnf pathways cooperate in regulating ureteric branching during metanephric kidney development. *Development* **130,** 3175–3185 (2003).

42. Li, X. *et al.* Eya protein phosphatase activity regulates Six1-Dach-Eya transcriptional effects in mammalian organogenesis. *Nature* **426,** 247–254 (2003).

43. Nie, X., Sun, J., Gordon, R. E., Cai, C.-L. & Xu, P.-X. SIX1 acts synergistically with TBX18 in mediating ureteral smooth muscle formation. *Development* **137,** 755–765 (2010).

44. Ruf, R. G. *et al.* SIX1 mutations cause branchio-oto-renal syndrome by disruption of EYA1-SIX1-DNA complexes. *Proc. Natl. Acad. Sci. U. S. A.* **101,** 8090–8095 (2004).

45. Grieshammer, U. *et al.* SLIT2-mediated ROBO2 signaling restricts kidney induction to a single site. *Dev Cell* **6,** 709–717 (2004).

46. Kume, T., Deng, K. & Hogan, B. L. Murine forkhead/winged helix genes Foxc1 (Mf1) and Foxc2 (Mfh1) are required for the early organogenesis of the kidney and urinary tract. *Development* **127,** 1387–1395 (2000).

10. Manuscript II

Misexpression of *Tbx18* in the ureter wall and renal stroma prevents *lamina propria* development and alters distribution of stromal cells

Eva Bettenhausen[1], Anna-Carina Weiss[1], Mark-Oliver Trowe [1], Henner Farin and Andreas Kispert[1],*

[1]Institut für Molekularbiologie, Medizinische Hochschule Hannover, Hannover, Germany

*Corresponding author Address:
Institut für Molekularbiologie, OE5250, Medizinische Hochschule Hannover, Carl-Neuberg-Str. 1, D-30625 Hannover, Germany. TEL.: +49 (0)511 5324017; fax: +49 (0)511 5324283.
e-mail address: kispert.andreas@mh-hannover.de (A. Kispert)

Manuscript in preparation

ABSTRACT

The T-box transcription factor Tbx18 is expressed in an early mesenchymal progenitor population which gives rise to the ureteric smooth muscle and connective tissue coat and contributes to the renal stroma. In the course of ureter differentiation *Tbx18* expression is restricted to the ureteric smooth muscle layer. Analysis of *Tbx18*-loss of function mutant mice revealed, that Tbx18 is needed in this tissue to allow ureteric smooth muscle development and ureter extension.

In this study we analyzed the consequences of permanent expression of *Tbx18* in all cells derived from the early mesenchymal progenitor population via a conditional misexpression approach. Furthermore, we addressed the question if Tbx18 functions as a transcriptional repressor by expressing *Tbx18* fused to the transcription activating herpes simplex-VP16-domain.

We found that misexpression of *Tbx18* in the ureteric mesenchyme leads to the loss of the *lamina propria* connective tissue layer, most likely due to ectopic smooth muscle differentiation, as well as to changes in the distribution of *Tbx18*-derived cells in the renal stroma. Expression of *Tbx18VP16* prevented smooth muscle differentiation cell-autonomously. The results of this study revealed that an exact temporal regulation of *Tbx18* is necessary to allow normal *lamina propria* and renal stroma development. Additionally, first *in vivo*-evidence for a transcription repressing function of Tbx18 in ureteric smooth muscle-development was found.

INTRODUCTION

Kidney and ureter of the mouse embryo arise from the urogenital ridge (UGR), a strand of mesenchyme which stretches along the dorsal body wall of the embryo. The ridge gives rise to the Wolffian- or nephric duct (ND). From the forelimb bud level the duct grows out along the ridge. It produces an epithelial protrusion, the so called ureteric bud (UB) near its caudal end, at the level of the hindlimb bud [1]. This UB is the precursor structure of both the ureter and the branching collecting duct system (CDS) of the kidney. With the outgrowth of the UB from the ND at E10.5 different mesenchymal sub-lineages, which will contribute to the developing organs of the UGS, are established within the surrounding mesenchyme of the so called metanephrogenic field. One of these mesenchymal precursor populations, the metanephric mesenchyme (MM), is invaded by the tip of the outgrowing UB. The condensed cluster of MM tissue is surrounded by a loose layer of fibroblasts, the early renal stroma progenitor population, which is marked by *Foxd1* after E11.5. The third sub-lineage is the ureteric mesenchyme (UM) progenitor population. It becomes detectable with the outgrowth of the ureter from the ND at about E10.5, as a narrow band of mesenchymal tissue, located between the MM and the ND. It is marked by expression of the T-box transcription factor *Tbx18* and surrounds the part of the ureteric bud which does not invade the MM. This part of the UB will give rise to the ureter. After the establishment of the early organ primordia, further signal exchange between the UB epithelium and the surrounding mesenchyme produces the collecting duct system via repetitive branching within the MM. Clusters of nephron progenitors, the so called cap mesenchyme (CM), cover the tips of the branching UB and the fetal renal stroma, a fibroblast frame work of the developing kidney, is established [2–4]. The stroma cells fill the interstitial space between the epithelial structures. Until E18.5, the stroma becomes organized into four sub-populations, the outermost layer of renal capsule cells [5], the stroma of the renal cortex, the medullary stroma [6] and the inner medullary stroma, which reaches into the papilla. The developmental function of the stroma is still under investigation. After it has been considered as a mere framework which provides structural support to the developing kidney, there are now some indications for an active role of the stroma in the regulation of ureteric branching morphogenesis and nephrogenesis [6]. Cells derived from this interstitial or stromal lineage were found to give rise to the mesangial cells between the capillaries of the glomerula tuft and to renal pericytes in the mature kidney [7].

Until E18.5 also the wall of the ureter undergoes a patterning process. Its mesenchymal coat, which is derived from the early stripe-like UM progenitor population of the metanephrogenic field [8], establishes a three layered architecture around the innermost ureteric epithelium. The UM gives rise to an inner fibroblast layer, the so called *lamina propria*, which covers the ureteric epithelium, followed by the smooth muscle layer and the outermost *lamina adventitia*, another connective tissue layer, which anchors the ureter to the dorsal body wall [9]. Two important paracrine signaling

pathways known to be involved in this process are the *Sonic hedgehog* (Shh)-pathway [10] and the canonical Wnt-signaling-pathway [11]. Most interestingly, Shh seems to regulate both proliferation and differentiation of the UM [10]. Canonical Wnt-signaling is involved in radial patterning and proliferation of the ureteric smooth muscle precursors [11].

Expression of Tbx18 is maintained in the undifferentiated UM after E11.5. Between E11.5 and E12.5, it is restricted to the mesenchymal coat of the ureter. After E14.5 *Tbx18* expression is maintained in the layer of UM which will give rise to the ureteric smooth muscle tissue, where it is expressed until about E16.5. Between E16.5 and E18.5, with smooth muscle differentiation, it is downregulated. A fate mapping of *Tbx18*$^{+}$ cells in the urogenital organ system (UGS) revealed, that the UM progenitor population does not only give rise to all tissue layers of the ureter wall, but contributes to most organs of the UGS. *Tbx18*-derived cells were found in the smooth muscle tissue of the bladder wall, in the gonads, the adrenal glands. Furthermore they were detectable in all regions of the stroma, as well as in the mesangium inside the glomeruli and the smooth muscle tissue of renal arteries [8]. In the stroma *Tbx18*-derived cells showed a medial to lateral gradient in their distribution with the highest density in the cortex around the ureter entry side and lowest in the lateral cortex, farthest away from the ureter.

Fate mapping in the *Tbx18*-loss of function mutant showed, that *Tbx18* is dispensable for the development of all organs of the UGS except for ureteric smooth muscle development. Contribution to the renal stroma was still detectable in the mutant although the distribution of *Tbx18*-derived cells in the stroma was slightly altered.

As it has been shown before that *Tbx18* is restricted to the inner ring of ureteric mesenchyme during ureter development [8,12], we decided to examine in this study, if this confined expression of *Tbx18* is significant for the development of the of the ureter wall and the *Tbx18*-derived stroma population. To address this question we used conditional misexpression mutants which showed permanent expression of *Tbx18* in all *Tbx18*-derived cells and analyzed the consequences of this misexpression *in vivo*. The aim of another approach was to find out if *Tbx18* functions as a transcriptional repressor during UGS development, as indicated before by the results of an *in vitro* study [13]. To answer this question we investigated the effect of expression of a strongly activating version of Tbx18 fused to the VP16-domain, derived from the herpes simplex virus *in vivo*.

MATERIAL AND METHODS

Mice

Mice showing conditional misexpression of *Tbx18* or *Tbx18VP16* were generated by mating *Tbx18*$^{tm4(cre)Akis}$ (synonym *Tbx18*^{cre}) males to females homozygous for either the *Hprt*^{Tbx18} or the *Hprt*^{Tbx18VP16} misexpression allele which were described before [11,14]. Cre-mediated recombination of these alleles led to permanent expression of *Tbx18* or *Tbx18VP16* together with cytoplasmatic

expression of Venus-*GFP*. In the male offspring from these matings misexpression occurs in all recombined cells, while the female mutants show misexpression in a mosaic-pattern due to random X-inactivation as the *Hprt*-allele is located on the X-chromosome. For permanent labeling of all recombined cells by expression of a membrane bound GFP, we used a *Gt(ROSA)26Sor*$^{tm4(ACTB-tdTomato-EGFP)Luo}$ (*R26*^{mTmG}) reporter allele in these mutants [15]. Controls which expressed membrane bound GFP permanently in all *Tbx18*-derived cells and which do not show any phenotypical changes concerning UGS morphology were generated by mating *Tbx18*$^{cre/+}$;*R26*$^{mTmG/mTmG}$ males to NMRI females. To generate *Tbx18*-loss of function-mutants we used mice harboring a *Tbx18*^{tm2Akis} (synonym *Tbx18*^{GFP}) allele mating heterozygous females to heterozygous males to obtain *Tbx18*$^{GFP/GFP}$ homozygous embryos. Heterozygous offspring from these matings was used as controls. All mice were maintained on an NMRI outbred background.
For timed pregnancy vaginal plugs of mated females were checked in the morning. Noon of the day when a plug was detected was designated E0.5. Embryos were dissected in PBS. After dissection isolated tissues of decapitated embryos were fixed in 4% paraformaldehyde/PBS overnight and washed in PBS and dehydrated in methanol for storage at -20°C on the following day.

***In situ* hybridization**

We performed whole-mount RNA *in situ* hybridizations following a standard procedure with digoxigenin-labeled antisense riboprobes [16]. Stained specimens were transferred in 80% glycerol for documentation. *In situ* hybridization on 10-µm paraffin sections was done essentially as described [17]. For each marker we analyzed at least three independent specimens.

Histological and immunohistochemical analyses

Tissue for histological or immunohistochemical analyses was fixed in 4% PFA in PBS, dehydrated and stored in methanol at -20°C or embedded in paraffin immediately. 5 µm sections were used for immunohistochemical and histological analysis. For histological examination tissue sections were stained with haematoxylin and eosin. The following antibody combinations were used for immunohistochemical detection of antigens in tissue sections: rabbit anti-CDH1 (kindly provided by R. Kemler, MPI for Immunobiology and Epigenetics, Freiburg, Germany, 1:200), rabbit anti-GFP (sc-8334, Santa Cruz, 1:200) and mouse anti-ACTA2 (F3777 and C6198, Sigma, 1:200). For fluorescent detection of primary antibodies we used Alexa 488/555-conjugated secondary antibodies (A11034; A11008; 711-487-003; A21202; A21422; A21428, Invitrogen/Dianova; 1:500) Procedure: After deparaffination and rehydration of the sections we performed antigen unmasking in acidic antigen unmasking solution (Vector Laboratories) for 10 min. in a pressure cooker. Blocking with the blocking solution provided with the Tetramethylrhodamine Amplification Kit (TSA-kit) (Perkin-Elmer) was followed by blocking with the anti-mouse IgG blocking solution provided with the Mouse-on-Mouse Kit (Vector Laboratories) when a mouse primary antibody was used.

Labeling with the primary antibodies was performed over night at 4°C. Sections were mounted with Mowiol (Roth) or Permount mounting medium (Thermo Fisher Scientific) after H&E staining.

Organ cultures

Explant culture of metanephric primordia of E11.5 embryos for *ex vivo* lineage tracing and lysotracker assays was performed as described in [18] using CO_2-independent medium (Gibco). Medium was exchanged every 24h. For the lysotracker assay, culture medium was exchanged with medium containing the Lysotracker dye red DND-99 (Invitrogen) (1yl/0,42ml) after the explanted metanephric primordium had settled on the membrane. After incubation for one hour at 37°C and 5% CO_2, the dye was removed by exchanging the medium again. The first microscopic documentation followed immediately, the second documentation was performed 24h after explantation. With this assay we detected apoptotic processes indirectly in the living tissue via the accumulation of a red fluorescent dye.

Image analysis

Whole-mount specimens were photographed on Leica M420 with Fujix digital camera HC-300Z, sections on Leica DM5000B with Leica digital camera DFC300FX. GFP epifluorescence in living tissues was documented with the Leica DMI 6000 microscope, and the images and movies were processed with Leica Application Suite Advanced Fluorescence Version 2.3.0 software. Confocal images were taken on Leica Inverted-2 with TCS SP2 scan head. Images for figure files were processed in Adobe Photoshop CS4.

RESULTS

Misexpression of *Tbx18* in cells derived from the UM progenitor population causes ectopic tissue accumulation along the ureter and in the renal cortex

To analyze the effect of *Tbx18* misexpression on ureter and stroma development, we examined $Tbx18^{cre/+};Hprt^{Tbx18}$-embryos at E18.5. Due to random X-inactivation female mutants showed *Tbx18* misexpression statistically only in 50% of the recombined cells while in male mutants all *Tbx18*-derived cells permanently expressed *Tbx18* after recombination. In male $Tbx18^{cre/+};Hprt^{Tbx18/y}$-embryos we found excessive connective tissue which coated all organs of the upper urinary tract, including the kidneys, the ureters and the adrenal glands (**Fig. 1 A-D**), fixing the gonads to the kidney surface. The testes were elongated while the epididymes were morphologically not detectable. The phenotype showed full penetrance (N=20). In female embryos the phenotype was more variable (N=11). Subsequently only male mutants were analyzed. The histological analysis at E18.5 confirmed the superficial accumulation of connective tissue and revealed an altered organization of the renal stroma. We found an accumulation of cells in the cortex on the medial side of the kidney, close to the ureter entry site (**Fig. 1 E`** and **G`**). Loosely packed ectopic tissue piled up in this region in the mutant, while in the control kidney the cortical stroma was tightly packed. A thickened layer of connective tissue was also found lining the complete pelvis underneath the epithelium. The renal capsule, which normally consists of one to two cell layers, was histologically not detectable as a separate layer (**Fig. 1 E`** and **G`**). The amount of stroma cells in the medulla on the other hand appeared reduced in the misexpression mutant (**Fig. 1 E``** and **G``**). Proximal and distal segments of the convoluted tubules of nephrons, which were confined to the cortex in the control, were displaced to the medulla region in the mutant. The cortex on the lateral side of the kidney showed an unchanged histology (**Fig. 1E```**and **G```**). The histological analysis of transverse sections through the proximal ureter revealed a thickened adventitial fibroblast layer in $Tbx18^{cre/+};Hprt^{Tbx18/y}$-embryos. The *lamina adventitia* was continuous with the connective tissue which covered the ventral surface of the kidney. The diameter of the ureter was strongly reduced (**Fig. 1 F** and **H**). The ureteric smooth muscle layer was detectable as a ring of condensed spindle-shaped cells in the control and misexpression mutant. Together, this suggests that permanent expression of *Tbx18* in cells derived from the common UM and stroma precursor population interferes with the normal organization of the ureter wall and renal stroma.

In vivo lineage tracing reveals that accumulating cells in the $Tbx18^{cre/+};Hprt^{Tbx18/y}$-mutant are *Tbx18*-derived

After we found that *Tbx18* misexpression leads to tissue accumulation around the pelvis region, in the medial renal cortex and along the ureter and on the kidney surface, we wanted to find out if the ectopic tissue was of $Tbx18^{+}$ origin. For a lineage tracing of *Tbx18* misexpressing cells at E18.5

we used the *R26*^{mTmG}*-reporter*-allele [15] in *Tbx18*$^{cre/+}$;*R26*$^{mTmG/+}$-controls and *Tbx18*$^{cre/+}$;*R26*$^{mTmG/+}$;*Hprt*$^{Tbx18/y}$-mutant mice. Initially all cells of these embryos express a membrane bound red fluorescent Tomato protein. After cre-mediated recombination the expression switches to a membrane bound GFP. In this way all "*Tbx18*-derived" cells are marked by GFP expression, which we detected via epifluorescence in the whole UGS and via IHC in tissue sections.

In the organs of *Tbx18*$^{cre/+}$;*R26*$^{mTmG/+}$-control UGS, we found GFP$^+$ cells in the ureter wall, the renal stroma, the adrenal gland, the testis, the epididymis, the *vas deferens* and the bladder wall (**Fig. 2 A**), as described before (Bohnenpoll et al. 2013). *Tbx18* misexpressing, GFP$^+$ cells appeared to be distributed less evenly in the renal interstitium. Also the layer of loosely packed connective tissue, which covered parts of the ventral and medial side of the kidney, was GFP$^+$ (**Fig. 2 B**). Detection of GFP$^+$ cells in sagittal sections of kidneys and ureters (**Fig. 2 C-H**) confirmed a patchy, uneven distribution of *Tbx18* misexpressing cells in the renal stroma. We found accumulations of GFP$^+$ tissue around the pelvis, in the medial cortex and along the ureter in the mutant. Contribution of *Tbx18* misexpressing cells to the medullary stroma on the other hand appeared strongly reduced (**Fig. 2 G** and **H**).

Examination of transverse sections of the proximal ureter showed an increase in the thickness and density of the outer, *Tbx18*-derived connective tissue layer, the *lamina adventitia* (**Fig. 2 I** and **J**). Hence lineage tracing of *Tbx18* misexpressing cells in the UGS showed that ectopic tissue in the renal cortex, on the kidney and ureter surface and around the pelvis of *Tbx18* misexpressing mutants consists of *Tbx18*misexpressing cells, while the contribution of this cell population to the medullary stroma is reduced.

Accumulating cells in the renal cortex show expression of stroma markers, while medullary stroma is reduced in *Tbx18* misexpression mutants

To better define the molecular character of the ectopic *Tbx18* misexpressing tissue in the affected medial cortical zone, we decided to analyze the expression of markers for the different stroma populations, the CM and smooth muscle tissue.

Expression of *Wilms tumor 1 (Wt1)*, a marker for the CM and podocytes was comparable between *Tbx18* misexpressing and control embryos but the space between the clusters of CM was strongly increased in the mutant and filled with *Wt1*$^-$ tissue (**Fig. 3 A-B`**). Next we checked the expression of specific markers for different stroma sub-populations. *Aldehyde dehydrogenase family 1, subfamily A2* (*Raldh2),* showed expression in the stroma throughout the nephrogenic zone, in the renal capsule, in the Loop of Henle and renal vesicles in the control. In the misexpression mutant it was not detectable in the ectopic tissue in the renal cortex or in the thickened outer connective tissue layer. Only some scattered clusters of stromal cells in the nephrogenic zone of the mutant

still expressed *Raldh2* in the medial cortex (**Fig. 3 C-D`**). No *Raldh2*$^{+}$ renal capsule was distinguishable. *Forkhead-box D1* (*Foxd1*), which is expressed exclusively in the renal stroma lineage [19,20], was detectable in the cortical stroma and renal capsule at E18.5 in the control. In the mutant we found that the tissue accumulations in the medial cortex and the superficial tissue covering the kidney were *Foxd1*$^{+}$ (**Fig. 3 E- F`**). *Secreted frizzled-related protein 1* (*Sfrp1*) showed a strong expression in the Loop of Henle and a slightly weaker expression in the medullary stroma and the renal capsule in the control. In *Tbx18* misexpressing embryos it was also detectable in the tissue accumulations in the cortical stroma and around the renal pelvis, but not in the ectopic tissue on the kidney surface. The overall amount of *Sfrp1*$^{+}$ renal interstitial cells appeared to be increased in the misexpression mutant (**Fig. 3 G-H`**). *Wingless-type MMTV integration site family, member 11* (*Wnt11*) is a specific marker for medullary stroma at E18.5. Most interestingly, this marker was not detectable in the tissue accumulations around the pelvis in *Tbx18* misexpressing embryos. The expression analysis for *Wnt11* showed prongs of cortical tissue, containing bundles of convoluted tubules, invading into the *Wnt11*$^{+}$ medulla region and the overall amount of *Wnt11*$^{+}$ cells in the renal interstitium appeared slightly decreased in the mutant. (**Fig. 3 I- J`**). *Wnt4*, which is expressed in the medullary and papillary stroma as well as in renal vesicles of the control, was undetectable in the accumulated tissue around the pelvis in *Tbx18*$^{cre/+}$;*Hprt*$^{Tbx18/y}$-kidneys. The overall amount of *Wnt4*-expressing cells again seemed to be slightly reduced (**Fig. 3 K-L`**) and there were prongs of cortical tissue, invading into the medullary zone in the mutant. To find out if permanent expression of *Tbx18* can activate the smooth muscle program ectopically in the tissue accumulations in the renal cortex or on the surface of the kidney we detected α-smooth muscle actin (ACTA2) immunohistochemically (**Fig. 3 M-N`**). We did not find ectopic smooth muscle differentiation in these tissues. It has been shown previously, that the smooth muscle tissue in medulla and papilla, is partly derived from *Tbx18*$^{+}$ cells [8], Expression analysis of ACTA2 additionally showed that this smooth muscle tissue is present in the misexpression mutant, in spite of the overall reduction of *Tbx18*-derived cells in the medullary stroma.

Taken together the results of the molecular marker expression analysis revealed a reduction of the medullary stroma which does not affect medullary smooth muscle development. The accumulated cells in the medial cortex and around the pelvis seem to be of a stroma-like character, as they express cortical/capsule stroma markers. Formation of a distinguishable renal capsule layer was not detectable in *Tbx18* misexpression mutants. We conclude from this, that temporal misexpression of *Tbx18* interferes with the contribution of *Tbx18*-derived cells to all sub-populations of renal interstitial cells.

Misexpression of *Tbx18* in the UM leads to a loss of the *lamina propria*

To analyze the effect of prolonged expression of *Tbx18* on smooth muscle differentiation and expression of molecular markers in the ureter wall, we analyzed expression of ACTA2 and E-

Cadherin (CDH1), which mark the smooth muscle layer and the urothelium respectively. Expression of pathway components involved in UM development were likewise checked by RNA *in situ* hybridization in transverse ureter sections of *Tbx18*$^{cre/+}$;*Hprt*$^{Tbx18/y}$-embryos at E18.5.

Verifying ectopic expression of *Tbx18* in *Tbx18*$^{cre/+}$;*Hprt*$^{Tbx18/y}$-embryos via *in situ*-hybridization, we found *Tbx18* to be detectable throughout the UM at E18.5 while in the control we detected only very weak expression in the ureteric smooth muscle coat at this time point (**Fig. 4 E** and **F**).

Immunohistochemical detection of ACTA2 showed strong expression in the wall of control and mutant ureter (**Fig. 4 A** and **B**). Examining the ureter wall at higher magnifications, using confocal laser scanning microscopy we found that in the control about one to two ACTA2$^-$ cell layers were detectable between the epithelium, marked by expression of CDH1 and the smooth muscle layer marked by ACTA2. This sub-epithelial mesenchyme has been described before by Yu and colleagues [10]. It is the *lamina propria* which becomes detectable at E16.5 [9,21]. In the mutant we found CDH1$^+$ and ACTA2$^+$ cells to be in direct contact with each other (**Fig. 4 C** and **D**) with no *lamina propria* detectable between them. Expression of *Ptch1* which is restricted to the sub-epithelial mesenchyme at this stage in the wildtype, appeared comparable between control and misexpression mutant (**Fig. 4 G** and **H**), while *Bmp4*, which was also expressed in the sub-epithelial mesenchyme in the control, was undetectable in the mutant (**Fig. 4 I** and **J**). The same was true for *Retinaldehyde dehydrogenase 2* (*Raldh2*), another marker for the *lamina propria* at this stage (**Fig. 4 K** and **L**). *Myocd*, an important transcriptional activator for the smooth muscle differentiation program [22] was strongly expressed in the control as well as in the *Tbx18* misexpression mutant (**Fig. 4 M** and **N**). Although our detection method did hardly allow the resolution of a layer of one to two cells, it appeared that *Myocd* was expressed in the sub-epithelial mesenchyme in the misexpression mutant, a domain which did not show *Myocd*-expression in the control (**Fig. 4 M`** and **N`**). The transcription factor *Teashirt 3* (*Tshz3*), another target of *Bmp4* and regulator of *Myocardin* (*Myocd*) expression and activity [23], was strongly expressed throughout the UM in control and misexpression mutant (**Fig. 4 O** and **P**) *Id2*, a known target gene of *Bmp*-signaling [24], was slightly down-regulated in the *Tbx18* misexpressing UM (**Fig. 4 Q** and). Expression of *Axin2* and *Secreted frizzled-related-protein 2* (*Sfrp2),* two target genes and regulators of *Wnt*-signaling [25,26], were also unchanged at E18.5 (**Fig. 4 S**-**V**). We also checked the expression of *Uroplakin 1 b* (*Upk1b), Myosin heavy polypeptide 11 (Myh11)*, and *Dermatopontin* (*Dpt*) as differentiation markers for the urothelium, the ureteric smooth muscle layer and the *lamina adventitia* respectively. All markers were unchanged at E18.5 (**Suppl. Fig.1**). The results of this analysis indicate that maintained expression of *Tbx18* throughout the UM does not interfere with smooth muscle differentiation but with *lamina propria* development.

Misexpression of *Tbx18* does not prevent apoptosis in the UM precursor population

The analysis of the *Tbx18*$^{cre/+}$;*Hprt*$^{Tbx18/y}$-mutant at E18.5 had shown that the number of *Tbx18*-derived cells is strongly increased on the kidney surface and in the medial cortex and pelvis entry region. We wanted to find out if prolonged expression of *Tbx18* can prevent apoptosis, which normally occurs in the lateral part of the early UM-progenitor population after down regulation of *Tbx18* [8]. If apoptosis is prevented in these cells, they might give rise to the ectopic tissue on the renal surface. We detected apoptotic events by lysotracker analysis in metanephric explant cultures of *Tbx18*$^{GFP/+}$ heterozygous controls compared to *Tbx18*$^{cre/+}$; *Hprt*$^{Tbx18/y}$-mutant tissue. In both cases *GFP* expression marks cells which are expressing *Tbx18*.

At E11.5 GFP expression was detectable in the *Tbx18*$^{GFP/+}$ explant in a stripe-like domain which is known to express *Tbx18* at this stage [8,12] (**Fig. 5 A**). In the *Tbx18*$^{cre/+}$;*Hprt*$^{Tbx18/y}$-explant *Tbx18* and GFP expression was maintained in the cells which had left this domain. At this stage only very few apoptotic spots were detectable in the epithelium of the ureter-ND-junction region, and in some cells on the surface of the MB (**Fig. 5 A** and **C**) in control and mutant explants. After one day of culture GFP-expression was only maintained in the mesenchyme in direct contact with the UE in the control (**Fig. 5 B**). In the misexpression mutant the remaining cells of the lateral population showed strong expression of *GFP* and the lysotracker revealed massive apoptosis in the lateral UM population in control and misexpression-mutants (**Fig. 5 B`** and **D`**). An overlay of GFP- and lysotracker- detection showed a comparable number of apoptotic events in the lateral mesenchymal population in the misexpression mutant and the control (11/15 explants from 8 mutant individuals) (**Fig. 5 B``** and **D``**). Hence misexpression of *Tbx18* is not sufficient to prevent apoptosis in the lateral UM population between E11.5 and E12.5.

***Tbx18* misexpressing cells pile up along the ureter over time and their invasion of the renal stroma is impaired**

To further explore the fate of *Tbx18* misexpressing cells and analyze the process leading to their accumulation, we decided to do an *ex vivo* lineage tracing experiment in metanephric explant cultures. We used again the *R26*^{mTmG}-allele to mark all *Tbx18*-derived cells. By explanting the metanephric primordium at E11.5 (d0) we could exclude the possibility that the observed cell population had an origin different from the early *Tbx18* expressing mesenchymal subpopulation of the metanephrogenic field (**Fig. 6 A** and **E**). The explant cultures were documented for 7 days after explantation.

Invasion of the renal stroma was detectable in control and *Tbx18* misexpressing explants after E11.5. The intensity of the GFP-signal along the ureter in control and misexpression mutant was comparable until the third day of culture (**Fig. 6 B** and **F**). After this time point the GFP^{+} tissue layer increased much stronger and the *Tbx18*-derived cells in the renal stroma appeared to be distributed less evenly in the *Tbx18* misexpression mutant than in the control.

Finally, in the *Tbx18*$^{cre/+}$;*R26*$^{mTmG/+}$-control, at day 7 of culture *Tbx18*-derived cells spread throughout the renal stroma of the explanted renal primordium and even left the explant to cover the membrane of the culture dish around the explant (**Fig. 6 C** and **D**). In the *Tbx18*$^{cre/+}$;*R26*$^{mTmG/+}$;*Hprt*$^{Tbx18/y}$-mutant the distribution was less even and parts of the stroma appeared completely devoid of GFP^{+} cells while in other areas clusters of GFP^{+} tissue were found. Regions of low and very high GFP^{+} cell density had clearly demarcated borders between them (**Fig. 6 G**). In most cultures we also found a thin layer of GFP^{+} cells lining the outer border of the explanted tissue. This superficial layer is most likely the culture equivalent to the accumulating tissue on the renal surface we detected *in vivo*. We only found GFP^{+} cells on the membrane in close proximity to the ureter in the mutant explant but not further away from the explanted tissue like in the control (**Fig. 6 D** and **H**).

From these results we conclude that *Tbx18* misexpressing cells accumulate along the ureter over time. The altered distribution of misexpressing cells along the ureter, in the renal stroma and on the membrane of the culture dish argues for an altered migration behavior and/or increased proliferation of the cell population after day 3 of culture.

Mosaic-expression of the transcription activating *Hprt*^{Tbx18VP16}-allele results in hydroureter, hydronephrosis and failing smooth muscle development

Although there were indications for a repressing function of Tbx18 from an *in vitro* study [27], it has not been analyzed if Tbx18 functions as a repressor *in vivo* and if this function is relevant for ureteric smooth muscle development. We therefor wished to analyze the effect of expression of a strongly activating version of Tbx18 in the *Tbx18*-derived population on ureteric smooth muscle and stroma development. If *Tbx18* functions as a repressor in these cells, we expect to find a phenotype similar to the *Tbx18*-loss of function phenotype. For this analysis we generated *Tbx18*$^{cre/+}$;*Hprt*^{Tbx18VP16}-embryos. Because male *Tbx18*$^{cre/+}$;*Hprt*$^{Tbx18VP16/y}$-embryos die at E14.5 [14], the analysis at E18.5 was possible only in *Tbx18*$^{cre/+}$;*Hprt*$^{Tbx18VP16/+}$ female mutants, which show a mosaic expression of *Tbx18VP16*.

For the morphological examination we dissected 10 female *Tbx18*$^{cre/+}$;*Hprt*$^{Tbx18VP16/+}$ UGS at E18.5 and found that their phenotype was very variable, ranging from wildtype appearance to severe hydroureter and hydronephrosis with ventrally rotated kidneys (**Fig. 7 A** and **B** and **Supplementary. table 1**). The UGS depicted in **Fig. 7 B** shows all morphological changes observed. (For information about the frequency of the different phenotypic features please see **Supplementary table 1**) Histological analysis at E18.5 showed a strong reduction of the ureteric smooth muscle layer and severe hydronephrosis (**Fig. 7 C** and **D**). Histological examination of transverse sections of the proximal ureter showed a complete absence of the smooth muscle and outer connective tissue layer in severe cases (**Fig.7 E-F`**).

To find out if the contribution of *Tbx18*–derived cells to the UGS is altered in *Tbx18VP16*-expressing embryos we traced affected cells via epifluorescence and immunohistochemistry in whole dissected UGS and tissue sections, respectively. In female mutants statistically 50% of the cells recombined by the $Tbx18^{cre}$ allele show expression of *Tbx18VP16* and are marked by GFP. For this reason in females the amount of GFP^+ cells is not directly comparable to the $Tbx18^{cre/+};R26^{mTmG/+}$ control and we could only examine if *Tbx18VP16*-expressing cells contributed to a certain tissue, but not if the amount of contributing cells was changed.

Epifluorescent detection of GFP^+ cells in whole UGS showed *Tbx18VP16*-expressing cells in the pelvis region, the adrenal glands and along some of the blood vessels, e.g. the dorsal aorta and the big renal arteries branching of the dorsal aorta and entering the kidney close to the ureter. The smooth muscle of the bladder wall was devoid of GFP^+ cells. Immunohistochemically, we detected the majority of the *Tbx18VP16*-expressing cells in the renal interstitium directly underneath the epithelial lining of the pelvis. Interestingly no affected cells were detectable in the medial renal cortex while in the control most of the medial cortical stroma was GFP^+ (**Fig. 7 K**+**M** and **L**+**N**). Patches of *Tbx18VP16*-expressing cells were detectable in the thin ureter wall in $Tbx18^{cre/+},Hprt^{Tbx18VP16/+}$ hydroureters while in the control *Tbx18*-derived, GFP^+ cells give rise to all layers of the ureter wall except the epithelium(**Fig. 7 O** and **P**).

To analyze the contribution of *Tbx18VP16*-expressing cells to the smooth muscle tissues of the different organs of the UGS we traced GFP and the smooth muscle marker ACTA2 via double-immunohistochemistry in tissue sections at E18.5. We found that clusters of *Tbx18VP16*-expressing cells in the ureter wall were $ACTA2^-$ (**Fig. 7 U** and **U`**). A strongly reduced ACTA2 expression was also found in *Tbx18VP16*-expressingcells in the renal pelvis and medulla region (**Fig. 7 V** and **V`**). In the smooth muscle layer of the bladder wall no *Tbx18VP16*-expressing cells were detectable, in contrast to the control, while some *Tbx18VP16*-expressing cells which were found, associated with blood vessels (**Fig. 7X** and **X`**)were $ACTA2^+$ (**Fig. 7W** and **W`**).

Taken together the phenotypical analysis of female $Tbx18^{cre/+},Hprt^{Tbx18VP16/+}$ -mutants has showed several morphological features, which were also found in *Tbx18*-loss of function mutant. *Tbx18VP16* expressing cells showed impaired smooth muscle differentiation and contributed only to the smooth muscle layer of blood vessel. From this we conclude that the transcription activating *Tbx18VP16*-allele functions as a dominant negative allele of *Tbx18*, and that Tbx18 has a transcription repressing function in ureteric smooth muscle development.

***Tbx18VP16* expressing cells accumulate in the pelvis region and are scarcely detectable along the ureter in male mutant metanephric explants**

Since the phenotype of male $Tbx18^{cre/+}R26^{mTmG/+};Hprt^{Tbx18VP16/y}$-mutants cannot be analyzed *in vivo* after E14.5, we decided to explant male metanephric primordia, and document their

development *ex vivo* for 7 days. As in male mutants expression of *Tbx18VP16* occurs in all recombined cells, the amount of GFP^+ cells is now comparable to the control.

At E11.5, the day of explantation (d0), the amount of *Tbx18*-derived cells is comparable between control and misexpression mutant (**Fig. 8 A** and **B**). One day later GFP^+ cells spread over the medial surface of the developing kidney in the control while they were mainly found along the ureter and, along the first branches of the CDS in mutant explant cultures (**Fig. 8 C** and **D**). After day 2 of culture (**Fig. 8 E** and **F**) *Tbx18*-derived cells established a coat of mesenchyme around the ureteric epithelium and the diameter of the ureter increased considerably in the control culture. In the *Tbx18VP16* expressing explant in contrast *Tbx18*-derived cells were more and more restricted to the pelvis region of the explant. No mesenchymal coat around the ureteric epithelium was detectable and the diameter of the ureter stayed the same after day 3 of culture. At day 7 of culture (**Fig. 8 I-L**) the ureter of the *Tbx18VP16* expressing explant appeared severely hypoplastic and the *Tbx18*-derived cells were more or less restricted to the pelvis region of the explant. Invasion of the renal stroma appeared strongly reduced.

The *ex vivo* lineage tracing revealed a strong reduction of *Tbx18*-derived cells along the ureter and in the stroma of *Tbx18VP16* expressing explant cultures. In the male explant cultures the amount of GFP^+, *Tbx18*-derived cells can be compared directly to the control, as expression of *Tbx18VP16* is activated in all recombined cells in this case. The result of the *ex vivo* analysis confirms the *in vivo* finding in female mutant which also showed an extremely low overall number of *Tbx18*-derived cells.

DISCUSSION

In this study we examined the consequences of temporal misexpression of the transcription factor Tbx18 and of a strongly activating *Tbx18VP16*-allele *in vivo*. Misexpression was activated in a *Tbx18*$^{+}$ mesenchymal precursor population of the metanephrogenic field. This precursor population contributes to the renal stroma and establishes the mesenchymal coat of the ureter, which gives rise to the ureteric smooth muscle and connective tissue [8]. Maintained expression of *Tbx18* resulted in a loss of the *lamina propria*, an accumulation of *Tbx18* misexpressing cells along the ureter and an altered distribution of affected cells in the renal stroma. While misexpressing stromal cells accumulated in the medial cortex, the amount of *Tbx18*-derived cells in the medullary stroma was reduced. Expression of *Tbx18VP16* prevented smooth muscle development cell-autonomously along the ureter and in the pelvis region, resulting in severe cases in hydroureter and hydronephrosis development.

Tbx18 and the control of cellular adhesion or proliferation in the UM

Our analysis of *Tbx18* misexpressing mouse mutants showed that prolonged expression of *Tbx18* resulted in hyperplasticity of UM coat and an accumulation of misexpressing cells in the renal cortex, while their contribution to the medullary stroma was strongly reduced. The complementary analysis of metanephric explant cultures confirmed these findings and revealed additionally that accumulation of misexpressing cells along the ureter occurs only after day 3 of culture. In our opinion the reduced contribution of *Tbx18* misexpressing cells to the medullary stroma occurs due to impaired stromal invasion. This impairment might be the result of decreased motility and/or increased adhesion of the affected cells. Results from earlier analyses of wildtype and *Tbx18*-loss of function embryos support this theory. In the wildtype *Tbx18* expression is maintained only in cells which stay part of the UM coat after E11.5. This has been shown in a previous expression analysis of *Tbx18* in the developing UGS and in the detailed analysis of stroma invasion by cells derived from the *Tbx18*$^{+}$-progenitor population [8,12]. A loss of *Tbx18* on the contrary led to the dispersal of the complete UM population at about the same time. This dispersal left the ureter completely devoid of mesenchymal cells, while the number of *Tbx18*-derived cells in the pelvis was increased [8,12].

The increased number of misexpressing cells along the ureter might be the result of impaired migration of supernumerary cells away from the ureter or it might occur due to increased proliferation. Up to now it is unclear if invasion of UM-derived cells continues after E11.5.

If the renal interstitium is still invaded after E11.5 by cells of the UM coat, which show a downregulation of *Tbx18*, maintained expression of *Tbx18* might prevent them from leaving the ureter and so cause the late accumulation. A reduction of proliferation was found previously in the *Tbx18*-loss of function mutant UM at E15.5 [12]. Also the strongly reduced amount of *Tbx18*-derived

cells along the ureter and in the renal stroma of *Tbx18VP16* expressing explants argues for a function of Tbx18 in UM proliferation. In the future it should be analyzed, if maintained expression of *Tbx18* or the expression of *Tbx18VP16* alters the number of proliferating cells or the response to proliferation-promoting signals like Shh. This analysis should be done at E14.5, when *Tbx18* is normally restricted to the layer of smooth muscle precursors.

Misexpression of *Tbx18* in the UM interferes with *lamina propria* development

The *lamina propria* is a connective tissue layer of the ureteric wall, between the ureteric epithelium and the smooth muscle tissue. It becomes detectable as one to two layers of ACTA2$^-$ cells at about E16.5 [9,21]. In the *Tbx18* misexpression mutant the ureteric smooth muscle layer was well developed, however the ACTA2$^-$ tissue layer was not detectable at E18.5. Expression of ACTA2 and of *Myocd,* the master regulator of smooth muscle differentiation [28] was ectopically detectable in the sub-epithelial mesenchyme.

These results led us to the conclusion that prolonged expression of *Tbx18* does not prevent smooth muscle differentiation, as hypothesized after the first *Tbx18* expression analysis [12], but expands the smooth muscle fate into the sub-epithelial mesenchyme layer. It was shown before that Shh-signaling is required for *lamina propria* development [10]. *Shh* is expressed in the epithelial lining of the ureter, the pelvis and the distal collecting duct system from E11.5 until the new born stage. The Shh receptor and target gene *Ptch1* and the Shh downstream mediator *Bmp4* are detectable in the adjacent mesenchyme of the ureter wall and the renal medulla. At newborn stage *Ptch1* and *Bmp4* finally become restricted to the thin sub-epithelial layer of mesenchyme. The analysis of mouse mutants with a conditional loss of *Shh* in the epithelium revealed that Shh-signaling is needed for UM proliferation but also, via *Bmp4*-activation, for ureteric smooth muscle differentiation. Most interestingly an epithelial loss of *Shh* also led to a loss of the *lamina propria* [10].

In the *Tbx18*-loss of function mutant expression of *Ptch1* and *Bmp4* were massively down regulated in the UM at E12.5 [8,12]. This led to the conclusion that *Tbx18* is needed in the mesenchyme to allow the reception of *Shh*-signals from the epithelium or to regulate the reaction to these signals. In the *Tbx18* misexpression mutant *Ptch1* was normally expressed in the sub-epithelial mesenchyme but we did not detect *Raldh2* or *Bmp4* expression at E18.5. The loss of *Raldh2* and *Bmp4* might indicate that ectopic *Tbx18* in the sub-epithelial mesenchyme interferes with *Shh*-signaling, causing the loss of the *lamina propria,* or the markers might be lost secondary to the loss of the *lamina propria*. As *Tbx18* and *Bmp4* are co-expressed in the wildtype UM at E12.5 a direct repression of *Bmp4*-expression by Tbx18 appears unlikely. The same is true for *Raldh2* [12].

Our study revealed furthermore that misexpression of *Tbx18* affects the outermost *lamina adventitia* and the inner *lamina propria* in different ways. In the outer layer we only found an

increased amount of connective tissue but no expression of the smooth muscle marker ACTA2, like in the inner sub-epithelial mesenchyme layer. Accordingly the effect of prolonged *Tbx18* expression on the UM depends on additional, is radially distributed factors. A factor secreted by the UE, which reaches the sub-epithelial mesenchyme but not the outer *lamina adventitia* layer, which might limit ectopic smooth muscle development to the UM close to the epithelium.

Known secreted signals from the UE affecting the UM are Shh and Wnt signals. Canonical Wnt-signaling is mediated by the transcriptional regulator *β-catenin* (*Ctnnb1*) in the. The role of canonical Wnt signaling in ureteric smooth muscle development and its connection to *Tbx18* has been analyzed in a previous publication from our group UM [11]. It revealed that a loss of canonical Wnt-signaling resulted in an expansion of the outermost connective tissue layer towards the UE at the expense of the ureteric smooth muscle layer, whereas a gain of canonical Wnt signaling, achieved by stabilization of β-catenin in the UM, triggered premature smooth muscle differentiation. The analysis also revealed that expression of Tbx18 depends on functional canonical Wnt signaling, as *Tbx18* was undetectable in the UM at E12.5 after the loss of β-catenin. Re-expression of *Tbx18 in the β*-catenin-loss of function background, using the same $Hprt^{Tbx18}$-misexpression-construct and $Tbx18^{cre}$-line applied in this study, did not rescue ureteric smooth muscle development. This experiment showed that the function of *Tbx18* in ureteric smooth muscle development depends on active Wnt signaling. Hence Wnt, secreted by the UE might be the factor which limits ectopic smooth muscle development in $Tbx18^{cre/+}$;$Hprt^{Tbx18/y}$ misexpression-mutants to the sub-epithelial mesenchyme. These findings are compatible with a function of *Tbx18* in regulating the extent of ureteric smooth muscle development by making the UM responsive to signals emanating from the UE without expanding the range of these signals.

Expression of *Tbx18VP16* in *Tbx18*-derived stroma and UM interferes with smooth muscle differentiation cell-autonomously

With the analysis of the *Tbx18VP16* expressing mutant we wanted to find out if Tbx18 functions as a repressing transcription factor during ureteric smooth muscle development. If the *Tbx18VP16* expressing mutant shows phenotypical features of the loss of function mutant this would be an indication for a repressing function of Tbx18 *in vivo*. From previous analyses it is known that in the *Tbx18*-loss of function mutant the loss of smooth muscle tissue is restricted to the ureter wall, while *Tbx18*-derived cells contribute normally to the smooth muscle tissue of the bladder, the pelvis, the medulla and the renal blood vessels [8,12]. In the *Tbx18VP16* expressing mutant in contrast, $ACTA2^{+}$ *Tbx18VP16* expressing cells were found only in the smooth muscle tissue of renal blood vessels. This might indicate that Tbx18 regulates genes in the UM, which are involved in smooth muscle differentiation in general and not specifically in the ureteric mesenchyme. While a loss of *Tbx18* only lead to a de-repression of its target genes, Tbx18VP16 causes the strong activation of their expression. This might explain the active prevention of smooth muscle

development in all *Tbx18VP16* expressing cells although Tbx18 is required only in the ureteric mesenchyme.

The mosaic expression pattern in female *Tbx18V16* expressing mutants gave us the opportunity to trace the fate of affected cell clusters embedded in the wildtype tissue of a phenotypically normal ureter. Affected cells, in the ureter wall and also in the pelvis failed to differentiate into smooth muscle tissue. This result demonstrated that the loss of smooth muscle differentiation in the *Tbx18VP16* expressing mutant is a cell-autonomous effect. Most likely *Tbx18VP16* expressing cells were either unable to receive a differentiation signal or they were unable to react to it.

The phenotypic similarities between the *Tbx18*-loss of function and the *Tbx18VP16* expressing mutant and the cell autonomous loss of smooth muscle differentiation in *Tbx18VP16* expressing cells reveal first *in vivo* evidence for a function of *Tbx18* as a transcriptional repressor in the regulation of ureteric smooth muscle differentiation.

FIGURES AND FIGURE LEGENDS

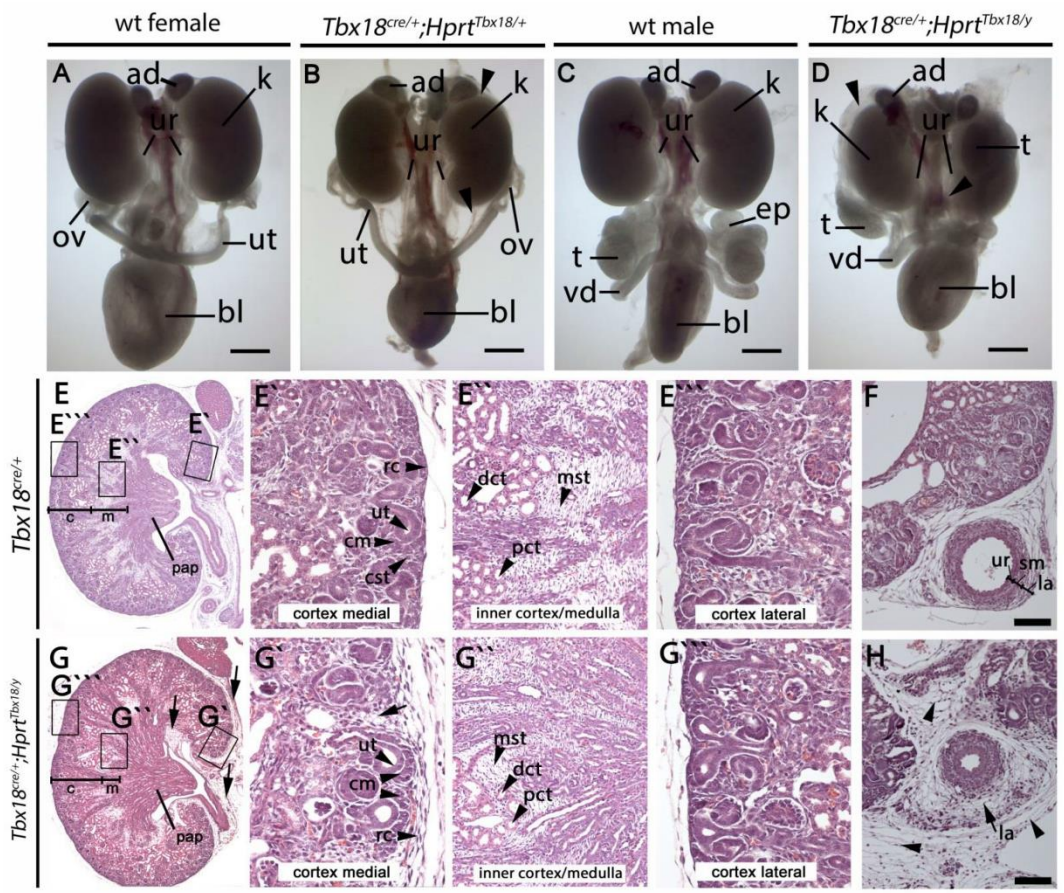

Fig.1: Kidney and urogenital tract anomalies of *Tbx18*$^{cre/+}$;*Hprt*^{Tbx18} misexpression mutants at E18.5.
Morphology of whole urogenital systems of female (**A** and **B**) and male embryos (**C** and **D**). Arrow heads in **B** and **D** indicate ectopic connective tissue. Hematoxylin and eosin (H&E) stainings of sagittal (**E** and **G**) and transverse (**F** and **H**) sections of kidney and proximal ureter. Frames in **E** and **G** indicate regions which are shown in higher magnification in **E`-E```** and **G`-G```**. Arrows in **G** and **G`** indicate ectopic tissue accumulations. ad, adrenal gland; bl, bladder; c, cortex; cm, cap mesenchyme; cst, cortical stroma; dct, distal convoluted tubule; ep, epididymis; k, kidney; m, medulla; ov, ovary; pap, papilla rc, renal capsule; t, testis; ur, ureter; ut, uterus; vd, *vas deferens*. Scale bars: A-D: 1mm; F+H: 0,1mm.

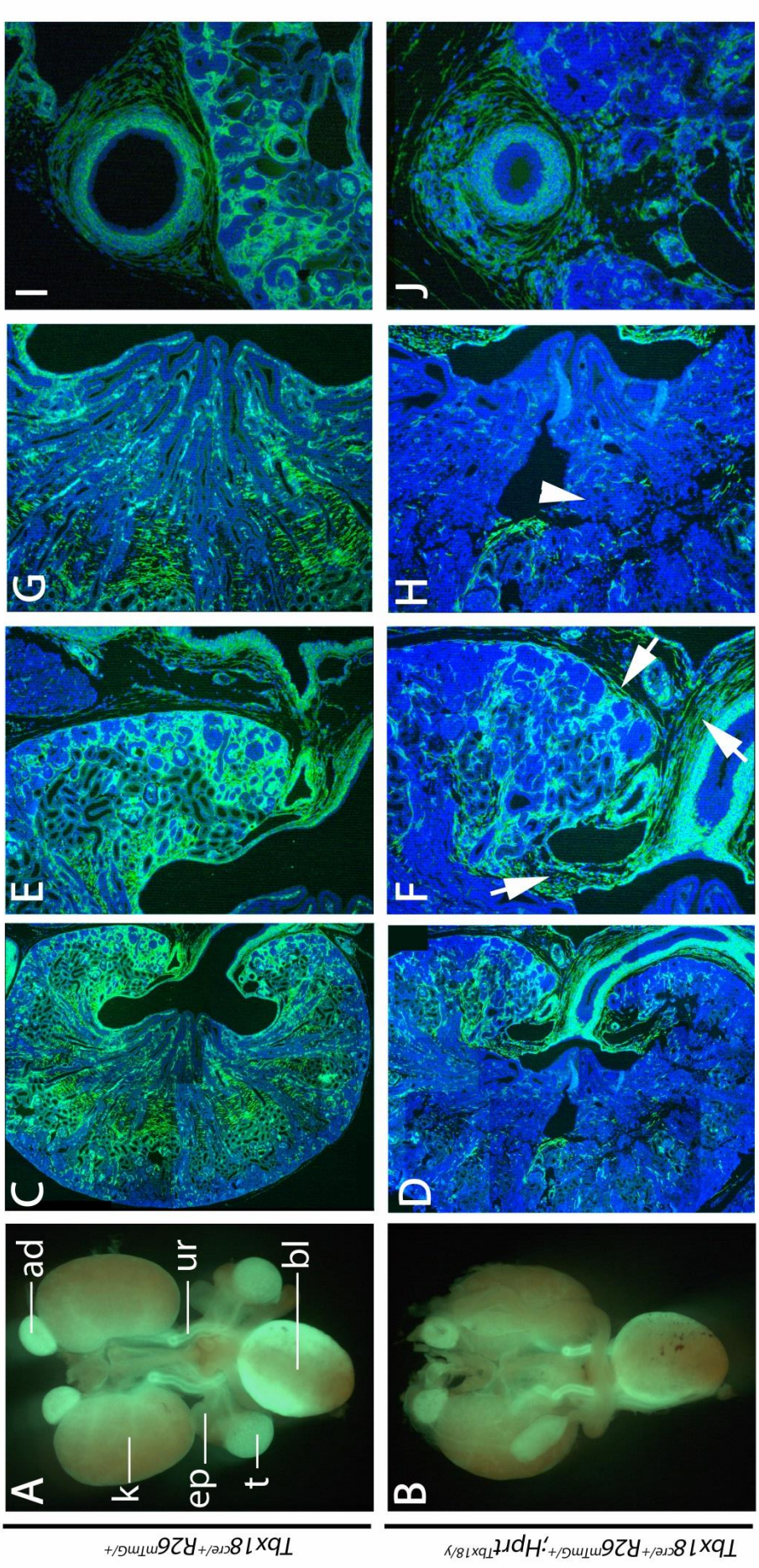

Fig.2: *In vivo*-lineage tracing of *Tbx18*-derived cells in the *Tbx18*$^{cre/+}$;*R26*$^{mTmG/+}$;*Hprt*$^{Tbx18/y}$ -mutant at E18.5
Membrane bound GFP and Tomato were detected via epifluorescence in dissected urogenital systems (**A** and **B**). In sagittal sections of kidney (**C** and **D**) and proximal ureter (**I** and **J**) *Tbx18*-derived, GFP^{+} cells were detected immunohistochemically. Higher magnification of the medial cortex and pelvis region (**E** and **F**) and the medulla region (**G** and **H**). Arrows in F indicate regions of ectopic *Tbx18*-derived tissue accumulations. Arrow in H indicates a region of reduced *Tbx18*-derived cell contribution in the medullary zone. ad, adrenal gland; bl, bladder; ep, epididymis; k, kidney; t, testis; ur, ureter; vd, vas deferens.

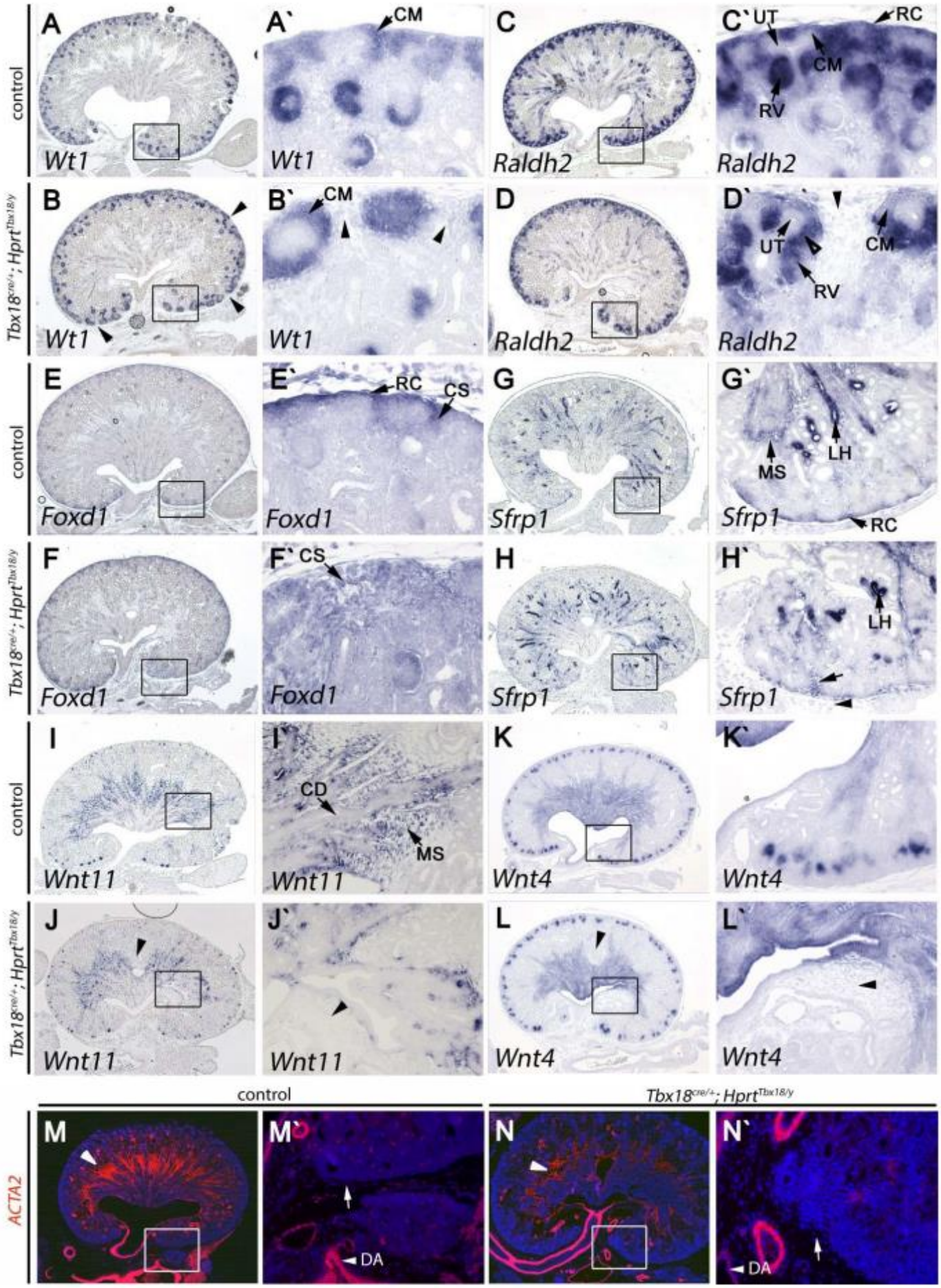
control
Tbx18cre/+; HprtTbx18/y
A
A`
CM
C
C`
UT
RC
CM
RV
Wt1
Wt1
Raldh2
Raldh2
B
B`
CM
D
D`
UT
CM
RV
Wt1
Wt1
Raldh2
Raldh2
E
E`
RC
CS
G
G`
LH
MS
Foxd1
Foxd1
Sfrp1
Sfrp1
RC
F
F`
CS
H
H`
LH
Foxd1
Foxd1
Sfrp1
Sfrp1
I
I`
CD
MS
K
K`
Wnt11
Wnt11
Wnt4
Wnt4
J
J`
L
L`
Wnt11
Wnt11
Wnt4
Wnt4
control
Tbx18cre/+; HprtTbx18/y
ACTA2
M
M`
N
N`
DA
DA

Fig.3: Molecular characterization of the accumulated tissue on the kidney surface and in the renal cortex of *Tbx18*$^{cre/+}$;*Hprt*$^{Tbx18/y}$-mutants at E18.5. Detection of molecular markers by *in situ*-hybridization (**A**-**L`**). Detection of the smooth muscle marker smooth muscle α-actin (ACTA2)by immunohistochemistry (**M**-**N`**) Frames indicate the regions shown in a higher magnification on the right side, next to the overview pictures. Arrow heads in **B`**, **D`**, **H`**, **L`** and **J`** indicate ectopic tissue accumulations in *Tbx18*$^{cre/+}$;*Hprt*$^{Tbx18/y}$-mutant kidneys. Arrow heads in **J** and **L** indicate prongs of cortical tissue reaching into the medullary zone of the renal parenchyme. Hollow arrow head in **D`** indicates *Raldh2*$^{+}$ renal stroma. White arrow heads in **M** and **N** indicate medullary smooth muscle tissue. White arrows in M` and N` indicate ACTA2^{-} ectopic tissue in the renal cortex. CM, cap mesenchyme; DA, dorsal aorta; RC, renal capsule; UT, ureteric tip; RV, renal vesicle; CS, cortical stroma; MS, medullary stroma; LH, Loop of Henle, CD, collecting duct.

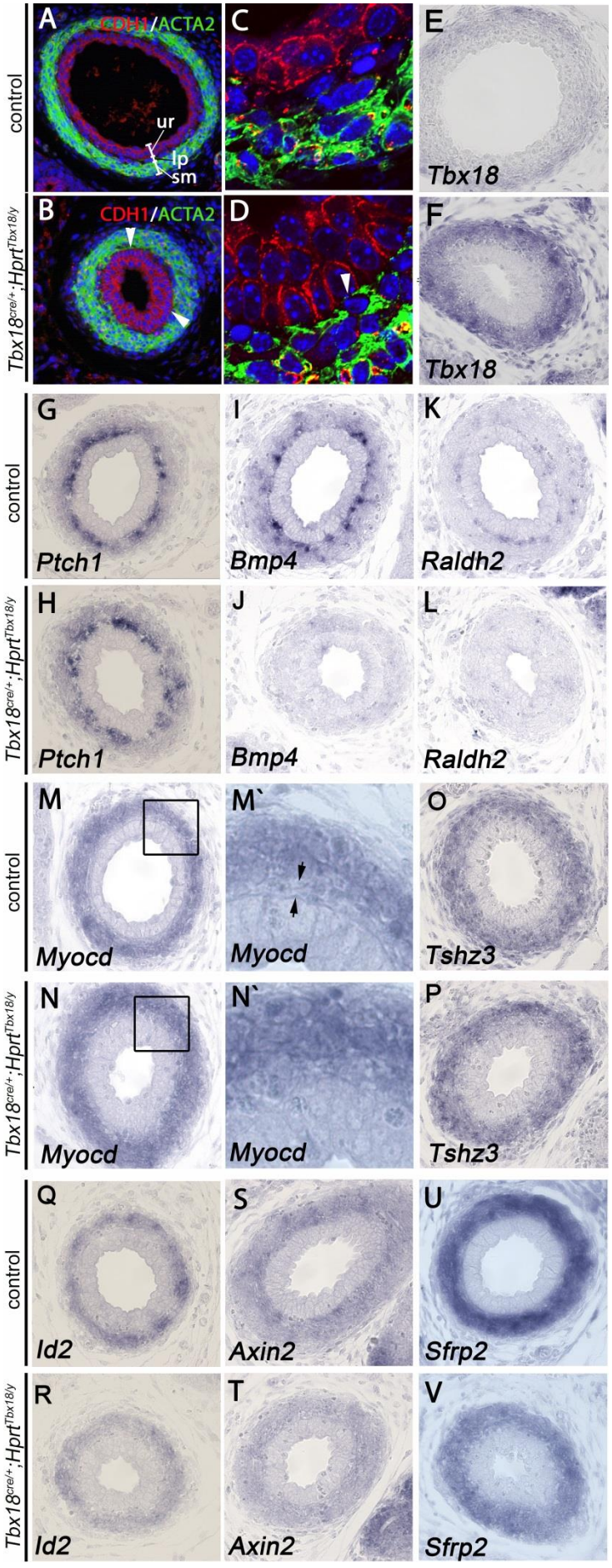
control
Tbx18cre/+;HprtTbx18/y
A
CDH1/ACTA2
ur
lp
sm
B
CDH1/ACTA2
C
D
E
Tbx18
F
Tbx18
G
Ptch1
I
Bmp4
K
Raldh2
H
Ptch1
J
Bmp4
L
Raldh2
M
Myocd
M`
Myocd
O
Tshz3
N
Myocd
N`
Myocd
P
Tshz3
Q
Id2
S
Axin2
U
Sfrp2
R
Id2
T
Axin2
V
Sfrp2

Fig. 4: Molecular characterization of the proximal ureter of *Tbx18*$^{cre/+}$;*Hprt*$^{Tbx18/y}$-mutants at E18.5.
Proximal transverse ureter sections were taken close to the ureter-pelvis-junction region. Immunohistochemical detection of the epithelial marker E-Cadherin (CDH1) and ACTA2 (**A** and **B**). Higher magnification pictures, of the epithelium-smooth muscle interface, taken with a confocal laser scanning microscope (**C** and **D**). Arrow heads in **B** and **D** in higher magnification in **D** indicate sections of the epithelium-smooth muscle interface where epithelial cells of the urothelium are in direct contact with the smooth muscle layer. ur, urothelium; sm, smooth muscle layer; la, *lamina adventitia*; lp, *lamina propria.* Expression analysis of *Tbx18* (**E** and **F**) and of other molecular markers of the UM (**G**-**V**) by RNA *in situ* hybridization.

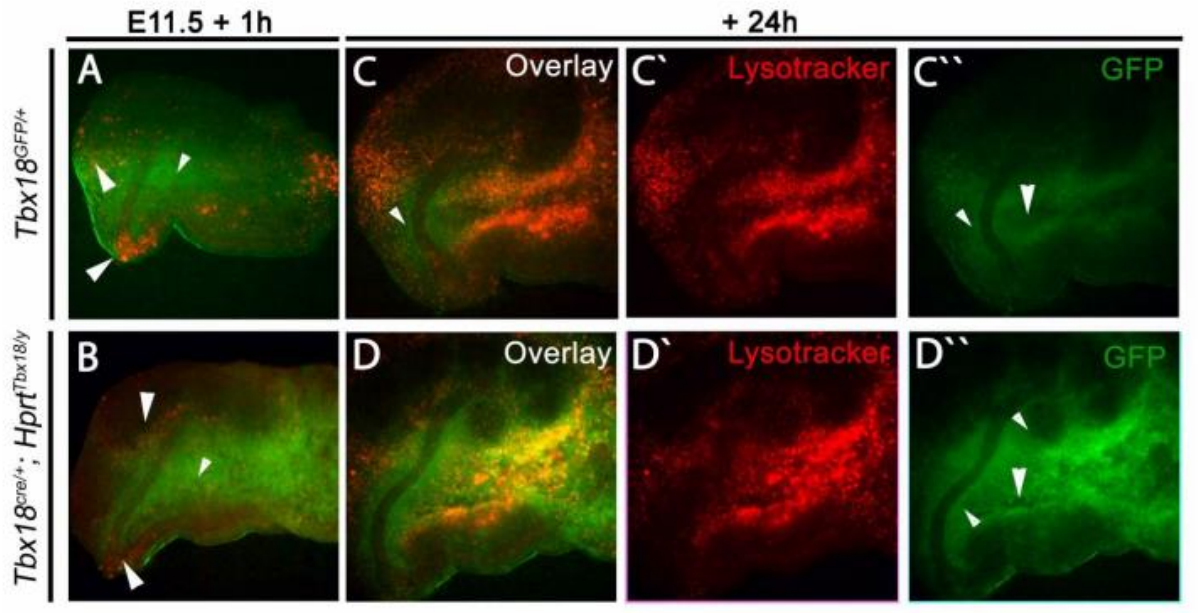

Fig.5: Detection of apoptosis in the *Tbx18*-derived UM-progenitor population in *Tbx18$^{cre/+}$;Hprt$^{Tbx18/y}$* metanephric explant cultures

Metanephric primordia of Tbx18$^{cre/+}$;Hprt$^{Tbx18/y}$-mutants and heterozygous Tbx18$^{GFP/+}$-controls were explanted at E11.5. Apoptosis was detected in the explant via the lysotracker assay 1h (**A+B**) and 24h (**C-D`**) after explantation. Big white arrow heads in **A** and **B** indicate spots of apoptotic processes. Small arrow heads in A and B indicate the early,Tbx18^{+}UM-progenitor population, marked by GFP-expression. The small arrow head in **C** indicates the mesenchyme along the ureter, where *Tbx18* expression is maintained after E11.5 in the control wile it persists in all cells derived from the progenitor population in the misexpression mutant in **D**.

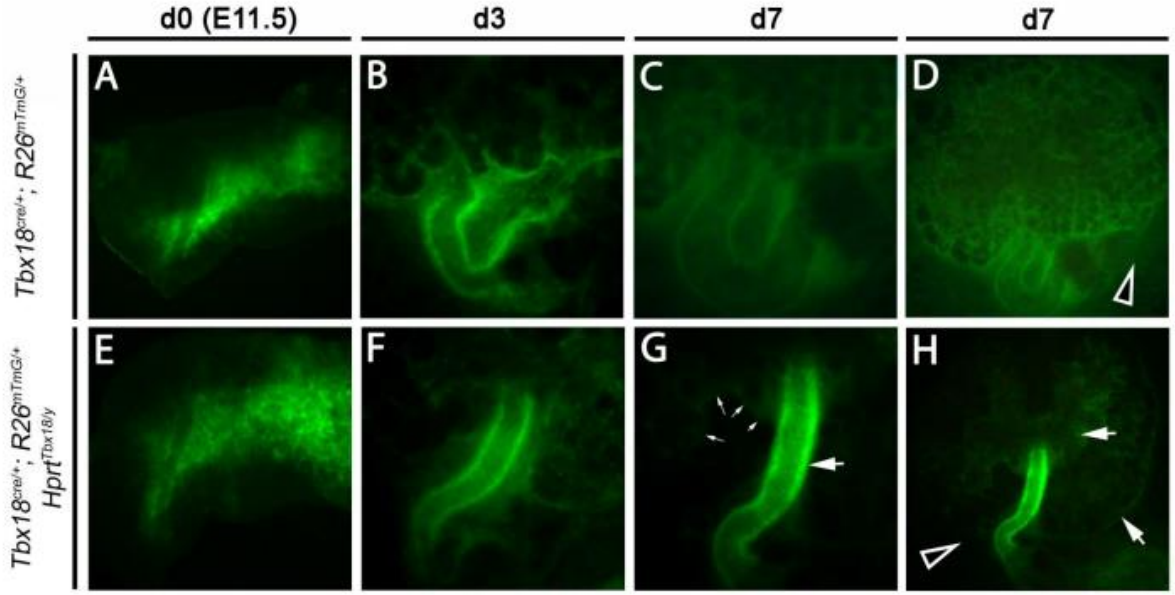

Fig.6: Lineage tracing of *Tbx18*-derived cells in *Tbx18*$^{cre/+}$;*R26*$^{mTmG/+}$;*Hprt*$^{Tbx18/y}$ metanephric explant cultures
Metanephric primordia were explanted at E11.5 (d0 of culture). *Tbx18*-derived cells were traced by epifluorescent detection of GFP Explant cultures were documented 3 and 7 days after explantation. The big arrow in **G** indicates accumulation of *Tbx18*$^{+}$ cells along the ureter. Small arrows in **G** indicate the border of a patch of *Tbx18* misexpressing cells in the renal interstitium. Arrows in **H** indicate accumulations of *Tbx18* misexpressing cells on the surface of the explant and in the interstitium. Hollow arrow heads in **D** and **H** indicate where we found *Tbx18*-derived cells which spread over the culture dish membrane in the control (**D**) but not in the misexpression mutant (**H**).

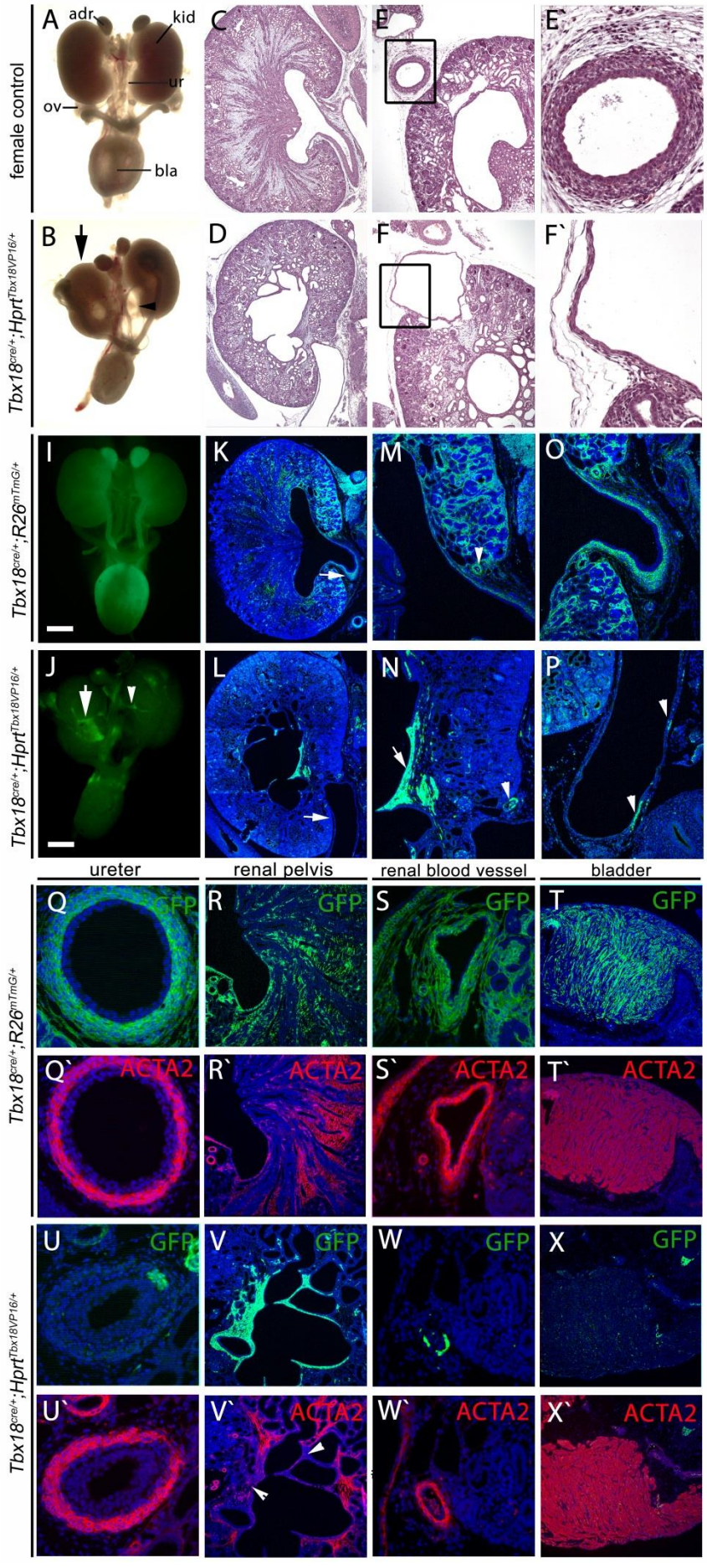
female control
Tbx18cre/+;HprtTbx18VP16/+
Tbx18cre/+;R26mTmG/+
Tbx18cre/+;HprtTbx18VP16/+
A
adr
kid
ur
ov
bla
B
C
D
E
E`
F
F`
I
J
K
L
M
N
O
P
ureter
renal pelvis
renal blood vessel
bladder
Q
R
S
T
GFP
Q`
R`
S`
T`
ACTA2
U
V
W
X
U`
V`
W`
X`

Fig.7: Kidney and ureter anomalies of *Tbx18*$^{cre/+}$;*Hprt*$^{Tbx18VP16/+}$-mutants at E18.5.
Morphology of whole dissected female UGS (**A** and **B**). Arrow in **B** indicates a ventrally rotated kidney. H&E staining of mid-sagittal sections of kidney and proximal ureter (**C** and **D**) and transverse proximal ureter sections (**E** and **F**). Frames indicate the region which is shown in higher magnification in **E`** and **F`**. Detection of all *Tbx18*-derived cells in dissected female *Tbx18*$^{cre/+}$;*R26*$^{mTmG/+}$-control UGS (**I**) and detection of *Tbx18VP16*-expressing cells in female *Tbx18*$^{cre/+}$;*Hprt*$^{Tbx18VP16/+}$-mutant UGS (**J**) using epifluorescent detection of GFP. Arrow in **J** indicates *Tbx18VP16*-expressing cells in the pelvis region. Arrow head in **J** indicate *Tbx18VP16*-expressing cells along a renal blood vessel. Immunohistochemical detection of GFP^{+} cells in mid-sagittal sections of kidney and proximal ureter (**K** and **L**) and in higher magnification images in the cortex and pelvis region (**M** and **N**) and the ureter (**O** and **P**). Arrows in **K** and **L** indicate the ureter wall. Arrow head in **M** and **N** indicate the renal artery. Arrow in **N** indicates accumulation of *Tbx18VP16*-expressing cells in the renal pelvis of the mutant. Arrow heads in **P** indicate remaining Tbx18VP16-expressing cells along the hydroureter wall in the mutant. Immunohistochemical analysis of the contribution of *Tbx18*-derived cells to smooth muscle tissue in the ureter (**Q** – **U`**), the renal pelvis and medulla (**R**-**V`**), renal blood vessels (**S**-**W`**) and the bladder wall (**T**-**X`**) by double staining for GFP and ACTA2. Arrow heads in **V`** indicate regions of reduced ACTA2 expression in the renal pelvis/medulla smooth muscle tissue.

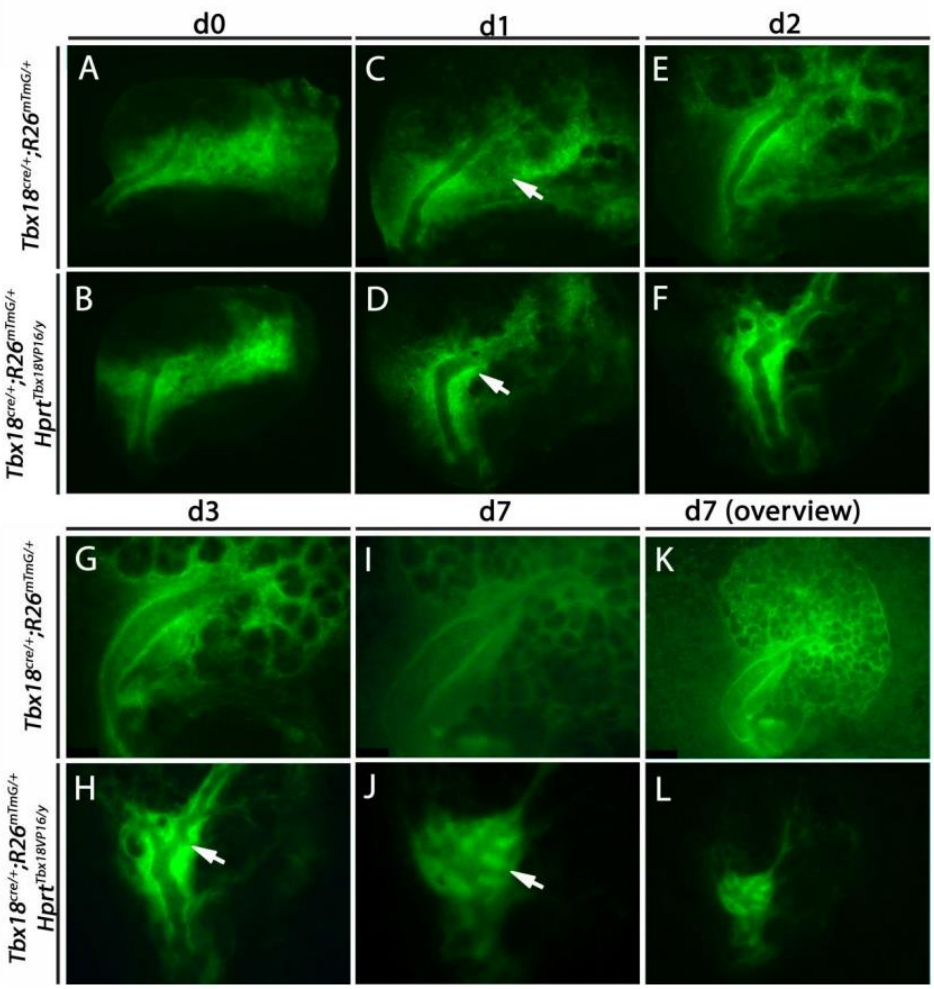

Fig.8: Lineage tracing of *Tbx18*-derived cells in *Tbx18$^{cre/+}$;R26$^{mTmG/+}$;Hprt$^{Tbx18VP16/y}$* metanephric explant cultures

Metanephric primordia were explanted at E11.5 (d0 of culture). *Tbx18*-derived cells were traced by epifluorescent detection of GFP Explant cultures were documented for 7 days after explantation (**A-J**). Overview picture of the complete explant at d7 in a lower magnification (**K** and **L**).

SUPPLEMENTARY FIGURES

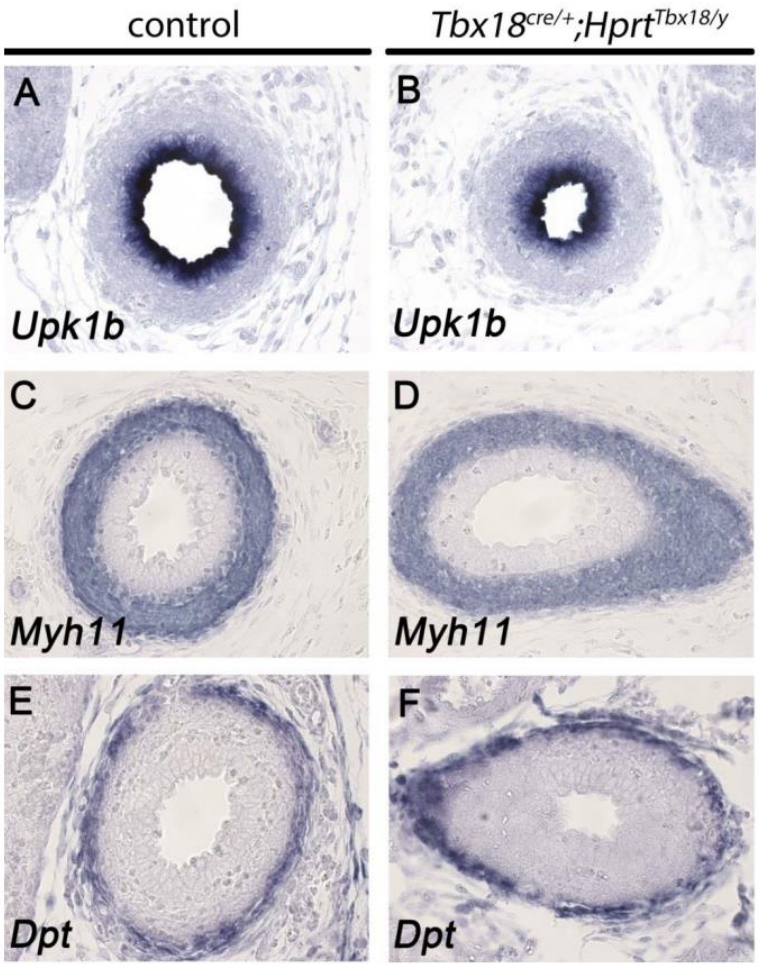

Fig. S1: Expression analysis of differentiation markers in transverse proximal ureter sections from *Tbx18*$^{cre/+}$;*Hprt*$^{Tbx18/y}$-mutants by RNA *in situ*-hybridization at E18.5.

Phenotypic changes observed in *Female Tbx18*$^{cre/+}$;*Hprt*$^{Tbx18VP16/+}$ UGS, dissected at E18.5	**N**
Total:	10
Wild-type phenotype	2
Unilateral hydroureter	4
Bilateral hydroureter	1
One or both kidneys rotated, pelvis opening on ventral side	5
(The hydroureter and rotated kidney phenotype also occurred in combination)	

Tab. S1: Morphological changes found in female *Tbx18*$^{cre/+}$;*Hprt*$^{Tbx18VP16/+}$-mutants and their prevalence

REFERENCES

1. Airik, R. & Kispert, A. Down the tube of obstructive nephropathies: the importance of tissue interactions during ureter development. *Kidney Int* **72,** 1459–1467 (2007).

2. Alcorn, D., Maric, C. & McCausland, J. Development of the renal interstitium. *Pediatr. Nephrol.* **13,** 347–354 (1999).

3. Ekblom, P. & Weller, A. Ontogeny of tubulointerstitial cells. *Kidney Int.* **39,** 394–400 (1991).

4. Zeisberg, M. & Kalluri, R. Physiology of the Renal Interstitium. *Clin. J. Am. Soc. Nephrol.* **10,** 1831–1840 (2015).

5. Li, W., Hartwig, S. & Rosenblum, N. D. Developmental origins and functions of stromal cells in the normal and diseased mammalian kidney. *Dev. Dyn.* **243,** 853–863 (2014).

6. Cullen-McEwen, L. A., Caruana, G. & Bertram, J. F. The where, what and why of the developing renal stroma. *Nephron. Exp. Nephrol.* **99,** e1–8 (2005).

7. Kobayashi, A. *et al.* Identification of a Multipotent Self-Renewing Stromal Progenitor Population during Mammalian Kidney Organogenesis. *Stem cell reports* **3,** 650–662 (2014).

8. Bohnenpoll, T. *et al.* Tbx18 expression demarcates multipotent precursor populations in the developing urogenital system but is exclusively required within the ureteric mesenchymal lineage to suppress a renal stromal fate. *Dev. Biol.* **380,** 25–36 (2013).

9. Bohnenpoll, T. & Kispert, A. Ureter growth and differentiation. *Semin. Cell Dev. Biol.* **36,** 21–30 (2014).

10. Yu, J., Carroll, T. J. & McMahon, A. P. Sonic hedgehog regulates proliferation and differentiation of mesenchymal cells in the mouse metanephric kidney. *Development* **129,** 5301–5312 (2002).

11. Trowe, M.-O. *et al.* Canonical Wnt signaling regulates smooth muscle precursor development in the mouse ureter. *Development* **139,** 3099–3108 (2012).

12. Airik, R., Bussen, M., Singh, M. K., Petry, M. & Kispert, A. Tbx18 regulates the development of the ureteral mesenchyme. *J. Clin. Invest.* **116,** 663–674 (2006).

13. Farin, H. F., Mansouri, A., Petry, M. & Kispert, A. T-box protein Tbx18 interacts with the paired box protein Pax3 in the development of the paraxial mesoderm. *J. Biol. Chem.* **283,** 25372–25380 (2008).

14. Greulich, F., Farin, H. F., Schuster-Gossler, K. & Kispert, A. Tbx18 function in epicardial development. *Cardiovasc. Res.* **96,** 476–483 (2012).

15. Muzumdar, M. D., Tasic, B., Miyamichi, K., Li, L. & Luo, L. A global double-fluorescent Cre reporter mouse. *Genesis* **45,** 593–605 (2007).

16. Wilkinson, D. G. & Nieto, M. A. Detection of messenger RNA by in situ hybridization to tissue sections and whole mounts. *Methods Enzymol.* **225,** 361–373 (1993).

17. Moorman, A. F., Houweling, A. C., de Boer, P. A. & Christoffels, V. M. Sensitive nonradioactive detection of mRNA in tissue sections: novel application of the whole-mount in situ hybridization protocol. *J. Histochem. Cytochem.* **49,** 1–8 (2001).

18. Airik, R. *et al.* Hydroureternephrosis due to loss of Sox9-regulated smooth muscle cell differentiation of the ureteric mesenchyme. *Hum. Mol. Genet.* **19,** 4918–4929 (2010).

19. Hatini, V., Huh, S. O., Herzlinger, D., Soares, V. C. & Lai, E. Essential role of stromal mesenchyme in kidney morphogenesis revealed by targeted disruption of Winged Helix transcription factor BF-2. *Genes Dev.* **10,** 1467–1478 (1996).

20. Hum, S., Rymer, C., Schaefer, C., Bushnell, D. & Sims-Lucas, S. Ablation of the renal stroma defines its critical role in nephron progenitor and vasculature patterning. *PLoS One* **9,** e88400 (2014).

21. Xu, J. *et al.* Fstl1 antagonizes BMP signaling and regulates ureter development. *PLoS One* **7,** e32554 (2012).

22. Wang, D. *et al.* Activation of cardiac gene expression by myocardin, a transcriptional cofactor for serum response factor. *Cell* **105,** 851–862 (2001).

23. Caubit, X. *et al.* Teashirt 3 is necessary for ureteral smooth muscle differentiation downstream of SHH and BMP4. *Development* **135,** 3301–3310 (2008).

24. Nakahiro, T., Kurooka, H., Mori, K., Sano, K. & Yokota, Y. Identification of BMP-responsive elements in the mouse Id2 gene. *Biochem. Biophys. Res. Commun.* **399,** 416–421 (2010).

25. Kikuchi, A. Modulation of Wnt signaling by Axin and Axil. *Cytokine Growth Factor Rev.* **10,** 255–265 (1999).

26. Lescher, B., Haenig, B. & Kispert, A. sFRP-2 is a target of the Wnt-4 signaling pathway in the developing metanephric kidney. *Dev. Dyn.* **213,** 440–451 (1998).

27. Farin, H. F. *et al.* Transcriptional repression by the T-box proteins Tbx18 and Tbx15 depends on Groucho corepressors. *J. Biol. Chem.* **282,** 25748–25759 (2007).

28. Wang, Z., Wang, D.-Z., Pipes, G. C. T. & Olson, E. N. Myocardin is a master regulator of smooth muscle gene expression. *Proc. Natl. Acad. Sci. U. S. A.* **100,** 7129–7134 (2003).

11. Conclusions

The aim of this thesis was to investigate the function of Tbx18 during ureteric smooth muscle development and to analyze its connection to other pathways involved in this process. The results of this study revealed the early establishment of a multipotent Tbx18$^+$ progenitor lineage, which contributes to most organs of the UGS, while only ureteric smooth muscle development depends on the function of Tbx18.

The analysis of Tbx18-gain- and loss-of-function mutants showed, that Tbx18 is not only necessary for smooth muscle development but also sufficient to expand it into neighboring tissue layers, most likely in cooperation with epithelium derived signals, like Wnt-signaling.

Analysis of mutants expressing the artificial, transcription activating *Tbx18VP16*-allele gave first *in vivo* indications for the requirement of Tbx18 as a repressor during smooth muscle development.

Finally we were able to show, that the early missexpression of *Tbx18* is insufficient to expand the UM precursor population, while the early analysis of the Tbx18-loss-of-function mutant showed that Tbx18 is necessary to repress the early metanephric expression program in the UM precursor population to allow ureteric smooth muscle development.

Tbx18 marks a new multipotent progenitor population of the metanephrogenic field

We were able to show that the *Tbx18*$^+$ lineage is established along the urogenital ridge between E9.5 and E10.5 as a mesenchymal sub-population which never showed an overlap with nephrogenic tissue of the ridge. Also this lineage is distinct from the renal stroma precursors from E11.5 on. The segregation of cells contributing either to the UM or the renal stroma at E11.5 was visualized for the first time in our publication by DiI-labeling of single cell clusters in metanephric explant at E11.5 cultures. It revealed that the cells of the Tbx18$^+$ UM-precursor population in young E11.5 embryos can actually be assigned to three different fractions depending on their distance from the ureteric epithelium at this stage. The most cranial part of the population will be removed by apoptosis. The cells which are located 200 µm or less far away from the ureteric epithelium contribute to the stroma of the kidney and only a

small fraction close to the epithelium, which could not be distinctly labeled, remains part of the UM coat. It would be interesting to find out how long the invasion of the renal interstitium continues after E11.5 when *Tbx18* expression is restricted to the UM coat. It is possible, that the proliferating population of UM cells continues to contribute to the renal stroma. The lineage tracing of permanently labeled *Tbx18*-derived cells showed that cells from the two expression domains of *Tbx18* in the UGR, the cranial UGR mesenchyme and its surface epithelium as well as the population in the metanephrogenic field contribute to most organs of the UGS. The complementary fate mapping in the loss of function mutant revealed that its function is restricted to the control of ureteric smooth muscle development. Permanent labeling of the *Tbx18*-derived cell population in the *Tbx18*-loss of function mutant and heterozygous controls allowed a comparable *in vivo* and *ex vivo* lineage tracing and the quantification of *Tbx18*-derived cells in different zones of the renal stroma. It showed the increased contribution of *Tbx18*-mutant cells to the renal stroma, which lead us to the conclusion that these cells adopt a stroma-like default fate.

Tbx18 and ureteric smooth muscle development

The analysis of the $Tbx18^{cre/+};Hprt^{Tbx18}$-mutant revealed that maintained expression of *Tbx18* throughout the coat of ureteric mesenchyme is sufficient to expand ureteric smooth muscle development into the innermost layer of mesenchyme which normally differentiates into the $ACTA2^{-}$ fibrocytes of the *lamina propria*. The absence of ectopic smooth muscle differentiation in the outermost layer of *Tbx18* misexpressing ureteric mesenchyme indicates that smooth muscle development still depends on the presence of additional factors, which are restricted to the inner layers of the mesenchymal coat. The analysis of the conditional β-catenin-loss of function mutant and the examination of Wnt signaling pathway in the *Tbx18*-loss of function mutant, which are part of the publications in this thesis, indicate that expression of *Tbx18* after E11.5 and Wnt-signaling between the UE and UM depend on each other. The conditional *β-catenin*-loss of function mutant showed a loss of *Tbx18* expression and an expansion of *lamina propria* fibroblast markers into the inner layers of UM, while no ureteric smooth muscle layer was detectable. Re-expression of *Tbx18* in the conditional *β-catenin*-loss of function background, in $Tbx18^{cre/+};Hprt^{Tbx18/y};Ctnn1^{fl/fl}$-mutants did not rescue the loss of ureteric smooth muscle tissue. This indicates that the function of Tbx18 in ureteric smooth muscle development depends on functional

canonical Wnt-signaling. Thus UE-derived Wnt might be the factor which limits the diameter of the ureteric smooth muscle layer in the *Tbx18*$^{cre/+}$*; Hprt*$^{Tbx18/y}$-mutant. The results of the different publications in this thesis indicate that *Tbx18*-expression and functional canonical Wnt-signaling depend on each other in this context. Furthermore, canonical Wnt signals and Tbx18 seem to be needed in combination to allow ureteric smooth muscle development. It would be interesting to find out if expression of *Tbx18* in the UM and the presence of Wnt-proteins, which can activate the canonical signaling pathway, are also sufficient to activate smooth muscle development. It has been shown that forced activation of canonical Wnt-signaling in the UM can activate smooth muscle differentiation and that in this case, the process does not depend on Tbx18 [66]. To find out, if Tbx18 can expand the radius of the UM which reacts to Wnt signals, one could use an organ culture of E14.5 *Tbx18*$^{cre/+}$*;Hprt*$^{Tbx18/y}$ ureter primordia and add Wnt-coated beads to the outer surface of the ureter. If the combination is sufficient, to activate smooth muscle differentiation ectopically, we would expect smooth muscle differentiation in the outer UM, which normally differentiates into the *tunica adventitia* layer.

Taken together, these results are well compatible with a function of Tbx18 in making the ureteric mesenchyme responsive to epithelium derived signals to allow ureteric smooth muscle development, which was initially proposed after the analysis of the *Tbx18*-loss of function phenotype by Airik and colleagues.

New *in vivo* indications for a repressing function of Tbx18 in ureteric smooth muscle development

The examination of embryos, which showed expression of *Tbx18VP16* in all *Tbx18*-derived cells, revealed a cell-autonomous loss of smooth muscle differentiation in the affected cells. The strongly affected individuals, among the heterozygous female misexpression mutants, showed several features of the *Tbx18*-loss of function phenotype, like the very characteristic ventral rotation of the kidney, the shortened ureter and the loss of the ureteric smooth muscle layer. These results brought the first indication for a transcription repressing function of *Tbx18* in this context. The massive loss of *Tbx18*-derived cells in the *Tbx18VP16* expressing embryos might occur due to the fact that in this mutant, target genes which should be repressed are now strongly activated. Of course also off-target effects might be involved. If it will be

possible in the future to sort out false targets from true ones, this mutant might be a valuable tool for the identification of target genes which can be regulated by Tbx18 in an *in vivo* setting. This sorting might be done by overlaying the results of microarrays of *Tbx18*-loss and gain of function and *Tbx18VP16* expressing mutants compared to wildtypes.

Tbx18 and the specification of the ureteric mesenchyme

One of our initial questions was, if Tbx18 has an early function in the specification of the ureteric mesenchyme as the precursor population of the ureteric smooth muscle tissue. Our analysis of *Pax3-cre/+;Hprt*$^{Tbx18/y}$ misexpression mutants showed that Tbx18 is not sufficient to expand the UM-precursor population within the UGR, as there was no expansion of early markers of this compartment detectable. The analysis also revealed that Tbx18 is sufficient to suppress the development of nephrogenic mesenchyme in the ridge. We investigated the physiological relevance of the NM-repressing potential of Tbx18 and found that Tbx18 is also necessary to repress the early MM-expression program in the UM-progenitor population at this stage. We excluded the possibility of an expansion of MM marker expression due to boundary maintenance defects by immunohistochemical detection of GFP(Tbx18) and Eya1 in the metanephrogenic field at E11.5 in *Tbx18*$^{GFP/+}$ heterozygous controls and *Tbx18*$^{GFP/GFP}$-loss of function mutants. This examination showed Eya1/GFP-double positive cells in the UM-domain, arguing for a change to the molecular character of the UM. Altered expression of mesenchymal Eya1 and Gdnf was accompanied by secondary changes in the ureteric epithelium and we were able to show that first morphological changes in the loss of function mutant occurred concomitantly with the altered mesenchymal and epithelial marker expression. We wondered how far the ureteric mesenchyme was changed towards a metanephric character after a loss of *Tbx18*. The fate mapping of *Tbx18*-derived cells in the mutant partly answered this question. In this fate mapping we found no contribution of *Tbx18*-derived cells to the cap mesenchyme or the nephrons in either *Tbx18*-mutant or control embryos. Obviously the UM did not adopt a full CM-like character. The fact that *Eya1* expression is expanded only transiently and is basically restricted to the mesenchyme close to the ureteric epithelium implies that the function of Tbx18 lies in the regulation of the mesenchymal response to epithelium derived signals. By repressing the activation of *Eya1* and, most likely secondary, of *Gdnf* Tbx18 might

specify the UM as a distinct mesenchymal precursor population indirectly. The analysis of the two *Eya1*-misexpression mutants, which was done to determine the significance of ectopic Eya1 expression for the development of the *Tbx18*-loss of function phenotype, brought conflicting results. Misexpression of *Eya1* throughout the metanephrogenic field led to the expansion of *Gdnf* and *Six1* expression in the mesenchyme and to expanded expression of *Ret* in the UE. These molecular changes were accompanied by alterations in ureteric branching. These results indicate that ectopic Eya1 might be responsible for the early defects in the Tbx18-loss of function mutant. The ectopic expression of *Eya1* in the UM in contrast, showed only minor effect on ureter development. Overall ectopic *Eya1* expression and activation of other MM markers might rather be a symptom of the defective mechanism in the *Tbx18*-loss of function mutant than the causative agent. We did not address the question about a direct regulation of *Eya1* by Tbx18 on the level of chromatin immunoprecipitation in this analysis. This analysis might be interesting in the future, as soon as a suitable antibody is available. Even if Eya1 is not the main mediator of the *Tbx18*-loss of function phenotype, its expression might still be regulated by Tbx18. It would be a great progress to identify a gene which is regulated by Tbx18 under physiological conditions.

There is an accumulating amount of evidence for a function of Tbx18 in regulating the perception of or reaction to epithelial signals in the UM. Hence a promising approach for future identification of direct target genes of Tbx18 might be to analyze the overlap between transcriptional changes in the *Tbx18*-loss of function mutant and mutants for the pathway which are active between the epithelium and the mesenchyme. Transcription analysis might be done by microarrays. This would mean to approach the question on a large and unbiased scale.

12. References

1. Bohnenpoll, T. & Kispert, A. Ureter growth and differentiation. *Semin. Cell Dev. Biol.* **36,** 21–30 (2014).

2. Mugford, J. W., Sipilä, P., Kobayashi, A., Behringer, R. R. & McMahon, P. Hoxd11 specifies a program of metanephric kidney development within the intermediate mesoderm of the mouse embryo. **319,** 396–405 (2009).

3. Davidson, A. J., Mouse kidney development, StemBook, ed. The Stem Cell Research Community, StemBook (2009)

4. Erman, A., Veranic, P., Psenicnik, M. & Jezernik, K. Superficial cell differentiation during embryonic and postnatal development of mouse urothelium. *Tissue Cell* **38,** 293–301 (2006).

5. Shiroyanagi, Y. *et al.* Urothelial sonic hedgehog signaling plays an important role in bladder smooth muscle formation. *Differentiation.* **75,** 968–977 (2007).

6. Rasouly, H. M. & Lu, W. Lower urinary tract development and disease. *Wiley Interdiscip. Rev. Syst. Biol. Med.* **5,** 307–342 (2013).

7. Mugford, J. W., Sipila, P., McMahon, J. A. & McMahon, A. P. Osr1 expression demarcates a multi-potent population of intermediate mesoderm that undergoes progressive restriction to an Osr1-dependent nephron progenitor compartment within the mammalian kidney. *Dev. Biol.* **324,** 88–98 (2008).

8. Wang, C. *et al.* Six1 and Eya1 are critical regulators of peri-cloacal mesenchymal progenitors during genitourinary tract development. *Dev. Biol.* **360,** 186–194 (2011).

9. Bohnenpoll, T. *et al.* Tbx18 expression demarcates multipotent precursor populations in the developing urogenital system but is exclusively required within the ureteric mesenchymal lineage to suppress a renal stromal fate. *Dev. Biol.* **380,** 25–36 (2013).

10. Richardson, L. *et al.* EMAGE mouse embryo spatial gene expression database: 2014 update. *Nucleic Acids Res.* **42,** D835-44 (2014).

11. James, R. G., Kamei, C. N., Wang, Q., Jiang, R. & Schultheiss, T. M. Odd-skipped related 1 is required for development of the metanephric kidney and regulates formation and differentiation of kidney precursor cells. *Development* **133,** 2995–3004 (2006).

12. Bouchard, M., Souabni, A., Mandler, M., Neubuser, A. & Busslinger, M. Nephric lineage specification by Pax2 and Pax8. *Genes Dev* **16,** 2958–2970 (2002).

13. Sainio, K., Hellstedt, P., Kreidberg, J. A., Saxen, L. & Sariola, H. Differential regulation of two sets of mesonephric tubules by WT-1. *Development* **124,** 1293–1299 (1997).

14. Grote, D., Souabni, A., Busslinger, M. & Bouchard, M. Pax 2/8-regulated Gata 3 expression is necessary for morphogenesis and guidance of the nephric duct in the developing kidney. *Development* **133,** 53–61 (2006).

15. Carroll, T. J., Park, J.-S., Hayashi, S., Majumdar, A. & McMahon, A. P. Wnt9b plays a central role in the regulation of mesenchymal to epithelial transitions underlying organogenesis of the mammalian urogenital system. *Dev. Cell* **9,** 283–292 (2005).

16. Fujii, T. *et al.* Expression patterns of the murine LIM class homeobox gene lim1 in the developing brain and excretory system. *Dev. Dyn.* **199,** 73–83 (1994).

17. Pachnis, V., Mankoo, B. & Costantini, F. Expression of the c-ret proto-oncogene during mouse embryogenesis. *Development* **119,** 1005–1017 (1993).

18. Smith, C. & Mackay, S. Morphological development and fate of the mouse mesonephros. *J. Anat.* **174,** 171–184 (1991).

19. Georgas, K. M., Chiu, H. S., Lesieur, E., Rumballe, B. A. & Little, M. H. Expression of metanephric nephron-patterning genes in differentiating mesonephric tubules. *Dev Dyn* **240,** 1600–1612 (2011).

20. Sajithlal, G., Zou, D., Silvius, D. & Xu, P. Eya1 acts as a critical regulator for specifying the metanephric mesenchyme. **284,** 323–336 (2005).

21. Xu, J. & Xu, P.-X. Eya-Six are necessary for survival of nephrogenic cord progenitors and inducing nephric duct development prior to ureteric bud formation. *Dev. Dyn.* (2015).

22. Nishinakamura, R. *et al.* Murine homolog of SALL1 is essential for ureteric bud invasion in kidney development. *Development* **128,** 3105–3115 (2001).

23. Karl, J. & Capel, B. Sertoli cells of the mouse testis originate from the coelomic epithelium. *Dev. Biol.* **203,** 323–333 (1998).

24. McLaren, A. Gonad development: assembling the mammalian testis. *Curr. Biol.* **8,** R175-7 (1998).

25. Sun, J., Ting, M.-C., Ishii, M. & Maxson, R. Msx1 and Msx2 function together in the regulation of primordial germ cell migration in the mouse. *Dev. Biol.* (2016).

26. Dressler, G. R. Advances in early kidney specification, development and patterning. *Development* **136,** 3863–3874 (2009).

27. Brophy, P. D., Ostrom, L., Lang, K. M. & Dressler, G. R. Regulation of ureteric bud outgrowth by Pax2-dependent activation of the glial derived neurotrophic factor gene. *Development* **128,** 4747–4756 (2001).

28. Xu, P.-X. *et al.* Six1 is required for the early organogenesis of mammalian kidney. *Development* **130,** 3085–3094 (2003).

29. Kreidberg, J. A. *et al.* WT-1 is required for early kidney development. *Cell* **74,** 679–691 (1993).

30. Wellik, D. M., Hawkes, P. J. & Capecchi, M. R. Hox11 paralogous genes are essential for metanephric kidney induction. *Genes Dev.* **16,** 1423–1432 (2002).

31. Gong, K. Q., Yallowitz, A. R., Sun, H., Dressler, G. R. & Wellik, D. M. A Hox-Eya-Pax complex regulates early kidney developmental gene expression. *Mol Cell Biol* **27,** 7661–7668 (2007).

32. Costantini, F. & Shakya, R. GDNF/Ret signaling and the development of the kidney. *Bioessays* **28,** 117–127 (2006).

33. Karner, C. M. *et al.* Canonical Wnt9b signaling balances progenitor cell expansion and differentiation during kidney development. *Development* **138,** 1247–1257 (2011).

34. Xu, J. *et al.* Eya1 interacts with Six2 and Myc to regulate expansion of the nephron progenitor pool during nephrogenesis. *Dev. Cell* **31,** 434–447 (2014).

35. Dressler, G. R., Deutsch, U., Chowdhury, K., Nornes, H. O. & Gruss, P. Pax2, a new murine paired-box-containing gene and its expression in the developing excretory system. *Development* **109,** 787–795 (1990).

36. Pichel, J. G. *et al.* Defects in enteric innervation and kidney development in mice lacking GDNF. *Nature* **382,** 73–76 (1996).

37. Nie, X., Xu, J., El-Hashash, A. & Xu, P.-X. Six1 regulates Grem1 expression in the metanephric mesenchyme to initiate branching morphogenesis. *Dev. Biol.* **352,** 141–151 (2011).

38. Cullen-McEwen, L. A., Caruana, G. & Bertram, J. F. The where, what and why of the developing renal stroma. *Nephron. Exp. Nephrol.* **99,** e1-8 (2005).

39. Fanni, D. *et al.* Interstitial stromal progenitors during kidney development: here, there and everywhere. *J. Matern. Fetal. Neonatal Med.* 1–6 (2016).

40. Ekblom, P. & Weller, A. Ontogeny of tubulointerstitial cells. *Kidney Int.* **39,** 394–400 (1991).

41. Brenner-Anantharam, A. *et al.* Tailbud-derived mesenchyme promotes urinary tract segmentation via BMP4 signaling. *Development* **134,** 1967–1975 (2007).

42. Sainio, K. *et al.* Neuronal characteristics in embryonic renal stroma. *Int. J. Dev. Biol.* **38,** 77–84 (1994).

43. Airik, R., Bussen, M., Singh, M. K., Petry, M. & Kispert, A. Tbx18 regulates the development of the ureteral mesenchyme. *J. Clin. Invest.* **116,** 663–674 (2006).

44. Cunha, G. R., Young, P., Higgins, S. J. & Cooke, P. S. Neonatal seminal vesicle mesenchyme induces a new morphological and functional phenotype in the epithelia of adult ureter and ductus deferens. *Development* **111,** 145–158 (1991).

45. Lipschutz, J. H., Young, P., Taguchi, O. & Cunha, G. R. Urothelial transformation into functional glandular tissue in situ by instructive mesenchymal induction. *Kidney Int.* **49,** 59–66 (1996).

46. Baskin, L. S., Hayward, S. W., Young, P. & Cunha, G. R. Role of mesenchymal-epithelial interactions in normal bladder development. *J. Urol.* **156,** 1820–1827 (1996).

47. Wang, C., Ross, W. T. & Mysorekar, I. U. Urothelial generation and regeneration in development, injury, and cancer. *Dev. Dyn.* **246,** 336–343 (2017).

48. Yu, J., Carroll, T. J. & McMahon, A. P. Sonic hedgehog regulates proliferation and differentiation of mesenchymal cells in the mouse metanephric kidney. *Development* **129,** 5301–5312 (2002).

49. Farin, H. F. *et al.* Transcriptional repression by the T-box proteins Tbx18 and Tbx15 depends on Groucho corepressors. *J. Biol. Chem.* **282,** 25748–25759 (2007).

50. Kraus, F., Haenig, B. & Kispert, A. Cloning and expression analysis of the mouse T-box gene Tbx18. *Mech. Dev.* **100,** 83–86 (2001).

51. Greulich, F., Rudat, C. & Kispert, A. Mechanisms of T-box gene function in the developing heart. *Cardiovasc. Res.* **91,** 212–222 (2011).

52. Tada, M. & Smith, J. C. T-targets: clues to understanding the functions of T-box proteins. *Dev. Growth Differ.* **43,** 1–11 (2001).

53. Conlon, F. L., Fairclough, L., Price, B. M., Casey, E. S. & Smith, J. C. Determinants of T box protein specificity. *Development* **128,** 3749–3758 (2001).

54. Kispert, A. & Herrmann, B. G. The Brachyury gene encodes a novel DNA binding protein. *EMBO J.* **12,** 3211–3220 (1993).

55. Sinha, S., Abraham, S., Gronostajski, R. M. & Campbell, C. E. Differential DNA binding and transcription modulation by three T-box proteins, T, TBX1 and TBX2. *Gene* **258,** 15–29 (2000).

56. Farin, H. F., Mansouri, A., Petry, M. & Kispert, A. T-box protein Tbx18 interacts with the paired box protein Pax3 in the development of the paraxial mesoderm. *J. Biol. Chem.* **283,** 25372–25380 (2008).

57. Nie, X., Sun, J., Gordon, R. E., Cai, C.-L. & Xu, P.-X. SIX1 acts synergistically with TBX18 in mediating ureteral smooth muscle formation. *Development* **137,** 755–765 (2010).

58. Bussen, M. *et al.* The T-box transcription factor Tbx18 maintains the separation of anterior and posterior somite compartments. 1209–1221 (2004).

59. Trowe, M.-O., Maier, H., Schweizer, M. & Kispert, A. Deafness in mice lacking the T-box transcription factor Tbx18 in otic fibrocytes. *Development* **135,** 1725–1734 (2008).

60. Christoffels, V. M. *et al.* Formation of the venous pole of the heart from an Nkx2-5-negative precursor population requires Tbx18. *Circ. Res.* **98,** 1555–1563 (2006).

61. Wiese, C. *et al.* Formation of the sinus node head and differentiation of sinus node myocardium are independently regulated by Tbx18 and Tbx3. *Circ. Res.* **104,** 388–397 (2009).

62. Kapoor, N., Galang, G., Marban, E. & Cho, H. C. Transcriptional suppression of connexin43 by TBX18 undermines cell-cell electrical coupling in postnatal cardiomyocytes. *J. Biol. Chem.* **286,** 14073–14079 (2011).

63. Kapoor, N., Liang, W., Marban, E. & Cho, H. C. Direct conversion of quiescent cardiomyocytes to pacemaker cells by expression of Tbx18. *Nat. Biotechnol.* **31,** 54–62 (2013).

64. Greulich, F. *et al.* Misexpression of Tbx18 in cardiac chambers of fetal mice interferes with chamber-specific developmental programs but does not induce a pacemaker-like gene signature. *J. Mol. Cell. Cardiol.* **97,** 140–149 (2016).

65. Airik, R. & Kispert, A. Down the tube of obstructive nephropathies: the importance of tissue interactions during ureter development. *Kidney Int* **72,** 1459–1467 (2007).

66. Trowe, M.-O. *et al.* Canonical Wnt signaling regulates smooth muscle precursor development in the mouse ureter. *Development* **139,** 3099–3108 (2012).

13. Curriculum vitae

Personal information

Name:	Eva Christina Bettenhausen
Date of birth:	14/10/1984
Place of birth:	Kassel
Citizenship:	German
E-mail:	bettenhausen.eva@mh-hannover.de

School education

1991-1995	Grundschule Körle
1995-2001	Integrierte Gesamtschule IGS Guxhagen
2001-2004	Oberstufengymnasium Geschwister-Scholl-Schule, Melsungen Degree: Abitur

University studies

2005-2008	Bachelor studies in Biology at Philipps-Universität Marburg/Lahn Degree: Bachelor of Science
2008-2010	Master`s program Biomedizin at Hannover Medical School Degree: Master of Science
2010-2015	Employment as research assistant and preparation of doctoral thesis at the Institute for Molecular Biology in the lab of Prof. Dr. Andreas Kispert

Current position

2015-	Research assistant at the Clinic for Dental Prosthetics at Hannover Medical School

Practical experiences

2004-2005	Nursing internship at Kreiskrankenhaus Melsungen Stage Design Internship at Staatstheater Kassel Internship at the Clinic of Veterinary Surgery (Kleintierklinik Doering & Partner, Kassel)
2007	Fieldwork internship in Southafrica and Namibia with the Department of Ecology at Philipps-Universität Marburg/Lahn

Language skills

English, fluent, written and spoken
Italian, basic knowledge
French, basic knowledge

14. Publications

2013 **„*Tbx18* expression demarcates multipotent precursor populations in the developing urogenital system but is exclusively required within the ureteric mesenchymal lineage to suppress a renal stroma fate“**

Bohnenpoll T (1) and Bettenhausen E (2), Weiss AC, Foik AB, Trowe MO, Blank P, Airik R and Kispert A.

Developmental Biology 2013, August 380(1), 25-36

Authors 1 and 2 share first authorship

2012 **„Canonical Wnt signaling regulates smooth muscle precursor development in the mouse ureter“**

Trowe MO and Airik R, Weiss AC, Farin HF, Foik AB, Bettenhausen E, Schuster-Gossler K, Taketo MM and Kispert A.

Development 2012, September 139(17), 3099-108.

15. Acknowledgement

First of all I would like to thank my supervisor Prof. Dr. Andreas Kispert for giving me the opportunity to work on this very interesting and challenging project. I am very thankful for his constant scientific support and advise. In his very well organized lab it was possible to fully concentrate on the project, while he took care of the organization and of bureaucratic and financial issues. Also he was constantly available for questions and discussion. Thanks a lot for that!

I want to thank Dr. Roland Schmitt for his kind offer to co-examine my thesis and Prof. Dr. Hansjörg Küster for accepting the duty as chair of my disputation.

I also want to thank my colleagues for their constant support in the lab and lots of interesting discussions. I found inspiring co-workers, good friends and one especially good friend during my time with you. Most of all I want to thank Dr. Mark-Oliver Trowe for being my supervisor during my first months in the lab and introducing me to ureter and kidney development, Tobias Bohnenpoll, Patrick Blank, Dr. Anna-Carina Weiss and Dr. Anna Foik with whom I worked on the publications and manuscript, which are part of this thesis and the technicians Marianne Petry and Dr. Imke Peters for technical support and lots and lots of genotyping!

I want to thank all my friends who had to be very patient with me during all this time und who never stopped supporting me in all possible ways.

Finally I thank my parents and Patrick, without you I could never have done this!!!